DOT/FAA/TC-14/42

Federal Aviation Administration
William J. Hughes Technical Center
Aviation Research Division
Atlantic City International Airport
New Jersey 08405

Innovative, Wide-Area, Image-Based Nondestructive Inspection Techniques for Modern Rotorcraft Composites

June 2015

Final Report

This document is available to the U.S. public through the National Technical Information Services (NTIS), Springfield, Virginia 22161.

This document is also available from the Federal Aviation Administration William J. Hughes Technical Center at actlibrary.tc.faa.gov.

U.S. Department of Transportation
Federal Aviation Administration

NOTICE

This document is disseminated under the sponsorship of the U.S. Department of Transportation in the interest of information exchange. The U.S. Government assumes no liability for the contents or use thereof. The U.S. Government does not endorse products or manufacturers. Trade or manufacturers' names appear herein solely because they are considered essential to the objective of this report. The findings and conclusions in this report are those of the author(s) and do not necessarily represent the views of the funding agency. This document does not constitute FAA policy. Consult the FAA sponsoring organization listed on the Technical Documentation page as to its use.

This report is available at the Federal Aviation Administration William J. Hughes Technical Center's Full-Text Technical Reports page: actlibrary.tc.faa.gov in Adobe Acrobat portable document format (PDF).

Technical Report Documentation Page

1. Report No.	2. Government Accession No.	3. Recipient's Catalog No.
DOT/FAA/TC-14/42		

4. Title and Subtitle	5. Report Date
INNOVATIVE, WIDE-AREA, IMAGE-BASED NONDESTRUCTIVE INSPECTION TECHNIQUES FOR MODERN ROTORCRAFT COMPOSITES	June 2015
	6. Performing Organization Code
7. Author(s)	8. Performing Organization Report No.
Robert J. Barry and Jeffrey P. Nissen	299-100-950
9. Performing Organization Name and Address	10. Work Unit No. (TRAIS)
Bell Helicopter Textron Inc. 600 E. Hurst Blvd. Hurst, TX 76053	
	11. Contract or Grant No.
	DTFACT-09-C-00011
12. Sponsoring Agency Name and Address	13. Type of Report and Period Covered
U.S. Department of Transportation Federal Aviation Administration FAA National Headquarters 950 L'Enfant Plaza North, SW Washington, DC 20024	FINAL REPORT
	14. Sponsoring Agency Code
	AFS-300

15. Supplementary Notes

The Federal Aviation Administration William J. Hughes Technical Aviation Research Division COR was David Westlund.

16. Abstract

This research was funded to develop inspection technologies to ensure safety of flight for composite aircraft in operational service. As these new composite airframe structures and material designs are fielded and experience subsequent damage, new inspection technologies and techniques are required to ensure safety of flight. The failure modes of the new composite structures are substantially different from metallic structures; for example, a bird strike or blunt object impact damage can be detected visually on legacy metallic structures, but may be well hidden on a composite structure. This report documents developed and demonstrated inspection technologies and techniques that can inspect composite airframe structures effectively and efficiently for various defects and damage.

This report includes the development of innovative, image-based, wide-area, and portable inspection technologies to address common inspection-related challenges within the industry, including: impact damage; inspection of repaired structures; detection of porosity or foreign materials; detection of fluid ingression in composite structures; and methods to enhance visual inspection. Technologies and techniques developed to address these challenges include Digital Acoustic Video, phased array ultrasonics, and field deployable infrared imaging. These technologies use wide-area coverage and intuitive, visual-based displays in contrast to the oscilloscope, or flying dot displays, in conventional inspection technology.

17. Key Words	18. Distribution Statement
Composite aircraft, Nondestructive inspection, Nondestructive evaluation, Impact damage, Porosity, Image-based inspection	This document is available to the U.S. public through the National Technical Information Service (NTIS), Springfield, Virginia 22161. This document is also available from the Federal Aviation Administration William J. Hughes Technical Center at actlibrary.tc.faa.gov.

19. Security Classif. (of this report)	20. Security Classif. (of this page)	21. No. of Pages	22. Price
Unclassified	Unclassified	196	

Form DOT F 1700.7 (8-72) Reproduction of completed page authorized

ACKNOWLEDGEMENTS

The author would like to acknowledge the Federal Aviation Administration for sponsoring this research, as well as the Industry Advisory Board, consisting of Air Logistics; Cessna; Petroleum Helicopters Inc (PHI); Rotor Blades, Incorporated (RBI); and Sandia National Laboratories. The author would also like to thank the validation participants consisting of PHI, RBI, and Sandia National Laboratories, as well as the technology development participants, particularly Imperium Inc. and Thermal Wave Imaging Inc.

TABLE OF CONTENTS

Page

EXECUTIVE SUMMARY xii

1. INTRODUCTION 1

1.1 Overview of Selected Nondestructive Evaluation Technologies 1

1.1.1 Phased Array Ultrasonic Testing Technology 2
1.1.2 The DAV Technology 3
1.1.3 The FDIR Technology 5

2. TECHNOLOGY VALIDATION PLAN 8
3. TECHNOLOGY EVALUATION 13

3.1 Porosity Evaluation 13

3.1.1 The DAV Results of Porosity Specimens 17
3.1.2 The PAUT Results of Porosity Specimens 19

3.2 Impact Panel Evaluation—BVID and Visible Impact Damage 20

3.2.1 The FDIR Impact Panel Evaluation 25
3.2.2 The DAV Impact Panel Evaluation 37
3.2.3 The PAUT Impact Panel Evaluation 40
3.2.4 Repaired Impact Panel Evaluation 45

3.3 The FOD Panel Evaluation 53

3.3.1 The PAUT Evaluation of FOD Panel #1 and FOD Panel #2 56
3.3.2 The DAV Evaluation of FOD Panel #1 and FOD Panel #2 58
3.3.3 The FDIR Evaluation of FOD Panel #1 and FOD Panel #2 59

3.4 THE FDIR Evaluation of Fluid Ingression in Control Surfaces 61

3.4.1 The FDIR Evaluation of Fluid Ingression in Fiberglass Skin Over Nomex Core 61
3.4.2 The FDIR Evaluation of Fluid Ingression in Aluminum Skin Over Aluminum Core 63
3.4.3 The FDIR Evaluation of Large Water Volumes in Control Surfaces via Passive Excitation 64

4. ASSESSMENT OF SELECTED TECHNOLOGIES 66

4.1 Assessment of FDIR Technology 66

4.1.1 Potential Future Work on FDIR 68

4.2 Assessment of DAV Technology 68

4.2.1 Potential Future Work on DAV 69

4.3 Assessment of PAUT Technology. 69

4.3.1 Potential Future Work on PAUT 69

5. SUMMARY OF SANDIA EVALUATIONS 69
6. CONCLUSION 70

APPENDICES

A—Field-Deployable Infrared Inspection Technique
B—Phased Array Ultrasonic Technique
C—Digital Acoustic Video-Inspection Technique
D—Large-Scale Impact Panel
E—Sandia Evaluation Results

LIST OF FIGURES

Figure		Page
1	Relation Between Technology, Applications, and Technology Readiness Level	2
2	The PAUT Technology Inspects Large Areas and Provides a Permanent Data Record	3
3	The DAV Camera Cross-Section	4
4	Imperium Inc.'s DAV Technology and the FAA-Bell Helicopter Textron, Inc. Prototype	5
5	The DAV C-Scan Image Development Progress	5
6	The FDIR Camera	6
7	The FDIR Examples of Impact Damage Imaging Development	8
8	Innovative NDE Validation Plan	9
9	Test Panel Configurations	11
10	Porosity Panel Baseline TTU C-Scan Images	14
11	Porosity Panel Baseline ToF C-Scan Images	15
12	Porosity Optical Evaluations, Panels 0°, 90° Orientation	16
13	The DAV Porosity Panel Images; A-Scan Shows Multiple Depths	18
14	The DAV Porosity Panels After Technology Development	19
15	The PAUT Porosity Output Screenshot	20
16	Ultrasonic Baseline Acceptance TTU C-Scans for I-Beam Panels #3, 2, and 1	21
17	Ultrasonic Baseline Acceptance TTU C-Scan for Hat Panels #1 and #2	21
18	Ultrasonic Baseline Acceptance TTU C-Scan for Hat Panel #3	22
19	Impact Test Plan Layout Map for Hat Panel #2	22
20	Impact Test Plan Layout Map for I-Beam Panel #2	23
21	The Impact Panel in the Impact Test Rig and Impact Test Rig	24
22	The ToF C-Scans of I-Beam Panel #1, I-Beam Panel #2, and I-Beam Panel #3	24
23	The ToF C-Scans of Hat Panel #1, Hat Panel #2, and Hat Panel #3	25
24	The I-Beam Panel #1 TWI Flash IR Image Compared to the FDIR Image	26
25	The I-Beam Panel #3 Photograph, FDIR Image , and ToF C-Scan	27
26	The FDIR Comparison Between Gloss White and High-Emissive Flat Black Coating	27
27	The FDIR Results for all FAA-Bell Impact Panels	28
28	The FDIR Temperature vs. Time	29

29	The TWI TSR Images of I-Beam Panel #1	30
30	The TWI TSR Images of I-Beam Panel #2	31
31	The TWI TSR Images of I-Beam Panel #3	32
32	The TWI TSR Images of Hat Panel #1	33
33	The TWI TSR Images of Hat Panel #2	34
34	The TWI TSR Images of Hat Panel #3	35
35	All Post-Processed FDIR Impact Damage Images	36
36	Lumus PD-20 Video Glasses	37
37	Lumus PD-20 FDIR Image as Viewed Through the Glasses	37
38	Initial DAV Output Snapshot	38
39	Development of DAV C-Scan Imaging of Impact Damage	38
40	The DAV Snapshot of a Delamination 0.050″ Deep in a 0.165″ Laminate	39
41	The DAV Stitched Image, Hat Panel #1	40
42	Phased Array Amplitude C-Scan of Impacted Area Resolution Comparison	40
43	Hat Panel #1 PAUT Comparison to Baseline ToF C-Scan	41
44	Hat Panel #2 PAUT Compared to Baseline PE ToF C-Scan	42
45	Hat Panel #3 PAUT Compared to Baseline PE ToF C-Scan	42
46	The I-Beam Panel #1 PAUT Compared to Baseline PE ToF C-Scan	43
47	The I-Beam Panel #2 PAUT Compared to PE ToF C-Scan	44
48	The I-Beam Panel #3 PAUT Compared to Baseline ToF C-Scan	45
49	Baseline C-Scans With Circles Noting the Designated Plug and Taper Repair Areas	46
50	Hat Panel #2 With Material Removed for Plug Repair and Taper Repair	46
51	Repaired Impact Damage Panels After Paint	47
52	The TTU C-Scan of Repaired I-Beam Panel #3 and Hat Panel #2	47
53	Baseline Ultrasonic ToF C-Scan Images of Impact Repairs	48
54	Repaired FAA-I-003 PAUT Amplitude C-Scans Compared to Baseline Amplitude C-Scan	49
55	Repaired FAA-H-002 PAUT Amplitude C-Scans Compared to Baseline Amplitude C-Scan	49
56	The DAV Evaluation of I-Beam Panel #3 Taper Repair	50
57	The DAV Evaluation of I-Beam Panel #3 Plug Repair	51
58	The DAV Snapshot of Hat Panel #2 Plug Repair	51

59	The I-Beam Panel #3 Bell Flash IR, FDIR, and Post-Processed FDIR	52
60	The Hat Panel #2 Bell Flash IR, FDIR, and Post-Processed FDIR	53
61	The FOD Panel #1 Design	54
62	The FOD Panel #2 Design	55
63	Baseline ToF C-Scan of FOD Panel #1 and FOD Panel #2	56
64	The PAUT Evaluation for FOD Panel #1 and FOD Panel #2	57
65	The PAUT C-Scan Dimensional Measurement Capability	57
66	The DAV FOD Panel #1 and FOD Panel #2 C-Scans	58
67	The DAV Snapshot of FOD Implant and Digital Depth of Reflector	59
68	Baseline Flash IR of FOD Panel #1 and FOD Panel #2	60
69	The FDIR Image of FOD Panel #1 and FOD Panel #2	61
70	Fiberglass and Nomex Control Surface Panel #1	62
71	Fiberglass Skin Over Nomex Core Fluid Ingression FDIR Evaluation	63
72	Aluminum Skin Over Aluminum Core Control Surface FDIR Evaluation	64
73	Insertion of Gross Fluid Ingression Into an Aluminum Control Surface	65
74	The FDIR of Aluminum Control Surface Exposed to Sunlight With 500 mL of Water	65
75	The DAV Images of Impact Damage Before and After Improvements	71
76	The FDIR of Impact Damage Before Optimization and at Project Conclusion	72

LIST OF TABLES

Table		Page
1	Technology Performance Metrics	10
2	Test Specimen Matrix	12
3	Attenuation of Porosity Panels	14
4	Porosity Content Evaluation Table	17
5	Technology and Technique Performance Metrics	66
6	The FDIR Impact Damage Results	67
7	Selected Technology Performance Evaluated by Application	73

LIST OF ACRONYMS

AANC	Airworthiness Assurance NDI Validation Center
AMP	Amplitude
A-scan	Ultrasonic time base signal display (similar to oscilloscope)
Bell	Bell Helicopter Textron, Inc.
B-scan	Ultrasonic depth base signal display
BVID	Barely visible impact damage
CEP	Carbon epoxy
C-scan	Ultrasonic raster scan display of recorded signal
CCW	Counterclockwise
CW	Clockwise
DAV	Digital Acoustic Video
FDIR	Field deployable infrared imaging
FOD	Foreign object debris
IR	Infrared
NDE	Nondestructive evaluation
NDI	Nondestructive inspection
PAUT	Phased array ultrasonic testing
PE	Pulse echo
PHI	Petroleum Helicopters Inc.
RBI	Rotor Blades, Incorporated
PPB	Pulse per burst
S-scan	Sectoral scan
ToF	Time of flight
TSR	Thermographic Signal Reconstruction
TTU	Through-transmission ultrasonic
TWI	Thermal Wave Imaging Inc.
UT	Ultrasonic testing

EXECUTIVE SUMMARY

Composite materials enable aircraft to fly faster and farther, and to carry more payload while costing less to maintain. As new composite commercial airframe structures are fielded and experience subsequent damage, new inspection technologies and techniques are required to ensure flight safety.

Although legacy metallic structures are heavier than modern composite structures, they show impact damage with a visible dent. Most composite structures show very little evidence of impact damage, thereby increasing the need for innovative, wide-area nondestructive inspection (NDI) technology.

Most of the commercial aircraft in service are metallic structures; therefore, most of the aircraft NDI techniques are based on metallic aircraft structures. The transition of legacy aircraft operational NDI to modern composite aircraft operational NDI will be less of a hurdle if the technology implemented is intuitive, visual, and easy to learn.

The following visual-based NDI technologies were evaluated, and the technology and techniques were optimized for composite aircraft inspections: field deployable infrared imaging (FDIR), Digital Acoustic Video (DAV™), and phased array ultrasonic testing (PAUT). A summary of the technology performance results is as follows:

- The FDIR provided wide-area inspection and an enhanced visual inspection of composite aircraft components. The FDIR performed well in fluid ingression, impact-damage detection, and substructure imaging of wide-area composite structures.

- The DAV provided visual ultrasonic raster scan display of recorded signal imaging of impact damage, porosity, and foreign object debris (FOD) in composite structures with limited diagnostic capabilities. The large touchscreen display and intuitive data output were easily understood with very little training.

- The PAUT provided the most diagnostic capability of impact damage, porosity, and FOD in composite structures. The full-waveform capture enabled full data reconstruction and manipulation.

Test panels were designed and fabricated to evaluate porosity, impact damage, impact-damage repairs, substructure, and fluid ingression using FDIR, DAV, and PAUT. Inspection techniques for each of these technologies were written and demonstrated for feedback at the Airworthiness Assurance NDI Validation Center, Cessna, Petroleum Helicopters Incorporated, and Rotor Blades, Incorporated.

1. INTRODUCTION.

The growing use of complex composite structures in modern aircraft has brought to light a growing need for improvements in composite inspection technology. Metals are usually more consistent or homogeneous in nature than composite materials. For example, a variance in composite material thickness (e.g., a resin-rich area could be thicker or a tooling impression may be thinner) is often acceptable and can make two similar parts appear different when only one surface is available, which is often the case when working with fielded aircraft.

The use of visualization often provides perspective and increases the speed of an inspection while enhancing the quality of the data produced. This adds a level of confidence to nondestructive inspection (NDI) personnel with limited experience, and provides a tool for those inspectors to make high-value decisions and accurate damage assessments.

Fielded aircraft are susceptible to several types of damage. The composite material challenges evaluated in this report are:

- Detection and characterization of barely visible impact damage (BVID)
- Detection and characterization of impact damages before and after repair
- Detection of fluid ingression in sandwich structures (core stiffened structures)
- Detection of porosity and foreign materials in cured laminate structures
- Methods to enhance visual inspection schemes detecting critical defects and damage
- Fast, low-cost, large-area inspection for BVID in laminated structures

1.1 OVERVIEW OF SELECTED NONDESTRUCTIVE EVALUATION TECHNOLOGIES.

The technologies developed for the composite material challenges were selected for their visual output, which improves their ability to be implemented in service with a minimal amount of training required. Figure 1 shows an illustration of the selected technologies and their intended applications.

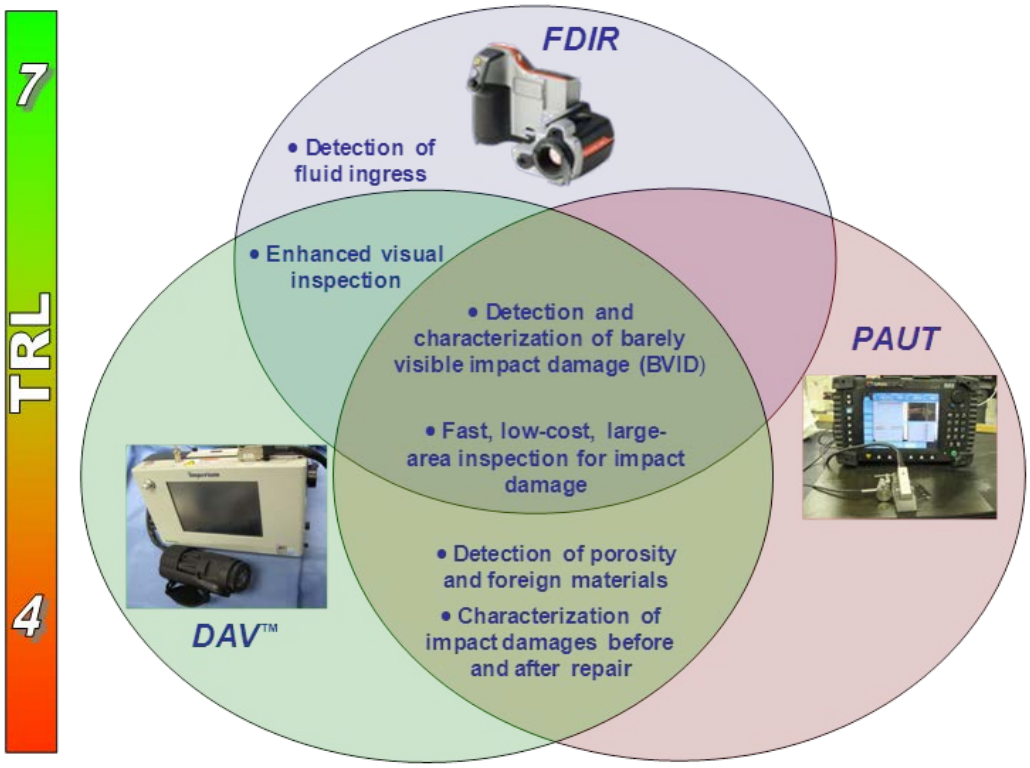

DAV = Digital Acoustic Video; FDIR = Field deployable infrared imaging, PAUT = phased array ultrasonic testing

Figure 1. Relation Between Technology, Applications, and Technology Readiness Level

The technologies shown in figure 1 were selected based on their ability to provide a visual display of the material being inspected and their intuitive use. The TRL bar on the left represents their technology readiness level at the beginning of the project.

1.1.1 Phased Array Ultrasonic Testing Technology.

Ultrasonic techniques using phased array probes provide several advantages over conventional ultrasonic testing (UT). Phased array probes can contain several to hundreds of small piezoelectric elements housed in a handheld case. Many phased array units are also equipped with a full range of display menus that provide the operator with the enhanced capability to visualize ultrasonic time base signal display (A-scan), ultrasonic depth base signal display (B-scan), and ultrasonic raster scan display of recorded signal (C-scan) data simultaneously. Though conventional UT equipment can provide the visualization capability when coupled to encoders and scanning arms, it fails to compete with the portability, low-cost, and speed of phased array ultrasonic testing (PAUT). The advantages of using PAUT include the increased sensitivity to smaller flaws as well as the ability to adjust sensitivity to known depths within a structure. This makes characterization of internal anomalies (e.g., porosity) easier to define. Having several display schemes becomes important when characterizing flaws or hidden structures, and the speed at which this can be done using PAUT allows for more rapid inspections in comparison to conventional methods. The full-waveform capture of PAUT lends itself to post-processing manipulation or reconstruction. The complexity of the PAUT technology makes it more challenging to learn than field deployable infrared imaging (FDIR)

and Digital Acoustic Video (DAV). Modern PAUT units, such as the one shown in figure 2, allow preprogrammed setups to be stored in the system for less-experienced personnel to use.

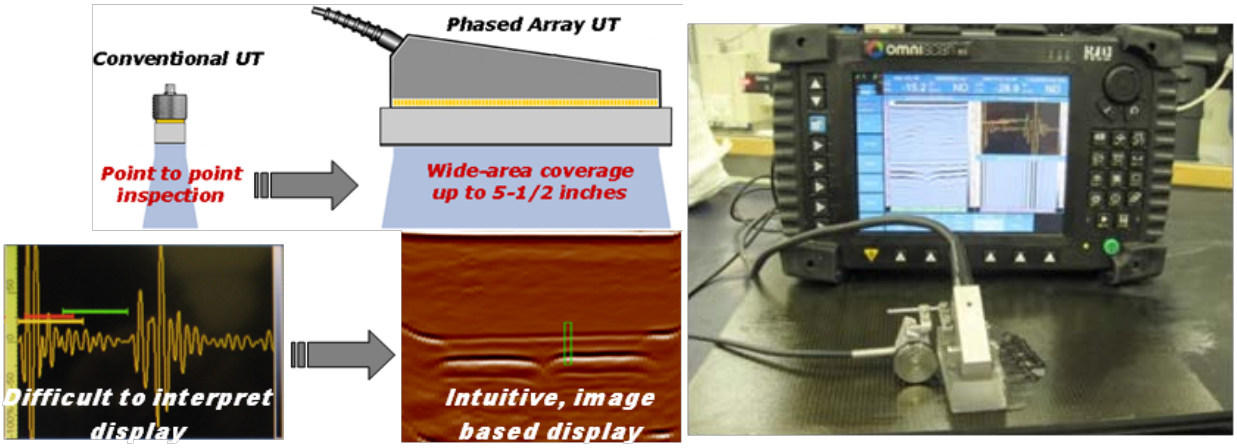

Figure 2. The PAUT Technology Inspects Large Areas and Provides a Permanent Data Record

The PAUT technology and technique development for usage on composite aircraft includes:

- Probe selection
- Focal law development
- Encoder method and arrangement
- Display optimization
- Signal acquisition optimization (via gating)
- Establishment of the resolution required to interrogate anomalies in composite materials

1.1.2 The DAV Technology.

Imperium Inc. DAV camera technology uses a piezoelectric sensor combined with a 120 x 120 charge-coupled device imaging chip (see figure 3) which allows for real-time ultrasonic imaging. The camera is placed on the sample and focuses the transmitted and received ultrasound beams to and from the unit's sensor. Standard video electronics and image processing are used to format the image for presentation to the user on a touchscreen liquid crystal display. This system produces pulse echo (PE) ultrasonic C-scan images at 30 frames per second with 0.008″ spatial resolution.

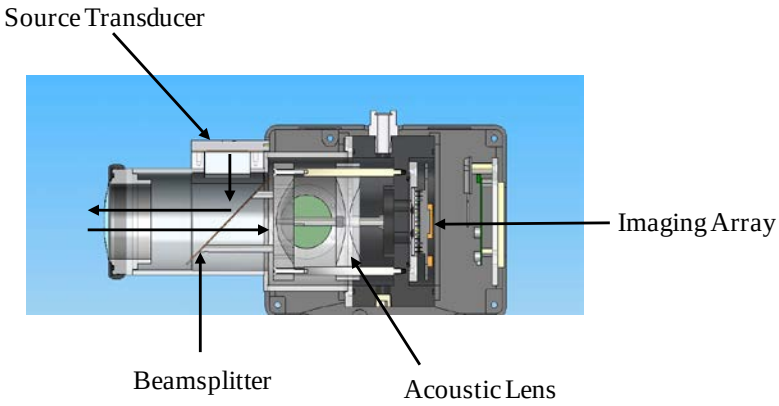

Figure 3. The DAV Camera Cross-Section

Figure 4 shows the final design configuration as part of this technology development. The technology developments made on the DAV were:

- The frequency was increased from 5 MHz to 7.5 MHz to improve near surface resolution
- The pulser voltage was increased from 800 volts to 990 volts to improve penetration of composites
- A software improvement provided digital thickness depth in the C-scan image, which can be saved as a still image (snapshot) or as a digital video recording
- The signal processing frequency was slightly increased to improve the A-scan display
- The pillow at the front of the camera was replaced with a membrane that does not snag on rough surfaces (as shown in figure 4(b))

(a) (b)

Figure 4. (a) Imperium Inc.'s DAV Technology and (b) the FAA-Bell Helicopter Textron, Inc. Prototype

Figure 5 shows the improvements made to the C-scan image output. The final 7.5 MHz transducer was found to perform best at 6.2 MHz.

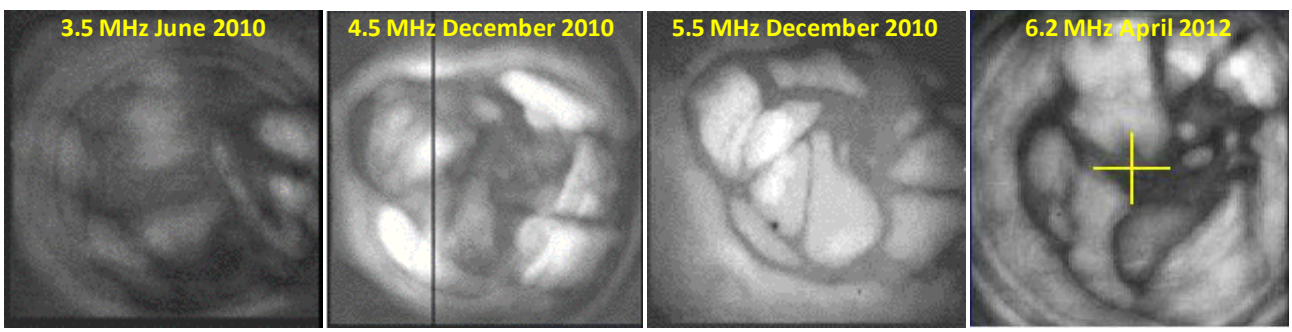

Figure 5. The DAV C-Scan Image Development Progress

The DAV technology provides a visual image of composite structures with the ability to scan faster than phased array, but slower than FDIR. The DAV technology can image a wider variety of anomalies than FDIR, but does not have the diagnostic capability (e.g., B-scan) of PAUT. Further detail on the DAV technology evolution is illustrated in the impact panel evaluations in section 3.2.2.

1.1.3 The FDIR Technology.

The FDIR technology provides ultra-portable, low-cost NDI tools to rapidly assess airframe and rotor composites for critical (gross) damage, and provides enhanced visual inspection data to aid conventional visual and NDI techniques. The FDIR tools give unskilled NDI personnel a way to quickly evaluate damage to aircraft before or after flight. Many times during detailed NDI inspection (e.g., contact ultrasonics) on complex composites (e.g., rotor or airframe structures),

inspection time can be prolonged because an inspector is unfamiliar with the structure of the component being inspected. Access to the backside surface is rarely allowed, preventing the inspector from seeing underlying component structures such as spars, stiffeners, stringers, or other complex configurations. A considerable amount of time may be spent familiarizing an inexperienced inspector with the structure. The FDIR can quickly show the inspector where the ribs, stiffeners, or spars are located, as well as previously repaired areas.

The simplistic, enhanced visual inspection technique involves an inspector walking around the aircraft before and after flight to ensure aircraft airworthiness. A wide-area technique using a low-cost infrared (IR) imager (see figure 6) has been evaluated in previous research to determine the applicability of detecting anomalies and composite damage, and providing an image-based aid to detailed NDI.

Figure 6. The FDIR Camera

The application of FDIR requires the operator to create a thermal flux between the component under evaluation and the surrounding environment. Some methods to create thermal flux in composite structures include:

- Using an auxiliary heating source to rapidly heat the surface ~10°F–15°F above ambient temperature
- Pulling an aircraft from a cool hangar (70°F–85°F) into sunlight
- Bringing an aircraft from a tarmac to a hangar
- Examining an aircraft immediately post-flight

The FDIR evaluation has also been used for detection of anomalies and damage in laminate and sandwich composite construction. In this report, delaminations, voids, water ingression, and impact damage were evaluated to determine their detectability.

The FDIR inspection technique was developed as part of this effort. The FDIR development in this project yielded the following focus areas to obtain the best possible image:

- Address thermal emissivity effects associated with high-gloss white paint typically found in commercial aircraft with the application of flat black or matte black paint

- Capture thermal images as soon as possible and as quickly as possible when the inspection area is exposed to thermal energy

- Utilize post-processing techniques, such as Thermal Wave Imaging Inc.'s (TWI's) Thermographic Signal Reconstruction (TSR®) software

Figure 7 shows these developments. Figure 7(a) is an initial FDIR panel evaluation of I-beam panel #2 with a low-emissive gloss-white finish. The substructure is clearly visible, but the impact damage is not. Figure 7(b) is I-beam panel #2 coated with a high-emissive flat black finish; four of the gross impact damage areas are visible as numbered. Figures 7(c and d) illustrate the results with optimized panel positioning of I-beam panel #2, with high-emissive coating and post-processing using TSR software. The FDIR development is described in more detail in section 3.2.1.

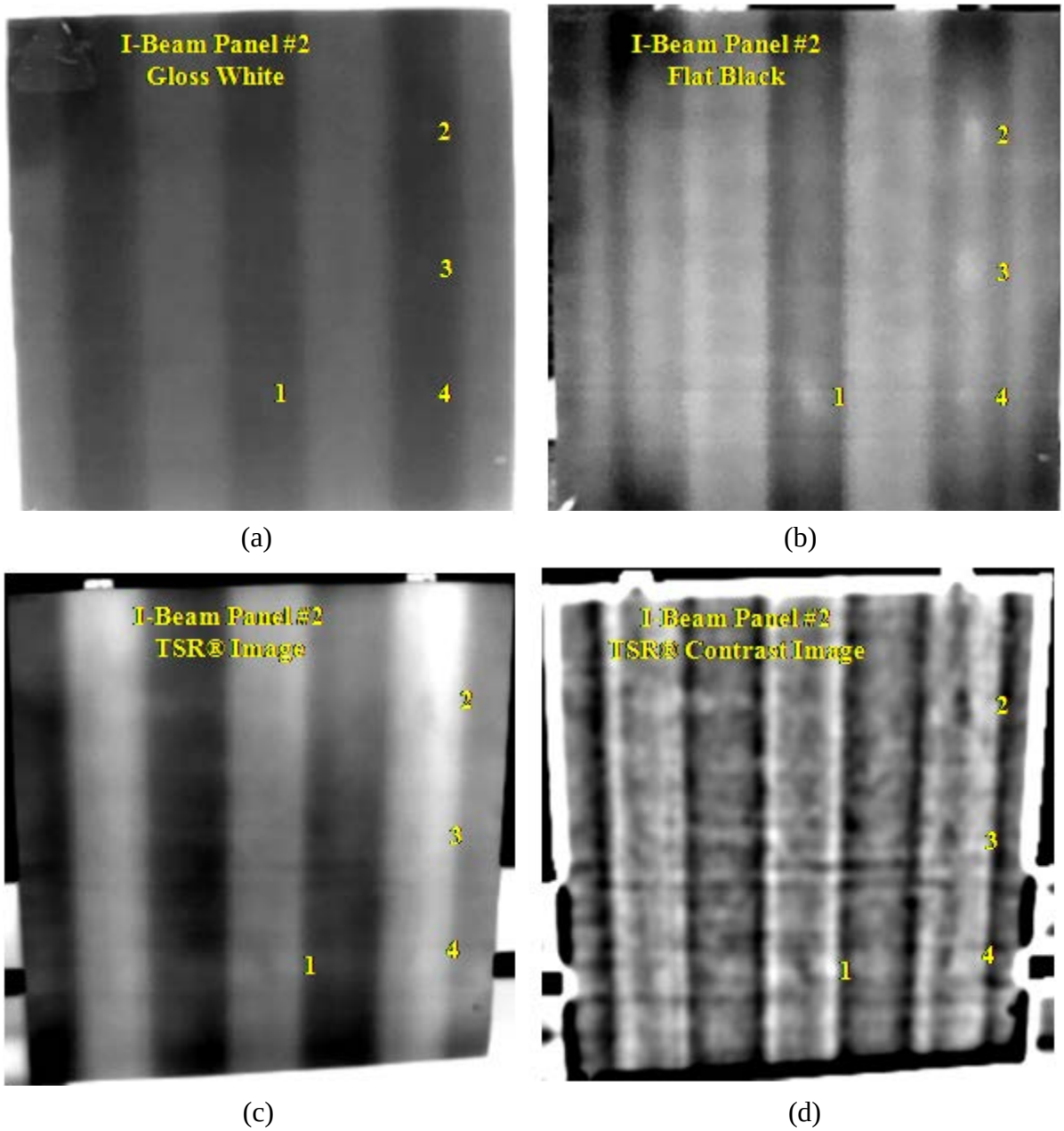

Figure 7. The FDIR Examples of Impact Damage Imaging Development

2. TECHNOLOGY VALIDATION PLAN.

A validation plan for the innovative nondestructive evaluation (NDE) research effort was established to ensure deliverables would be met (see figure 8). The validation plan integrates activities; testing and evaluations; and demonstrations.

An industry advisory board was established to provide input. The advisory board members were selected for their experience with fielding aircraft and with composite materials. The operational concepts and metrics were derived with the advisory board, and inspection/evaluation application requirements were formed.

Test specimens were then designed and fabricated. The test panels were baseline inspected to ensure they met the designed intentions. Evaluation of the panels with the selected technologies led to the identification of technology and technique gaps, and improvements were made.

The developed, optimized technology and techniques were then evaluated and validated. Technology demonstrations were performed at the Airworthiness Assurance NDI Validation Center (AANC) at Sandia National Laboratories. The techniques were further improved and then demonstrated at Petroleum Helicopters Inc. (PHI); Rotor Blades, Incorporated (RBI); and Cessna.

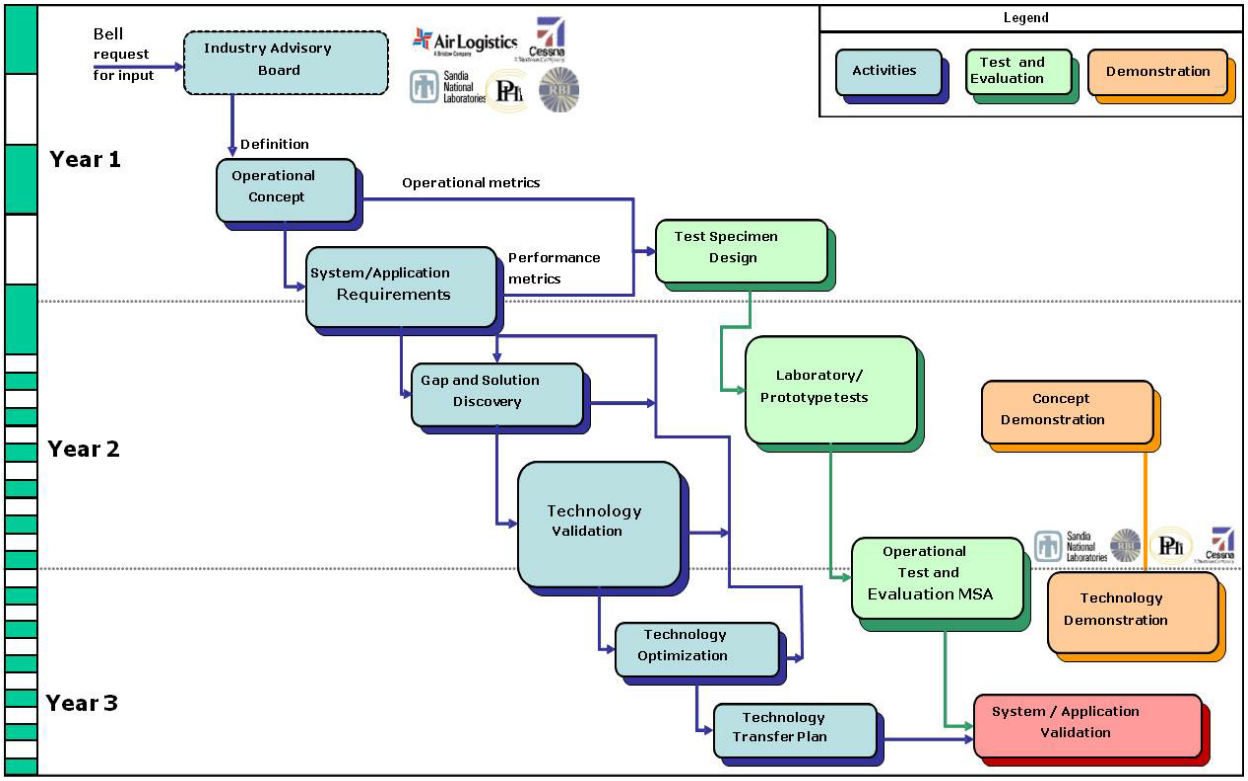

Figure 8. Innovative NDE Validation Plan

Table 1 shows the performance metrics for the selected technologies. The table illustrates a broad range of metrics pertinent to field inspection of composite aircraft structures.

Table 1. Technology Performance Metrics

Description	Originating Requirement	Measure
Are the results visualized?	Easy to interpret results	Yes or No
Data Resolution	Easy to interpret results	Inch
Instantaneous data points displayed	Easy to interpret results	Number
Technique throughput	Speed of inspection/Large area inspection	Ft^2/hr
Instant coverage area	Speed of inspection/Large area inspection	In^2
Equipment cost	Equipment Cost	$
Equipment weight	Portability	Lb
Parameter settings for usage (how many settings are necessary?)	Training required to perform	Number

Figure 9 shows illustrations of test specimens designed and fabricated for the technology and technique evaluations. These specimens represent typical composite aircraft components:

- The carbon epoxy (CEP) I-beam and hat-stiffened panels represent wing and fuselage panels

- The fiberglass over Nomex® and aluminum skin over aluminum core control panels represent flight control surfaces (e.g., flaps, ailerons, rudders, etc.) as well as rotor blades

- The CEP porosity laminate panels are three different thicknesses containing elongated porosity of about 5% by volume

- The CEP foreign object debris (FOD) laminate panels are of one thickness and contain five types of FOD, 1.25″ x 0.5″ in a dart shape, located at 25%, 50%, and 75% depths

Two large impact test panels were made (as requested by the FAA) for evaluation on another project. One is a 2′ x 5′ hat-stiffened panel, and the other is a 2′ x 6′ I-beam stiffened panel. The baseline scans before and after impact are attached in appendix D.

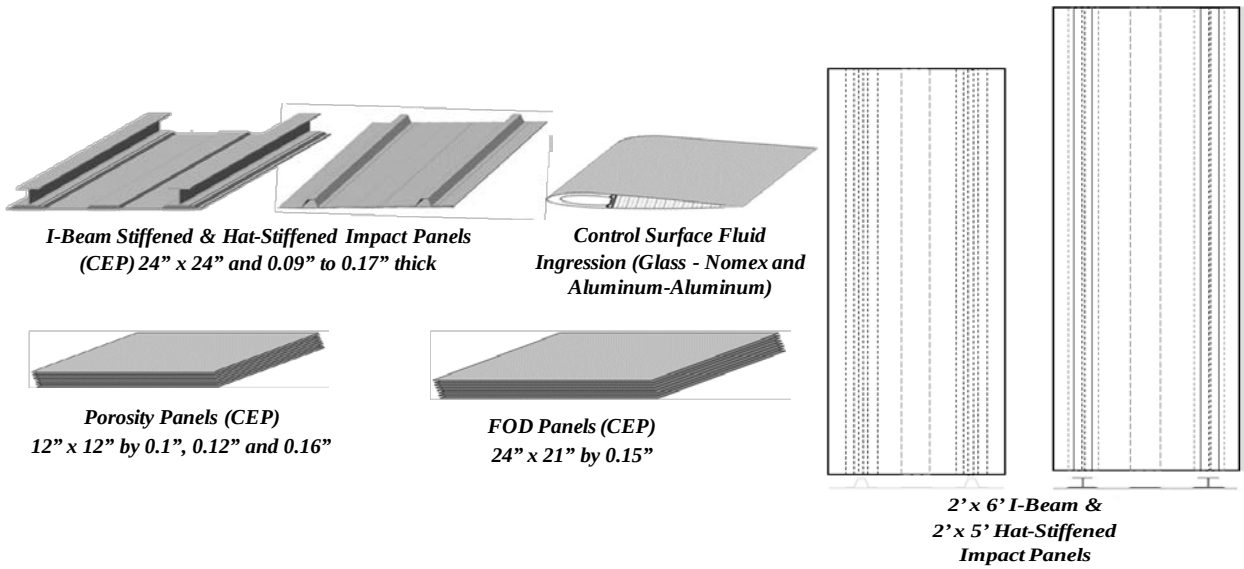

Figure 9. Test Panel Configurations

A matrix was made (see table 2) to illustrate the integration of technology application, specimen type, defect type, and location. The test panel configurations are described in the "Specimen Type/Materials" column, offering a correlation of what technology will be applied to each specimen type and the defects that will be in the various specimen types. The aircraft component or structure type being represented is shown in the right column.

Table 2. Test Specimen Matrix

Technology Application/Specimen Design	Specimen Type/Materials	Defects			Location of Defects	Application Aircraft/Component
		Flaw Simulated	Material	Defect Size		
Detection and characterization of BVID	Carbon composite laminate panels, with and without stiffeners, 0.09″ to 0.20″ thickness	BVID-VID	Natural	Impact size will be typical of imposed energy	In stiffened areas, in unstiffened areas, backside	Control surfaces, wing structure, fuselage
Detection and characterization of impact damages pre- and post-repair	Repaired carbon composite laminate panels, with and without stiffeners, 0.09″ to 0.20″ thickness	BVID-VID	Natural	Impact size will be typical of imposed energy	Repairs made over stiffened, unstiffened areas	Control surfaces, wing structure, fuselage
Detection of fluid ingress	Sandwich composite and metallic control surface structure (flaps, ailerons, rotorblades)	Water	Natural	0.5 to 250 mL	Near skin surface, near trailing edge	All control surfaces, rotorblades, sandwich construction
Detection of porosity and foreign materials in cured structure	Carbon composite laminate panels, 0.09″ to 0.20″ thickness varying porosity	Porosity	Natural	Natural porosity	Throughout, confined to depths	Rotor structures, control surfaces, wing structure
	Carbon composite laminate panels, 0.09″ to 0.20″ thickness containing FOD	FOD	A1, polymer, paper	0.31 in^2 (1.25″ x 0.5″)	Three depths, 25%, 50%, 75%	Rotor structures, control surfaces, wing structure
Methods to enhance visual inspection schemes detecting critical defects and damage	Samples from BVID tests, structural carbon laminate composite components with critical damage	Critical damage	End milled or natural	Critical size	In critical areas, high-stress areas	Control surfaces, wing structure, fuselage
Fast, low-cost, large-area for invisible impact damage in laminated structures	Samples from BVID tests, carbon laminate composite components with invisible simulated and natural flaws	Non-VID	End milled or natural	Impact size will be typical of imposed energy	In stiffened areas, in unstiffened areas, backside	Control surfaces, wing structure, fuselage

3. TECHNOLOGY EVALUATION.

After test specimens were fabricated, a baseline (or acceptance) scan was performed. An ultrasonic squirter system was used to establish a baseline scan for PAUT and DAV, and a flash IR system was used to establish an IR baseline for the FDIR technology.

3.1 POROSITY EVALUATION.

The first tests performed during this research included evaluation of porosity in carbon laminate composites. Once the panels were fabricated, baseline scans were performed to characterize the severity and distribution of porosity as cured in the panels using through-transmission ultrasonics (TTU) and PE ultrasonics. The TTU inspections were used to verify that a rejectable level of porosity had been created (see figure 10). In these scans, a reference standard of similar material containing less than 0.5% porosity is compared to the porosity panels. A dark or black color shows a high value of ultrasonic attenuation or resistance to passing ultrasonic energy through the part as compared to the reference standard on the left of figure 10. In this case, the attenuation is because of the high volume of porosity scattered in the panel.

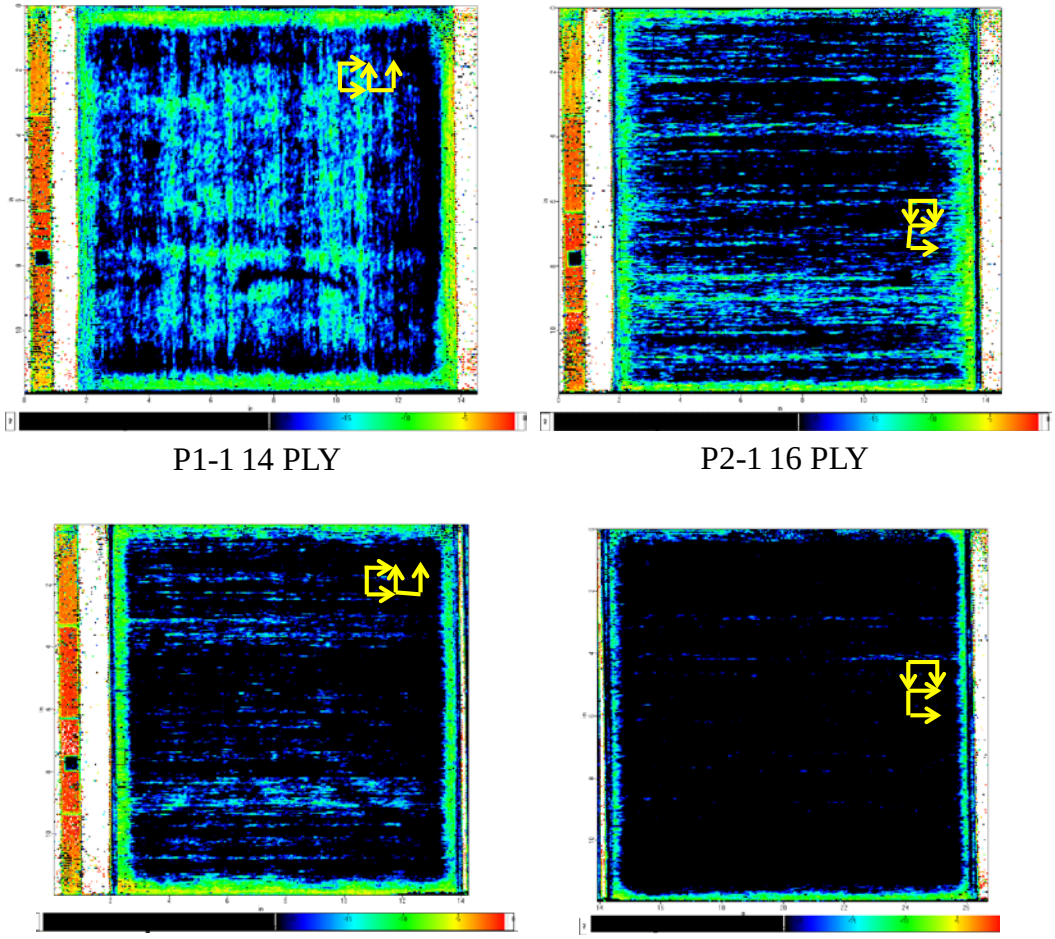

Figure 10. Porosity Panel Baseline TTU C-Scan Images

Table 3 shows the TTU attenuation for the four porosity panels.

Table 3. Attenuation of Porosity Panels

Panel	Average Attenuation (dB)	Max Attenuation (dB)
P1-1 14 ply	13 dB	24 dB
P2-1 16 ply	18 dB	25 dB
P1-2 20 ply	21 dB	28 dB
P2-2 20 ply	25 dB	28 dB

After the porosity panels were inspected using TTU, PE was used and time of flight (ToF) C-scans were created. Figure 11 shows that these scans plot the depth of all interfaces or indications in the panel. In these scans, changing colors correspond to various depths of the indication or porosity pore. These scans show elongated porosity parallel to fiber orientation and distributed throughout the panel.

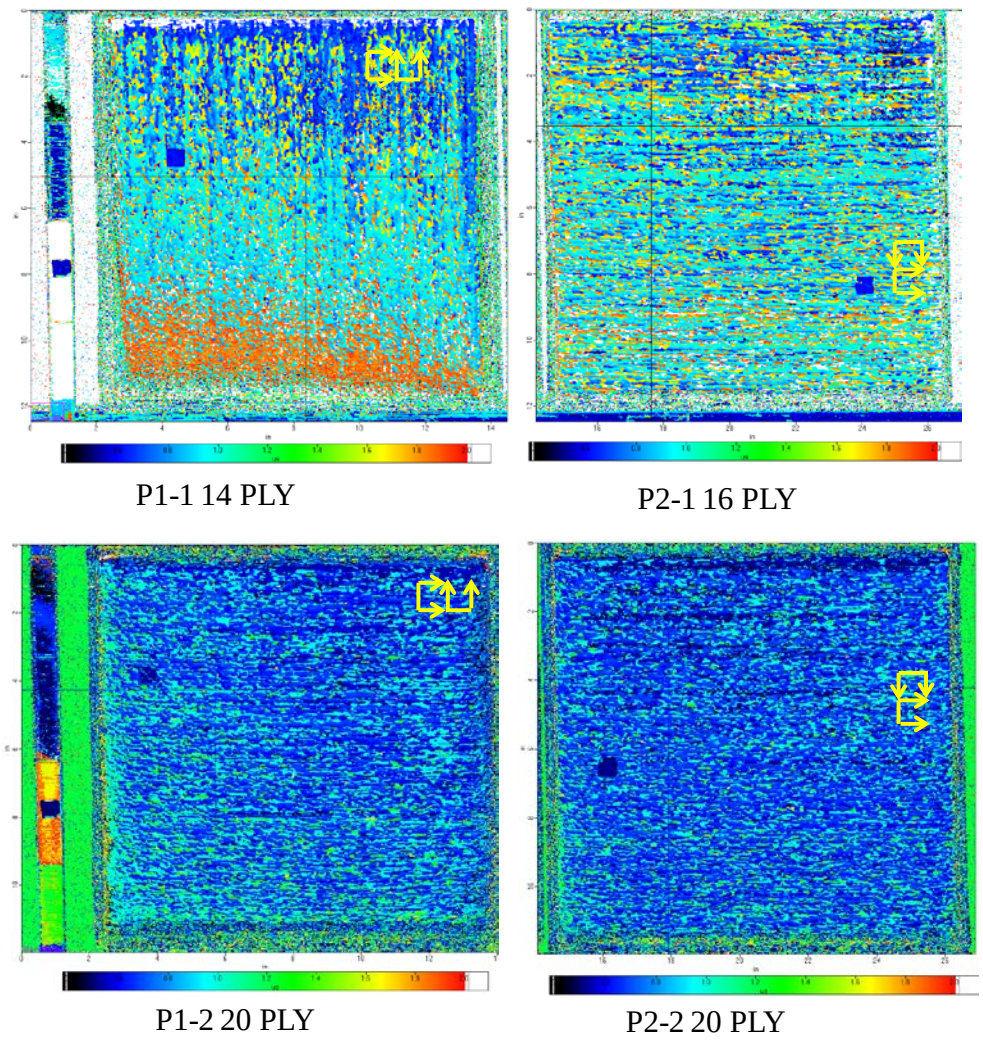

Figure 11. Porosity Panel Baseline ToF C-Scan Images

The porosity panels were then sectioned and micrographed at fiber directions of 0° and 90°, as shown by the arrows in figures 10 and 11. In this notation, 90° direction is along the fiber direction.

Figure 12 shows the micrograph images of the severe, elongated, and distributed porosity, which correlates well to baseline inspections. Each 0° and 90° cross section was photographed with off-angle lighting at the left side, center, and right side of the polished specimen.

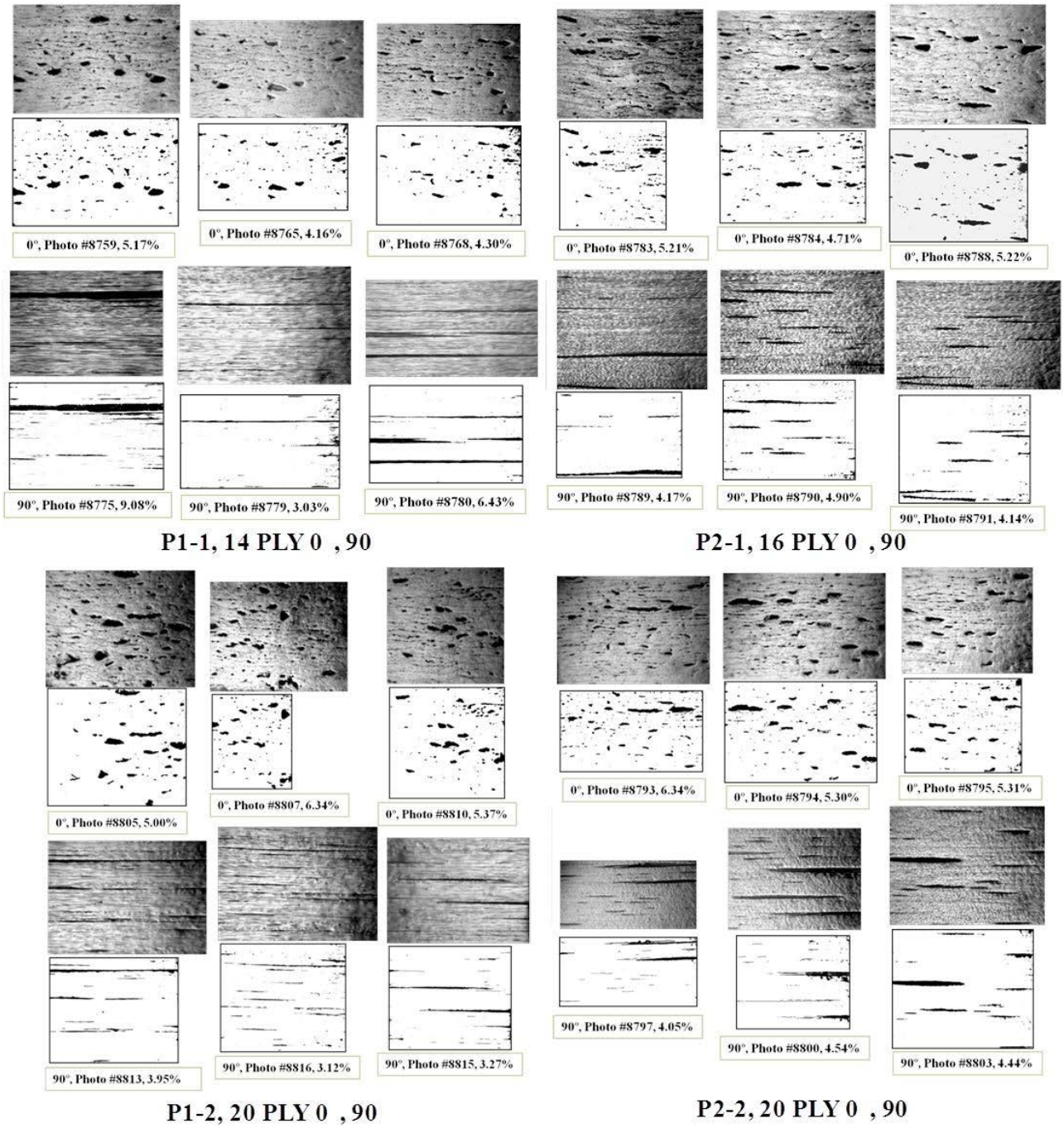

Figure 12. Porosity Optical Evaluations, Panels (P1-1, P2-1, P1-2, P2-2) 0°, 90° Orientation

The photographs were then evaluated with imaging software measuring area to provide a close estimate of the porosity percentage of each image. Table 4 shows that the average porosity quantity for the 4 panels was found to be ~5.2% by volume. The porosity content varies significantly across the panel and within the cross-section micrographs noted below.

Table 4. Porosity Content Evaluation Table

Sample ID	Photo #	Pore Area	Total Area	Porosity %	
14 Ply, 0°, Left	8759	156328	3024216	5.169%	
14 Ply, 0°, CTR	8765	90262	2169135	4.161%	
14 Ply, 0°, Right	8768	102974	2394972	4.300%	Sample Avg = 4.543%
14 Ply, 90°, Left	8775	251408	2769228	9.079%	
14 Ply, 90°, CTR	8779	75530	2490660	3.033%	
14 Ply, 90°, Right	8780	159188	2475396	6.431%	
16 Ply, 0°, Left	8783	110423	2119740	5.209%	
16 Ply, 0°, CTR	8784	115236	2446425	4.710%	
16 Ply, 0°, Right	8788	148411	2844464	5.218%	Sample Avg = 5.046%
16 Ply, 90°, Left	8789	81572	1957184	4.168%	
16 Ply, 90°, CTR	8790	118269	2412032	4.903%	
16 Ply, 90°, Right	8791	106853	2583576	4.136%	
20 Ply P1-2, 0°, Left	8805	162667	3256920	4.995%	
20 Ply P1-2, 0°, CTR	8807	96239	1516880	6.345%	
20 Ply P1-2, 0°, Right	8810	138725	2581608	5.374%	Sample Avg = 5.571%
20 Ply P1-2, 90°, Left	8813	106209	2687680	3.952%	
20 Ply P1-2, 90°, CTR	8816	85564	2741200	3.121%	
20 Ply P1-2, 90°, Right	8815	82622	2529792	3.266%	
20 Ply P2-2, 0°, Left	8793	136909	2158912	6.342%	
20 Ply P2-2, 0°, CTR	8794	153562	2895328	5.304%	
20 Ply P2-2, 0°, Right	8795	109744	2065952	5.312%	Sample Avg = 5.652%
20 Ply P2-2, 90°, Left	8797	72575	1793616	4.046%	
20 Ply P2-2, 90°, CTR	8800	91374	2010744	4.544%	
20 Ply P2-2, 90°, Right	8803	139808	3148552	4.440%	
	Average porosity all views % = 4.898%				Grand Mean = 5.203%

3.1.1 The DAV Results of Porosity Specimens.

Two of the fabricated porosity panels were evaluated with the prototype DAV system. The system was set up using a 5 MHz broadband transmitter and a broadband receiver. Figure 13 shows that the elongated porosity appeared in these images as light and dark streaks.

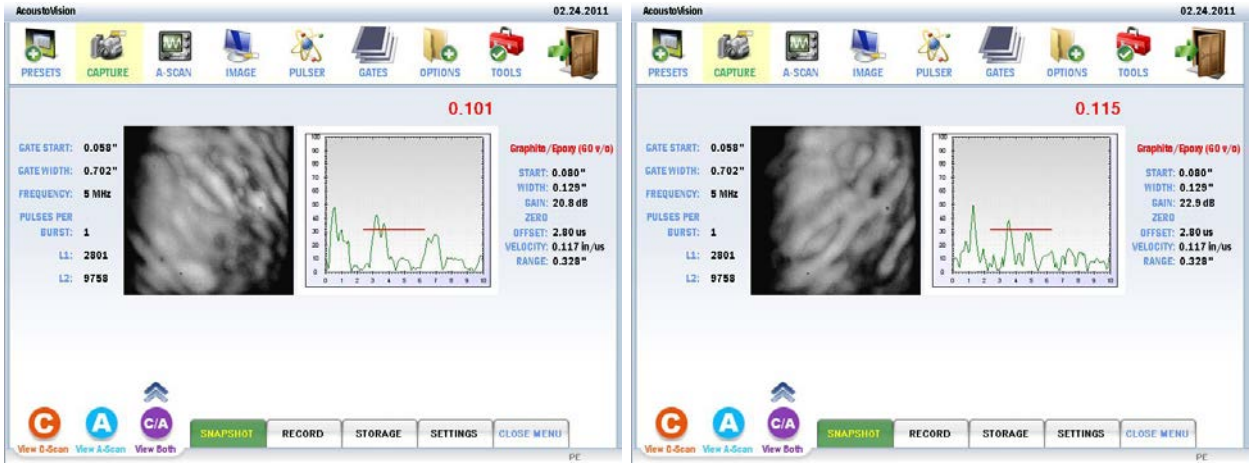

P1-1 14 PLY P2-1 16 PLY

Figure 13. The DAV Porosity Panel Images; A-Scan Shows Multiple Depths

Both of the DAV screenshots in figure 13 show the real-time C-scan image as well as the correlating A-scan signal, which can be used to determine panel acceptance. This technique demonstrated the capability to quickly detect and characterize porosity in laminate structures.

Further evaluation of porosity using this device included enhancing the resolution to 7.5 MHz. Evaluations on various porosity panels revealed that when the porosity was not elongated, it was sometimes more difficult to detect. The C-scan gate can be set to image the back-wall signal, and the C-scan turns black when excessive porosity is scanned. The A-scan display also shows the loss of back-wall signal and multiple reflectors from the porosity (see figure 13).

Figure 14 shows the porosity panel evaluations after the DAV technology was improved. The red digital depth of the nearest reflector from a pore is shown at the top of the DAV screen capture. The digital depth of the screen captures performed earlier in the project (see figure 13) were done using a lower frequency transmitter (3.5 MHz); the red digital depth reading is the back-wall echo. The 7.5 MHz transducer, with a central frequency of approximately 6.2 MHz, does not penetrate the porosity to the back wall of the laminate.

P1-1 14 PLY

P2-1 16 PLY

P1-2 20 PLY

P2-2 20 PLY

Figure 14. The DAV Porosity Panels After Technology Development

3.1.2 The PAUT Results of Porosity Specimens.

The 128-element, 5 MHz phased array system was used to image the porosity specimens. Figure 15 shows the image output of this system. The typical A-scan oscilloscope display is shown in the upper left.

The cross-section view, referred to as the sectoral scan (S-scan), is shown in the upper-right corner of figure 15. The top of the laminate is shown in the upper portion and the back of the panel is toward the middle portion of the image (indicating a depth just over 0.100″). This back surface signal is attenuated where the porosity concentrations are heavier. Through the cross-sectional S-scan view, porosity shows up as bright white and black specs scattered through the panel.

In addition to a cross-section view, PAUT can also provide a top-view C-scan of a large area. As shown in the lower portion of figure 15, the PAUT ToF C-scan matches the baseline ultrasonic ToF C-scan, showing the multicolor shades of porosity indications to correlate to the multiple depths. The C-scan data may be zoomed in on to assist in measurements.

Another benefit to phased array is that the C-scan data can be quickly changed to plot alternate data, such as signal amplitude. This postscan manipulation is a good example of the value of full-waveform capture.

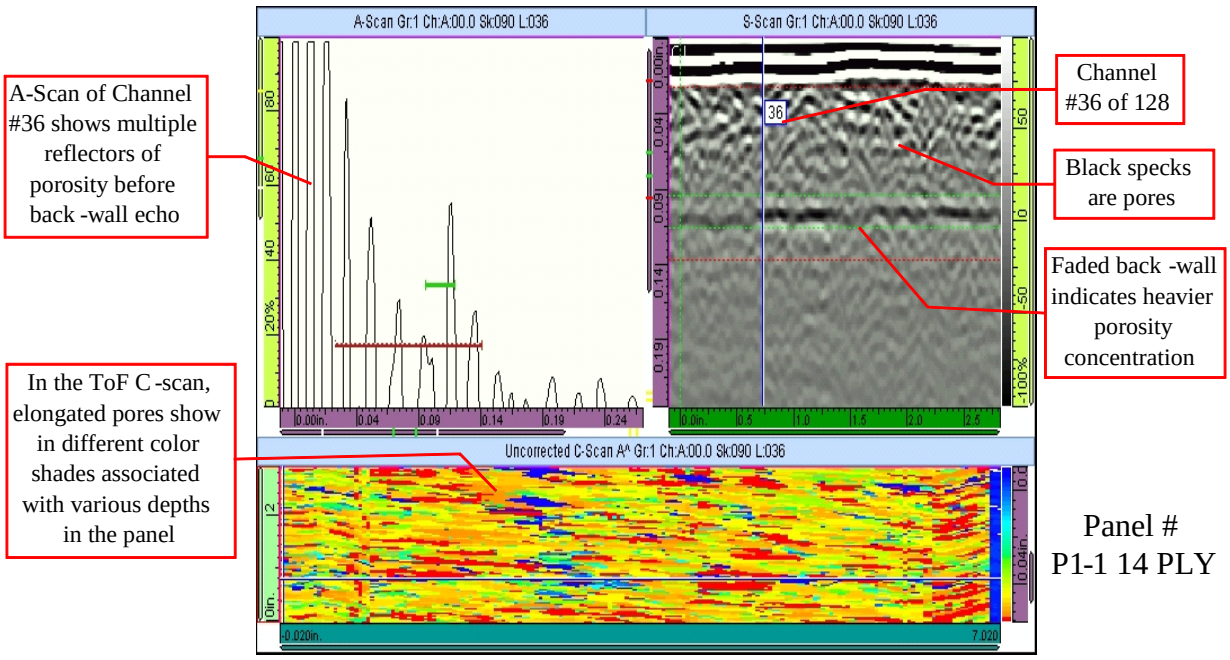

Figure 15. The PAUT Porosity Output Screenshot

The post-processing capability of the full-waveform capture also enables a technician to use a locked, preset program stored on the machine to gather data and send it to a skilled, offsite NDE engineer for evaluation.

3.2 IMPACT PANEL EVALUATION—BVID AND VISIBLE IMPACT DAMAGE.

The CEP I-beam stiffened panels were the first panels fabricated for the impact damage evaluation. After fabrication, the panels were painted with a common gloss white aircraft paint scheme to better exemplify fielded aircraft structures. Each I-beam panel was inspected and accepted per Bell Helicopter Textron, Inc.'s (Bell's) manufacturing quality assurance criteria. Figure 16 shows the UT acceptance C-scans of I-beam panels numbers 1, 2, and 3 inspected with 5 MHz transducers. A cross-section or profile of the panel is shown to the right.

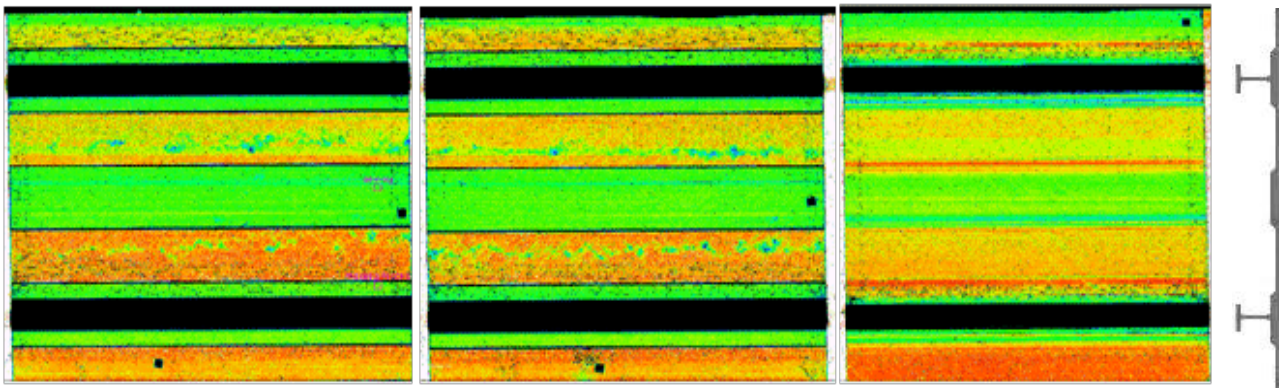

I-Beam Panel #3, (FAA-I-003) I-Beam Panel #2, (FAA-I-002) I-Beam Panel #1, (FAA-I-001)

Figure 16. Ultrasonic Baseline Acceptance TTU C-Scans for I-Beam Panels #3, 2, and 1

The dark horizontal lines are the shadowed area under the I-beam flanges. The small square spots are 1/2-inch x 1/2-inch attenuation tabs used for sensitivity and location purposes. The orange colors or lighter shades are materials that absorbed (attenuated) less sound than the green/darker areas because the material is thinner in the orange areas.

The hat panels were the next panels fabricated. The first two of these panels were fabricated successfully with the acceptance C-scans shown in figure 17. A cross-section of the panel is shown to the right.

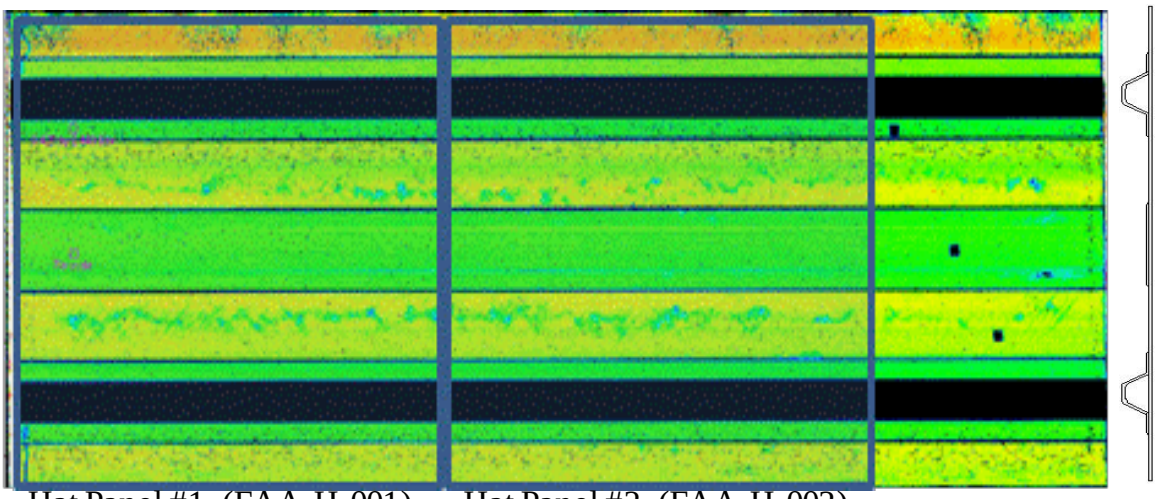

Hat Panel #1, (FAA-H-001) Hat Panel #2, (FAA-H-002)

Figure 17. Ultrasonic Baseline Acceptance TTU C-Scan for Hat Panels #1 and #2

The next hat panel contained higher levels of porosity as shown in the center area of figure 18. Hat panel #3 (FAA-H-003) was used from this fabricated panel.

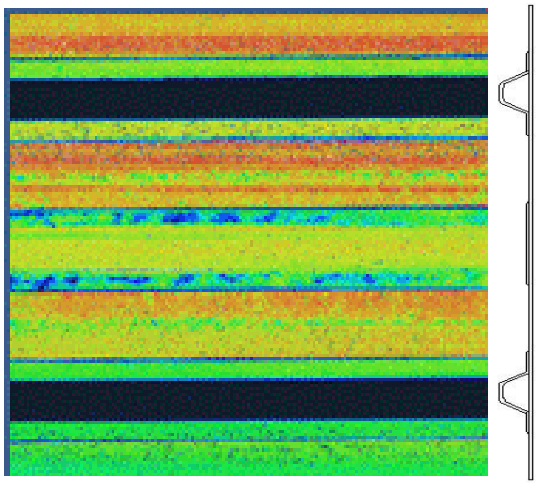

Hat Panel #3, (FAA-H-003)

Figure 18. Ultrasonic Baseline Acceptance TTU C-Scan for Hat Panel #3

An impact test plan was developed for the I-beam and hat impact test panels after they were evaluated for acceptance. A layout map was made to target a 6″ spacing between impact centers and panel edges. Figure 19 is an impact test plan layout map of hat panel #2. The map includes approximate target impact forces to be applied.

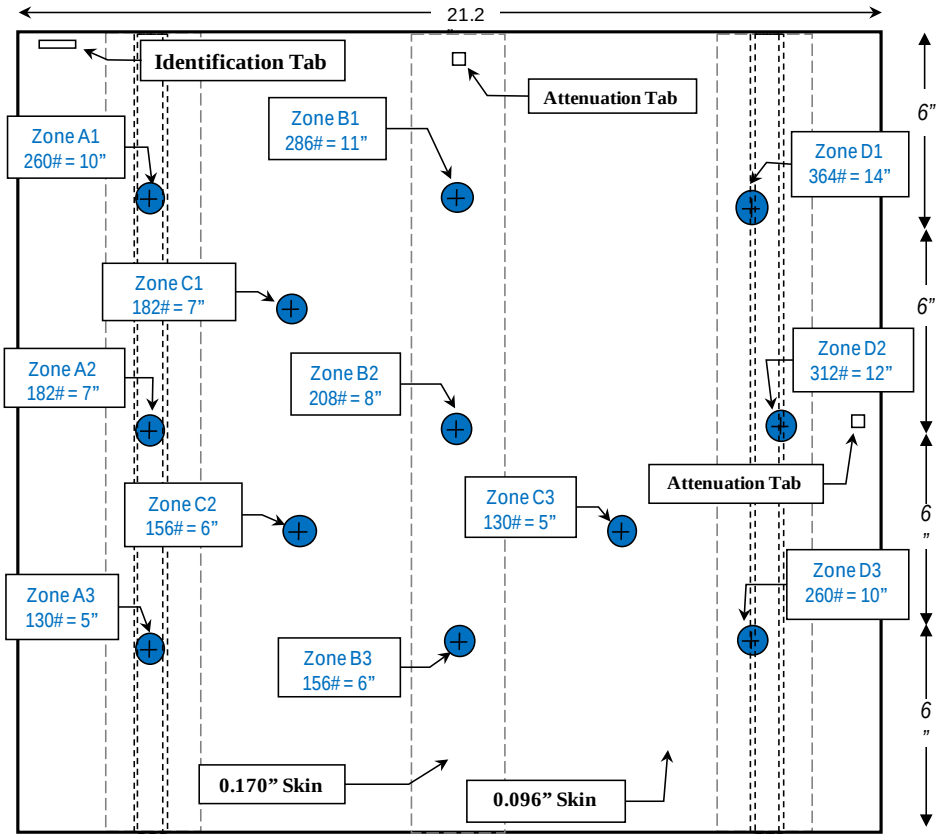

Figure 19. Impact Test Plan Layout Map for Hat Panel #2

Figure 20 is the impact test plan layout map for I-beam panel #2, (FAA-I-002), showing the various applied impact forces at the designated locations. The 6″ spacing between impact centers was intended to prevent impact damage from overlapping, and the 6″ spacing from the free edges was intended to minimize the effect of the unsupported edge of the panel. The impact forces are approximate impact force targets.

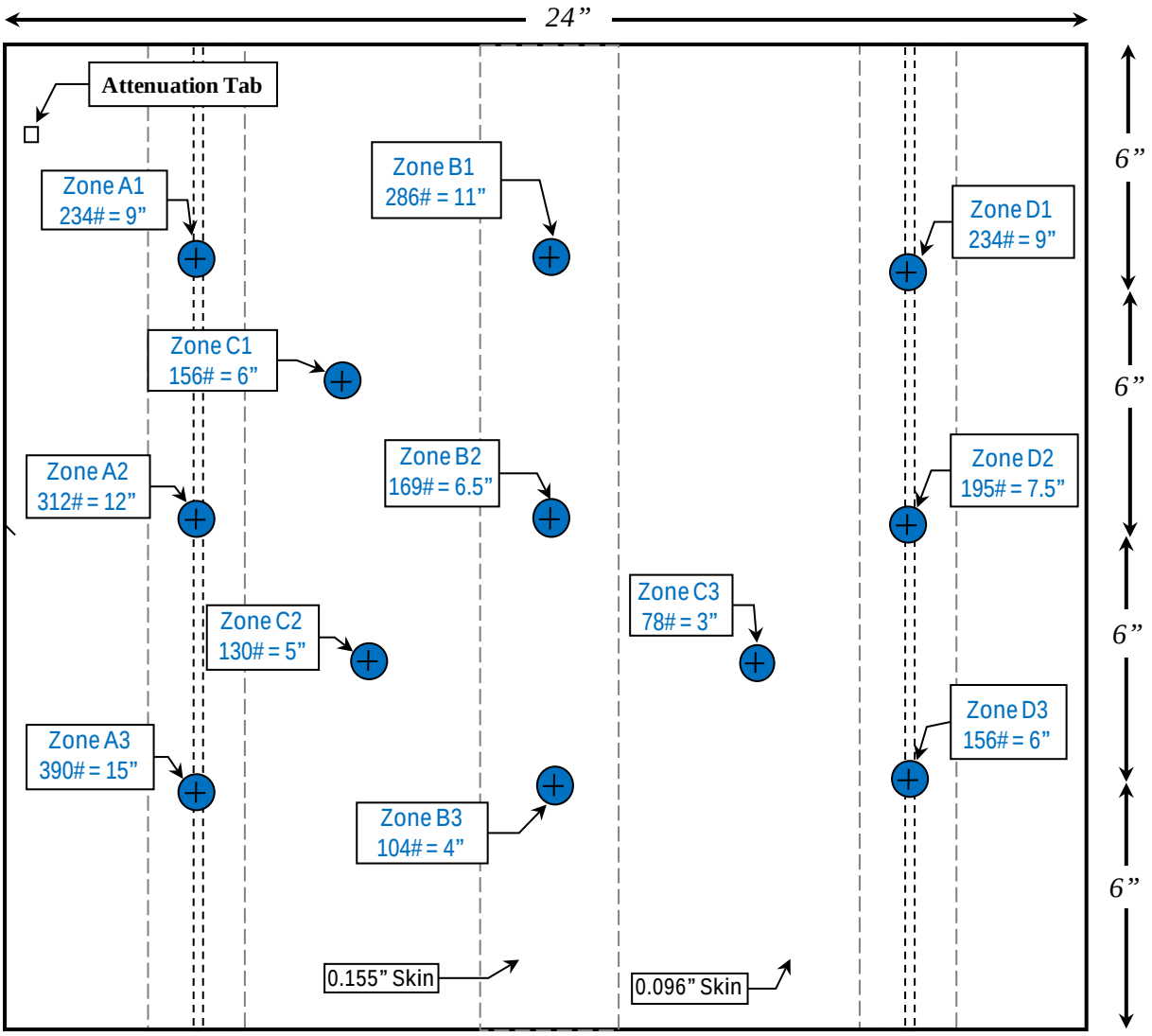

Figure 20. Impact Test Plan Layout Map for I-Beam Panel #2

Varying levels of impact forces were applied to simulate the blunt impacts experienced during aircraft operation. Several iterations were performed to select the proper impact force and impactor size; a 1″ diameter impactor was chosen because it created realistic multilevel impact damage with minimal surface damage. Figure 21 shows the calibrated impact test rig used at Bell for impact damage testing. Impact forces ranged from 26–494 in.-lb. This created surface depressions ranging from 0.002″–0.006″ and damage sizes ranging from just under 1″ diameter to over 3″ in diameter.

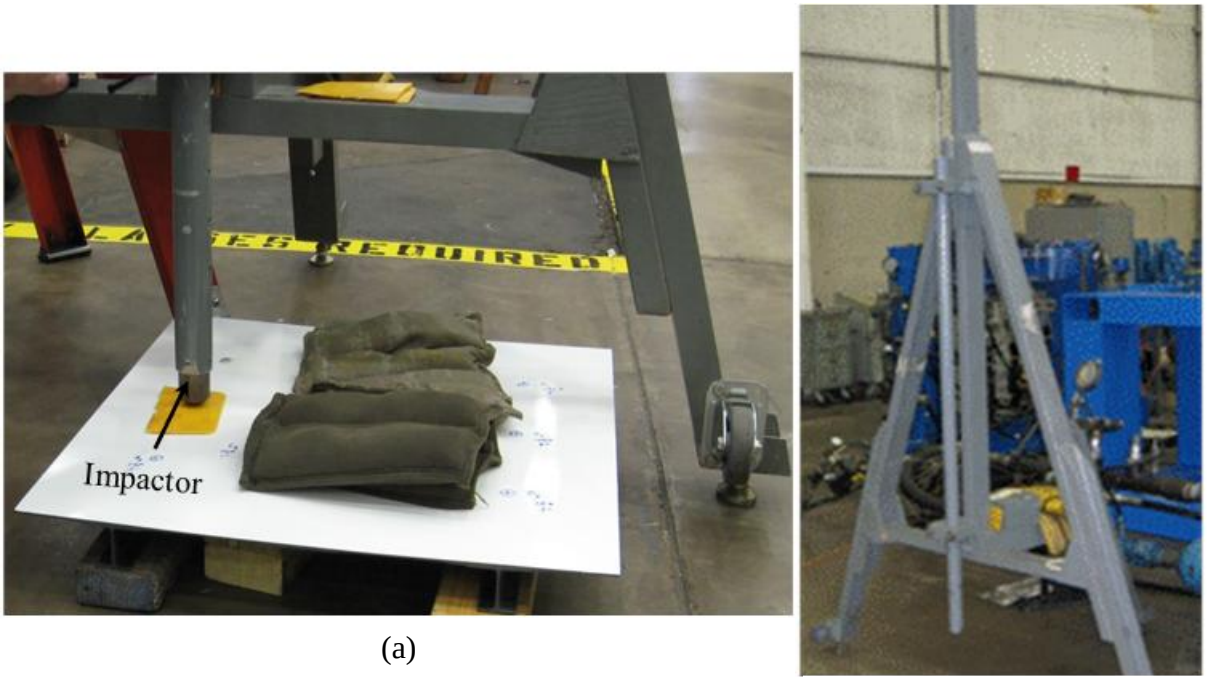

(a) (b)

Figure 21. The (a) Impact Panel in the Impact Test Rig and (b) Impact Test Rig

Once the I-beam and hat panels were impacted, each were baseline inspected using PE ultrasonics with full-waveform capture. Figures 22 and 23 show the baseline scans after impact damage tests. The ToF data clearly detects and accurately sizes all of the impact damage. In the ToF scans, darker colors/shades correspond to shallow delamination depths from the impacts.

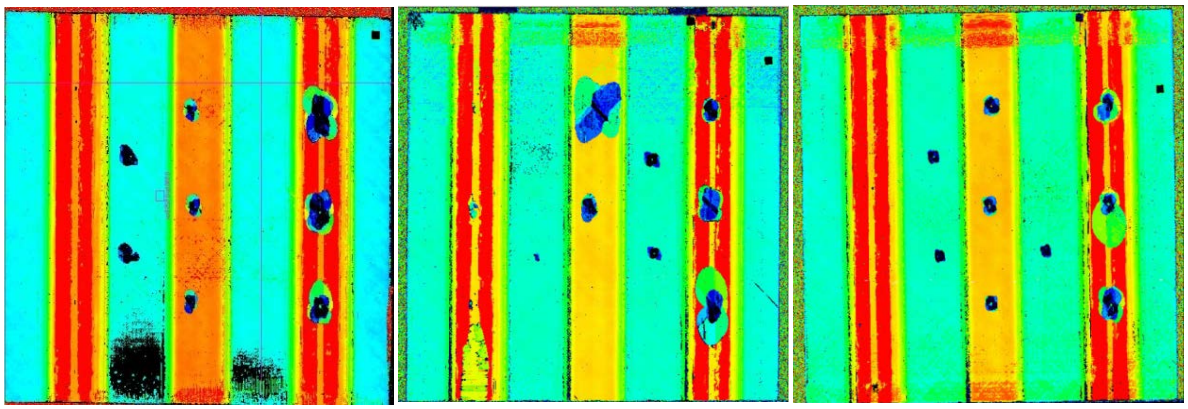

I-Beam Panel #1, (FAA-I-001) I-Beam Panel #2, (FAA-I-002) I-Beam Panel #3, (FAA-I-003)

Figure 22. The ToF C-Scans of I-Beam Panel #1, I-Beam Panel #2, and I-Beam Panel #3

As shown in the far right image of figure 23, the porosity found during baseline TTU scans of hat panel #3 are revealed during the post-impact PE C-scans as localized multicolored areas. The colors in the ToF C-scan of hat panel #3 show the porosity is at various depths.

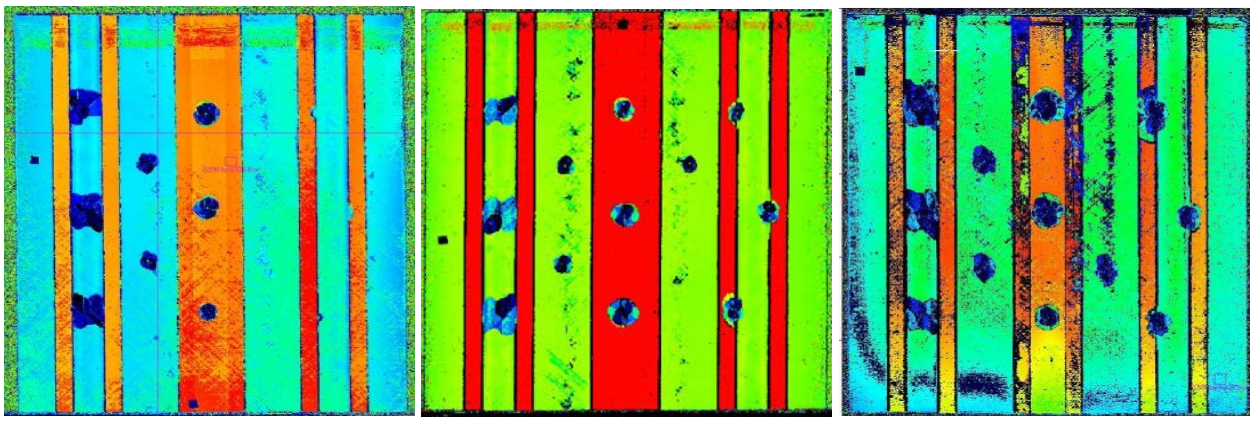

Hat Panel #1, (FAA-H-001) Hat Panel #2, (FAA-H-002) Hat Panel #3, (FAA-H-003)

Figure 23. The ToF C-Scans of Hat Panel #1, Hat Panel #2, and Hat Panel #3

3.2.1 The FDIR Impact Panel Evaluation.

Initial FDIR tests revealed substructure changes. However, FDIR evaluations of high-gloss white impacted panels did not detect multilayer delamination from impact damage. Further technique development was necessary to detect the impact damage with FDIR and is covered later in this report.

3.2.1.1 Baseline IR Evaluations.

A panel was selected to send to TWI for flash IR testing and evaluation. The TWI technology was used to evaluate a gloss white impacted panel.

The results of the flash IR using post-processing were compared to the baseline ToF C-scan. The flash IR image does not accurately show the impact damage sizes. Figure 24 shows that I-beam panel #1 has nine flash IR images that were manually stitched together. All eight of the impact damage areas are visible in the stitched IR image.

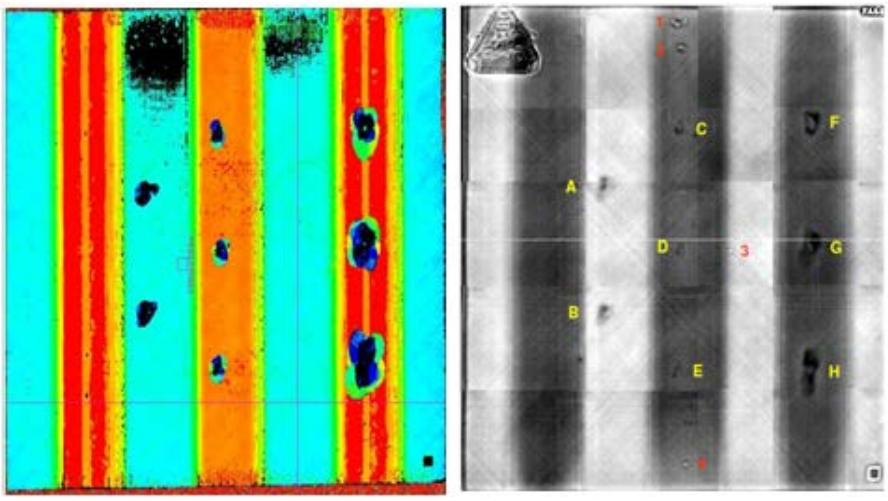

(a) (b)

Figure 24. The I-Beam Panel #1 (a) TWI Flash IR Image Compared to the (b) FDIR Image

The flash thermography data show that all of the impact defects were detected, but the extent of the subsurface damage was not accurately sized. This baseline technology did not accurately characterize the size of the impact damage because of its depth in the composite laminate. This means that additional technology will be required to characterize the full extent of the defect. I-beam panel #1 was not coated with a high-emissive paint; the short wavelength flash IR camera and TWI's advanced processing capabilities allow for imaging through the low-emissive gloss white.

3.2.1.2 The FDIR Technique Development.

All of the impact test panels were finished in a common gloss white aircraft paint scheme, which is a coating with very low emissivity. One of the difficulties was dealing with panel surface emissivity (low-emissive gloss white). The IR imaging is very sensitive to the surface emissivity of the inspected component (i.e., how well the component radiates IR energy to the viewer). A poorly emissive surface does not transmit the IR signal to the camera, effectively making a low signal-to-noise ratio regardless of the thermal changes occurring. Initial FDIR images could detect substructure changes, but could not detect the subtle thermal differences associated with impact damage.

To determine the effect of emissivity on impact damage tests, a section of one of the impact panels was painted in ultra-flat black, a very high-emissive coating. Figure 25 shows the results of this demonstration. The I-beam panel #3 was exposed to sunlight while being viewed with FDIR equipment. In the areas of low emissivity (gloss white), the temperature indicated had increased 8°F; in the ultra-flat black area, the recorded temperature change was 26°F. The difference is shown qualitatively in figure 25(a). Two of the impacts in the flat black appear, but very faintly, in figure 25(b). Figure 25(c) shows the accurate size of the impact damage. Figure 25(b) does not show the temperature change.

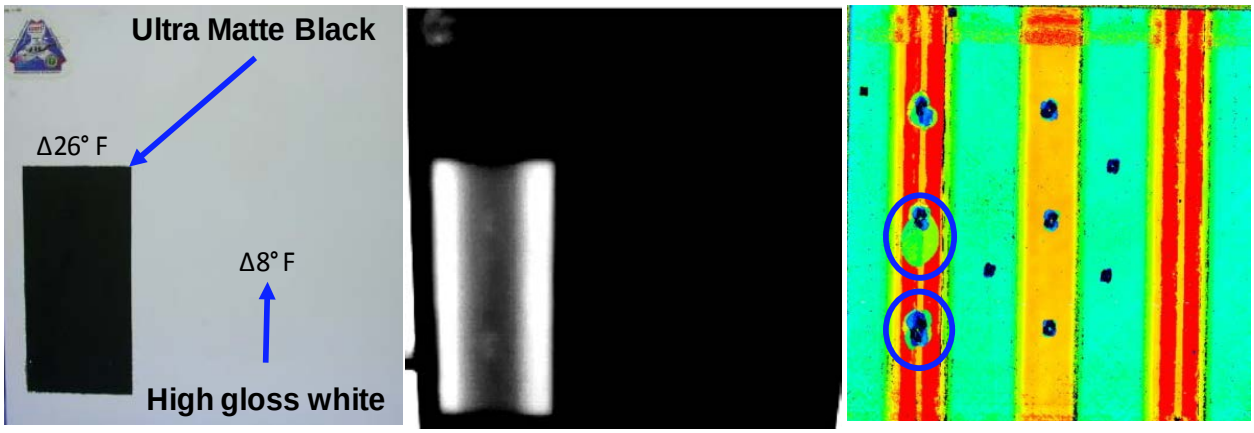

(a) (b) (c)

Figure 25. The (a) I-Beam Panel #3 Photograph, (b) FDIR Image , and (c) ToF C-Scan

Figure 26(a) shows an FDIR image of I-beam panel #2 with gloss white coating. Figure 26(b) shows I-beam panel #2 with flat black coating. The flat black coated I-beam panel #2 revealed four impact-damaged areas.

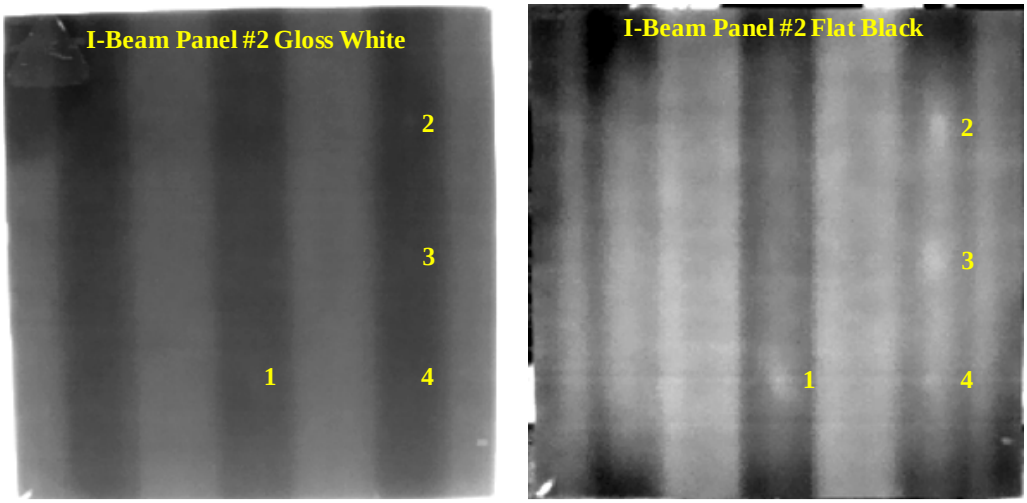

(a) (b)

Figure 26. The FDIR Comparison Between (a) Gloss White and (b) High-Emissive Flat Black Coating

3.2.1.3 The FDIR Evaluation of All Coated Impact Panels.

In figure 27, all of the impacted panels are painted flat black and the shallow impact damage, which is lighter in color, is easily seen. The substructure is also visible as darker shades of gray, representing cooler surface temperatures.

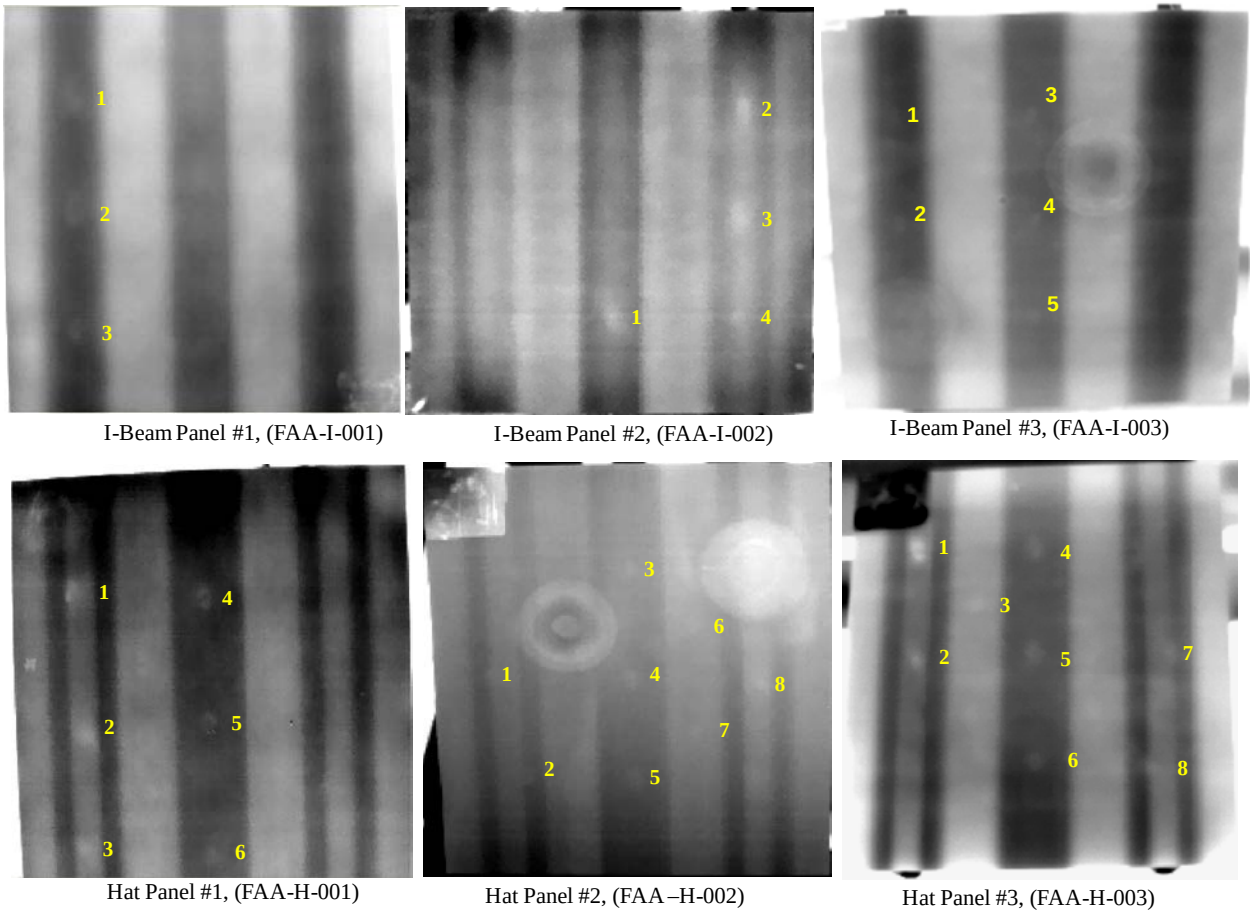

Figure 27. The FDIR Results for all FAA-Bell Impact Panels

3.2.1.4 The FDIR Image Capture Development.

As part of the development, Bell evaluated the effect of image capture rate during heating to evaluate how it relates to the detection of impact damage. Acquiring images as quickly as possible once the heat was exposed to the inspection surface yielded the best impact-damage detection. Figure 28 is a temperature-versus-time graph of the effect of sun exposure on panel warming. The temperature difference between impact-damaged and undamaged laminate decreases over time. A measurable thermal difference between the defect and surrounding area is required to detect defects. Each blue square represents a plot of panel temperature over time. Each red dot on the chart represents the previous image temperature minus the current surface temperature divided by the elapsed seconds (see the scale on the right).

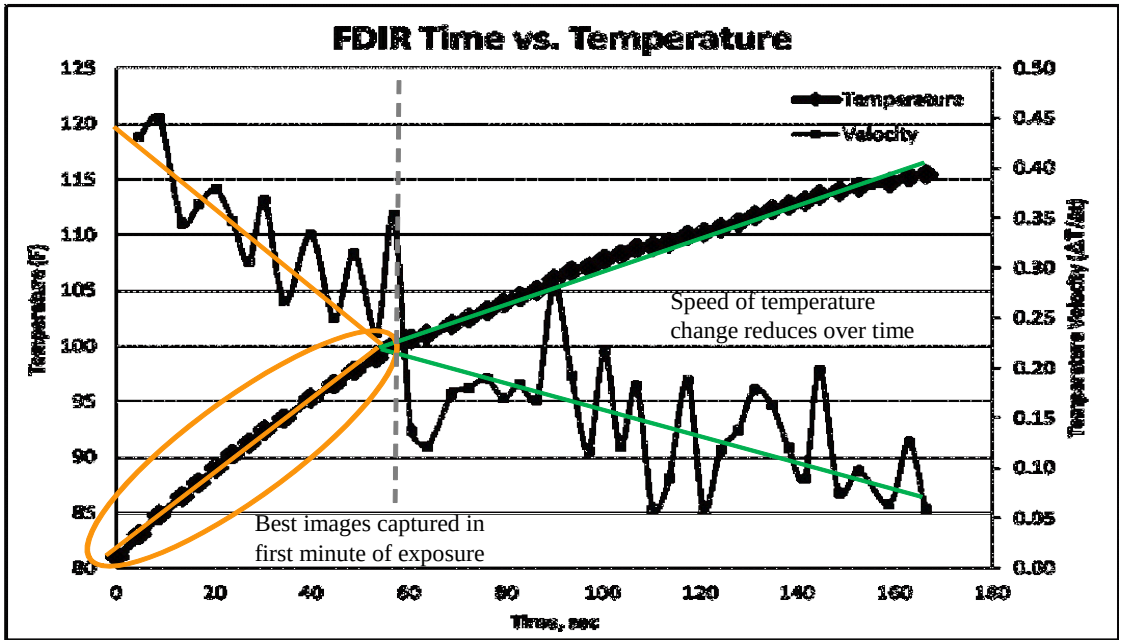

Figure 28. The FDIR Temperature vs. Time

3.2.1.5 The FDIR Post-Processing Development.

After the capture method was developed and optimized, effort was focused on post-processing options. One post-processing option explored was TWI's TSR software.

The TSR software is not commonly used with an inexpensive, long-wave, uncooled IR camera, so the first step was to identify a camera output format that would be compatible with the TSR software. A test was performed converting the FDIR camera images to a few formats (e.g., .fpf, .csv, etc.); the TWI verified the .csv format was compatible with their software. Subsequent tests revealed that TWI would also need image capture times as well as the temperature ranges for thick and thin areas of the panel. All of the impact panels were scanned, converted to .csv format, and sent to TWI for processing along with the image capture time range, the number of images captured, and the temperature range for thick and thin areas on the panel. Figures 29 through 34 show the test parameters, TWI's TSR images, and time and temperature charts for each of the six panels.

FDIR of FAA Impact Panel #: FAA-I-001

Date: 4/18/12, Time: 1:35:13 to 1:37:50 PM

Outside temp = 71°F Beginning panel temp = ~88°F

Camera set up on Manual

Fixed temperature range on camera: 35°F,
(Low end at 80°F and high end at 115°F.

#Images captured = 36 (~1 image every 4.36 seconds)

Imaging duration = 2 min 37 sec (157 seconds)
Rise in temperature at mid-elevation of panel:
Thick range at I-beam 87.7°F to 108.8°F (= Δ21.1°F)
Thick range at center 89.0°F to 113.9°F (= Δ24.9°F)
Thin range 91.3°F to 120.1°F (= Δ28.8°F)

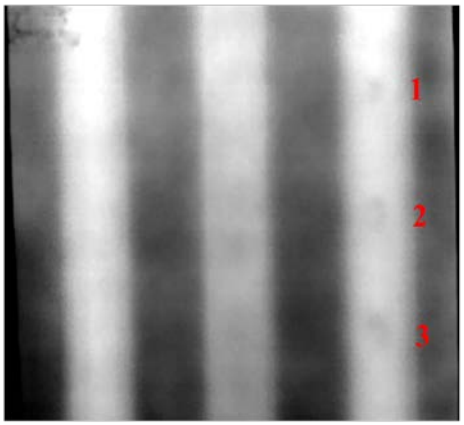

TSR Image

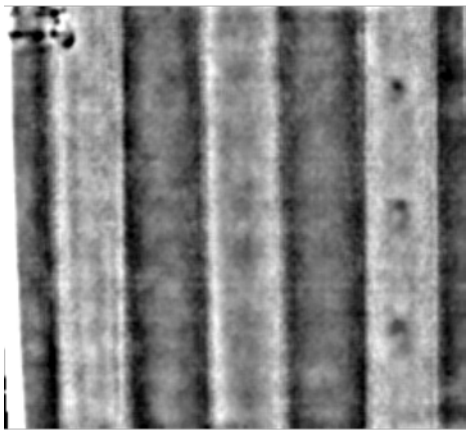
TSR Contrast Image

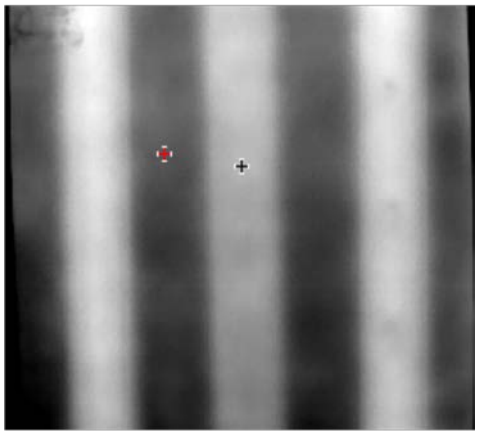
Thin (T1) and Thick (T2) Laminate Temperature Locations

I-Beam Panel #1, (FAA-I-001)

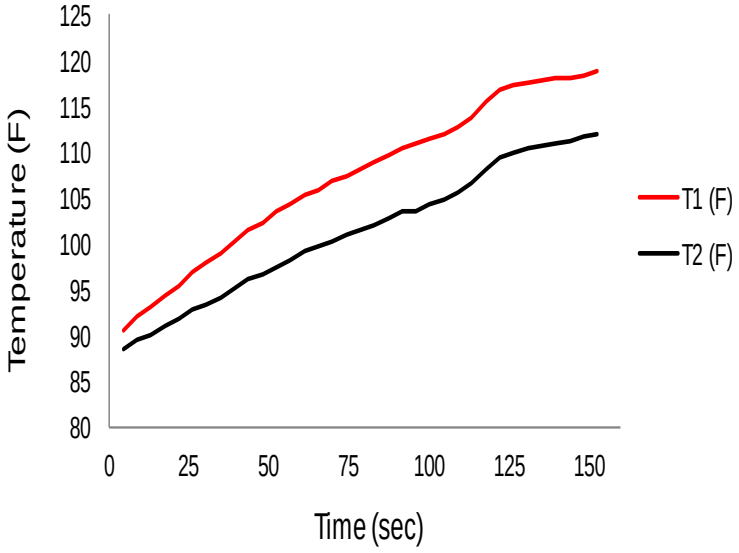

Figure 29. The TWI TSR Images of I-Beam Panel #1

FDIR of FAA Impact Panel #: FAA-I-002

Date: 3/23/12, Time: 1:46:04 to 1:47:43 PM

Outside temp = 79°F Beginning panel temp = ~89°F

Camera set up on Manual

Fixed temperature range on camera: 35°F,
(Low end at 75°F and high end at 110°F.

#Images captured = 20 (~1 image every 4.9 seconds)

Imaging duration = 1 min 39 sec
Rise in temperature at mid-elevation of panel:
Thick range at I-beam 89.4°F to 106.0°F (= ? 16.6°F)
Thick range at center 89.7°F to 111.8°F (= ? 22.1°F)
Thin range 90.4°F to 118.3°F (= ? 27.9°F)

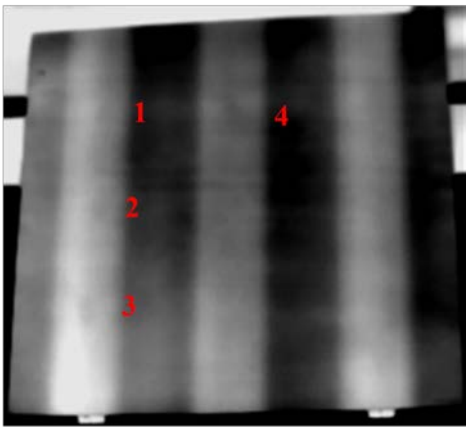

TSR Image

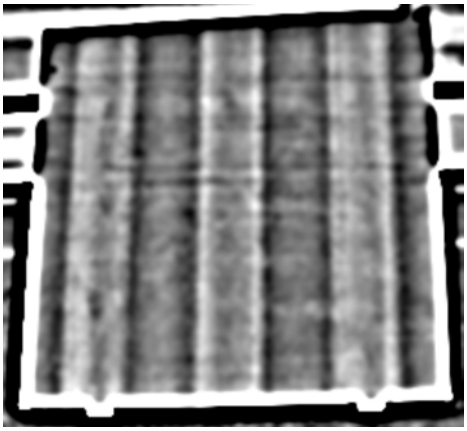
TSR Contrast Image

I-Beam Panel #2, (FAA-I-002)

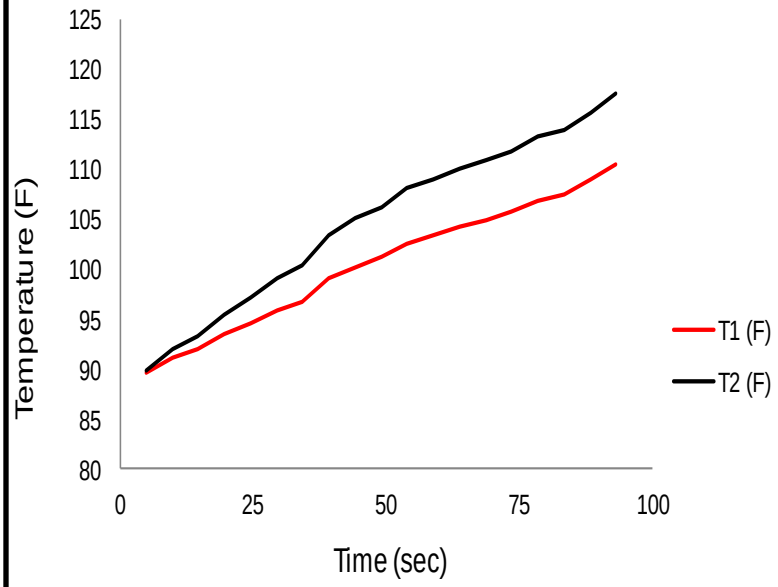

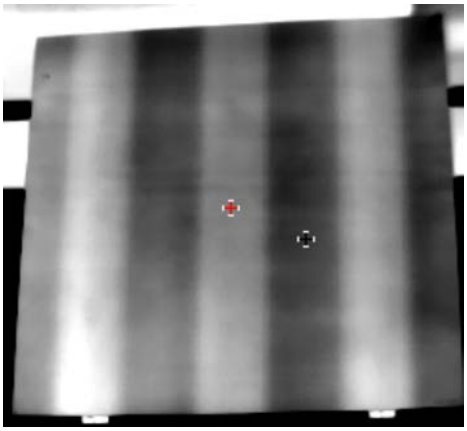
Thick (T1) and Thin (T2) Laminate Temperature Locations

Figure 30. The TWI TSR Images of I-Beam Panel #2

FDIR of FAA Impact Panel #: FAA-I-003

Date: 3/26/12, Time: 12:55:42 to 12:57:55 PM

Outside temp = 77°F Beginning panel temp = ~86°F

Camera set up on Manual

Fixed temperature range on camera: 35°F,
(Low end at 75°F and high end at 110°F.

#Images captured = 32 (~1 image every 4.2 seconds)

Imaging duration = 1 min 33 sec (93 seconds)
Rise in temperature at mid-elevation of panel:
Thick range at I-beam 85.6°F to 109.0°F (= Δ 23.4°F)
Thick range at center 86.5°F to 115.1°F (= Δ 28.6°F)
Thin range 90.5°F to 120.6°F (= Δ 30.1°F)

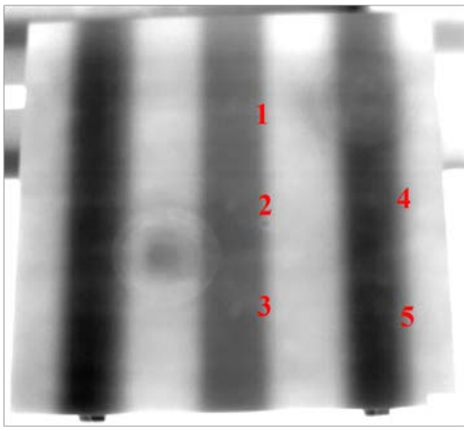

TSR Image

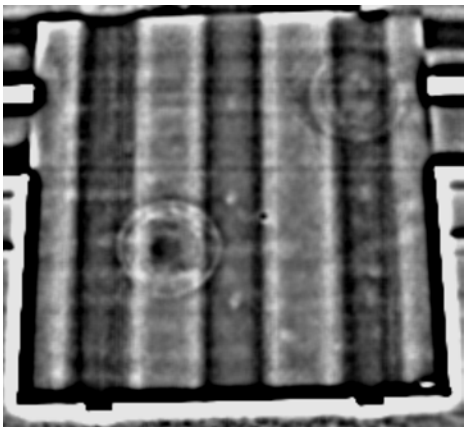

TSR Contrast Image

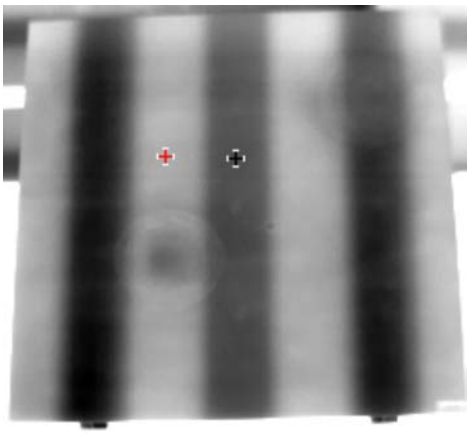

Thin (T1) and Thick (T2) Laminate Temperature Locations

I-Beam Panel #3, (FAA-I-003)

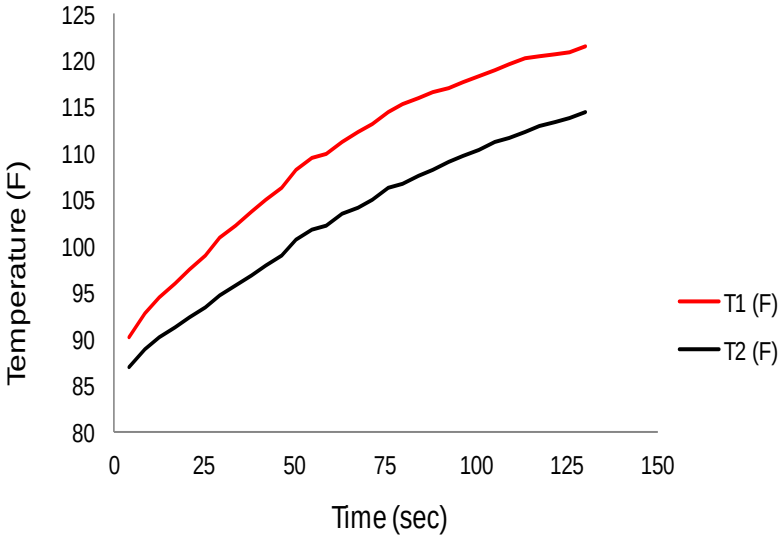

Figure 31. The TWI TSR Images of I-Beam Panel #3

FDIR of FAA Impact Panel #: FAA-H-001

Date: 4/18/12, Time: 1:29:58 to 1:32:53 PM

Outside temp = 70°F Beginning panel temp = ~80°F

Camera set up on Manual

Fixed temperature range on camera: 35°F,
(Low end at 80°F and high end at 115°F.

#Images captured = 42 (~1 image every 3.88 seconds)

Imaging duration = 2 min 43 sec (163 seconds)
Rise in temperature at mid-elevation of panel is:
Thick range at Hat flange 86.5°F to 112.5°F (= Δ 26°F)
Thick range at center 86.5°F to 111.4°F (= Δ 24.9°F)
Thin range 87.5°F to 118.8°F (= Δ 31.3°F)

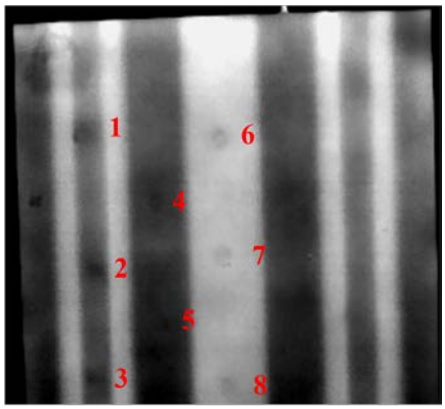

TSR Image

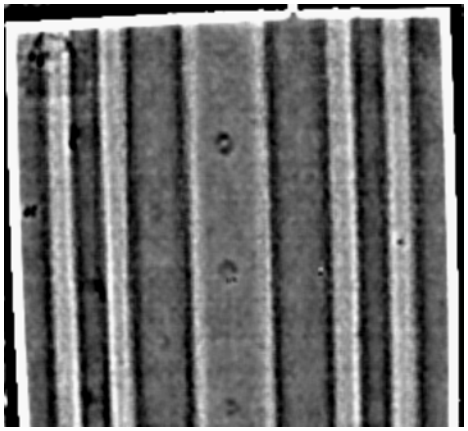

TSR Contrast Image

Hat Panel #1, (FAA-H-001)

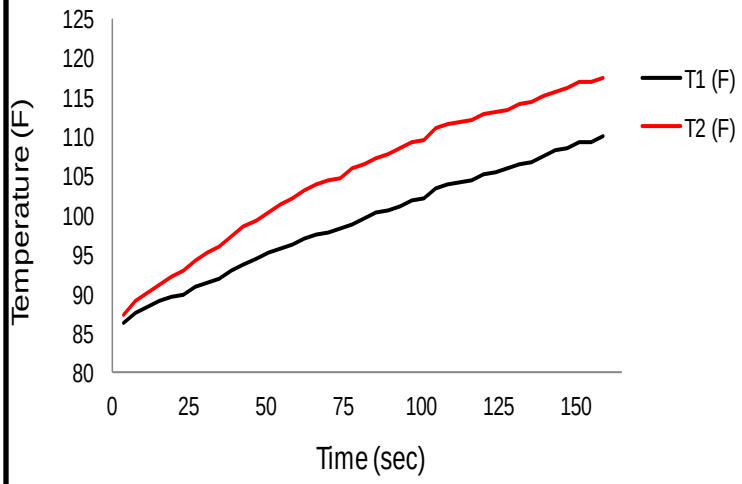

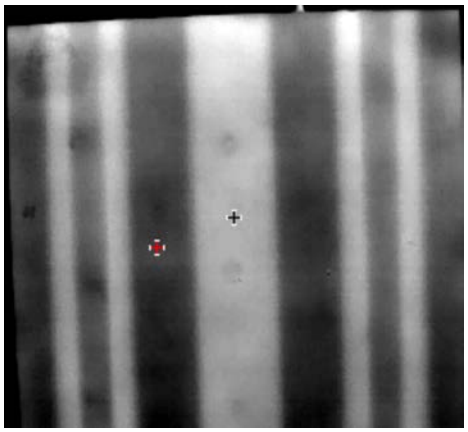

Thin (T2) and Thick (T1) Laminate Temperature Locations

Figure 32. The TWI TSR Images of Hat Panel #1

FDIR of FAA Impact Panel #: FAA-H-002

Date: 3/23/12, Time: 11:55:48 to 11:58:12 PM

Outside temp = 74°F Beginning panel temp = ~83°F

Camera set up on Manual

Fixed temperature range on camera: 35°F,
(Low end at 75°F and high end at 110°F.

#Images captured = 34 (~1 image every 4.2 seconds)

Imaging duration = 2 min 24 sec (144 seconds)
Rise in temperature at mid-elevation of panel is:
Thick range at Hat flange 82.4°F to 110.3°F (= Δ 27.9°F)
Thick range at center 82.7°F to 109.9°F (= Δ 27.2°F)
Thin range 86.0°F to 120.8°F (= Δ 34.8°F)

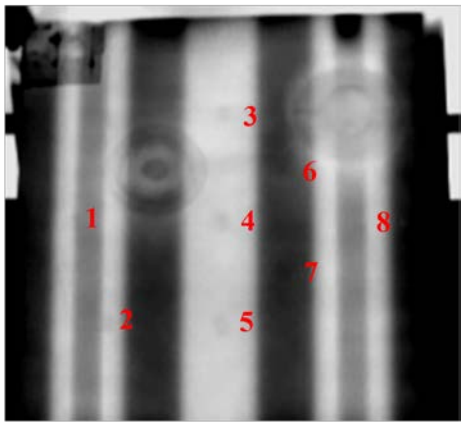

TSR Image

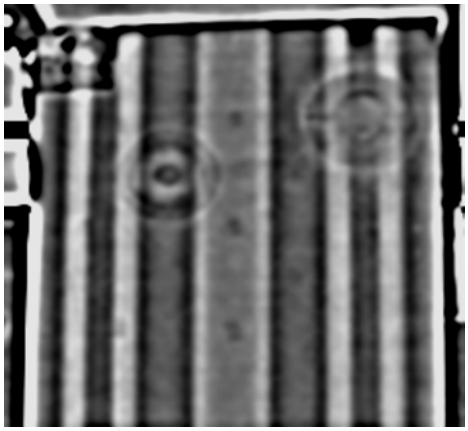

TSR Contrast Image

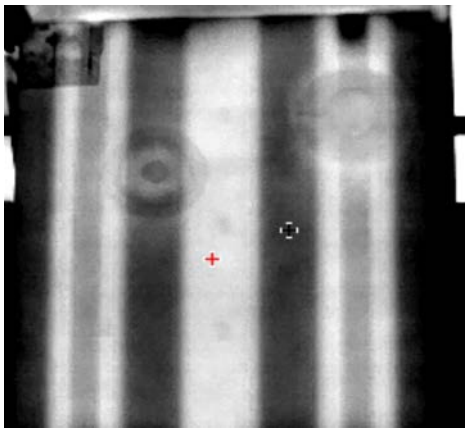

Thick (T1) and Thin (T2) Laminate Temperature Locations

Hat Panel #2, (FAA-H-002)

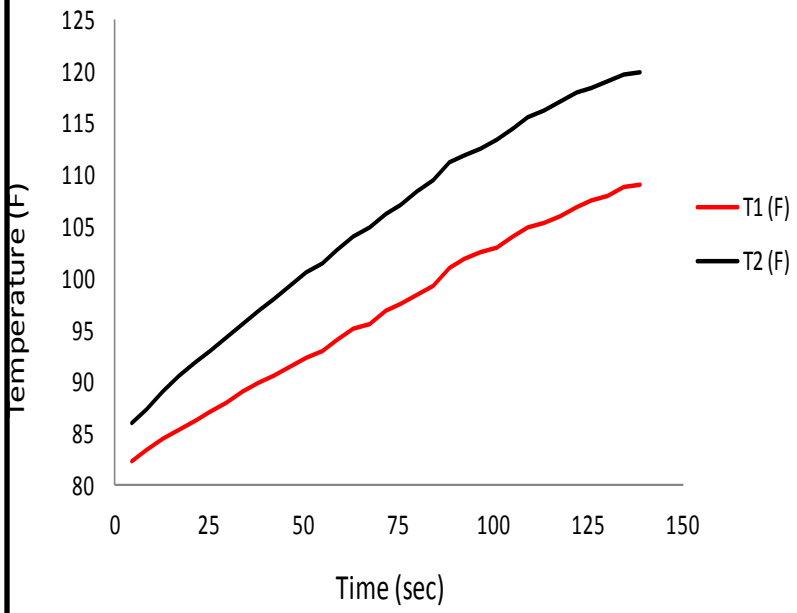

Figure 33. The TWI TSR Images of Hat Panel #2

FDIR of FAA Impact Panel #: FAA-H-003

Date: 3/23/12, Time: 1:43:21 to 1:45:03 PM

Outside temp = 79°F Beginning panel temp = ~83°F

Camera set up on Manual

Fixed temperature range on camera: 35°F,
(Low end at 75°F and high end at 110°F.

#Images captured = 22 (~1 image every 4.6 seconds)

Imaging duration = 1 min 42 sec (102 seconds)
Rise in temperature at mid-elevation of panel is:
Thick range at Hat flange 83.0°F to 107.0°F (= Δ 24.0°F)
Thick range at center 83.5°F to 106.9°F (= Δ 23.4°F)
Thin range 84.0°F to 115.1°F (= Δ 31.1°F)

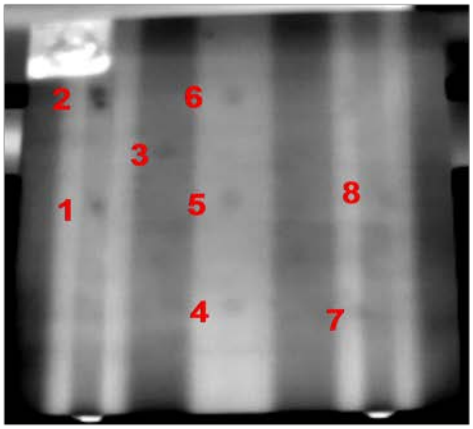

TSR Image

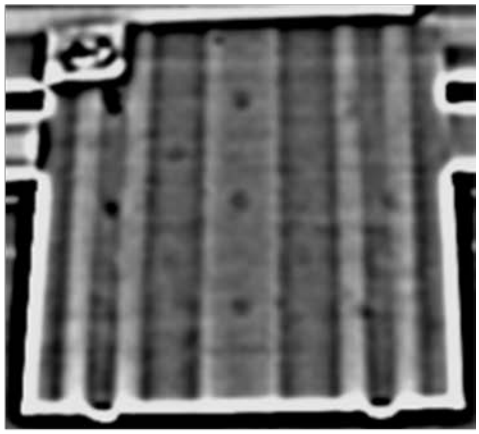

TSR Contrast Image

Hat Panel #3, (FAA-H-003)

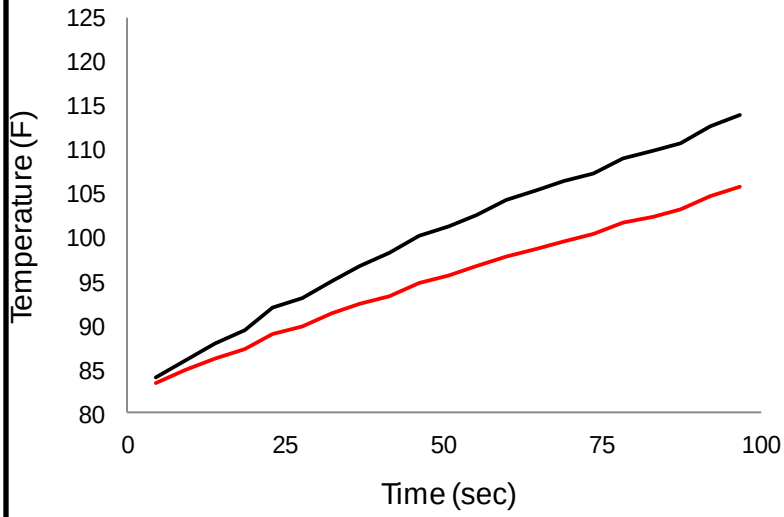

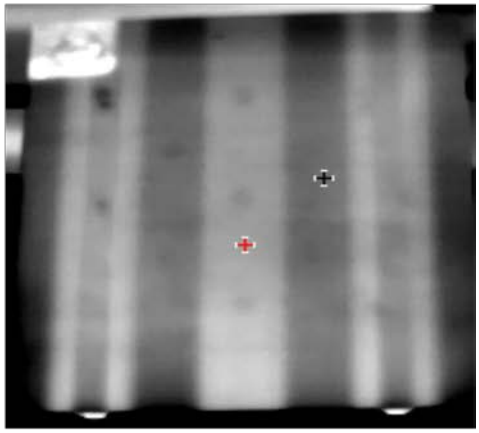

Thick (T2) and Thin (T1)
Laminate temperature locations

Figure 34. The TWI TSR Images of Hat Panel #3

Figure 35 shows the TSR contrast images of all six panels with numbered damage indications. The TSR contrast images are the result of an additional processing step in which the thermal data is processed through an algorithm that accentuates thermal differences from adjacent pixels in the image. The TSR contrast image algorithm often highlights the edge of thickness changes in the laminate.

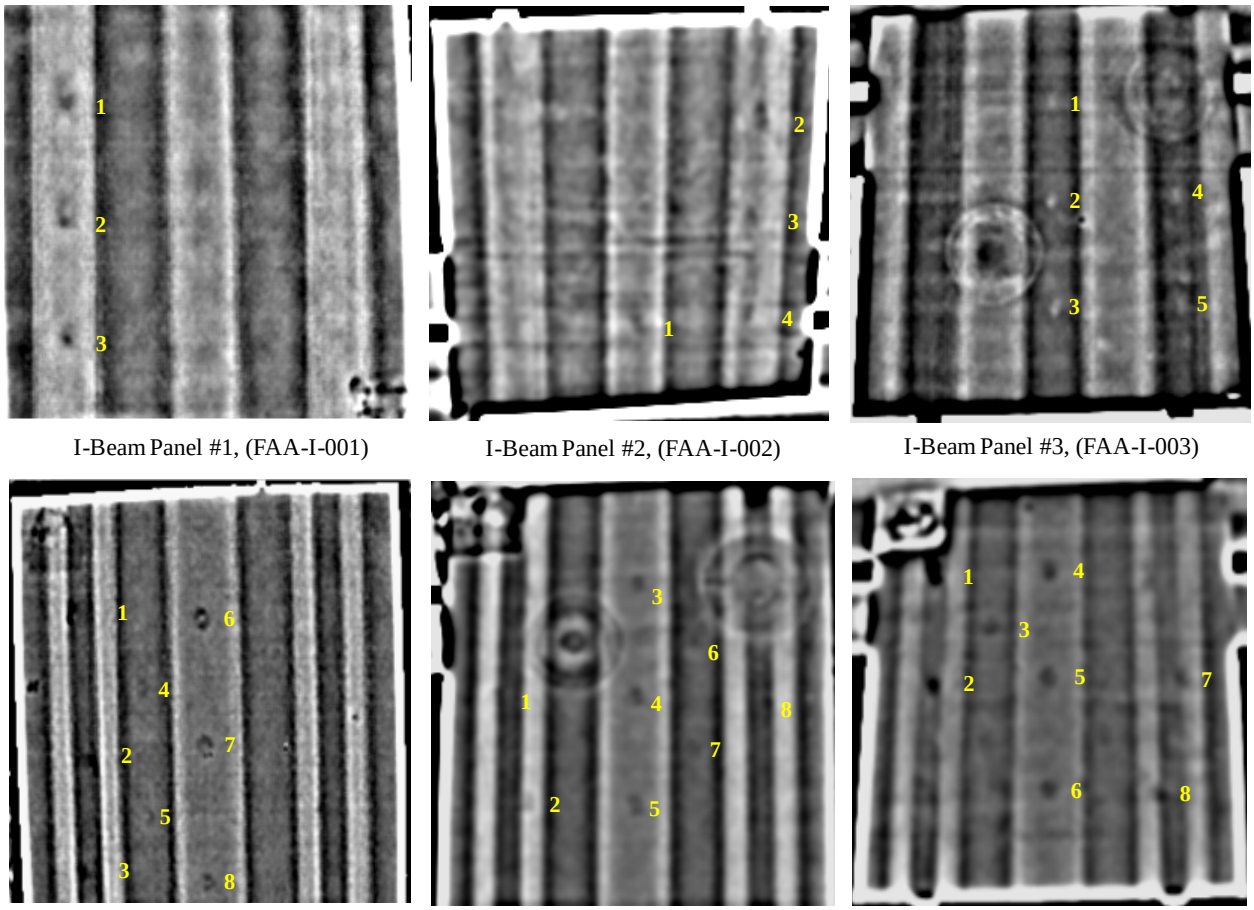

I-Beam Panel #1, (FAA-I-001) I-Beam Panel #2, (FAA-I-002) I-Beam Panel #3, (FAA-I-003)

Hat Panel #1, (FAA-H-001) Hat Panel #2, (FAA –H-002) Hat Panel #3, (FAA-H-003)

Figure 35. All Post-Processed FDIR Impact Damage Images

Post-processing improved the ability to detect damage by increasing the contrast of impact-damage indications in the FDIR image. When the research started, no impact damage was detected with FDIR on the gloss white panels. However, coating the panels with a flat black film, optimizing the capture process, and utilizing a post-process method to enhance the image has resulted in a repeatable method of detecting gross impact damage in composite structures.

After optimizing the image capturing and image processing techniques, efforts were focused on how to locate suspect damage areas on component surfaces. With the innovative imaging theme of the project in mind, effort was made to evaluate the use of real-time imaging technology that would allow an inspector to see a transparent video overlay of the FDIR camera image. Lumus PD-20 video glasses (see figure 36) were acquired to interface with the FDIR camera and provide the real-time video display.

Optical Engine Specifications*

Parameter	PD-20
Resolution	640 (H) x 480 (V)
FOV (Diagonal)	27.5º
Distortion	<2%
Brightness	1400 fL
Contrast	1:100
LOE Thickness	1.7 mm
Eye Motion Box @ 18 mm Eye Relief	10 mm x 10 mm
Color	Full color
Angle between LOEs	6.4º
LOE Transparency	>78%
Image focal plane	Infinity

Figure 36. Lumus PD-20 Video Glasses

The video glasses displayed the FDIR images well. The two lenses provided a visual stereo image that yielded better visual results when both lenses were functioning. The video display image is not the full size of the lens. Figure 37 shows an image of a Bell engineer taken through the Lumus PD-20.

Figure 37. Lumus PD-20 FDIR Image as Viewed Through the Glasses

The cable connecting the Lumus PD-20 glasses to the FDIR camera is 3-feet long. Wireless video glasses or a much longer cable would be necessary to use the glasses to map damages during field evaluation of large structures.

3.2.2 The DAV Impact Panel Evaluation.

The real-time video processing of the DAV C-scan allows for quick and intuitive scanning of large areas. Impact damage is easily detected in the C-scan because it appears as an irregular

shape with a sharp contrast in color from the undamaged laminate. Figure 38 shows the initial results for the DAV technology on impact damage.

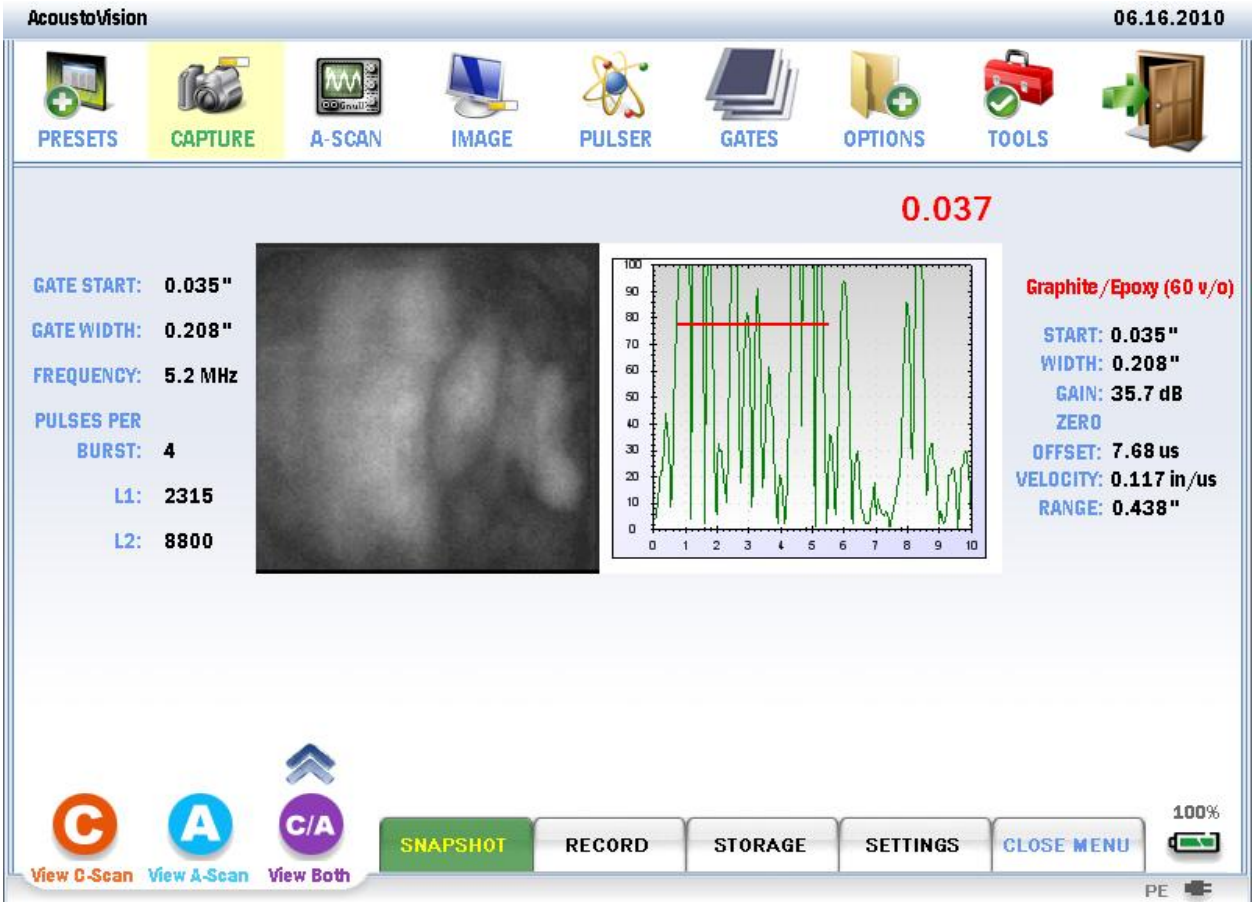

Figure 38. Initial DAV Output Snapshot

3.2.2.1 The DAV Technology and Technique Development

As the development transitioned to narrowband, high-frequency imaging, a noticeable improvement was observed, starting with the 4.5 MHz narrowband image from December 2010. Figure 39 shows incremental improvements of the DAV output during this development.

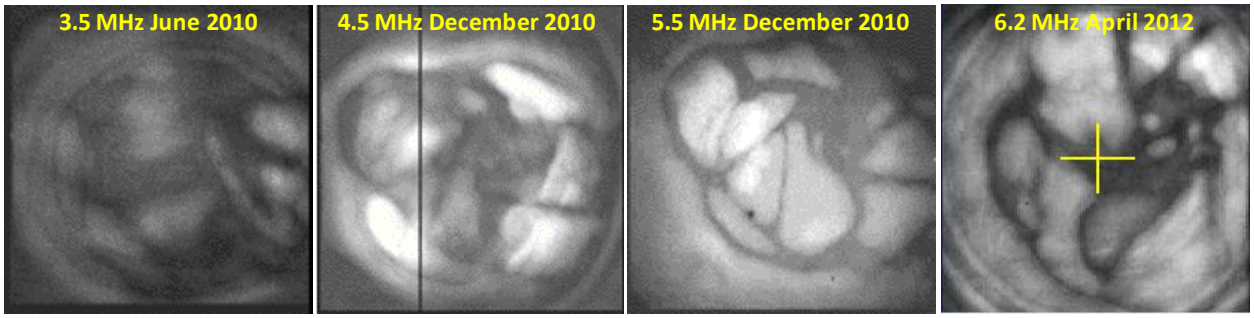

Figure 39. Development of DAV C-Scan Imaging of Impact Damage

Figure 40 shows that technology developments were also made in the software, including a cross-hair to identify where the digital depth is recorded. This image illustrates a screen capture or snapshot of the cross-hairs located at an impact-damaged area and indicates a delamination depth of 0.050″ in a 0.165″ thick laminate. The DAV image was acquired with a 7.5 MHz transducer and, with this resolution, fiber direction can be observed in these impact-damage panels. The DAV user interface allows display of the A-scan signal that can be used to characterize both the size and depth of this impact-damage defect. Impact damage is similar in appearance to a typical C-scan image when using automated PE techniques.

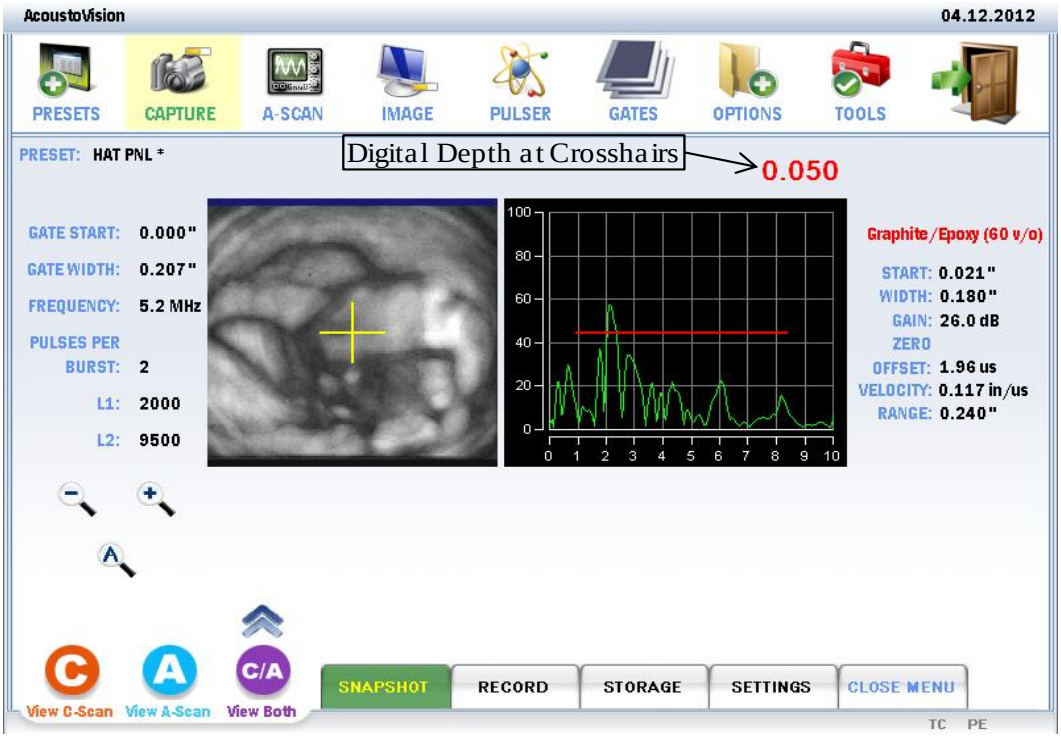

Figure 40. The DAV Snapshot of a Delamination 0.050″ Deep in a 0.165″ Laminate

3.2.2.2 The DAV Automated C-Scan Stitching.

The DAV automated C-scan stitching software was tested during this research. A panel was sent to Imperium Inc. for evaluation as a beta test article. Figure 41 shows the results from this test using hat panel #1.

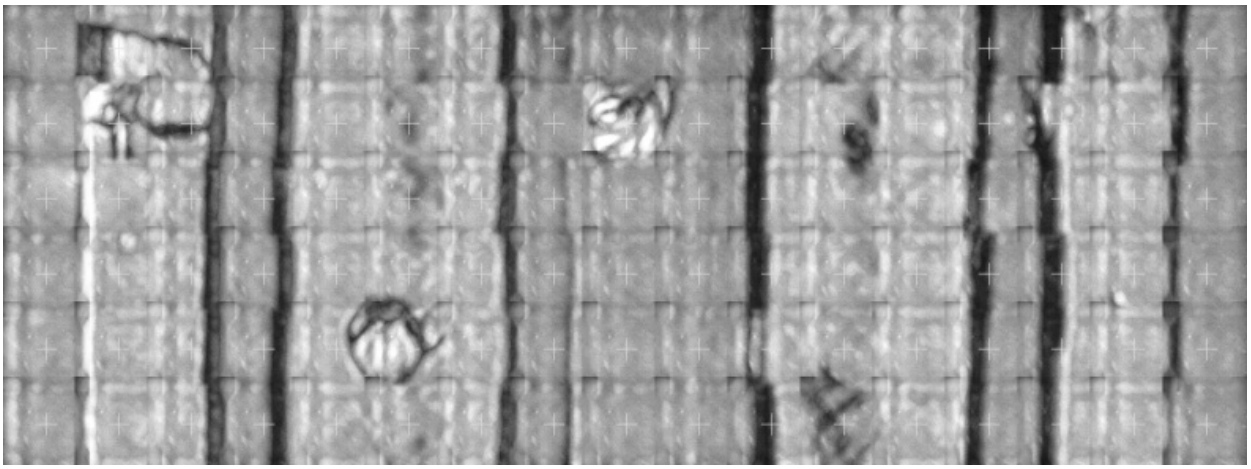

Figure 41. The DAV Stitched Image, Hat Panel #1 (FAA-H-001)

3.2.2.3 The DAV Comparison to PAUT.

Figure 42 shows that the current DAV equipment appears to exceed the performance of phased array systems. During the evaluation, it was found that the 14,400 pixels in each instant image provided a higher resolution capability than that of phased array. This increase in resolution occurs with no penalty in scan speed degradation. In phased array and conventional automated ultrasonic scanning systems, as resolution increases by reducing the size of each pixel, the capture rate is significantly slowed down (or data is lost/dropped). To get an image similar to DAV technology, a phased array system may take 2 seconds and a conventional system may take 112 seconds. The DAV system creates this data in 1/30th of a second, more than 2500 times faster than conventional scanning.

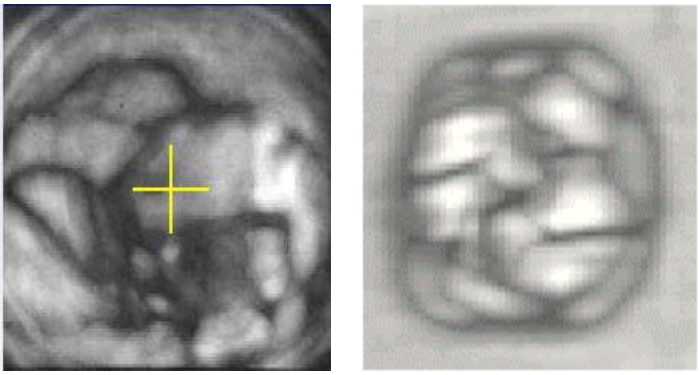

Figure 42. Phased Array Amplitude C-Scan of Impacted Area Resolution Comparison

3.2.3 The PAUT Impact Panel Evaluation.

The PAUT system is well suited for impact-damage evaluation with its 128-element, 5 MHz, phased-array probe and encoder to display a large, scaled area in a short amount of time. The C-scan display provides a plan-view image of the defect and the surrounding substructure

provides reference points for the evaluator. The S-scan provides a clear cross-sectional view of the damaged laminate.

3.2.3.1 The PAUT Technique Development.

The development of the PAUT technology focused on optimizing the scan results in thin CEP laminates while maintaining a reasonable scan speed. The shallow delaminations in the impact-damaged area were resolved with the final optimized technique. Figure 43 shows examples of some of the impacted areas of the panels.

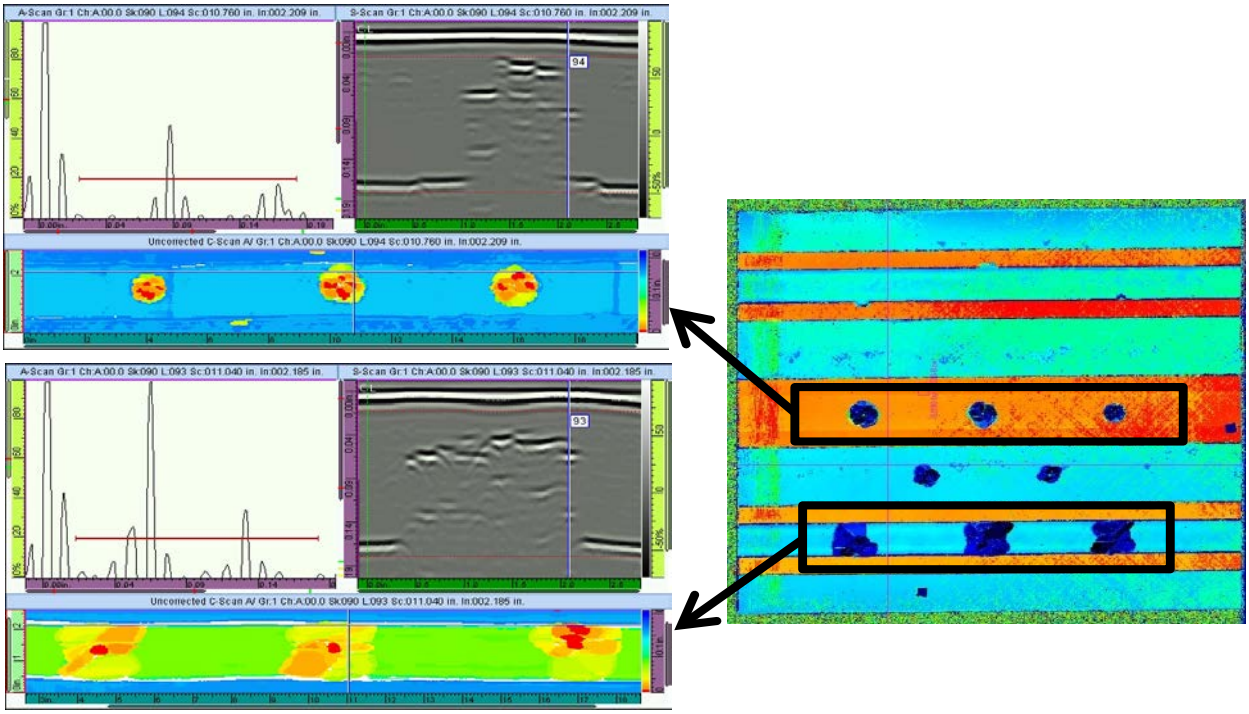

Figure 43. Hat Panel #1 PAUT Comparison to Baseline ToF C-Scan

The PAUT ToF C-scan, shown in the lower portion of the screenshot in figure 44, matches the rectangular area of the baseline ToF C-scan showing the multidepth indications. The A-scan display is presenting the signal responses for transducer element #92, which is indicated by the vertical line in the S-scan with the box containing "92."

The multilevel damage can be quickly seen in the S-scan display, appearing as a Christmas-tree-like indication in the upper-right black and white portion of figure 44. Impact damage sizes and depths can be interpreted in real time without additional evaluation. Just as the A-scan display has multiples, so does the S-scan display, and they appear as shadows below the relevant reflector. These can be misinterpreted as additional reflectors to the untrained eye.

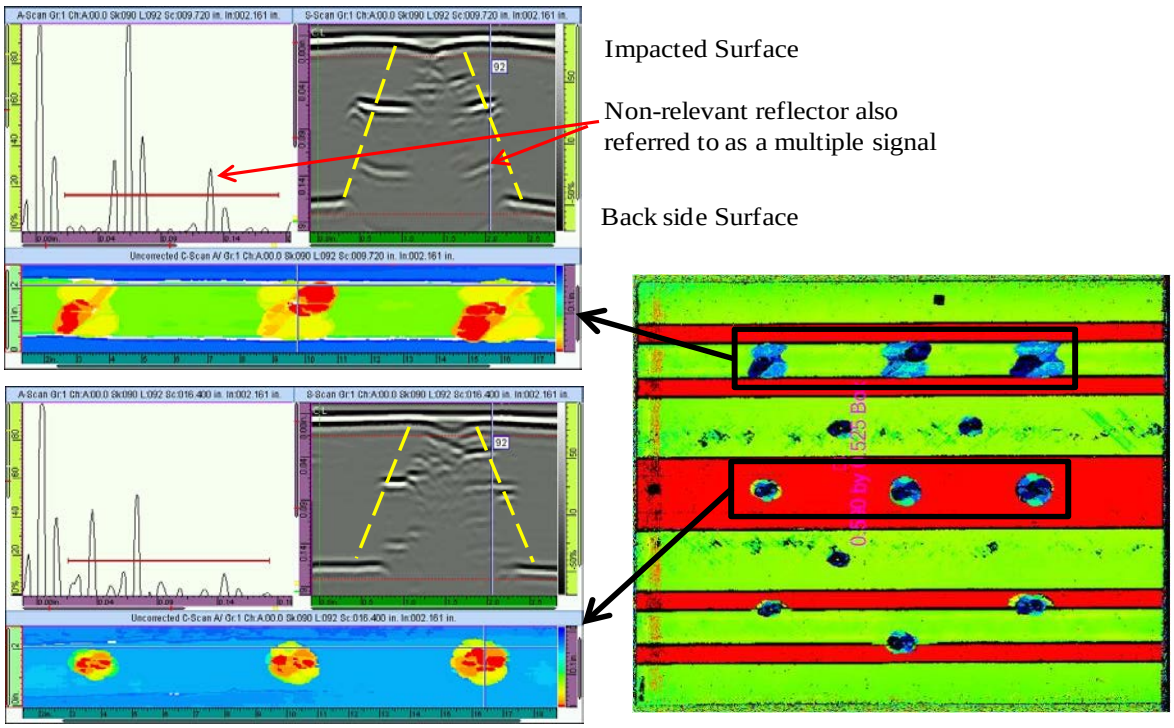

Figure 44. Hat Panel #2 PAUT Compared to Baseline PE ToF C-Scan

The PAUT evaluation of Hat panel #3 is shown in figure 45. The C-scan and S-scan of the upper PAUT image shows the porosity found in the baseline ToF C-scan.

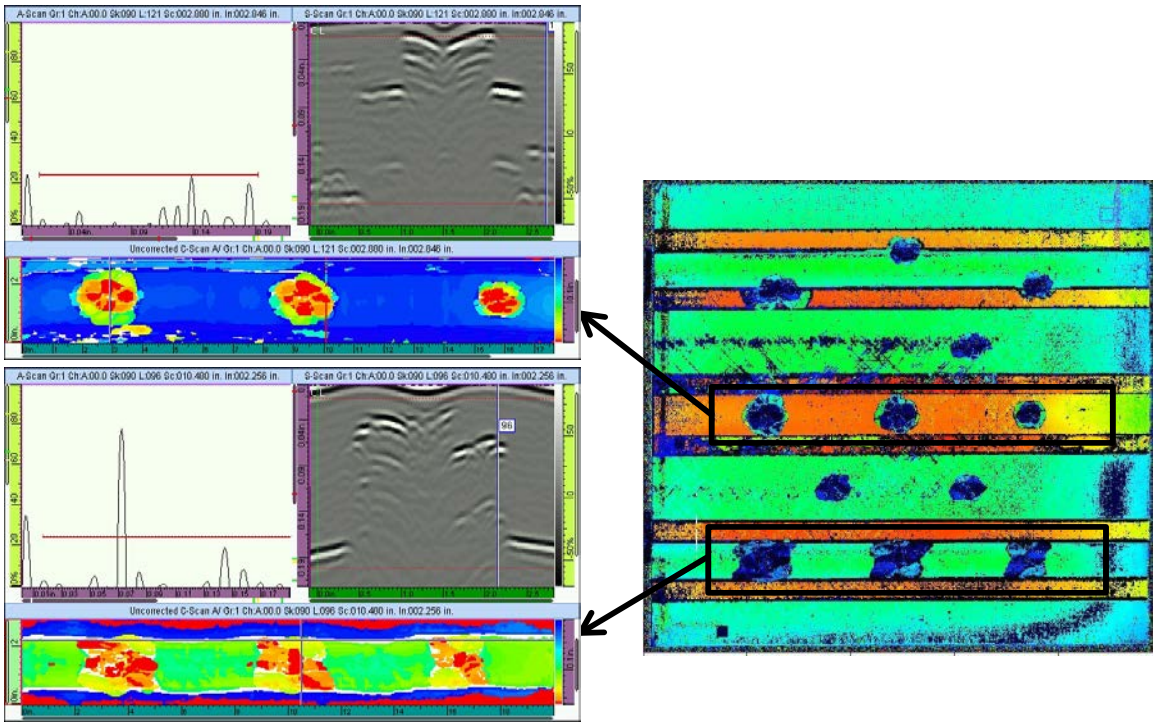

Figure 45. Hat Panel #3 PAUT Compared to Baseline PE ToF C-Scan

Figure 46 shows the PAUT C-scan of the thin area and thicker center laminate. The shading of the laminate is lighter because of the selected color palette.

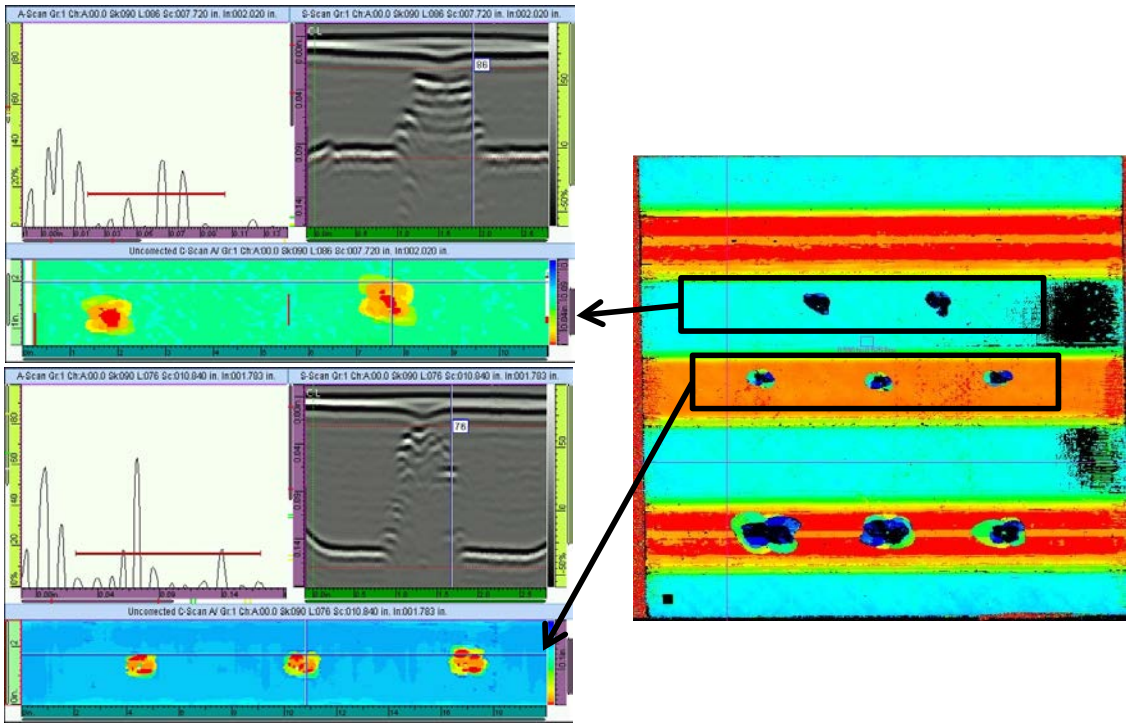

Figure 46. The I-Beam Panel #1 PAUT Compared to Baseline PE ToF C-Scan

Figure 47 shows the multiple colors in the I-beam panel #2 PAUT C-scan are arranged similarly to the baseline C-scan.

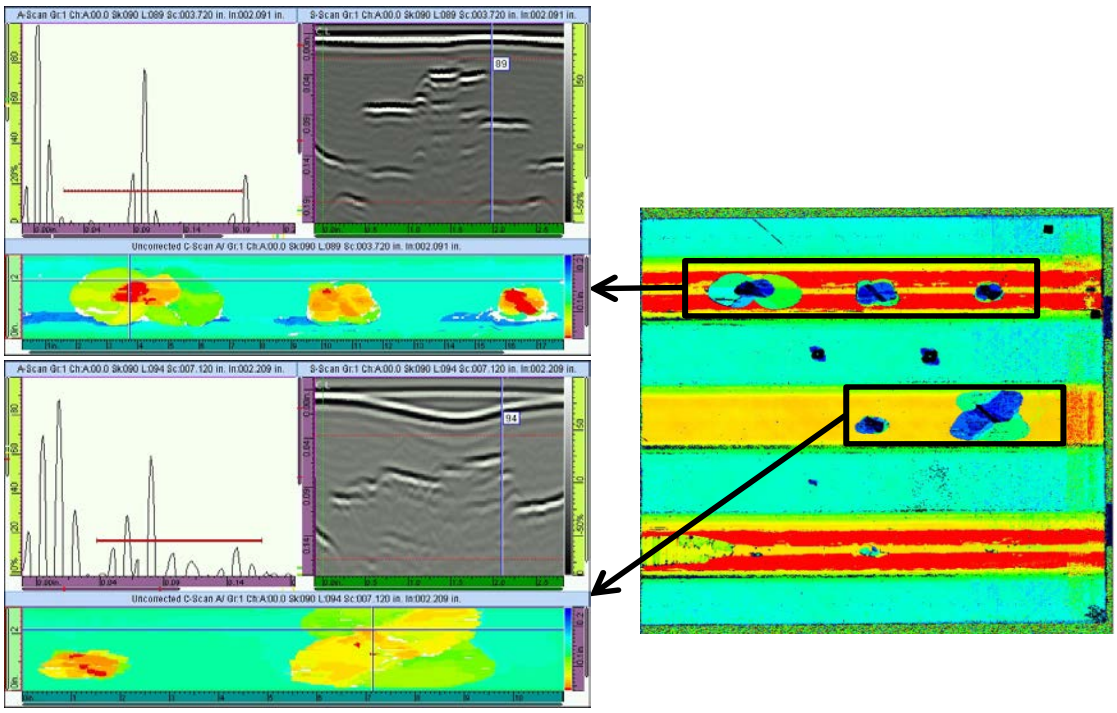

Figure 47. The I-Beam Panel #2 PAUT Compared to PE ToF C-Scan

Figure 48 shows I-beam panel #3 comparing PAUT scans to the PE scans noted in the rectangle. The area under the I-beam and the thin area of the laminate are compared in this view. The S-scan over the I-beam shows the cross-section of the laminate build-up and the impact damage. The size and shape of the damage in the PAUT images accurately correlate to the baseline images.

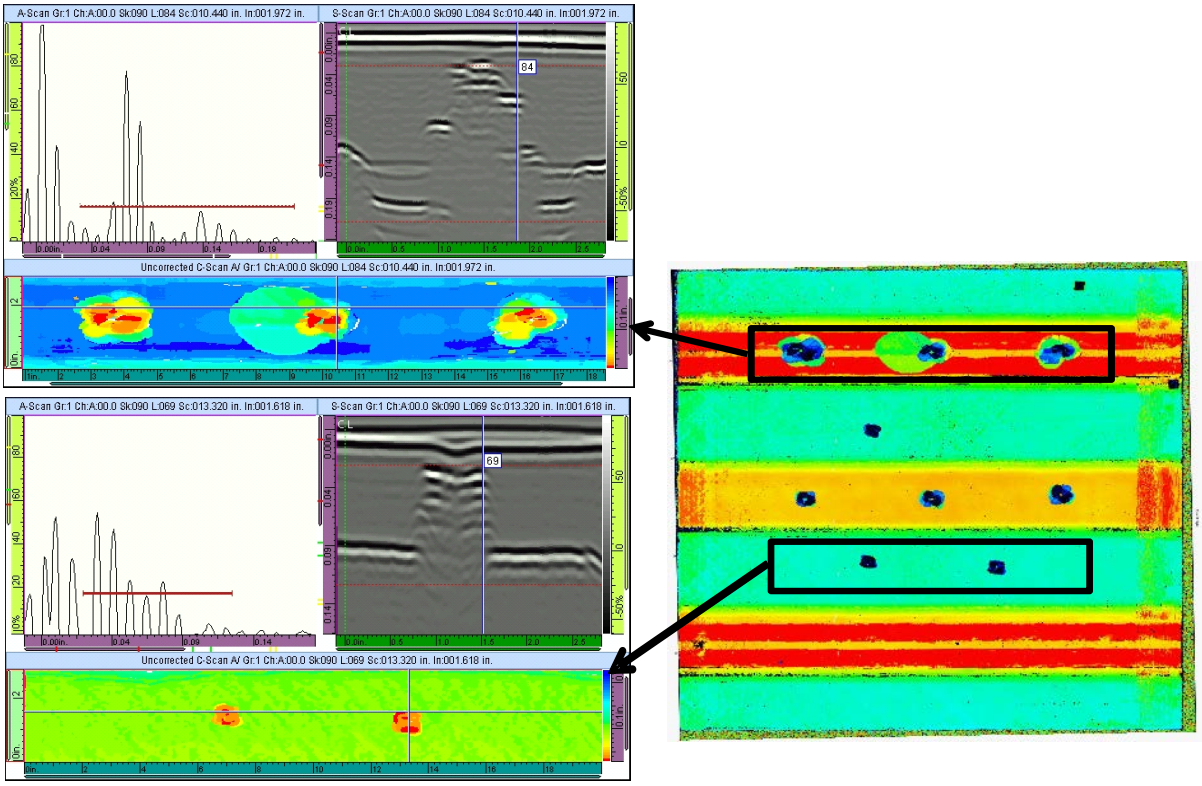

Figure 48. The I-Beam Panel #3 PAUT Compared to Baseline ToF C-Scan

3.2.4 Repaired Impact Panel Evaluation.

One hat-stiffened panel and one I-Beam-stiffened panel were selected for impact-damage repairs. This was done to simulate typical field repairs performed on composite aircraft. Taper and plug repairs are two common composite repair methods:

- A plug repair may be done when there is structure behind the skin to support the plug.
- A taper repair may be done on laminate when damage does not pierce the skin.
- Both repair methods are blended or smoothed well enough to yield a smooth, flush surface that is not detectible by visual inspection. The repaired surface profile will be very close to the surface profile before it was damaged.

Figure 49 illustrates the selected impact panels and the impact damage areas chosen for repair.

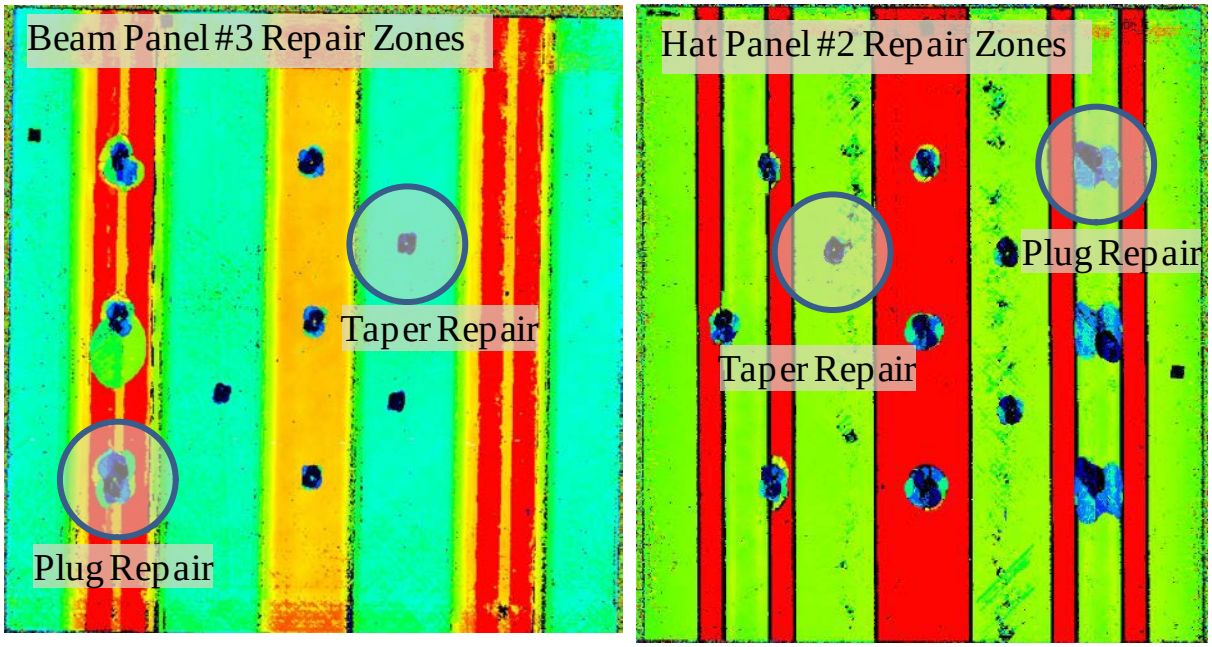

Figure 49. Baseline C-Scans With Circles Noting the Designated Plug and Taper Repair Areas

Figure 50 shows hat panel #2 plug and taper repair areas with the damaged material removed.

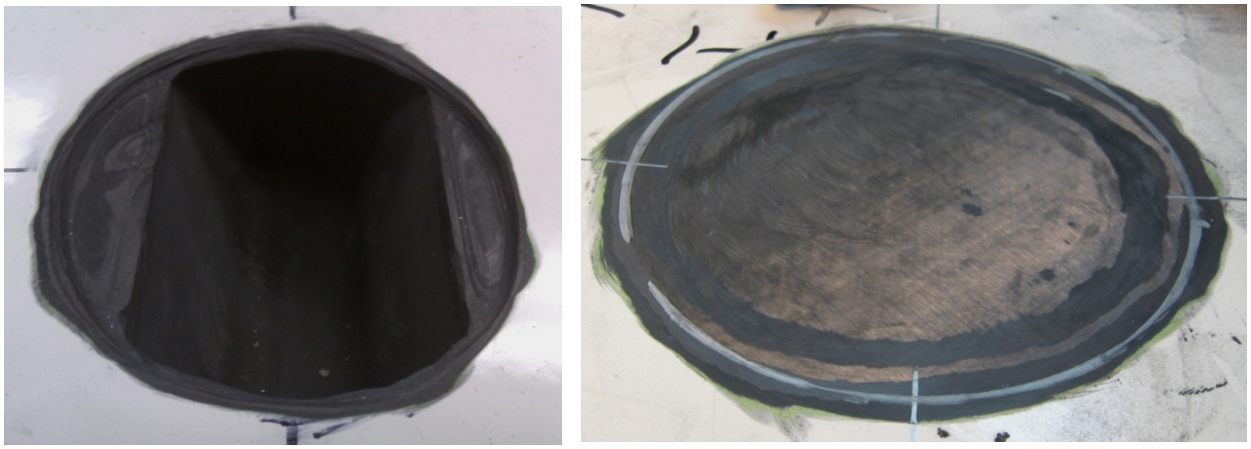

(a) (b)

Figure 50. Hat Panel #2 With (a) Material Removed for Plug Repair and (b) Taper Repair

The repaired panels were repainted to provide a smooth inspection surface similar to fielded aircraft repairs. Figure 51 is a photograph of the smooth surface of the panels after they were painted. A visual examination of the surface does not detect the repairs (i.e., there are no circular bumps or ridges where the circular repairs were made).

Figure 51. Repaired Impact Damage Panels After Paint

Figure 52 shows that a baseline TTU scan was performed of both panels with 5 MHz transducers. The unrepaired impact damage and stiffener cavities appear in black, and the repairs are more attenuative than the laminate.

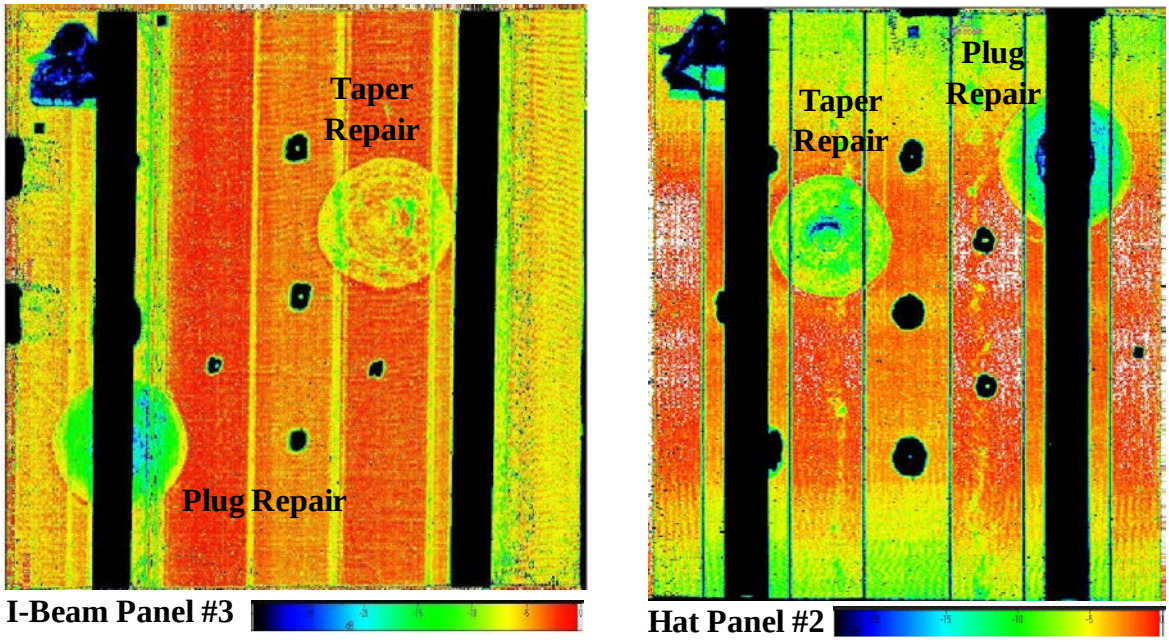

(a) (b)

Figure 52. The TTU C-Scan of (a) Repaired I-Beam Panel #3 and (b) Hat Panel #2

A PE ToF baseline C-scan was performed to compare the selected technologies. Figure 53(a) shows I-Beam panel #3 and figure 53(b) shows hat panel #2. The concentric circles of the

stepped layers in the taper repair are visible. The higher attenuation of the plug repair can be seen because two layers of adhesive were used to bond the precured plug in place. The feathering plies of the plug repair, which help blend the repair flush with the surface, can also be seen.

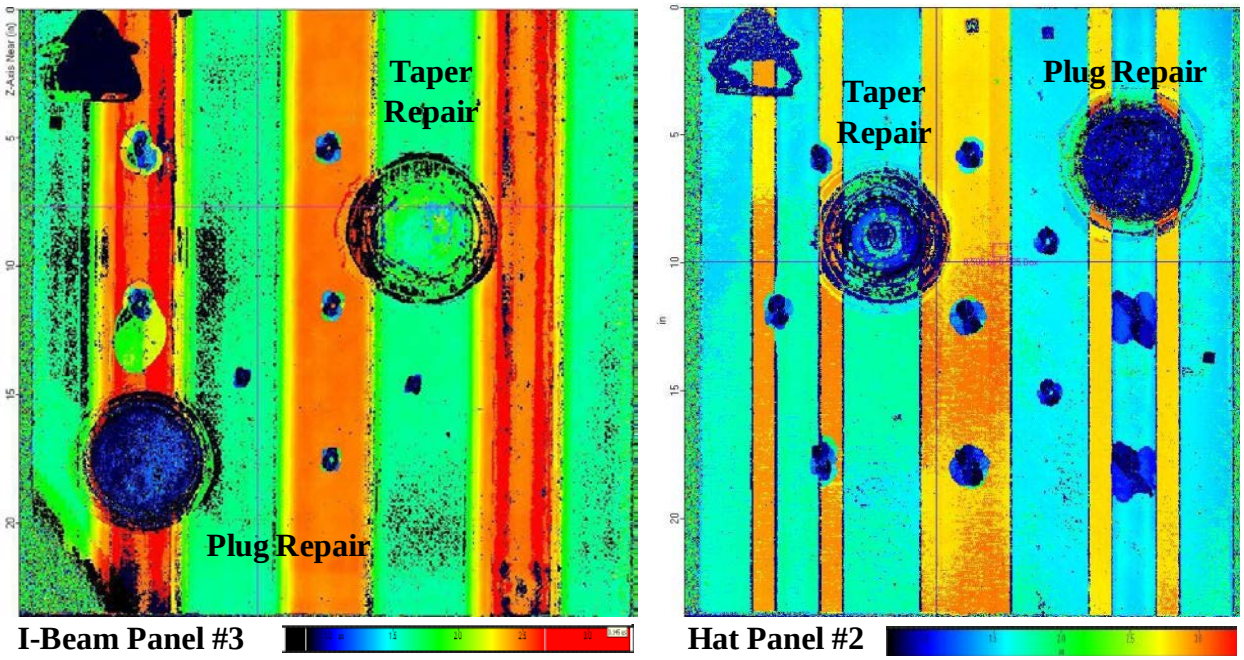

(a) (b)

Figure 53. Baseline Ultrasonic ToF C-Scan Images of Impact Repairs

3.2.4.1 The PAUT Evaluation of Impact-Damage Plug and Taper Repairs.

The initial PAUT evaluation of impact damage was done with a 64-element, 2.25 MHz probe; the results were not very clear, and the scan width was very narrow. A 128-element, 5 MHz probe was used on the repaired impact panels; the results differentiated the impact repairs and unrepaired impact damage.

3.2.4.2 The PAUT Impact-Damage Repair Evaluation.

Figure 54 shows the baseline amplitude C-scans and PAUT amplitude C-scans of the plug and taper repair. The area in the yellow box represents the PAUT scan areas. The PAUT C-scans covered the repairs, the undamaged area, and some unrepaired damage to evaluate the ability to show the difference in appearance.

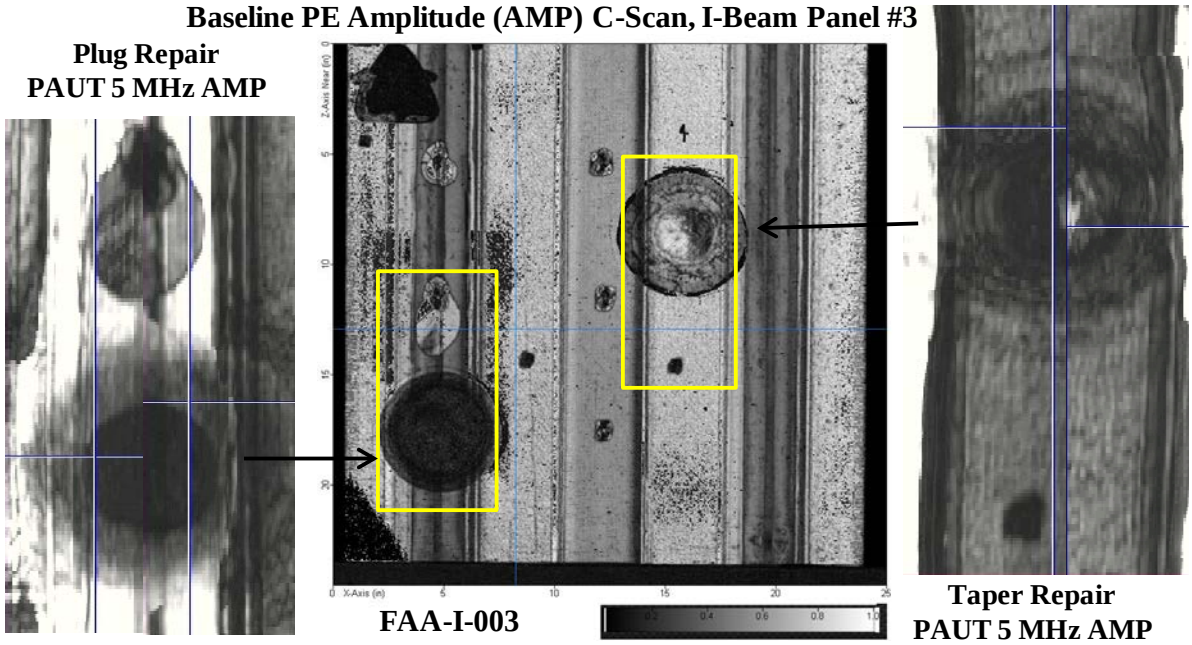

Figure 54. Repaired FAA-I-003 PAUT Amplitude C-Scans Compared to Baseline Amplitude C-Scan

Figure 55 shows that the hat panel #2 plug and taper repair areas are scanned with PAUT amplitude C-scan and compared to the baseline amplitude C-scan. The results are very similar to I-beam panel #3 in that the repair areas appear as regular defined shapes that are darker in color; the precured plug can be seen at the center of the plug repair, and the concentric rings of the taper repair as well as the feathering plies of the plug repair are visible.

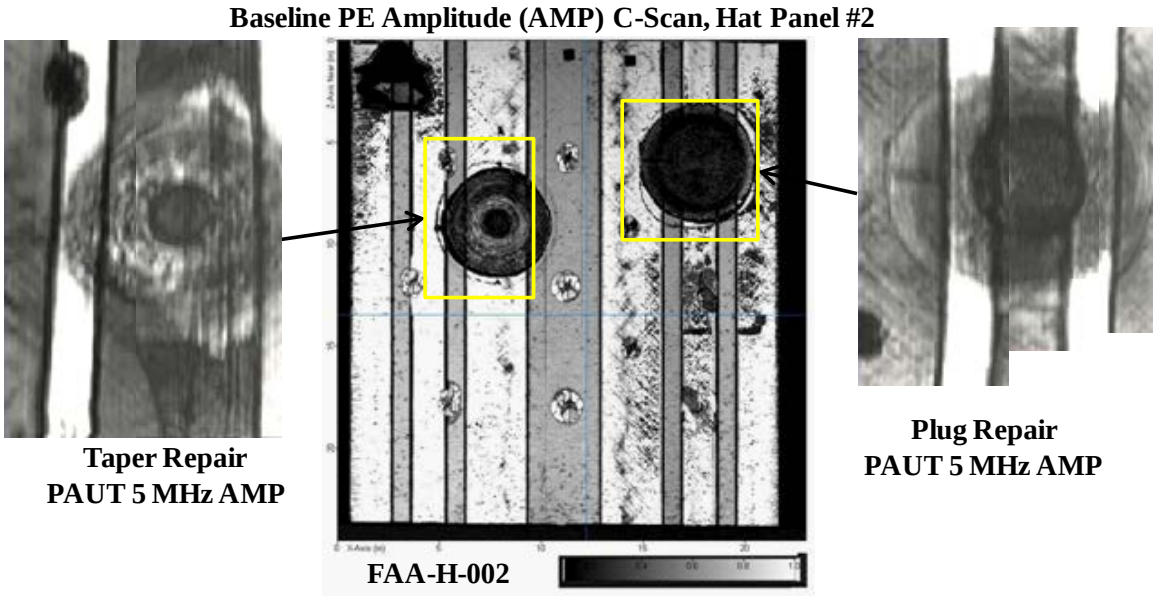

Figure 55. Repaired FAA-H-002 PAUT Amplitude C-Scans Compared to Baseline Amplitude C-Scan

Evaluation of the PAUT scans of the repaired impact damage reveals the following assessments:

- The concentric rings of the taper repair can be seen in the PAUT and baseline PE amplitude (AMP) C-scans.
- The plug repairs appear as darker, more attenuated areas (similar to the baseline PE AMP C-scan).
- The plug repair in the PAUT amplitude C-scans clearly show the outline of the precured plug inserted into the panel laminate (similar to the baseline PE AMP C-scan).
- The unrepaired impact damage appears as dark, irregular shapes, but the repairs have a more uniform appearance. The unrepaired damage can be differentiated from the repaired areas.

3.2.4.3 The DAV Evaluation of Impact Damage Plug and Taper Repairs

The DAV system performed well in the earlier impact damage evaluations, easily detecting and analyzing impact damage in the CEP laminate. The DAV C-scan areas will image impact damage repairs, undamaged laminate areas, and unrepaired impact damage to reveal the differences in how they are displayed.

A sequence of C-scan images (see figure 56) show the incremental C-scan views in the DAV on I-beam panel #3 taper repair edge. The yellow box in the baseline PE AMP C-scan image represents the area scanned with the DAV.

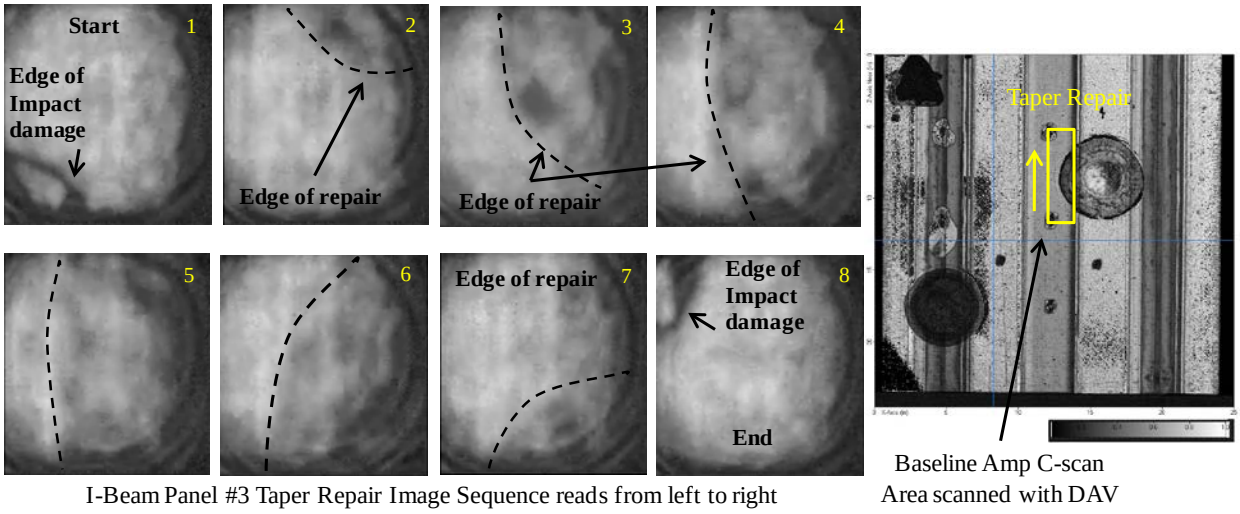

I-Beam Panel #3 Taper Repair Image Sequence reads from left to right

Figure 56. The DAV Evaluation of I-Beam Panel #3 Taper Repair

The plug repair area scanned with the DAV camera has similar results showing the higher attenuation as darker, defined geometric shapes. Figure 57 shows that the higher attenuation of the plug repair is expressed with darker C-scan images.

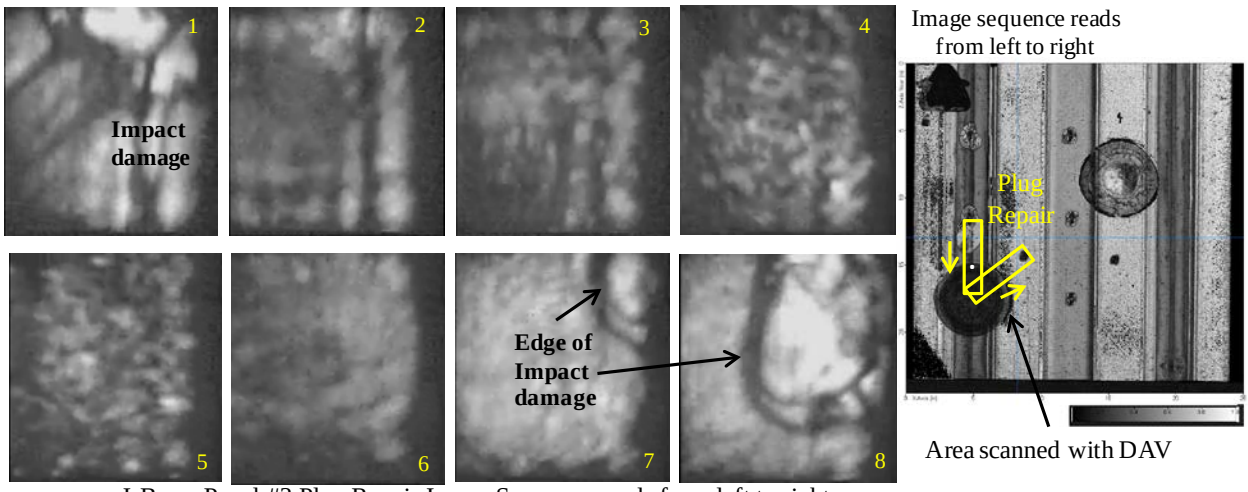

Figure 57. The DAV Evaluation of I-Beam Panel #3 Plug Repair

Figure 58 shows a DAV snapshot of a plug repair on hat panel #2. This image includes the A-scan display, which illustrates the signal amplitude of the adhesive bondline below the precured plug. The A-scan display provides the ability to characterize damage and differentiate delamination from porosity.

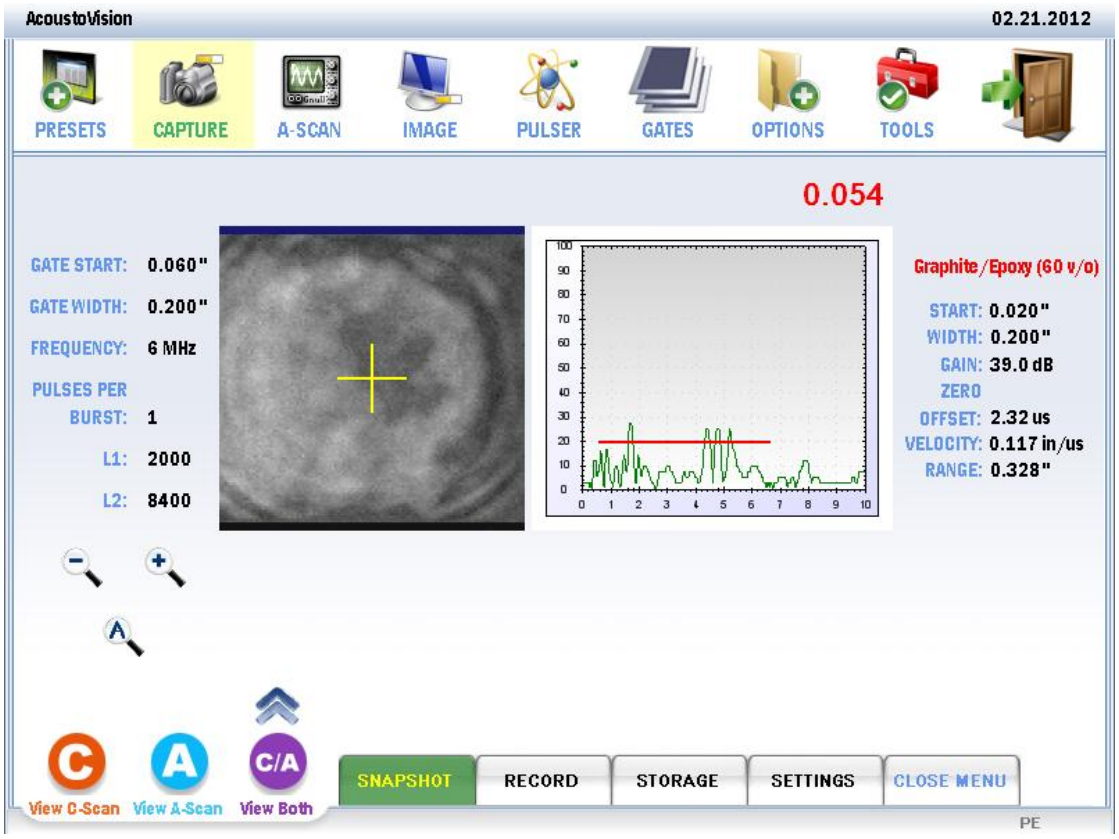

Figure 58. The DAV Snapshot of Hat Panel #2 Plug Repair

3.2.4.4 The FDIR Evaluation of Impact-Damage Plug and Taper Repairs.

Bell flash IR baseline images were acquired to evaluate the FDIR repair imaging capability. The field of view is smaller than the FDIR, so the flash IR images are manually stitched together.

Figure 59 shows the baseline Bell flash IR data and the accompanying FDIR data. Note that all seven of the unrepaired impact-damaged areas of I-beam panel #3 are shown in the flash IR image. In the FDIR image, all seven unrepaired impact-damaged areas are shown. The thin areas of I-beam panel #3 are darker in the flash IR image (see figure 59(a)) and lighter in the FDIR image (see figure 59(b)). The post-processed FDIR image shows five of the seven indications (see figure 59(c)).

In figure 59(a), the baseline flash IR image appears to mask the structure below the repair patch. The FDIR technique appears to image skin thickness variations and substructure through the repair patch (see figures 59(b and c)). The FDIR images can distinguish repair areas from unrepaired impact damage. One key benefit of post-processing is the improved contrast of the damage.

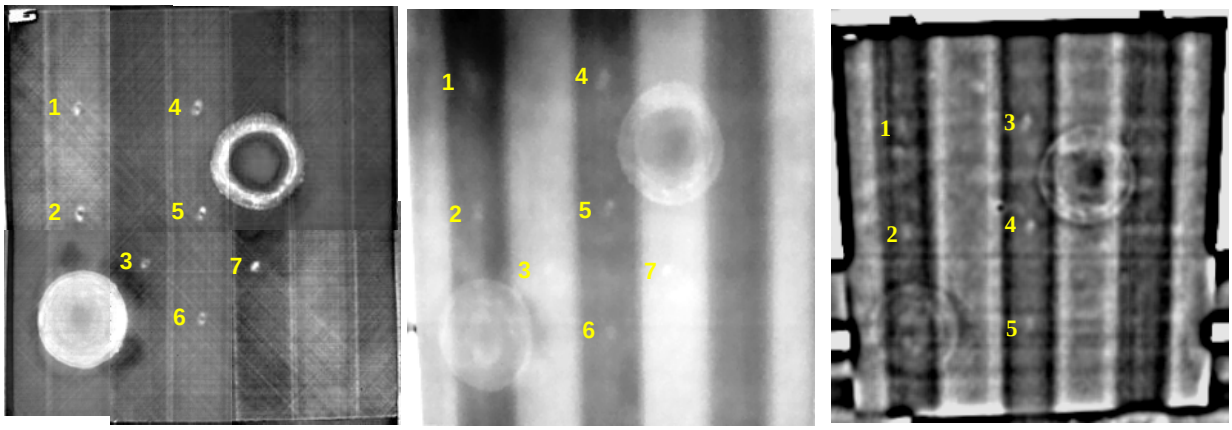

(a) (b) (c)

Figure 59. The I-Beam Panel #3 (a) Bell Flash IR, (b) FDIR, and (c) Post-Processed FDIR

In figure 60(a), the baseline flash IR reveals all ten of the unrepaired impact areas in hat panel #2. In the FDIR image, six of the ten unrepaired impact areas are clearly visible (see figure 60(b)). Again, the hat stiffener flanges and skin thickness variations are seen through the repair patches on the FDIR image and not the flash IR image. The post-processed FDIR image in figure 60(c) shows eight of the ten indications.

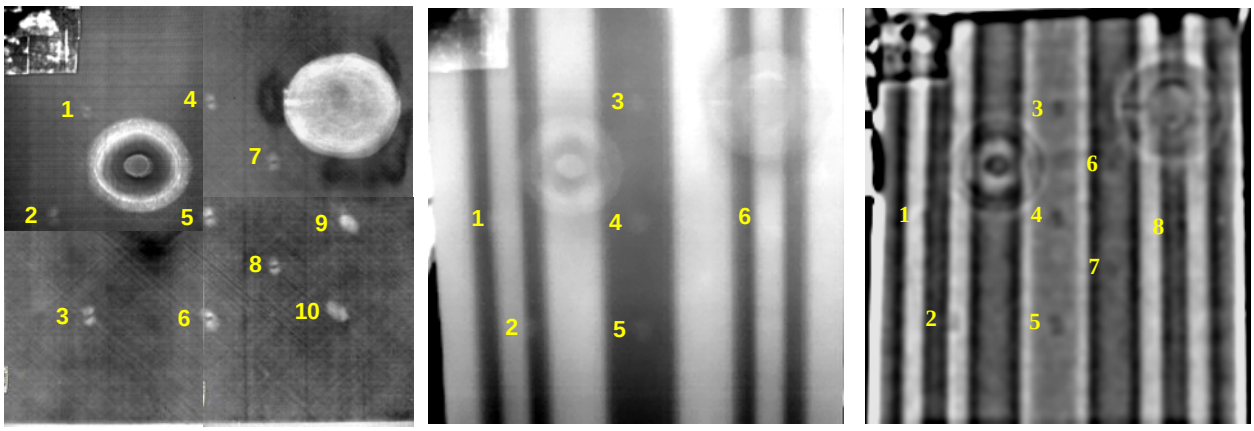

(a) (b) (c)

Figure 60. The Hat Panel #2 (a) Bell Flash IR, (b) FDIR, and (c) Post-Processed FDIR

One of the reasons for the difference in data is the technique. The flash IR images are gathered by measuring thermal energy from a brief exposure to a flash, whereas the FDIR image is gathered from a much longer exposure to direct sunlight. Flash IR will heat a panel as much as 4°F; the same panel will heat up more than 30°F after a few minutes of exposure to direct sunlight. The higher energy level from the sun enables the energy to soak deeper into the panel to reveal substructure, which helps provide location perspective in the visual image.

The FDIR images illustrate the capability to detect gross impact damage close to the surface on composite structures coated with flat black paint.

3.3 THE FOD PANEL EVALUATION.

The most common form of FOD in aerospace composites is single layers of various backing materials, which exist in layup rooms that use prepreg composite fabric or tape materials. When FOD creates an air gap between two layers, it can often be detected by many test methods, including visual and tap inspection. When FOD is bonded in a laminate, it becomes significantly more difficult to detect with conventional inspection methods.

The first FAA-Bell FOD panel has five common types of FOD that are found in a layup room: Teflon® tape, thick poly backing, coated paper backing, aluminum backing, and thin plastic/poly backing material.

Figure 61 shows FOD panel #1, which is 21 plies thick CEP (approximately 0.16″). A template was used to position the five triangular pieces of FOD at every five layers (i.e., 25% depth, 50% depth, and 75% depth) to yield 15 indications. A triangle was chosen to help compare the indication size to the true FOD insert size. Measuring the height and width of these triangles facilitates sensitivity comparisons of the selected technologies.

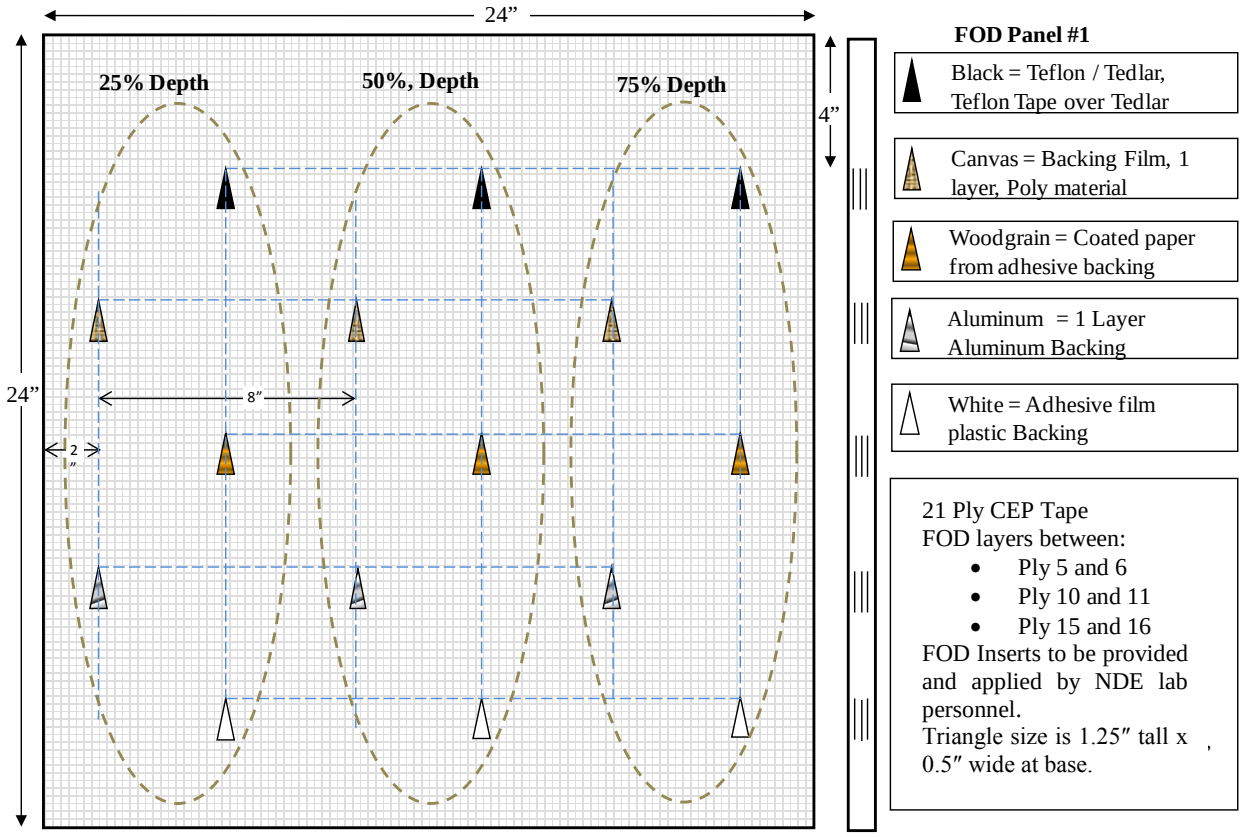

Figure 61. The FOD Panel #1 Design

Figure 62 shows FOD panel #2, which also has 15 indications; however, each indication represents a stack of three layers of FOD at 25%, 50%, and 75% depth. When FOD is located at several depths at the same location, it is only possible to see one layer. Although the FOD inserts were positioned with a template, the autoclave cure cycle and resin flow caused some layers to shift slightly, and this facilitated resolution comparisons of the selected technologies.

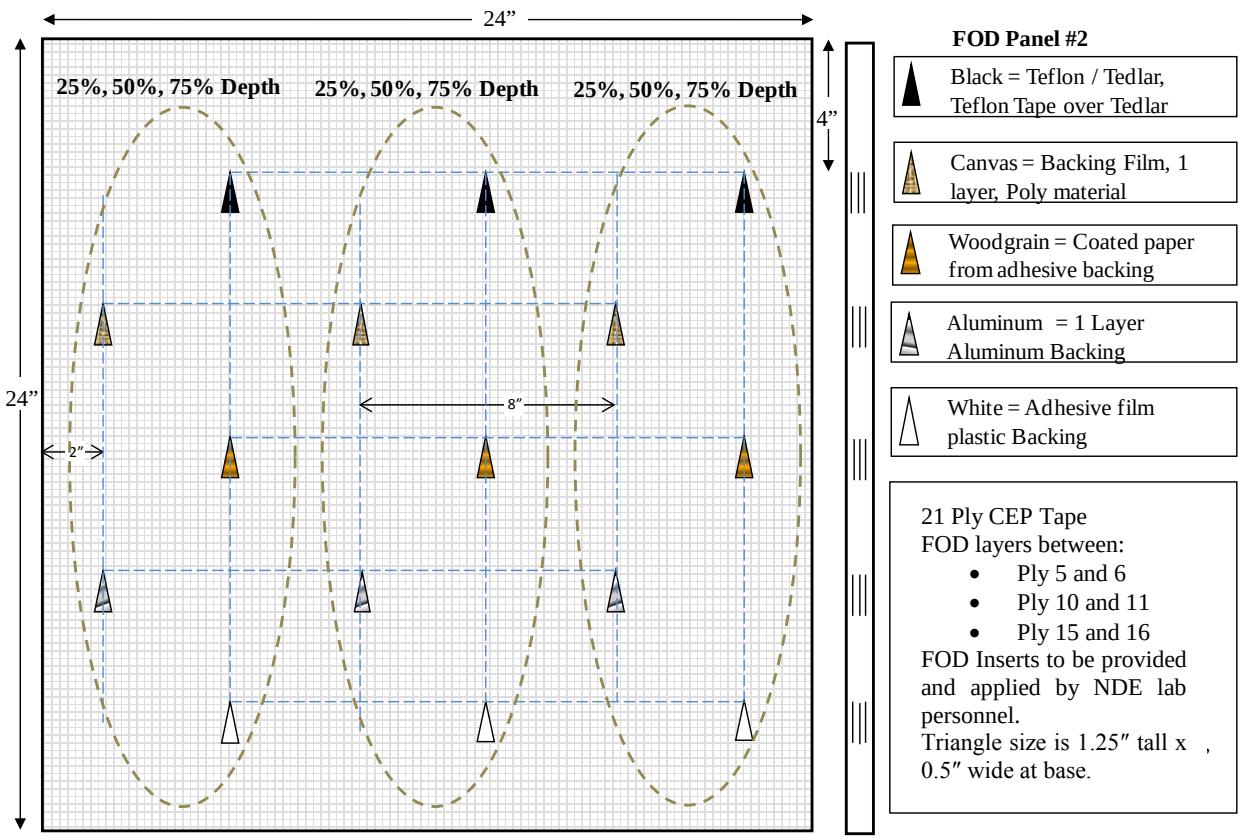

Figure 62. The FOD Panel #2 Design

Figure 63 shows the baseline ToF C-scans of the FOD panels. All 15 FOD insert locations are detected. Various levels of porosity are also visible. The baseline scans were captured with an acquisition and index increment of 0.040 inch; the scans did not reveal any staggered FOD inserts in FOD panel #2.

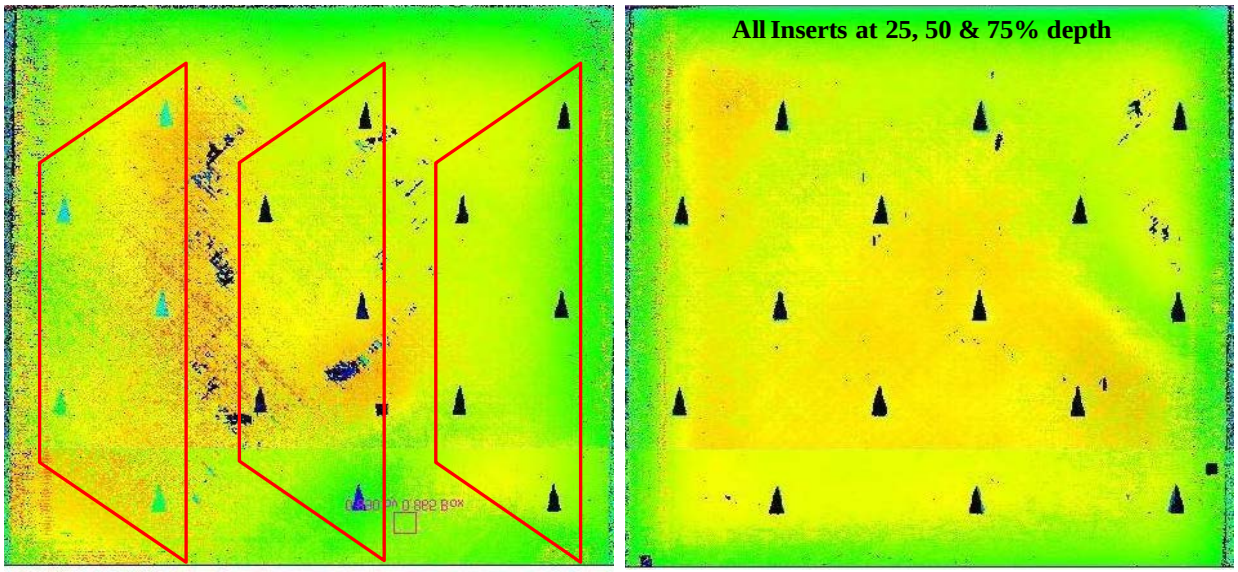

(a) (b)

Figure 63. Baseline ToF C-Scan of (a) FOD Panel #1 and (b) FOD Panel #2

3.3.1 The PAUT Evaluation of FOD Panel #1 and FOD Panel #2.

The PAUT evaluations of FOD panels #1 and #2 were done with a 128-element, 5 MHz transducer in ToF mode. The scans in figure 64 highlight the porosity in each panel. The scale below the ToF C-scans shows black for 0% depth, blue for approximately 25% depth, green for approximately 50% depth, yellow for approximately 75% depth, and red for 100% depth. A close look at a few of the FOD insert indications in FOD panel #2 reveals different shades of FOD at the edges below the 25% depth FOD layer, indicating a shifting of the different layers. These PAUT C-scans are approximately 2.8″ wide and manually stitched together. Figure 64 shows PAUT C-scans captured at an aperture of 0.020″; the shifted FOD inserts in FOD panel #2 are barely visible (see the zoomed-in image at the bottom right corner).

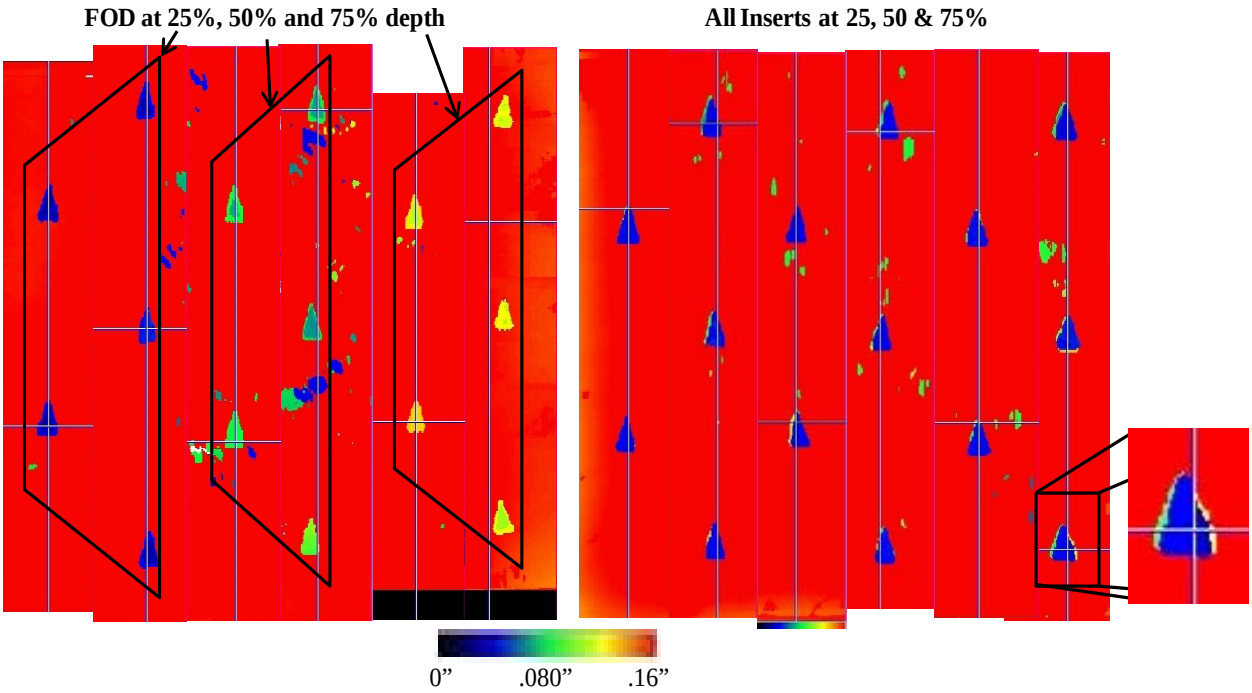

Figure 64. The PAUT Evaluation for FOD Panel #1 and FOD Panel #2

The ability to measure the length and width of indications after inspection is shown in the PAUT screen capture displaying an amplitude C-scan (see figure 65).

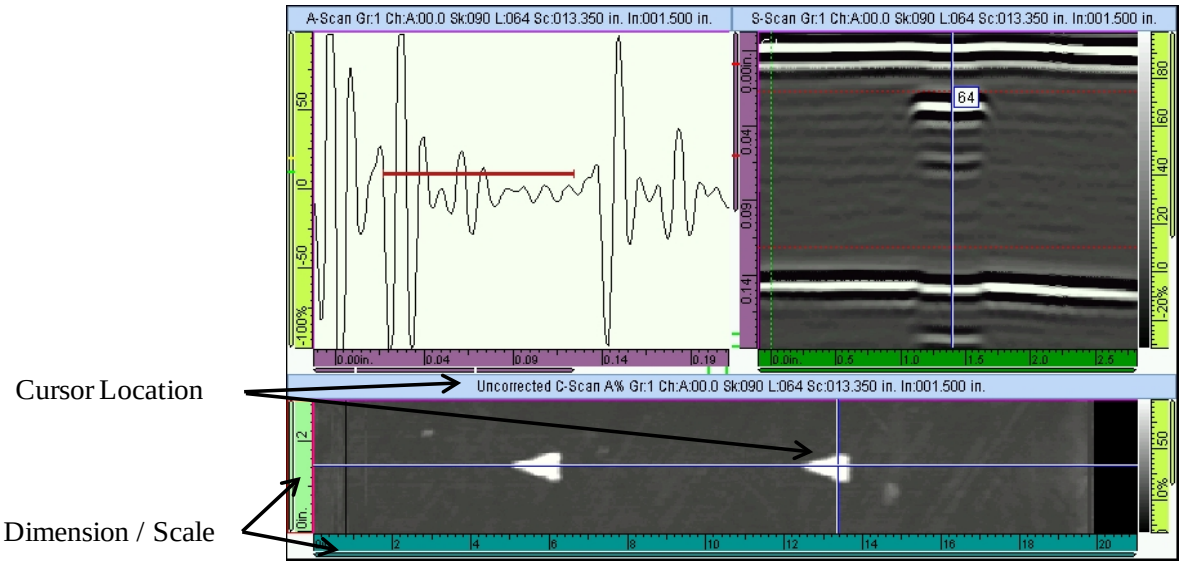

Figure 65. The PAUT C-Scan Dimensional Measurement Capability

The full-waveform capture of the PAUT inspection device enables the user to observe the C-scan data while scanning and perform various post-scan evaluations of suspect areas. Modifications

may be made to the gates, displays, color palette, etc., to highlight and measure indications after scanning.

3.3.2 The DAV Evaluation of FOD Panel #1 and FOD Panel #2.

The next technology used to evaluate the FOD panels is DAV. Figure 66 is a mosaic C-scan image that shows the fine C-scan resolution of the DAV. The higher imaging resolution of the DAV reveals a much more defined outline of the layered FOD in panel #2 as noted in the enlarged image at the right side of figure 66(b).

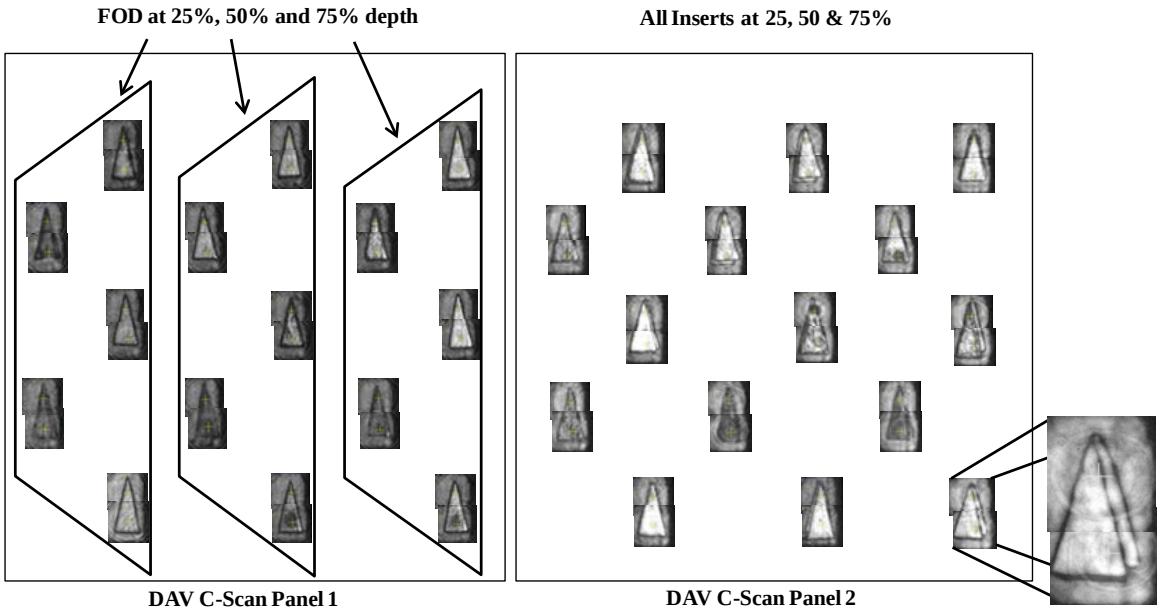

(a) (b)

Figure 66. The DAV (a) FOD Panel #1 and (b) FOD Panel #2 C-Scans

The DAV system C-scan output is amplitude data. The depth data is provided digitally at the cross-hairs at the center of the screen. The digital depth and A-scan display provide the ability to measure depth and characterize defects. When the DAV is positioned over the FOD inserts, the digital depth of the defect is displayed and may be recorded in snapshot or video mode. Figure 67 shows the informative and intuitive DAV display.

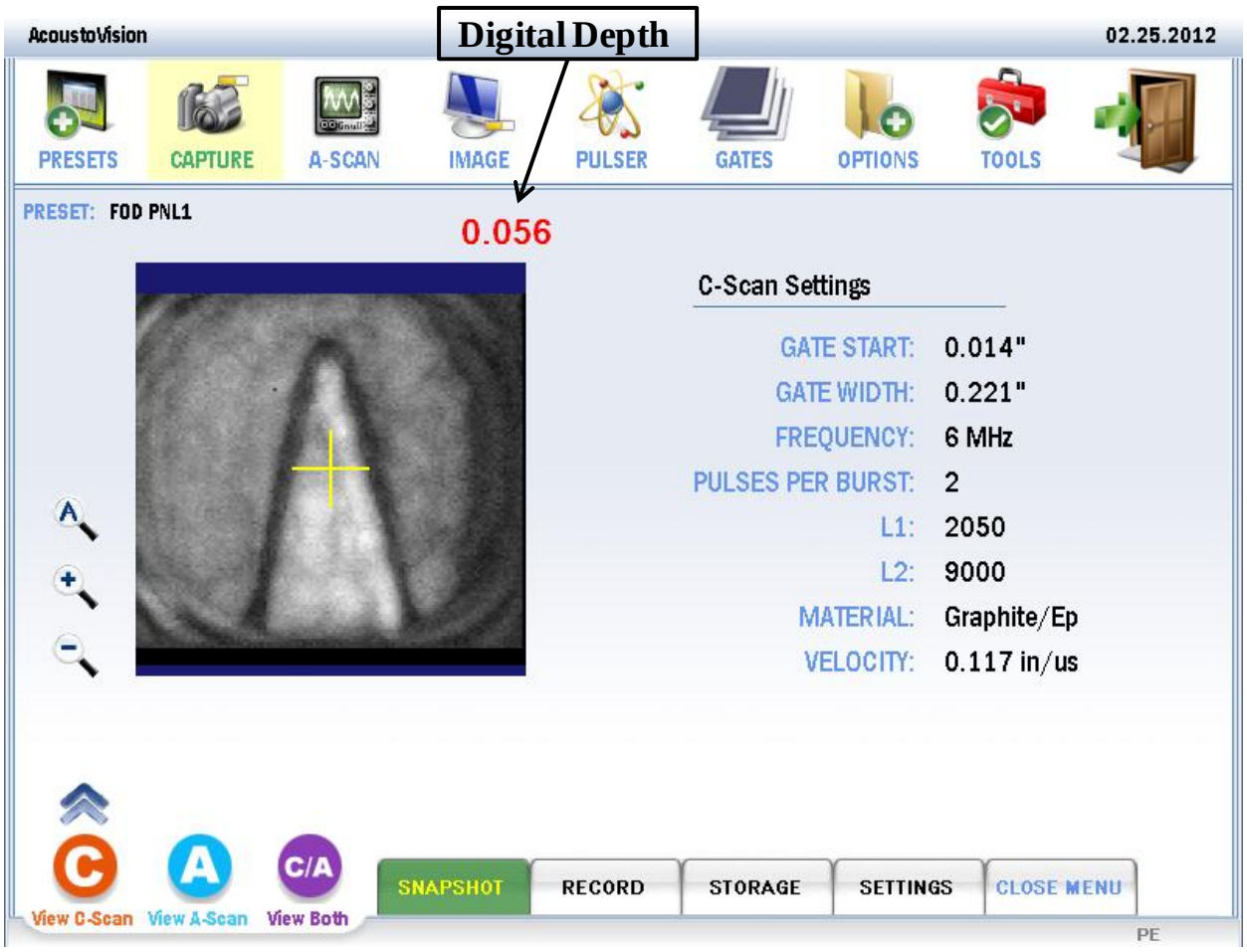

Figure 67. The DAV Snapshot of FOD Implant and Digital Depth of Reflector

The DAV technology provides the ability to scan suspect areas very quickly while performing real-time depth measurements. The C-scan display provides intuitive display of subsurface anomalies while the digital depth is recorded.

3.3.3 The FDIR Evaluation of FOD Panel #1 and FOD Panel #2.

The FDIR evaluation of FOD inserts was performed to determine which of the five types of FOD are more visible to the long-wave camera. The FOD panels were coated with ultra-flat black paint and then scanned with a flash IR short-wave camera to establish a baseline prior to performing FDIR. Figure 68 shows the flash IR baseline scans were manually stitched together.

In FOD panel #1, all of the embedded FOD inserts are visible at 25% depth (see figure 68(a)). Two of the five FOD inserts—Teflon/Tedlar® and coated paper—are visible at 50% depth. The Teflon/Tedlar is the only FOD insert visible at 75% depth.

The results for FOD panel #2 indicate that all 15 FOD inserts at 25% are visible, but the second and fourth rows are not as visible (see figure 68(b)). The second row of FOD inserts are made of thin poly/plastic backing and the fourth row is made of aluminized backing.

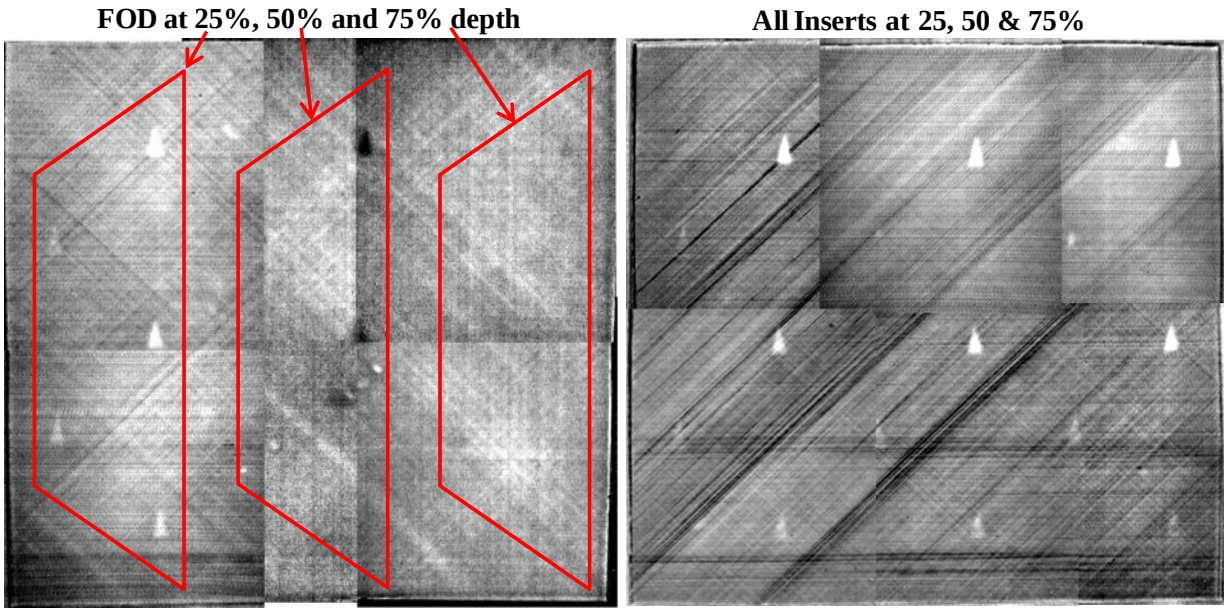

Baseline Flash IR results of FOD Panel #1 **Baseline Flash IR results of FOD Panel #2**

(a) (b)

Figure 68. Baseline Flash IR of (a) FOD Panel #1 and (b) FOD Panel #2

Figure 69(a and b) show the FDIR results of FOD panel #1 and FOD panel #2, respectively. The FOD panel #1 reveals one indication of Teflon at 25% depth. The FOD panel #2 reveals 7 of the 15 FOD implants. The low-cost, long-wave FDIR camera does not have the thermal sensitivity to adequately detect foreign materials embedded in laminates in a repeatable manner.

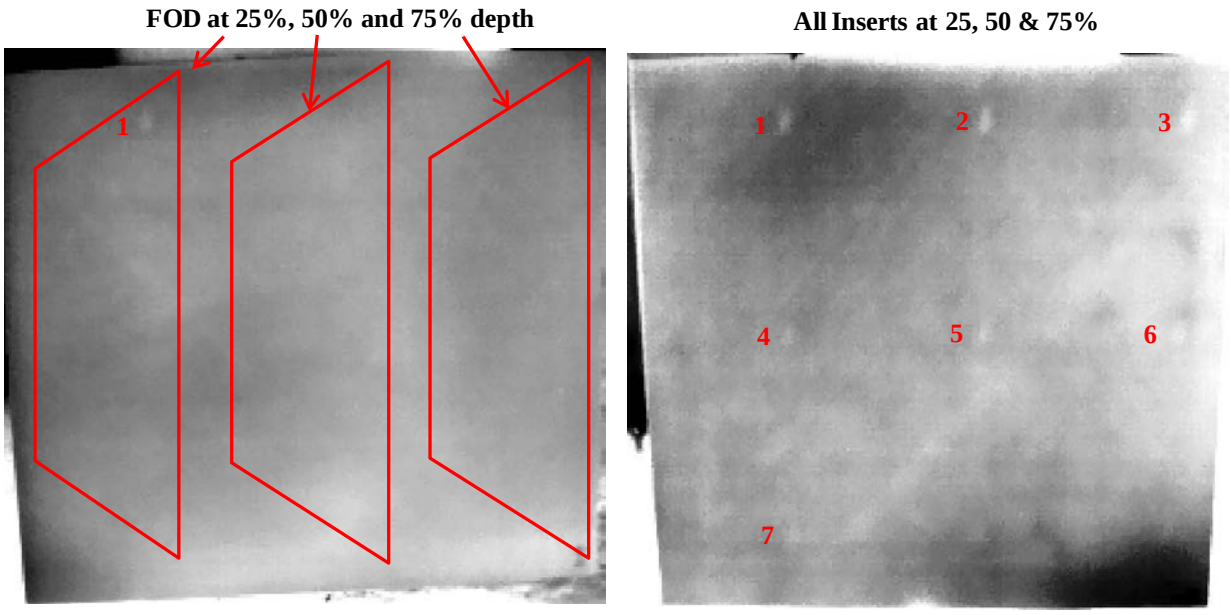

FDIR image of FOD Panel #1 **FDIR image of FOD Panel #2**

(a) (b)

Figure 69. The FDIR Image of (a) FOD Panel #1 and (b) FOD Panel #2

3.4 THE FDIR EVALUATION OF FLUID INGRESSION IN CONTROL SURFACES.

Fluid ingression in core-stiffened (sandwich) components has been observed in fielded aircraft. Though the long-term effect on the component and the potential threat to flight safety varies, the need to detect fluid ingression is valid. The FDIR can provide a wide-area imaging solution for this subsurface anomaly. The core section behind a rotor blade spar is a similar configuration to flight control components (e.g., ailerons, flaps, and rudders). Rotor blades with aluminum skin over aluminum core, as well as fiberglass skin over Nomex core, are two common configurations in commercial aviation that were evaluated. Metered quantities of water were inserted to determine the minimum quantity of fluid detectable in sandwich structures. The water inserted into the test panels was normalized to room temperature before insertion. Two forms of portable excitation were used to evaluate the sandwich panels.

3.4.1 The FDIR Evaluation of Fluid Ingression in Fiberglass Skin Over Nomex Core.

Fiberglass skin over Nomex core was the first test panel evaluated. A 2.5″ x 2″ square was cut into the upper and lower fiberglass skin over the Nomex core to provide access for fluid insertion (see figure 70). A metered syringe was used to inject quantified increments of water into individual 1/8″ core cells.

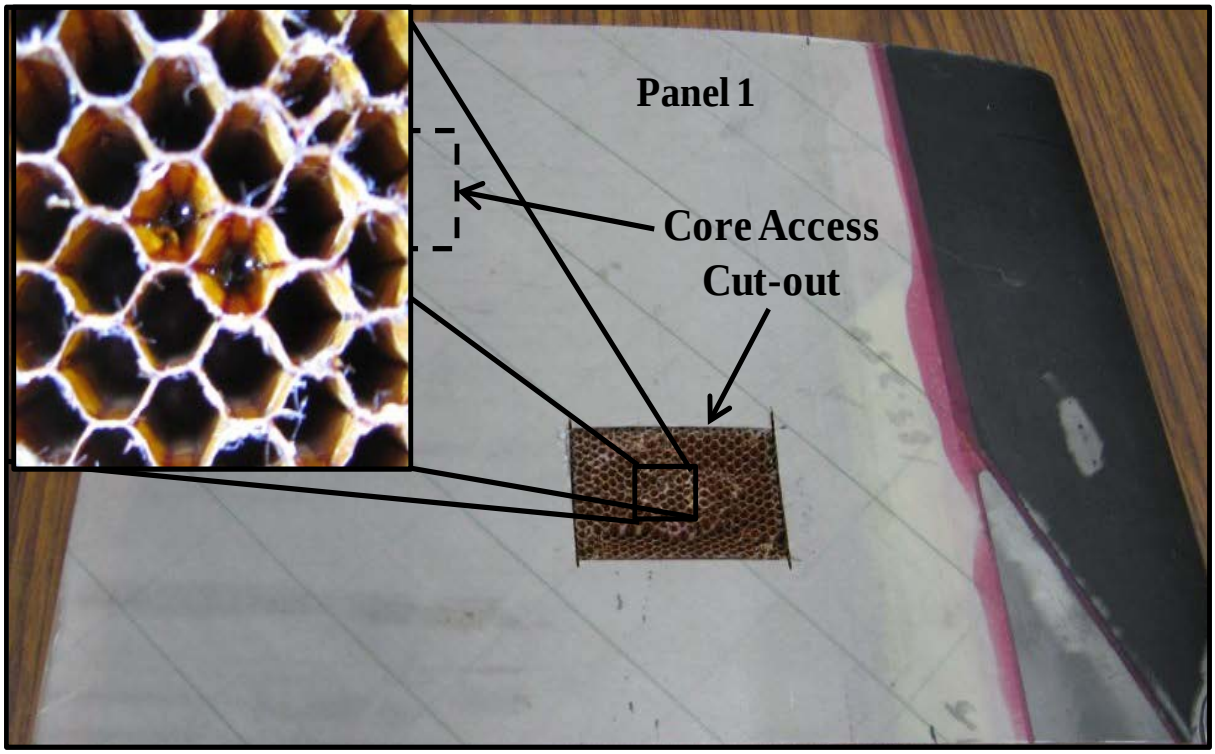

Figure 70. Fiberglass and Nomex Control Surface Panel #1

A baseline IR image of the panel was performed before fluid was inserted to ensure there were no nonrelevant indications in the panel. The panel was kept in a horizontal position to keep the water against the lower skin surface instead of spread out along the core cell wall. A 1000-watt halogen lamp placed 3 feet from the lower surface heated the panel for 1 second. Figure 71(a) shows no indications were found. The panel surface rose 9.8°F during the baseline test. Individual core cells were injected one at a time with 1/2 mL of water and the test repeated until a measurable IR indication was detected. Figure 71(b) shows evaluation of the images revealed a 4.1°F ΔT to the adjacent area. The two core cells injected with water were easily detected as the panel temperature rose 8.7°F from the heat exposure. The core access cutouts were not repaired.

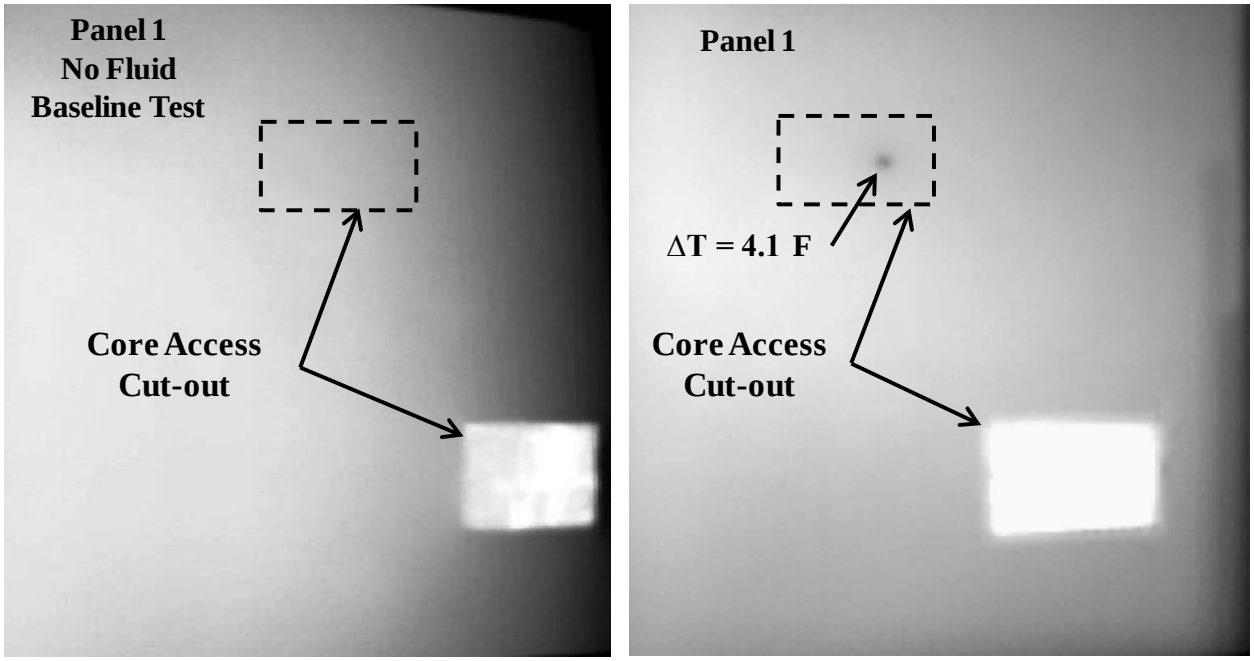

(a) (b)

Figure 71. Fiberglass Skin Over Nomex Core Fluid Ingression FDIR Evaluation

3.4.2 The FDIR Evaluation of Fluid Ingression in Aluminum Skin Over Aluminum Core.

Other materials, more commonly found on legacy aircraft, are aluminum skin over aluminum core. The high reflectivity of aluminum reflected away some of the heat. The higher thermal conductivity of aluminum dispersed the heat from the 1000-watt halogen lamp much faster, adding to the difficulty in imaging the water injected in the core cells. The low-emissive, shiny aluminum skin was coated with flat black paint to improve the imaging of the fluid through the aluminum skin by the FDIR camera.

A 2.5″ x 2″ square was cut into the upper and lower aluminum skin over the aluminum core to provide access for fluid insertion (see figure 72(a)). A metered syringe was used to inject quantified increments of water into individual 3/16″ core cells. This panel was also kept horizontal during testing to maintain the fluid on the lower skin surface. A 1/2 mL volume of water was injected in individual aluminum 3/16″ cells and imaged until a measurable thermal difference could be detected. No indications were found until three cells were each flooded with 1/2 mL of water. The panel surface was raised 18.2°F during the heat exposure. Figure 72(b) shows that this yielded a 1.9°F ΔT. The higher thermal conductivity of the aluminum skin and core transmits the temperature difference quickly, preventing a sharp outline of the cooler water-filled core cells like the previous fiberglass skin over Nomex evaluation.

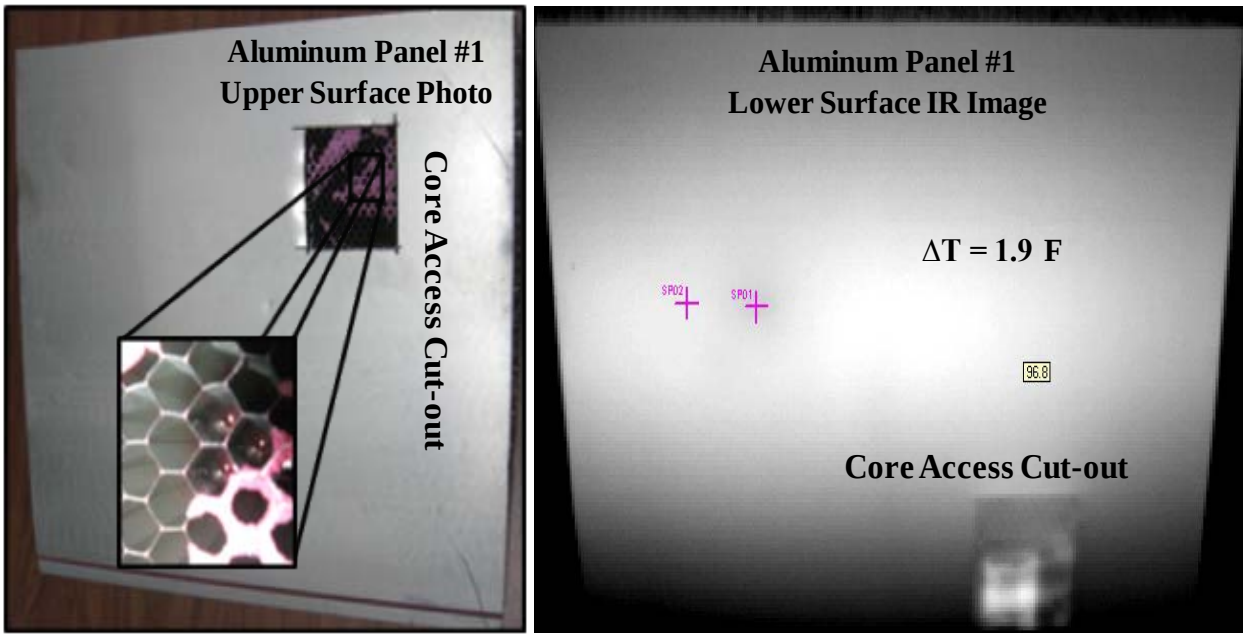

(a) (b)

Figure 72. Aluminum Skin Over Aluminum Core Control Surface FDIR Evaluation

3.4.3 The FDIR Evaluation of Large Water Volumes in Control Surfaces via Passive Excitation.

The next fluid ingression evaluation is a passive excitation evaluation using sunlight exposure of an aluminum core structure flooded with 500 mL of room-temperature water. The configuration has the panel almost vertical (i.e., core cells are almost horizontal), simulating a flaps-down condition.

A 1/4″ diameter cavity was made along the trailing edge and then sealed at each end. A similar cavity was then made connecting the 2.5″ x 2″ openings to the trailing edge. The surface of the panel to be evaluated was painted flat black to increase the thermal emissivity. Figure 73 shows 250 mL of water was injected into the upper and lower surfaces. The control surface was then exposed to sunlight.

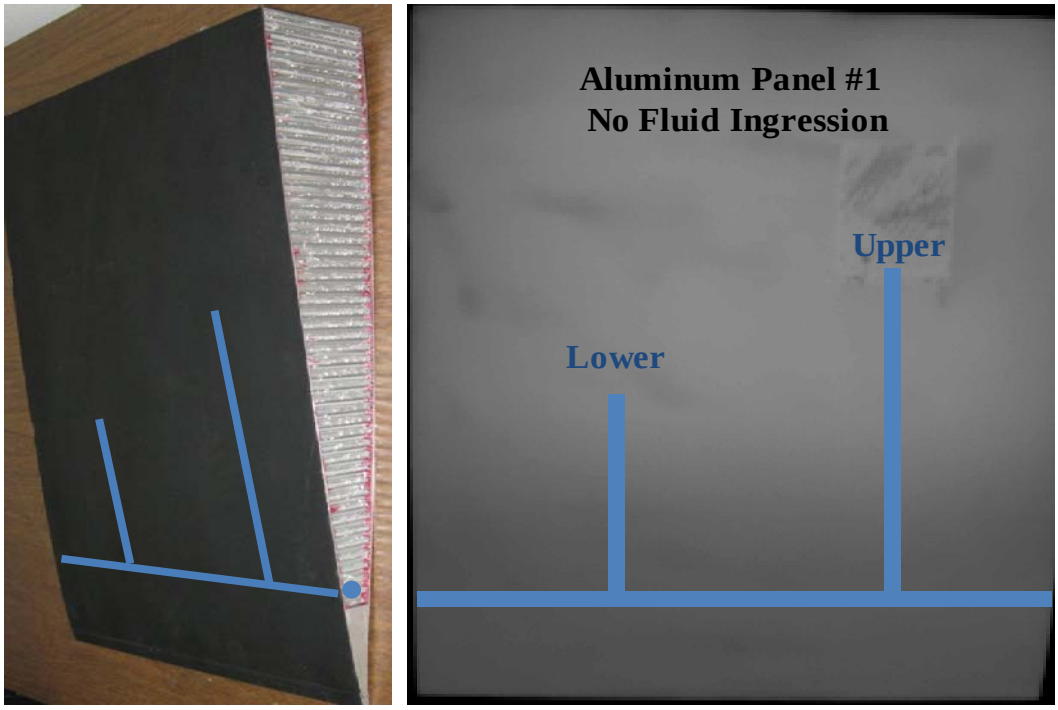

Figure 73. Insertion of Gross Fluid Ingression Into an Aluminum Control Surface

Figure 74 shows the aluminum control surface with 500 mL of water yielded 11.5°F ΔT from the adjacent area. The test panel surface increased 12.8°F during the test.

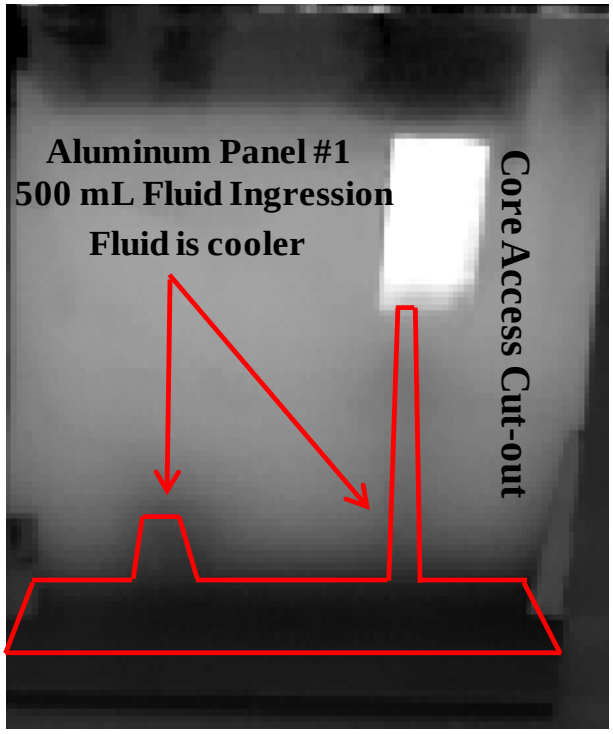

Figure 74. The FDIR of Aluminum Control Surface Exposed to Sunlight With 500 mL of Water

4. ASSESSMENT OF SELECTED TECHNOLOGIES.

As part of the validation plan, metrics were developed early in the project with input from the advisory board. Following the conclusion of the technology and technique development, each technique was evaluated against the metrics established in the validation plan. The assessments shown in table 5 serve as the summary of the technology performance on representative defects and structures.

Table 5. Technology and Technique Performance Metrics

Technology and Technique Performance Metrics					
Description	Originating Requirement	Measure	FDIR	DAV	PAUT
1) Are the results visualized	Easy to interpret results	Yes or No	Yes	Yes	Yes
2) Resolution	Easy to interpret results	Inch	0.1″	0.008″	0.040″
3) Instantaneous data points displayed	Easy to interpret results	Number	76,800	14,400	480,000
4) Technique throughput	Speed of inspection/Large area inspection	ft^2/hr	~1400 ft^2/hr	~72 ft^2/hr	~58ft^2/hr
5) Instant coverage area	Speed of inspection/Large area inspection	$in.^2$	~1024 $in.^2$	~1 $in.^2$	1.5 $in.^2$
6) Equipment cost	Equipment cost	$	$15,000	$45,000	$65,000
7) Equipment weight	Portability	lb	2 lb	12 lb	14 lb
8) Parameter settings for usage (how many settings are necessary)	Training required to perform	Number	1-Hour (without post-processing)	1-3, when preset program is used	2-4, when preset program is used

4.1 ASSESSMENT OF FDIR TECHNOLOGY.

Table 5 provides quantitative performance metrics used to compare FDIR to DAV and PAUT technologies. The screen resolution of 0.1″ was established by testing the composite panels from a distance of approximately 6′. The instant area captured at 6′ is approximately a 32″ x 32″ area with a 25° field-of-view lens. At this distance, each of the 76,800 pixels represents an approximately 0.013 $in.^2$ area, which is an increment of approximately 0.115″; when rounded to 0.1″, that is 320 pixels across 32″. The instantaneous data points displayed were established from the IR screen resolution of 320 x 240 pixels, for a total of 76,800 pixels. The speed of inspection was based on the image capture rate of approximately 4 seconds and an index time of 8 seconds per capture at ~6′, capturing a 32″ x 32″ area and an approximate 6″ overlap (26″ x 26″ = 676 $in.^2$/144 = 4.69 ft^2 per 4 second capture + 8 seconds for index = 5 captures per minute = 300 captures/hour x 4.69 ft^2 = 1407 ft^2). Data evaluation and image stitching is excluded from the assessment of all three selected technologies. The cost was based on the approximate cost when the unit was purchased in 2009. The approximate training time required to use the camera is based on the experience and knowledge level of the individual and the complexity of the component being evaluated. The FDIR camera does not have the ability to store preset programs. The manual temperature range setting is necessary to obtain a repeatable inspection. The optimized inspection technique is shown in appendix A.

In addition, a qualitative assessment of the FDIR technique was performed. During the technology demonstrations, the FDIR camera was the most appealing to the novice user because of the intuitive camera-based displays and ease of use. The FDIR camera's initial settings provided rapid setup for temperature and focus.

During evaluation of the FAA-Bell impact-damaged panels, challenges were encountered on high-gloss white paint panels because of the low emissivity. Substructure was visible through the gloss white paint, but defects were not detectible. Detection of impact damage improved when a thin coat of ultra-flat or flat black paint was applied and the images were captured as quickly as possible after exposure to sunlight. Application of post-processing with TSR software provided sharper contrast, and more defects were detected in almost every case (see table 6). There was a little improvement in the contrast of the defects on the I-beam panels, but the number of defects detected did not change.

Table 6. The FDIR Impact Damage Results

Panel ID	Impact Damage Detected (%) With Flat Black Applied	Impact Damage Detected (%) With Post Processing
Hat Panel #1	6 of 11 (54.5%)	8 of 11 (72.7%)
Hat Panel #2	6 of 10 (60%)	8 of 10 (80%)
Hat Panel #3	6 of 12 (50%)	8 of 12 (66.7%)
I-Beam #1	3 of 8 (37.5%)	3 of 8 (37.5%)
I-Beam #2	4 of 10 (40%)	4 of 10 (40%)
I-Beam #3	5 of 7 (71.4%)	5 of 7 (71.4%)

Even with the application of ultra-flat black paint, the FDIR technology did not accurately size known impact-damage defects. This was illustrated in the impact panel evaluation in sections 3.2.1 and 3.2.4.4.

Impact damage is easier to detect with FDIR when:

- The surface is painted flat black
- The impact damage is shallow (within ~0.040″ of the surface)
- The diameter is over 1″ in size

The FDIR technique in appendix A offers the largest area of inspection per hour of the three selected technologies. The FDIR technique performed well at identifying substructure in composite structures, even revealing substructure through composite repairs without a high-emissive coating applied. The FDIR evaluation of various FOD bonded in composite laminates revealed that Teflon is the easiest to detect at shallow depths (5 plies deep). The FDIR output data is easy to analyze, manipulate, and transfer.

The TSR post-processing software was used on long-wave, uncooled IR camera impact-damage data. This yielded improved data output and is not included in the performance metrics.

4.1.1 Potential Future Work on FDIR.

Section 3.2 showed the improved effects of capturing IR images as quickly as possible for the first 60 seconds after heat is applied to a test surface. It takes 3.7 seconds for the camera used in this evaluation to save an image. An IR camera, with the capability of capturing an image every second (like a modified video), would yield better results. A portable IR camera with TSR post-processing software would detect more impact damage than without the post-processing. There may be materials or technology that could reduce the need for a high-emissive coating to detect impact damage in large composite structures.

4.2 ASSESSMENT OF DAV TECHNOLOGY.

The next technology assessment was the DAV technology. Table 5 shows performance metrics used to compare DAV to FDIR and PAUT technologies. The 0.008″ resolution is derived by the 1″ receiver array, which is made up of 120 x 120 receiver transducer elements, for a total of 14,400 elements (1″/120 = 0.0083″). The technique throughput of 72ft²/hr is with a travel speed of approximately 4″/second with approximately 25% overlap. The equipment cost is based on the approximate purchase cost of the optimized high-frequency unit in April 2012. The approximate training time required to use DAV technology with a locked preset program is based on the experience and knowledge level of the individual and the complexity of the component being evaluated. This training will not yield an inspector capable of evaluating indications with the A-scan display.

The final version of DAV technology has a high-frequency transducer for improved resolution in composites, as well as higher voltage for improved penetration and digital depth recording at the center of the C-scan display. The DAV technology developed for this project did not include image-stitching capability, but a beta version was witnessed in development at Imperium Inc. in April 2012. The stitching capability has the option to display an A-scan during the video-recording playback.

Because the C-scan has its own gates, the DAV A-scan gates do not affect the C-scan image. This means the operator needs to exercise care when setting up the instrument to be sure a back-wall echo is being scanned and excessive porosity or another cause of attenuation has not absorbed or—more accurately—attenuated the back-wall echo signal of the A-scan. To be sure the back-wall echo is not being attenuated, only the back-wall echo signal should be gated, assuming the material thickness does not vary. Because the A-scan gate does not affect the C-scan gate, the loss of digital thickness indicates signal loss (a signal in the A-scan gate triggers the digital thickness reading in the C-scan display).

The DAV technology detected 100% of the porosity flaws and displayed the elongated pores in its C-scan display. The DAV technology detected 100% of the impact damage, and detected and evaluated composite repairs well. The DAV technology performed well, detecting and analyzing depth on the FOD panels.

4.2.1 Potential Future Work on DAV.

Further work on DAV technology to enable wide-area coverage should include the integration of an image-stitching capability. Development of real-time ToF depth-imaging would allow better characterization of defects and damage. The ability to inspect a large field of view instantaneously while maintaining equipment portability is another area for further development.

4.3 ASSESSMENT OF PAUT TECHNOLOGY.

The final technology assessment is the phased array technology. Table 5 provides performance metrics used to compare PAUT to FDIR and DAV technologies. The 0.040″ resolution is derived by the typical scan setup, which allows for a comfortable scan speed without missing data (faster scan speeds are more prone to missing data, which requires backing up or rescanning the area). The 480,000 instant data points refer to the 8.4″ real-time display, which has an 800 x 600 resolution with a 60 Hz A-scan refresh rate. The technique throughput of 58ft²/hr is with a scan speed of 1.88″/second with 15% overlap. The equipment cost is based on the approximate purchase cost of the unit in 2009; costs have likely changed since then. The approximate training time required to use PAUT is based on the student's data acquisition skill level and experience during the project technology validation. The training is only for PAUT use with preset programs; it is important that all preset functions are locked. The training hours do not include setup or data analysis. Changing the aperture, gain, gate, etc. will significantly affect the inspection output. This training will not yield an inspector capable of programming setups or evaluating data.

Of the three selected technologies, PAUT is the most capable analysis tool, but the most challenging to learn. The expanded capabilities include full-waveform capture, which provides a platform for numerous post-processing actions. An example of post-capture data manipulations include gate adjustments, the ability to change C-scan data (amplitude vs. ToF C-scans), and omitting an A-scan view, S-scan view, or C-scan view to allow more space on the screen for analysis.

The PAUT detected 100% of the porosity flaws and displayed the elongated shapes of the pore and the various depths as different colors in the ToF C-scan. The PAUT detected and analyzed 100% of the impact damage and impact repairs. The PAUT also detected, displayed, and analyzed 100% of the FOD indications in both FOD panels.

4.3.1 Potential Future Work on PAUT.

Phased array probes have the ability to provide valuable data on large areas, but are limited to relatively flat surfaces or subtle curves. The large, 128-element probes would be more useful if they could be used on curved components or compound curvatures.

5. SUMMARY OF SANDIA EVALUATIONS.

As the evaluation of test panels was completed at Bell, the panels were sent to the FAA AANC for validation using accepted inspection methods common to industry. The purpose of this validation is to provide verification of the baseline technology used on the test panels at Bell and

to provide additional methods of tests for the panels. The results of these validation tests are shown in appendix E. Sandia demonstrated some of their visual-based methods, including flash IR, MAUS V (PE/Resonance), and Omniscan® PAUT (e.g., PE contact, aqualene wedge, and plastic wedge), as well as conventional signal-type inspection devices (e.g., Ramp Damage Checker, Bondmaster, A-scan). A Bell evaluation summary of these data states that:

- The flash IR results at Sandia were comparable to the baseline flash IR results performed at Bell and TWI. The Sandia flash IR data also correlated to the Bell data in that the extent of impact damage through the panel thickness (i.e., depth) was not accurately characterized.

- Of the visual-based ultrasonic methods utilized, the MAUS V data provided comparable data resolution and clarity of imaging defects to the FDIR, DAV, and PAUT techniques developed at Bell as part of this research.

- Further correlations could be made by evaluating the Sandia inspection technology against the performance metrics defined as part of this research.

6. CONCLUSION.

Three industry-accepted baseline technologies were evaluated in this project, comparing their inspection output of realistic industry defects found in modern composite structures. The project began with the establishment of an industry advisory board consisting of industry representatives familiar with fielding composite structures. The industry advisory board helped establish the technology evaluation metrics and provided input on the test panel configurations, materials, and thicknesses. The test panel designs were revised to incorporate the advisory board input and were then fabricated. A validation plan was established with input from the industry advisory board. During the test and evaluation of the selected technologies, technology and technique improvement needs were identified. Improvements were made to the technology and techniques, and then the test specimens were retested and evaluated. Technology assessments were made after completion of the technology and technique development and optimizations.

Technology and technique validations were performed at Sandia, Petroleum Helicopters Inc. (PHI), Rotor Blades, Incorporated (RBI), and Cessna. The first validation was performed at Sandia, where the most feedback on the techniques was provided. Like Bell Helicoptor Textron, Inc., Sandia and Cessna already have phased array ultrasonic testing (PAUT) in use in various capacities, and PHI indicated that they were considering PAUT technology. PHI, RBI, and Cessna were aware of—but had limited experience with—the Digital Acoustic Video (DAV) and field deployable infrared imaging (FDIR) technology. Everyone who handled the FDIR camera found it to be intuitive, approachable, and user friendly (new users quickly found ways to improve their results).

The PAUT technology was an established portable evaluation tool with a high-technology readiness level at the beginning of the project to which the two other technologies could be compared. Most of the effort performed on PAUT focused on technique optimization. The PAUT technology is well-suited for detailed evaluation of foreign object debris (FOD), porosity,

or impact damage on flat or slightly curved surfaces and its full-waveform capture provides quantification of defect size and depth.

The DAV technology has programmable presets (similar to the PAUT unit) to save setup programs for less-trained operators. The DAV technology was significantly improved by increasing the frequency and processing speed, resulting in an intuitive video display. Figure 75 shows an example of the C-scan imaging at the beginning and end of the project. The DAV is well-suited for quick evaluations of impact damage and FOD, and can be used on more severe curves than the PAUT. Unlike PAUT, the DAV C-scan provides amplitude data only. Therefore, the DAV C-scan can miss porosity on laminates if the C-scan gate is not set on the back wall only. Also, if the laminate has multiple thicknesses, such as doublers and stiffeners, the gate will need to be wide enough to capture the back-wall echo of the various thicknesses, thus introducing the possibility of missing porosity.

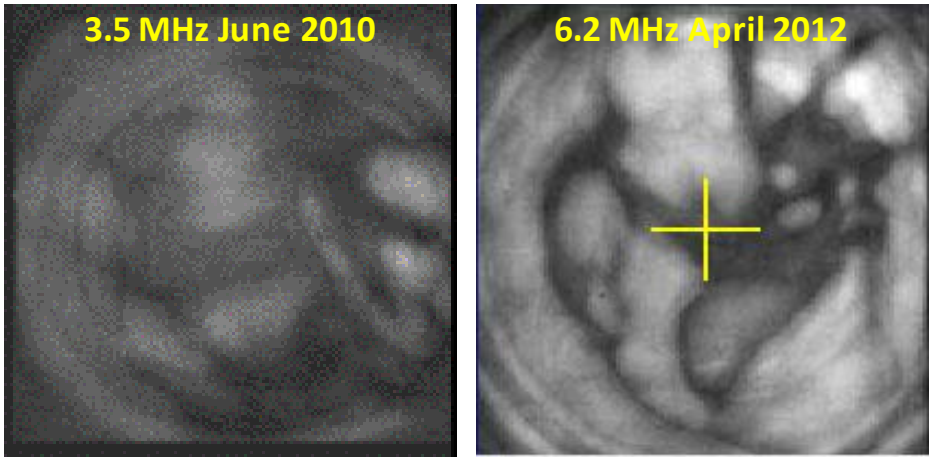

Figure 75. The DAV Images of Impact Damage Before and After Improvements

At the beginning of the project, FDIR was anticipated to be a strong performer in fluid-ingression detection and enhanced visual inspection, with hopes of being a low-cost, wide-area substructure and impact-damage detection tool, especially when the damage is over 1″ in size and within 0.050″ depth in the laminate. The FDIR exceeded expectations in the detection of substructure through plug and taper repairs. At the beginning of the project, FDIR could not detect impact damage on the gloss white impact-damage panels, but after the capture technique was optimized and the images were post-processed, most of the impact damage over one inch in size was detected (see figure 76).

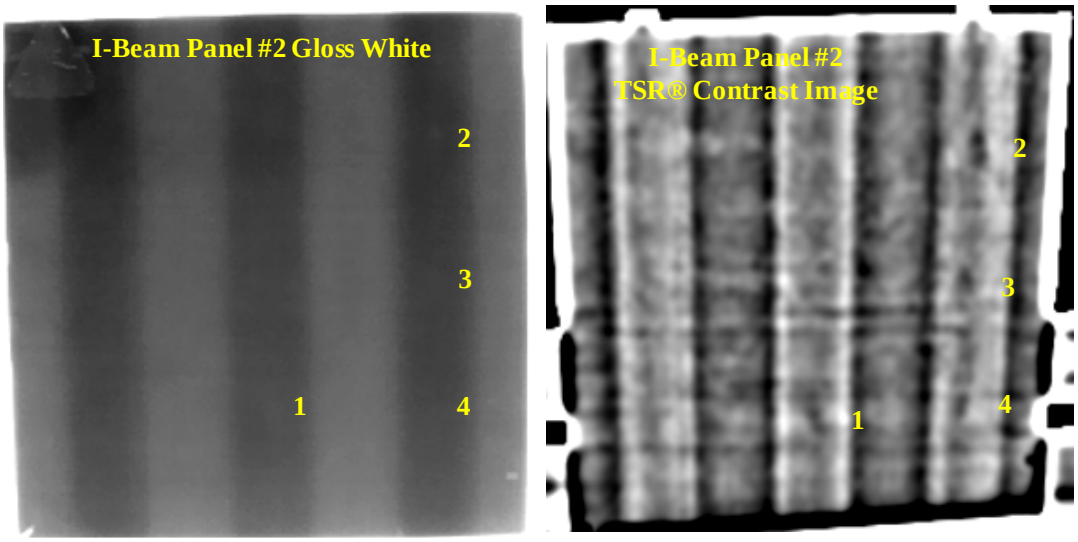

(a) (b)

Figure 76. The FDIR of (a) Impact Damage Before Optimization and (b) at Project Conclusion

FDIR detected 1.25″ x 0.5″ Teflon FOD up to 0.050″ deep, but did not detect the other four types of FOD consistently; therefore, FDIR is not recommended for FOD detection.

FDIR's greatest strength is the wide-area evaluation of composite materials for impact damage. FDIR's ability to cover over 1,400 ft^2/hr searching for gross impact damage when exposed to sunlight makes it a valuable wide-area imaging tool. The FDIR's next strength is its ability to detect fluid ingression, especially in fiberglass skin over Nomex core sandwich structures.

One drawback of FDIR is that it does not capture the full extent of impact damage, so subsequent inspection would be required and low-emissive (gloss white) surfaces would need to be coated with a high-emissive coating (water washable flat black).

Figure 1 shows the listed applications for the three selected technologies at the beginning of this project, before the technologies and techniques were improved. All three technologies proved their abilities to detect impact damage before and after repair. Table 7 identifies the preferred technology for each of the applications addressed in this project. Two stars are noted if a particular technology is considered most efficient or most effective.

Table 7. Selected Technology Performance Evaluated by Application

PAUT	DAV	FDIR	Application
		**	Detection of fluid ingression in core structures
	*	**	Enhanced visual inspection to detect critical composite defects or damage
*	**	*	Detection and characterization of impact damage and BVID
*	**	**	Fast, low-cost, large-area inspection to detect impact damage in laminate structures not clearly visible from the exterior surface
**	*		Detection of porosity and foreign materials in laminates
**	*	*	Characterization of impact damage before and after repair

APPENDIX A—FIELD DEPLOYABLE INFRARED INSPECTION TECHNIQUE

A.1 PURPOSE.

To provide nondestructive evaluation personnel a guideline procedure for using a portable, uncooled, long-wave infrared (IR) camera.

A.2 INSPECTION METHODS.

The IR thermography using long-wave, uncooled photo bolometer and sunlight excitation.

A.3 INSPECTION STANDARDS.

Carbon epoxy or fiberglass skin. Use a comparable substrate with known damage (verified with another nondestructive testing method).

A.4 EQUIPMENT SETUP.

1. Turn on the camera (power button is on the back of the camera, lower-right corner) and allow time for the camera to start up.

2. Open the lens cover.

3. On the back of the camera, an “A” or “M” will appear on the screen for the temperature grade control. If the “A” is showing, press the “A/M” button on the upper-right corner on the back of the camera to change the setting to “M.”

4. Use the toggle on the upper right of the back side of the camera to set the range to approximately 12°F to 20°F (moving the toggle left compresses the range and moving it right expands the range). The lower threshold should be just above room temperature if it is slightly warmer outside in the sun and 10°F higher than room temperature if it is more than 10°F warmer outside.

5. Use the toggle on the upper-right of the back side of the camera to shift the temperature scale so the bottom end of the scale is 1°F to 3°F above the temperature of the panel, which should be at a stable temperature out of the sun.

6. Mount the camera to a tripod and set up the camera 3′–5′ from where the inspection surface will be placed (if the camera is closer, it reduces the field of view). The sun should be at the operator’s back, slightly off angle (the shadow should point toward the panel, but not be in the image).

   Place a cone or support tripod where the panel will be placed and focus the camera on the object so the camera will be ready to capture images once the panel is in place.

   Note that if the purpose of the inspection is to detect substructure, often detected by significant differences in temperature (1°F to 5°F), then a high-emissive coating may not

be required. However, if very subtle indications—such as delamination from impact damage—are of interest, then a thin layer of flat black or ultra-flat black paint/coating will need to be applied to the inspection surface to detect very small thermal variations, such as 0.1°F ΔT.

7. Gloves should be worn to minimize the amount of heat that will transfer from fingers/hands to the panel (causing nonrelevant indications) before the panel is moved to the inspection area (direct sunlight). The inspection area where the panel will be placed should also be considered. Cardboard should be put down if the ground is very hot or cold so the panel does not conduct temperature from the ground.

8. If the temperature difference from room temperature is significant or if it is very sunny, it is important to move quickly to get the panel in the desired position and begin to capture images.

   The test panel should be moved to the intended position so that it is perpendicular to the sun.

9. Verify that the image is in IR camera focus, and then press the silver button on the front of the camera to capture the first picture image. As soon as one image is saved, another should be captured. The fastest capture rate possible is approximately one image every 3.7 seconds. At least three to seven images should be captured. If the thin areas begin to wash out or drift above the temperature range (turning white), the toggle should be used to move the range upward.

10. For further evaluation, the images should be downloaded to a PC using the cable provided or by removing the memory card from the top of the camera, inserting it into a card reader on a computer, and placing the images in a folder describing the performed inspection.

A.5 IMAGE EVALUATION (OPTIONAL EVALUATION ON PC).

The following steps should be taken to evaluate images:

1. Open ThermaCAM™ Researcher Pro 2.8 and open the group images.

   Use the "Open-Images" icon (or the Ctrl-I key) to open multiple images. Click "Add Files" and then "OK."

2. Change the images to grayscale using the palette selection pane.

3. Click on the "Flying Spotmeter," located on the left side of the screen, to activate the ability to read panel temperatures wherever the mouse is hovering.

4. Scroll through the images and select the ones that provide the best image (largest ΔT) of the suspect damage.

5. Use the upper and lower sliding scale palette controls to adjust/optimize the contrast of the image.

6. Save the image as a .jpeg by doing a screen capture and dropping the image in MS Paint, then cropping it to size.

APPENDIX B—PHASED ARRAY ULTRASONIC TECHNIQUE

B.1 PURPOSE.

To provide nondestructive evaluation personnel a guideline procedure for using the Olympus Phased Array Ultrasonic Testing (PAUT) with preprogrammed settings made by an ultrasonic testing (UT) level III or designated UT level II.

B.2 INSPECTION METHODS.

Ultrasonic inspection with the phased array pulse echo technique.

B.3 INSPECTION STANDARDS.

The inspection standard is carbon epoxy standard example (stepwedge or other material similar to what is to be inspected is acceptable).

B.4 EQUIPMENT SETUP.

All couplants used with the phased array system using an encoder wheel must be free of glycol. This is to preserve the life of the encoder wheel. The equipment setup consists of the following steps:

1. Press the green “Power” button to turn on the Olympus OmniScan® unit.

2. Check the battery indicator in the upper-left corner and attach the charger if the battery is low. Make sure the unit is plugged in and charging.

3. Press the “Folder” button (the green “4”) on the right side keypad.

4. Use the up and down arrows to navigate the options, and use the checkmark or “F7” button below the upper-right knob to select the preset program that best describes the part to be inspected.

5. Press “F7” to open the selected file (Hat Panel, I-Beam, or Porosity). The use of a mouse and keyboard is helpful in PAUT setup and operation.

6. Apply couplant to the reference standard and then place the probe on it to verify the preset program setup has not changed. If the delay shoe is worn, the entry surface is not present in the ultrasonic time base signal display and sectoral scan, and the preset needs revision by UT level III or designated UT level II.

7. Apply couplant to the part surface for which inspection is necessary. If a silver marker (or other paint marker) has been used to mark an area, it may need to be removed to prevent paint buildup on the shoe of the probe.

8. Set the encoder wheel to the “Start” position. Make a test scan 3 to 4 inches in length to verify the desired display has been obtained. Select the “Scan End” option and enter the desired scan length using the keypad.

9. To clear the screen for the scan, press the “Menu” button, and then select “Scan” and “Start.” Once the scan is made, save the inspection by naming the scan file in an incremental manner so the data may be traced back to a specific location or component. Save the inspection data on the PAUT unit.

10. To convert an image to .jpg, open the saved *.opd file by pressing the “Folder” button on the front panel. Select “File Type – Data” and double-click it to open it. Once the desired image is located, open the file, select “Screen” as the save mode, and enter the new file name using the keypad.

11. To improve the resolution of the ultrasonic depth base signal display image, reduce the number of transducer elements firing at once (select “Focal Law,” “Aperture,” “Elements,” and then reduce the quantity of elements). Note that changes to “Focal Law” removes time-corrected gain settings.

12. To change the ultrasonic raster scan display of recorded signal (C-scan) color, press ”F1” and then select “Display,” “Color,” “Load,” and then review the selections (optical nondestructive testing is usually preferred.) Note that if viewing amplitude data, the color display will default to black and white if the radio frequency display is selected.

The following steps should be followed to move a file from the OmniScan drive to a thumb drive:

1. Press “F1” on the left side of the unit.

2. Select “Preferences.”

3. Press “F4” to select “Service.”

4. Press “F9” to select “File Manager.”

5. Press “F2” to select “File Type,” and then select “Data” or “Image.”

6. Use the arrow keys or smart knob to scroll to the desired file, and then select the file by pressing the check-mark key beside the smart knob.

The following steps should be taken to set the scan length for the C-scan:

1. Press the blue “Menu” button on the left side of the unit.
2. Select the “Scan” option.
3. Select the “Area” option.
4. Select the “Scan End” option and then enter the desired scan length using the keypad.

APPENDIX C—DIGITAL ACOUSTIC VIDEO-INSPECTION TECHNIQUE

C.1 PURPOSE.

To provide nondestructive evaluation personnel a standard procedure for using the i600 Pulse-Echo (PE) AcoustoCam™.

C.2 INSPECTION METHODS.

The PE scanning via the i600 Camera AcoustoCam™ system.

C.3 INSPECTION STANDARD.

- Part-specific standards may be used for inspection.
- Setup to be completed on a reference standard of material similar to that which will be inspected (step-wedge is acceptable).
- Verify at least two depths of a known thickness (should read within +/- 0.005″ of a known material thickness).

C.4 EQUIPMENT SETUP.

All equipment setup instructions in this section are to be performed with the power supply unplugged and the battery removed.

1. Connect the main camera cable and its two thumb screws and then the BNC cable to the top of the control unit.

2. Turn the camera upside down (membrane facing upward) and look in the membrane to see if there are any air bubbles. If there are no air bubbles in the camera, skip the next step. If there are bubbles in the camera or the water level is low (membrane is not flush with contact surface), the following sequence should be followed:

   a. Camera Filling/Air Bubble Removal

3. Remove the transducer (this is not required, but is helpful) by pulling the cover off near the camera nozzle. Slide the transducer toward the nozzle to remove it. Take care not to get water in the transducer connection while filling the camera with the transducer removed.

4. If there is no water in the camera head, make sure the membrane is not perforated. If it is, rotate the nozzle ring counter-clockwise (CCW) to remove the nozzle cap and replace the membrane. Reinstall the nozzle cap, turning it clockwise (CW) until snug.

5. Install the fill tool (clear plastic cap with etched circle) until it is fully seated on the nozzle cap.

6. Remove the two rubber valve covers on the camera body. Pinch the in-line pinch lock closed on the vent line. Attach the vent line to either of the valves on the camera body.

7. Squeeze the in-line reservoir pinch locks until the line is closed. Fill the reservoir with deionized water and replace the reservoir cap, but do not tighten it; the cap must be loose to vent.

8. Open the pinch lock and allow water to flow through the line, which will help remove air from the line and in-line filter.

9. Insert the filler line into the other quick disconnect valve on the camera body. Water will begin rushing into the camera once the filler and vent lines are open. Unlock the pinch lock.

10. Tap and pinch the vent lines to help bubbles rise in the line. Look through the end of the camera or through the side if the transducer is removed to locate bubbles. Rock or tilt the camera to position the bubbles to the vent tube port.

11. Close the pinch lock on the fill tube and disconnect the fill tube. There should still be at least a few inches of water in the vent tube.

12. Repeatedly tap and pinch the vent tube while rocking the camera to position the air bubbles near the vent port.

13. When all visible air bubbles have been purged, make sure the membrane contact area matches the scribed circle on the fill tool.

14. Lock the pinch lock on the vent tube and disconnect the tube.

15. Remove the fill tool by pulling it off of the nozzle tip and rotating it CW.

16. Reapply the rubber valve covers over the valves.

17. Reinstall the desired transducer by applying a thin film of grade 10 couplant to the camera port face and gently sliding the transducer into its connector.

18. Visually inspect through the membrane to verify there are no air gaps, bubbles, or voids between the transducer and the camera.

19. Remove and reinstall the transducer by removing the transducer cover, sliding out the transducer, and adding grade 10 couplant if needed.

20. Attach the external power supply to the control unit by securing the circular weather-tight connector located on the left side of the unit (insert the power plug and turn CW), or insert a battery into the compartment located on the top of the unit. Do not apply external power to the camera while operating the camera with a battery.

C.5 INSPECTION SETUP.

1. Turn on the i600 AcoustoCam unit by briefly pressing the "Power" button on top of the unit at the left side and let it boot up.

2. Turn the pulser power all the way down by rotating the knob on the upper-left side CCW.

3. Press the "Presets" icon on the upper-left corner of the screen.

4. Select the desired program that best fits the part to be inspected and then press the "Refresh" key ( ) on the screen. Adjust the gain or gates slightly to optimize the ultrasonic raster scan display of recorded signal (C-scan).

5. Apply approved couplant as necessary to the area to be scanned.

6. Place the camera on the part or setup standard (membrane to the part surface). The image should show the flat-bottom drilled holes or steps in the setup standard and in some coarse material or fabric patterns. If it doesn't, adjust the focus on the i600 camera by rotating the focus wheel in the camera head. Impact damage appears as a lighter area with irregular shape and a dark border, whereas foreign object debris inserts appear as more regular/defined shapes. Porosity will appear as a darker, spotty image and, when severe enough, it will not allow finger damping on the backside surface. Impact repairs will appear as defined shapes with more attenuation.

7. Adjust the gain knob on the upper left face of the machine as needed to obtain the desired brightness and contrast.

8. Adjust the Pulse per burst (PPB) up if the image is too dark and the gain knob is at its limit (select Pulser at the top of the screen and PPB at the bottom of the screen, and then use the arrow keys to adjust PPB).

9. Verify that the C-scan gate is at or near zero if the image is going dark over shallow areas in the standard. If the C-scan has rings, the camera may not be filled correctly or the C-scan gate start may need to be moved out a little (to about 0.020″).

10. Use the camera-fill video procedure noted earlier if a small black spot appears on the C-Scan. A small bubble may be in the camera.

11. Make sure the part has not coupled to the surface of the test stand (table top) if an attenuated (darker) area appears in a scan.

12. Begin scanning with approximately 1/2″ index (~50% overlap of the 1″ x 1″ source transducer) once the desired image is acquired.

13. View the ultrasonic time base signal display (A-scan) and C-scan displays by pressing the "C/A" key on the lower-right area of the screen. Indication depth may be acquired with the A-scan gate set with the gate start just beyond the entry surface signal and about 0.1″ beyond the back wall echo signal. This may already be in the preset program.

14. Verify that the digital depths on the standard shown in section 3 match the digital reading within about 0.010″. Adjust the A-scan gate if necessary (select "Gates" at the top of the screen; "A-scan" at the bottom of the screen; and then "Gate Start," "Width," or "Height" and make adjustments as needed).

C.6 SCREEN CAPTURE–SAVING IMAGES.

A still image may be saved to a thumb drive for further evaluation by following this sequence:

1. Press the "Capture" button on the upper-left area of the touchscreen.

2. With the camera positioned at the area of interest, press the "Snapshot" button on the touchscreen.

   Note that when "Image Auto-Naming" is turned off, the keyboard display will automatically appear on the touchscreen. If it does not appear, then "Image Auto-Naming" is turned on. On a blade, it may be the "Station" number and distance from the leading edge (chord).

3. Press "Enter" on the keyboard display to save the image to the machine.

C.7 REVIEW OF CAPTURED IMAGES.

1. Press the "Capture" button on the touchscreen.
2. Press the "Storage" tab on the touchscreen.
3. Open the desired image by selecting it on the touchscreen.

C.8 DOWNLOAD OF CAPTURED IMAGE(S).

1. Insert the thumb drive in the bottom-right side of the control box.

2. Press the "Capture" button on the touchscreen.

3. Select the "Download" tab on the touchscreen.

4. Select images for transfer, then select "Start Copy" to leave images on the machine or "Start Move" to transfer the images from the machine to the thumb drive. Press "OK" to complete the transfer.

C.9 EQUIPMENT SHUTDOWN.

1. Press the “Close” button in the upper-right corner (which looks like a door with an arrow by it).

2. When asked, “Do you want to exit?”, select “Yes.” The machine will power itself down.

APPENDIX D—LARGE-SCALE IMPACT PANEL

The FAA requested a long, carbon epoxy, hat-stiffened impact test panel and a long I-Beam-stiffened impact test panel. The panels were to be similar in design to the impact test panels used to evaluate the selected technologies of this project. The panels were fabricated and painted, and then baseline through-transmission ultrasonic raster scanned display of recorded signal (C-scanned) to verify their acceptance. The panels were then impacted in the same manner as the impact panels in this report. After impact, the panels were pulse-echo C-scanned and shipped.

Figure D-1 shows the test panel layout.

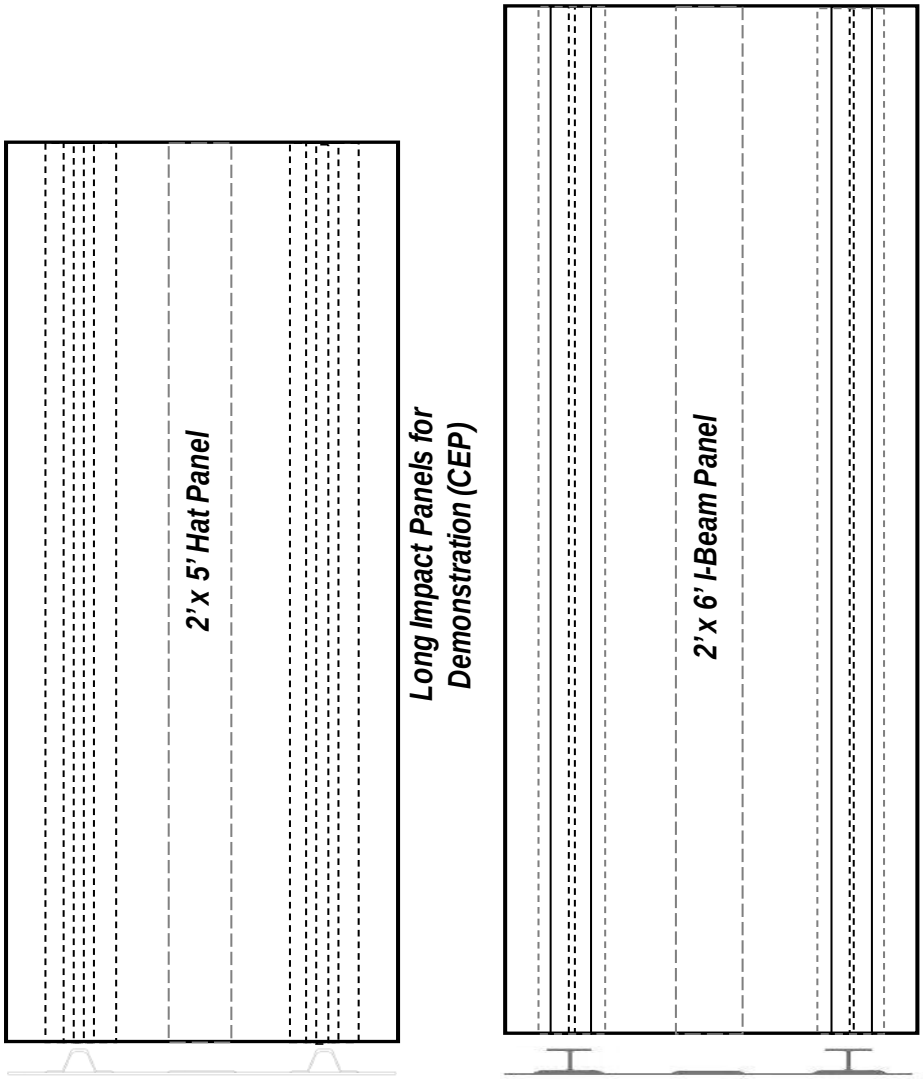

Figure D-1. Test Panel Layout

Figure D-2(a) shows the painted exterior surface. The project logo is attached in the upper-right corner. Figure D-2(b) shows the interior hat-side surface. Attenuation tabs appear as white squares in the photograph.

(a) (b)

Figure D-2. Panel (a) Outer and (b) Inner View After Paint (typical)

An impact force layout plan was created for the 2′ x 5′ hat panel and then mapped out onto the test panel (see figure D-3).

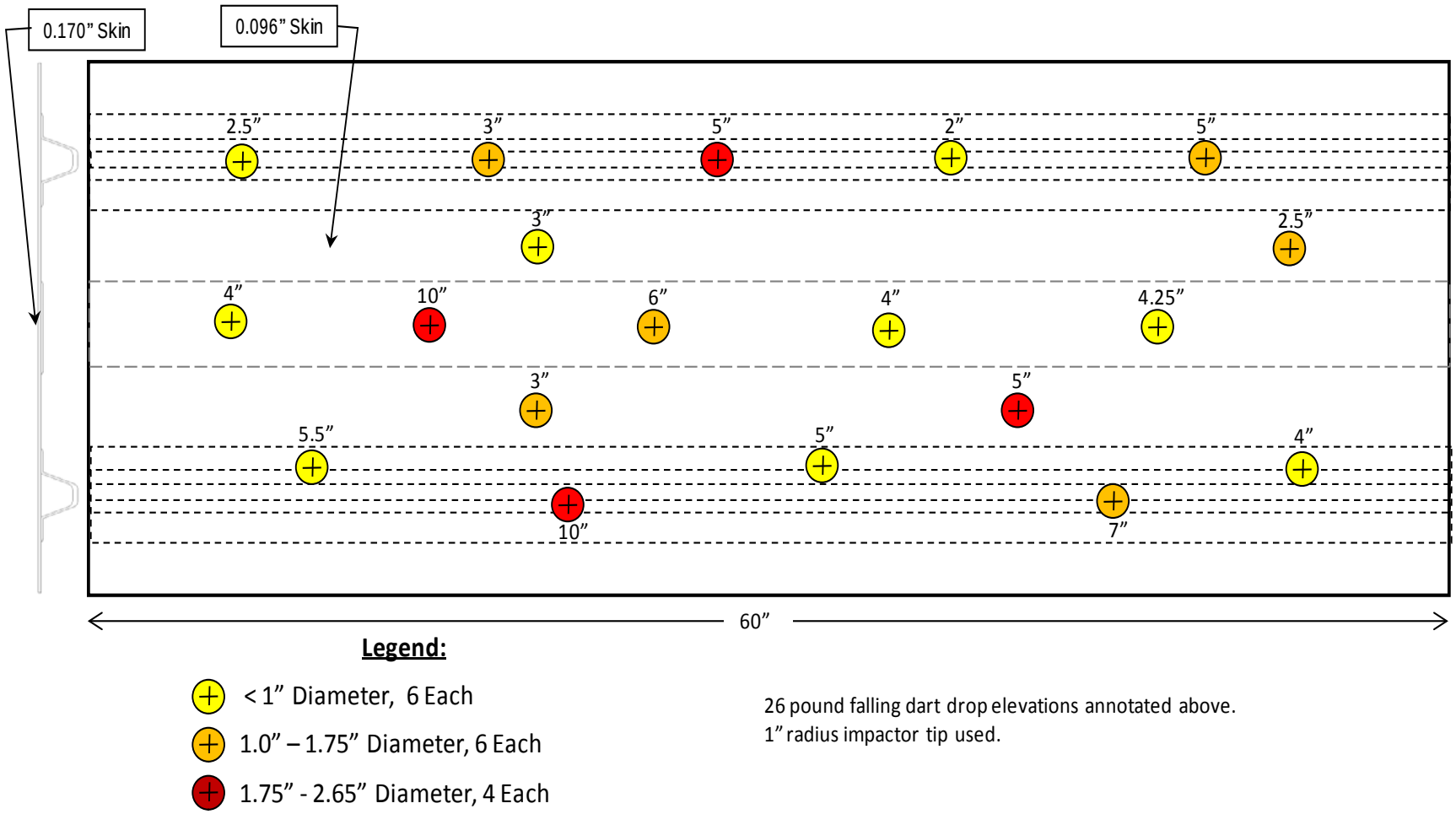

Figure D-3. Impact Force Layout Plan, Hat Panel

An impact force layout plan was created for the 2′ x 6′ I-Beam panel and then mapped out onto the test panel (see figure D-4).

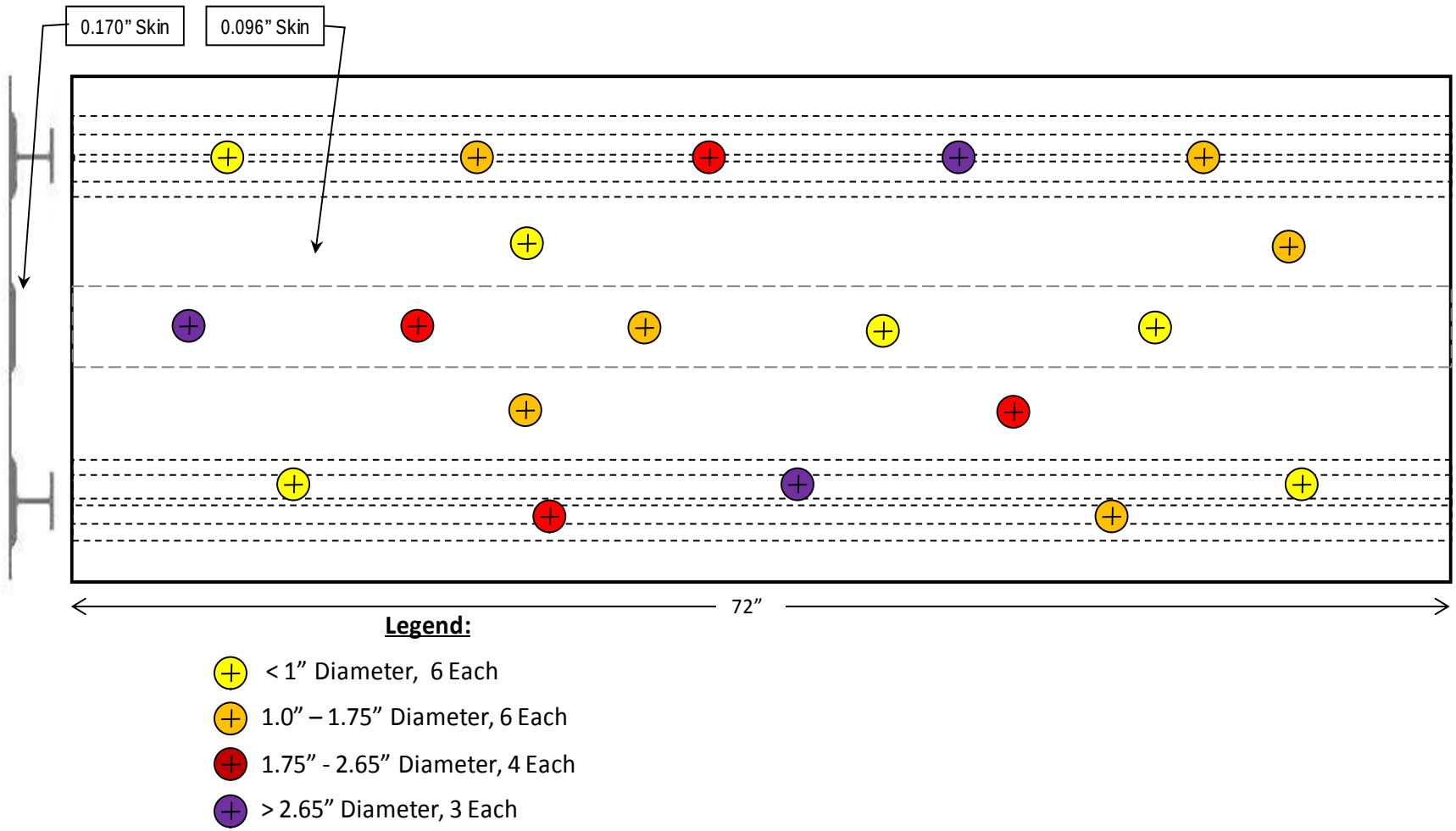

Figure D-4. Impact Force Layout Plan, I-Beam Panel

The planned impact locations and forces were noted on thin tape on the panel. The impacts were applied to the panel with a calibrated impact test rig. A portable ultrasonic testing machine was used to validate impact damage sizes (see figure D-5).

Figure D-5. A plastic isolator is inserted between impactor tip and panel to prevent multiple impacts during the falling dart impact test. Weights are used to keep the panel firmly in place.

The Ultrasonic PE time of flight (ToF) C-scan of the hat-stiffened panel after impact is shown in figure D-6(a). The project logo had already been applied to this panel, as seen in the top-right corner of the scan. The PE ToF C-scan of the I-beam stiffened panel after impact is shown in figure D-6(b). Shallow delaminations appear darker in color in the PE ToF C-scan.

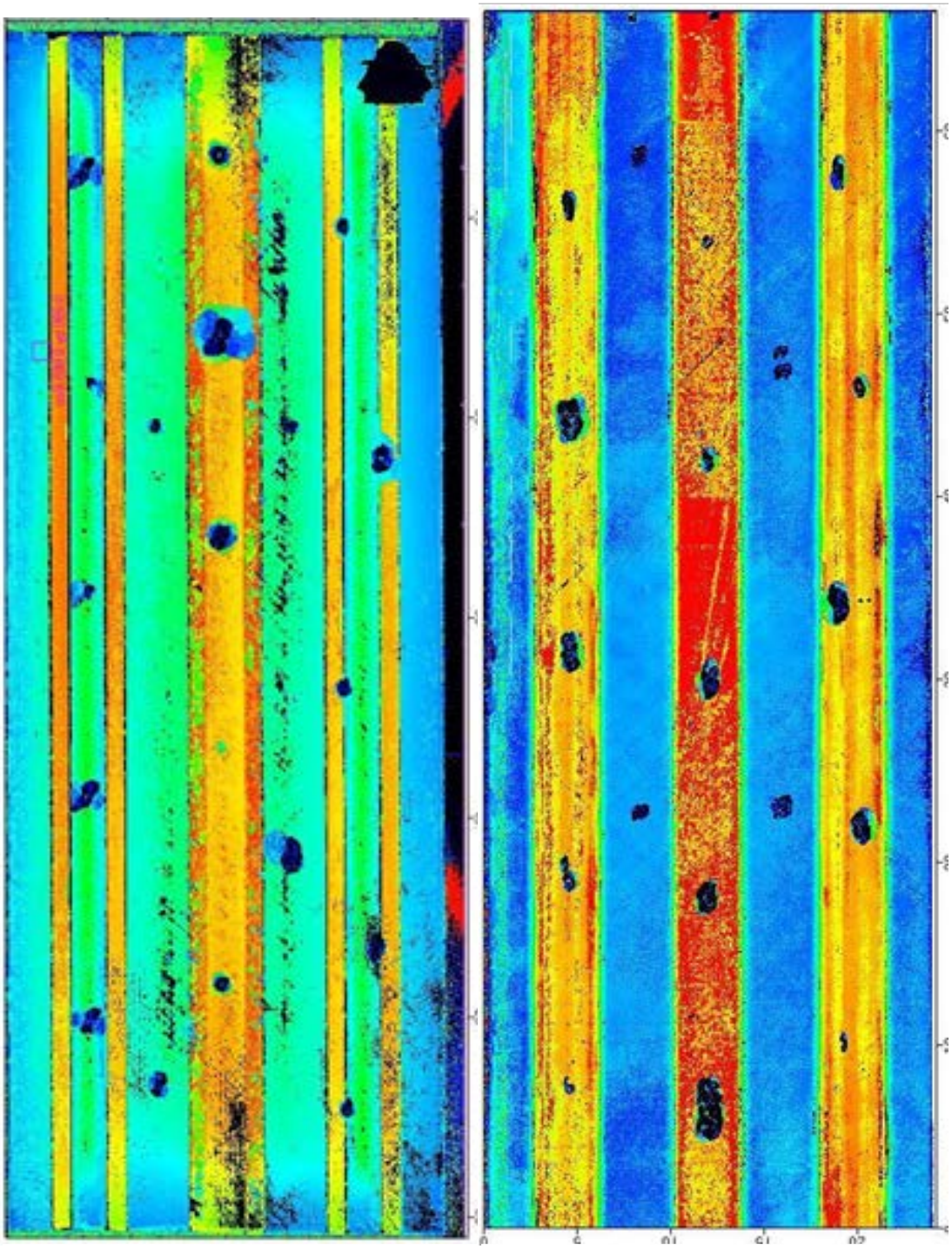

(a) (b)

Figure D-6. The (a) Hat Panel PE ToF C-Scan and (b) I-Beam PE ToF C-Scan

Table Of Contents

- **Panel FAA-I-1**

1. Omniscan Phased Array Plastic Wedge
2. Omniscan Phased Array Aqualene Wedge
3. Omniscan Pulse Echo Contact Testing
4. MAUS V Pulse Echo
5. MAUS V Resonance
6. Ramp Damage Checker/Bondmaster/A-Scan Impacts
7. Flash Thermography (IR)

- **Panel FAA-I-2**

1. Omniscan Phased Array Aqualene Wedge
2. Omniscan Pulse Echo Contact Testing
3. MAUS V Pulse Echo
4. MAUS V Resonance
5. Ramp Damage Checker/Bondmaster/A-Scan Impacts
6. Flash Thermography (IR)

Table Of Contents

- **Panel FAA-I-003**

1. Omniscan Phased Array Plastic Wedge
2. Omniscan Pulse Echo Contact Testing
3. MAUS V Pulse Echo
4. MAUS V Resonance
5. Ramp Damage Checker/Bondmaster/A-Scan Impacts
6. Flash Thermography (IR)

- **Panel FAA-H-001**

1. Omniscan Phased Array Aqualene Wedge
2. MAUS V Pulse Echo
3. MAUS V Resonance
4. Ramp Damage Checker/Bondmaster/A-Scan Impacts
5. Flash Thermography (IR)

National Nuclear Security Administration
Sandia National Laboratories

Table Of Contents

- **Panel FAA-FOD-01**

1. Omniscan Phased Array Aqualene Wedge
2. Omniscan Pulse Echo Contact Testing
3. MAUS V Pulse Echo
4. MAUS V Resonance
5. Ramp Damage Checker/Bondmaster/A-Scan Impacts
6. Flash Thermography (IR)

- **Panel FAA-FOD-02**

1. Omniscan Phased Array Aqualene Wedge
2. Omniscan Pulse Echo Contact Testing
3. MAUS V Pulse Echo
4. MAUS V Resonance
5. Ramp Damage Checker/Bondmaster/A-Scan Impacts
6. Flash Thermography (IR)

NNSA National Nuclear Security Administration
Sandia National Laboratories

Table Of Contents

- **Panel FAA-H-002**

1. Omniscan Phased Array Plastic Wedge
2. Omniscan Phased Array Aqualene Wedge
3. Omniscan Pulse Echo Contact Testing
4. MAUS V Pulse Echo
5. MAUS V Resonance
6. Ramp Damage Checker/Bondmaster/A-Scan Impacts
7. Flash Thermography (IR)

- **Panel FAA-H-003**

1. Omniscan Phased Array Plastic Wedge
2. Omniscan Phased Array Aqualene Wedge
3. Omniscan Pulse Echo Contact Testing
4. MAUS V Pulse Echo
5. MAUS V Resonance
6. Ramp Damage Checker/Bondmaster/A-Scan Impacts
7. Flash Thermography (IR)

National Nuclear Security Administration

Sandia National Laboratories

Bell-Innovative, Image Based NDE for Modern Rotorcraft Sustainment I-Beam Stiffened Panel FAA-I-1

Top

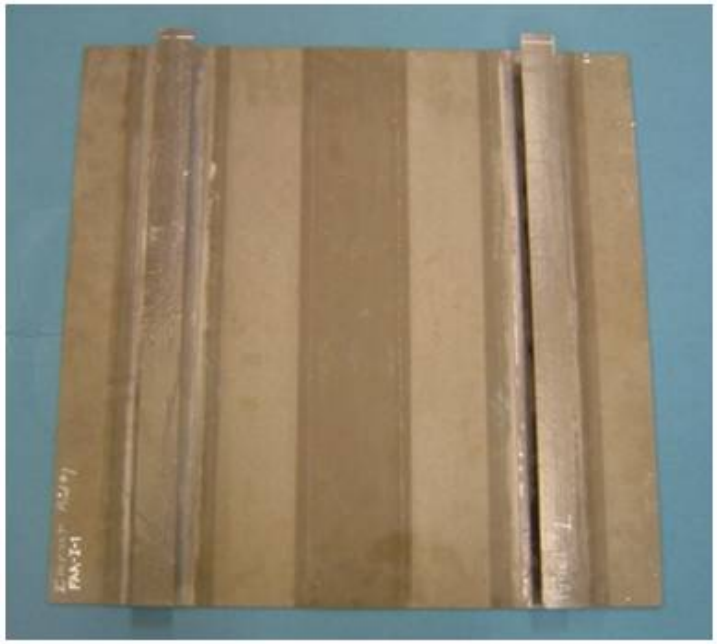

Bottom

National Nuclear Security Administration

Sandia National Laboratories

I Beam Stiffened Panel FAA-I-1 Bell-Innovative, Image Based NDE for Modern Rotorcraft Sustainment
Omniscan 10L64 (10 MHZ) Phased Array Plastic Wedge

Typical Backwall Signal

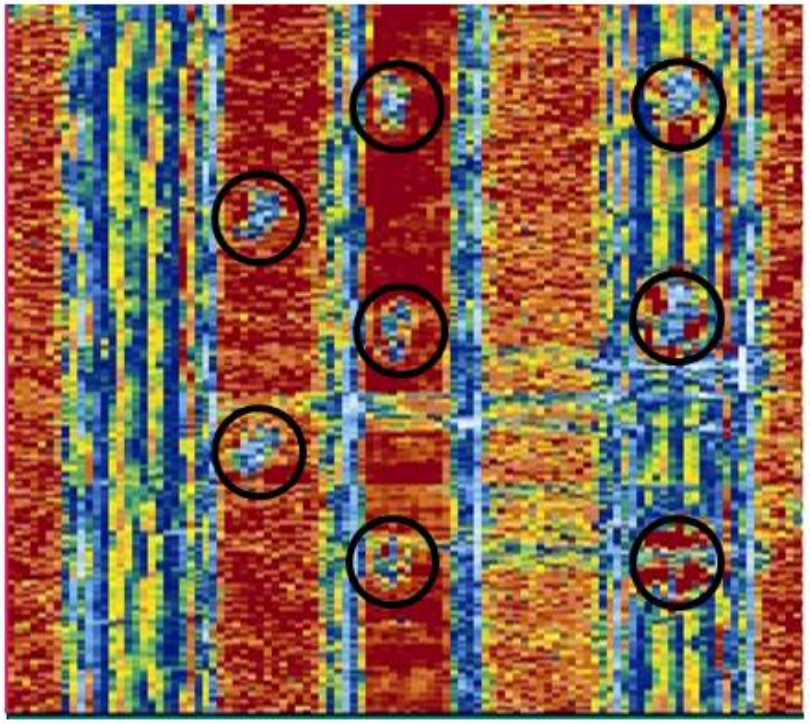

C-Scan Image

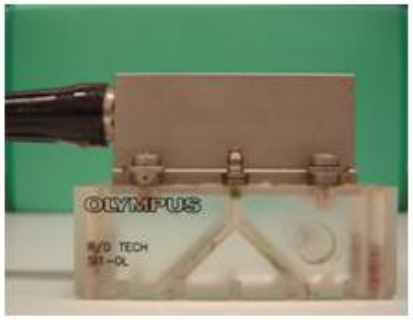

National Nuclear Security Administration

Sandia National Laboratories

I Beam Stiffened Panel FAA-I-1 Bell-Innovative, Image Based NDE for Modern Rotorcraft Sustainment
Omniscan 5L64 (5 MHZ) Phased Array Aqualene Wedge

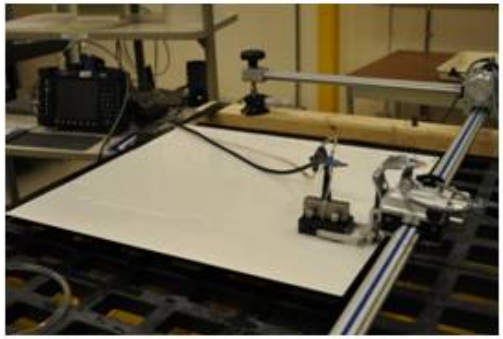

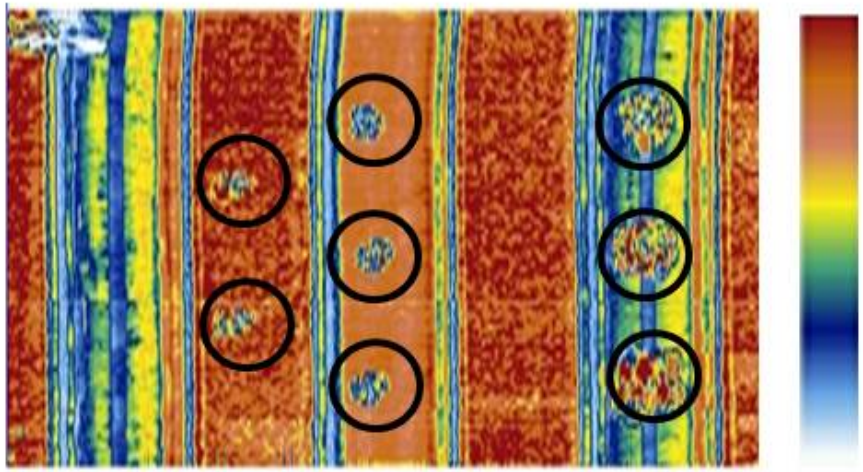

Amplitude

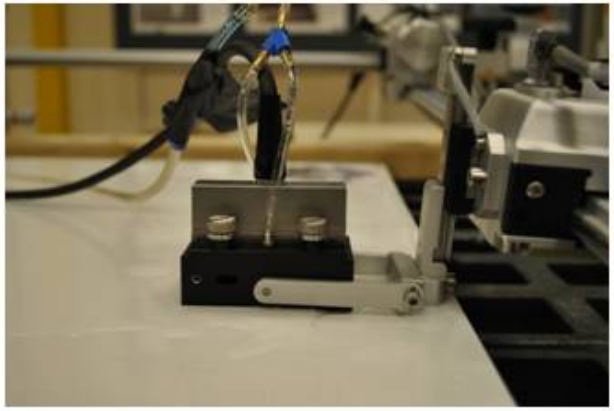

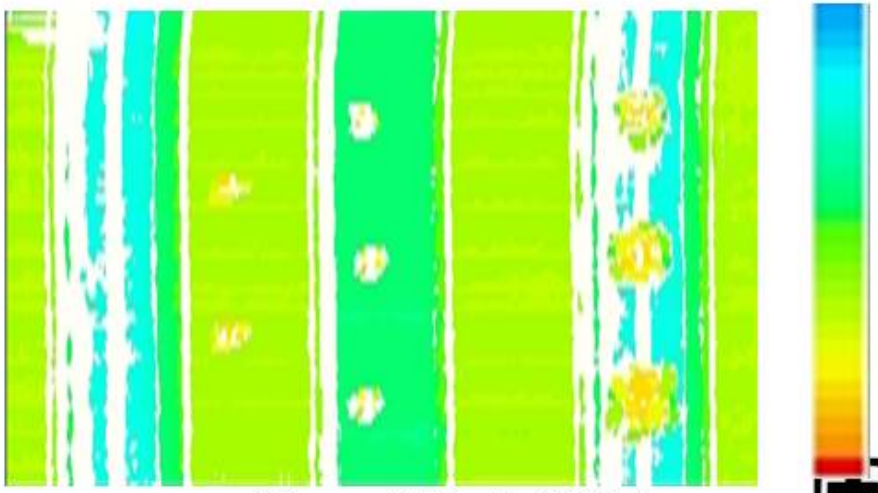

Time of Flight (TOF)

National Nuclear Security Administration

Sandia National Laboratories

I Beam Stiffened Panel FAA-I-1 Bell-Innovative, Image Based NDE for Modern Rotorcraft Sustainment Omniscan 5 MHZ/.5" Diameter PE Contact

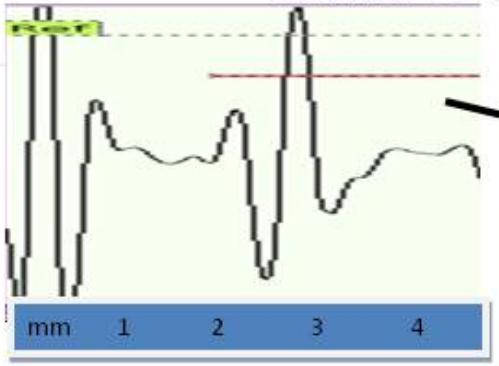

Typical Good
(2.97 mm)

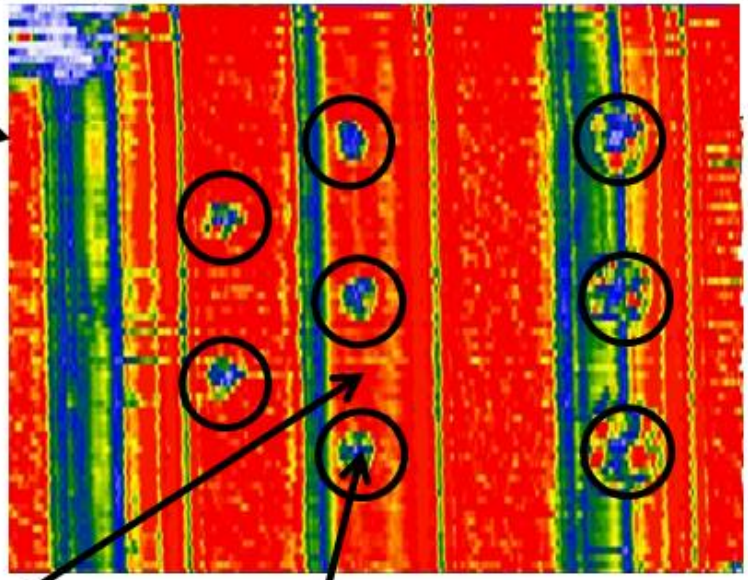

C-Scan
Image

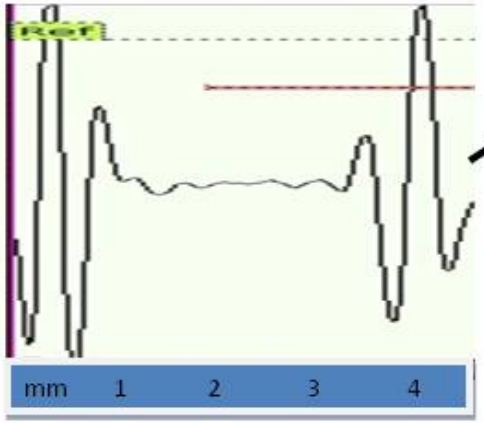

Typical Good Middle Area
(3.98 mm)

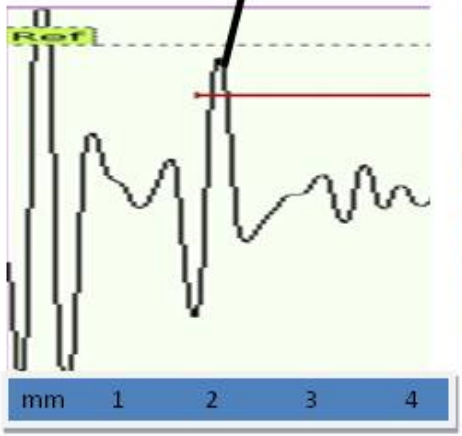

Typical Bad Middle Area

National Nuclear Security Administration

Sandia National Laboratories

I Beam Stiffened Panel FAA-I-1
Bell-Innovative, Image Based NDE for Modern Rotorcraft Sustainment
MAUS 5 Pulse Echo 5 MHZ

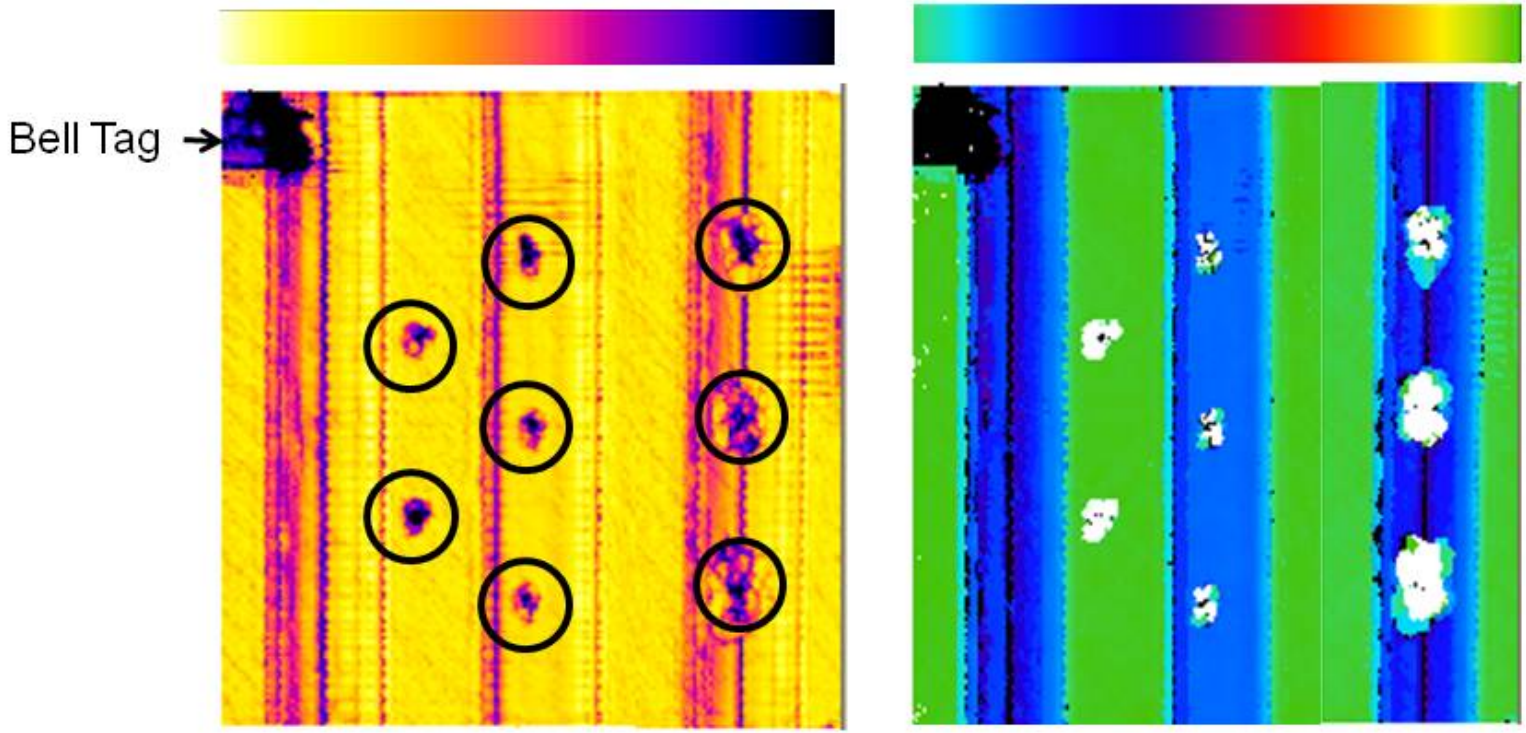

Amplitude

Time of Flight (Depth)

National Nuclear Security Administration

Sandia National Laboratories

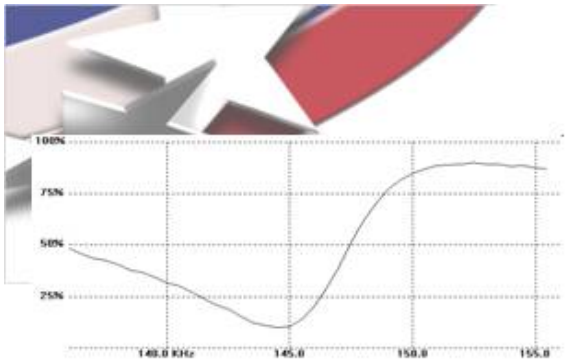

I Beam Stiffened Panel FAA-I-1
Bell-Innovative, Image Based NDE for Modern Rotorcraft Sustainment
MAUS 5 Resonance 145 KHZ

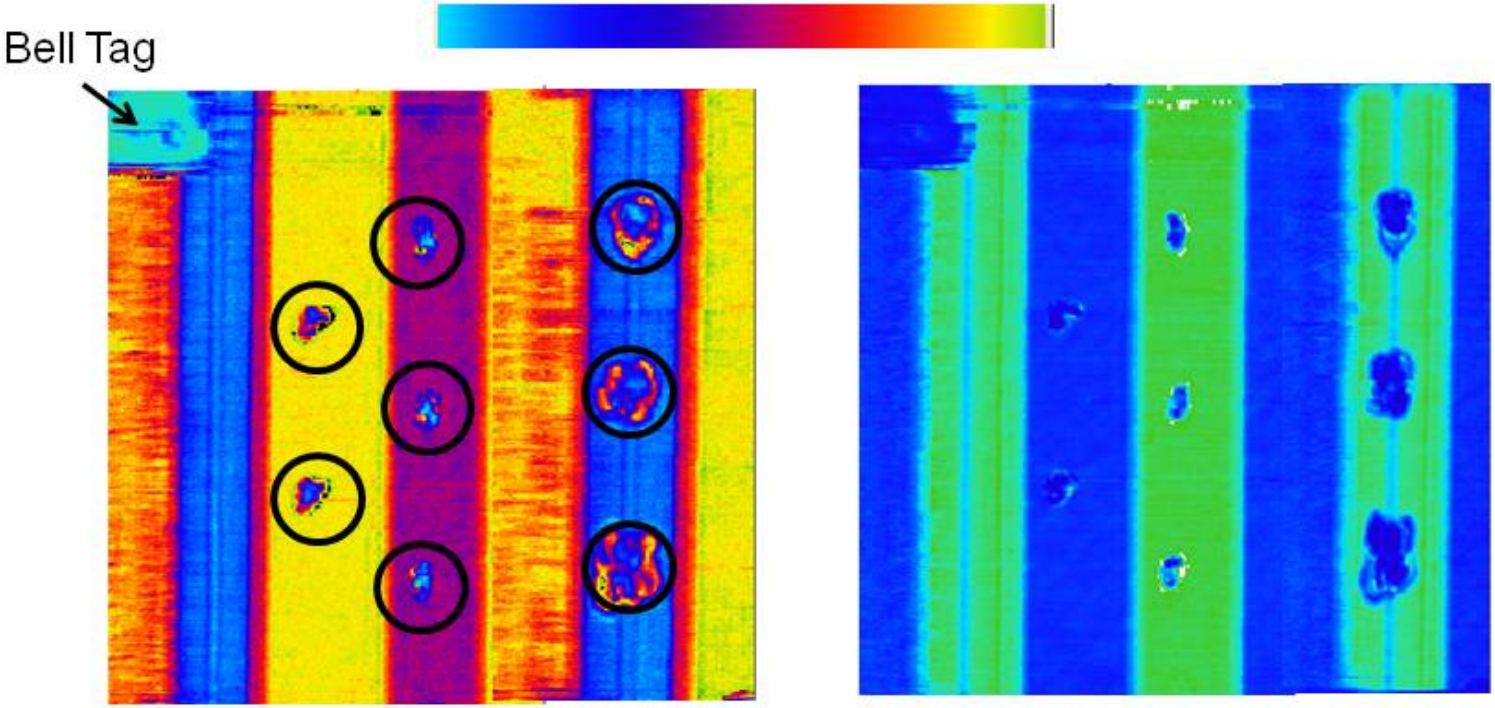

X-Plot

Y-Plot

National Nuclear Security Administration

Sandia National Laboratories

I Beam Stiffened Panel FAA-I-1Bell-Innovative, Image Based NDE for Modern Rotorcraft Sustainment Bondcheck- Pulse Echo 5 MHZ and Bondmaster- Resonance 312 KHZ

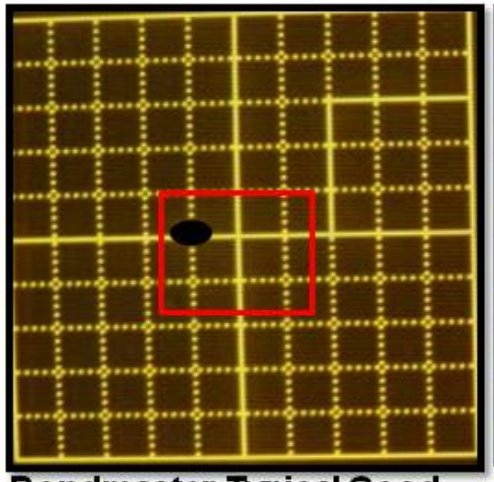

Bondmaster-Typical Good

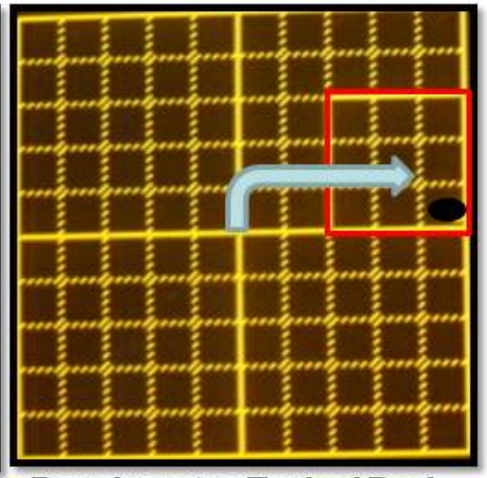

Bondmaster-Typical Bad

Olympus 35RDC Ramp Damage Checker

Note: Scanning technique for Ramp Damage Checker and Bondmaster . Scan started from the cal in point in a straight line from top to bottom of the panels. If thickness area changed, then re-cal was completed for that particular thickness.

National Nuclear Security Administration

Sandia National Laboratories

I Beam Stiffened Panel FAA-I-1BeII-Innovative, Image Based NDE for Modern Rotorcraft Sustainment 1000i Olympus Ultrasonic Tester 5 MHZ Contact A-Scans

Ramp Damage Checker/Bondmaster Results

Point A- Bad/Bad

Point B- Bad/Bad

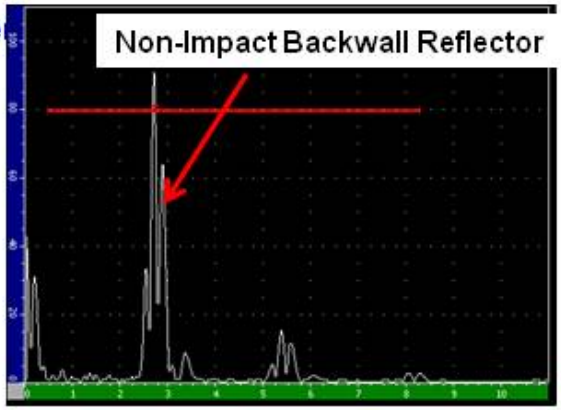

Cal In- 90% Amplitude/29.9db (2.66mm)

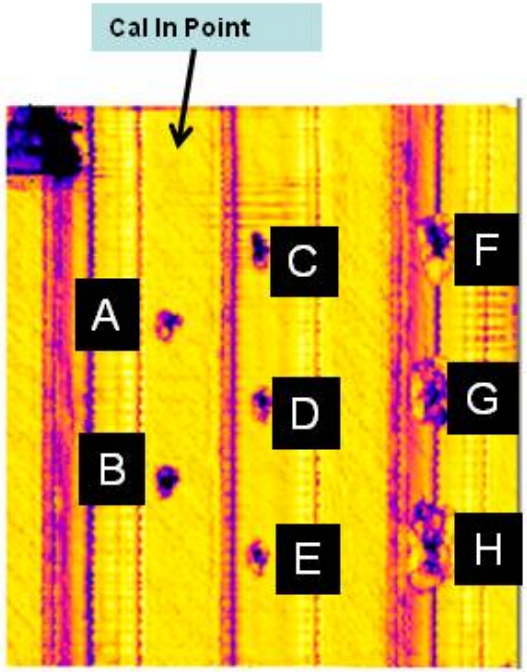

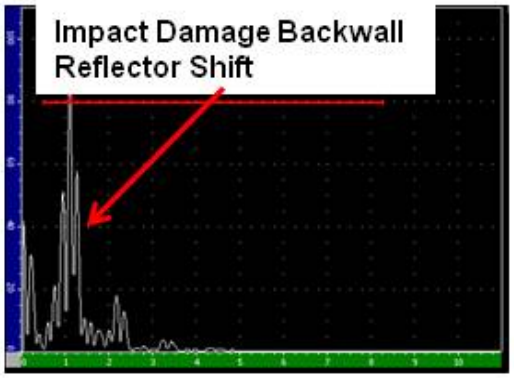

Point A-88% Amplitude

Point B- 107.5 Amplitude

NOTE: Noted dB and Amplitude Changes different from the Cal In

I Beam Stiffened Panel FAA-I-1BeII-Innovative, Image Based NDE for Modern Rotorcraft Sustainment 1000i Olympus Ultrasonic Tester 5 MHZ Contact A-Scans

Ramp Damage Checker/Bondmaster Results

Point C- Bad/Bad
Point D- Bad/Bad
Point E- Bad/Bad

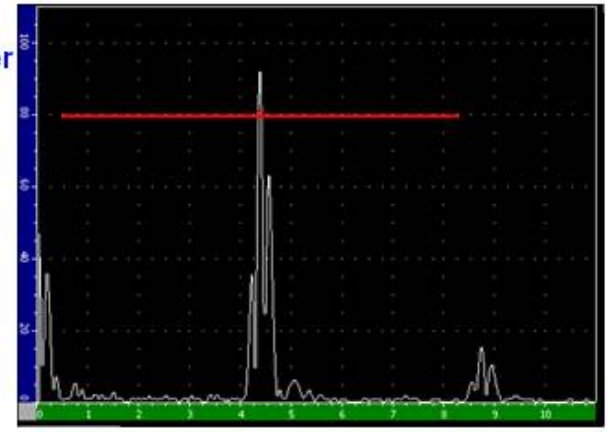

Cal In- 90% Amplitude/30.5dB (4.10mm)

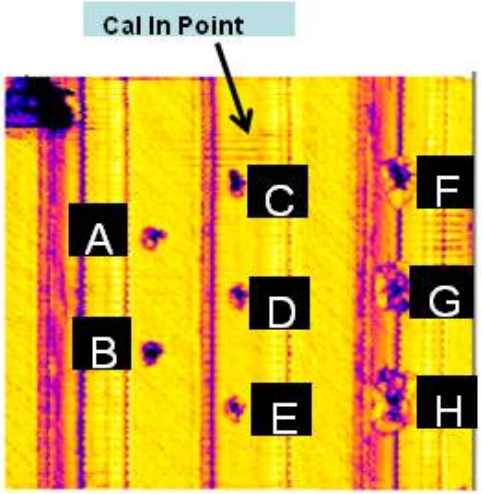

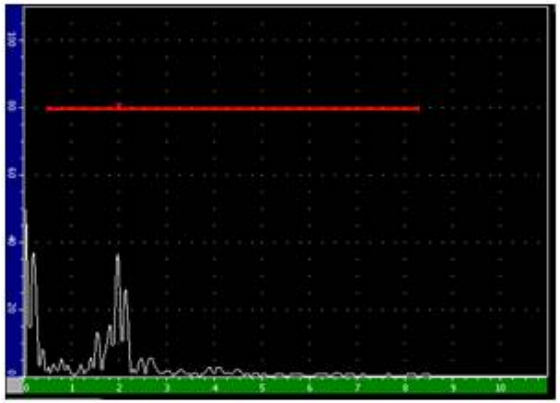

Point C- 36.75% Amplitude

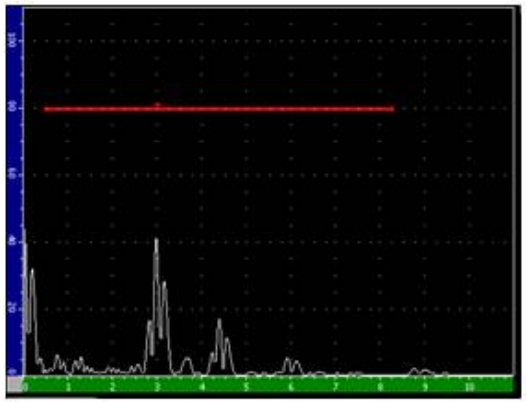

Point D- 41.50% Amplitude

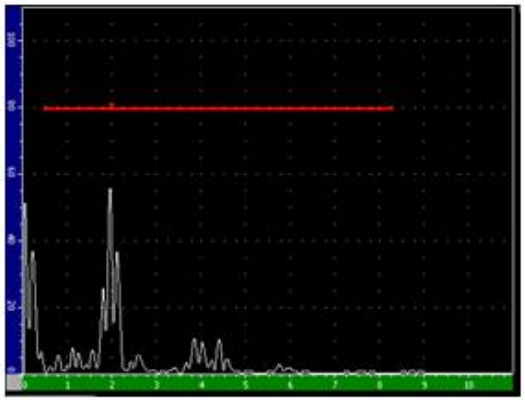

Point E- 56.25% Amplitude

NOTE: Noted dB and Amplitude Changes different from the Cal In

I Beam Stiffened Panel FAA-I-1BeII-Innovative, Image Based NDE for Modern Rotorcraft Sustainment 1000i Olympus Ultrasonic Tester 5 MHZ Contact A-Scans

Ramp Damage Checker/Bondmaster Results

Point F- Bad/Bad
Point G- Bad/Bad
Point H- Bad/Bad

NOTE: Noted dB and Amplitude Changes different from the Cal In

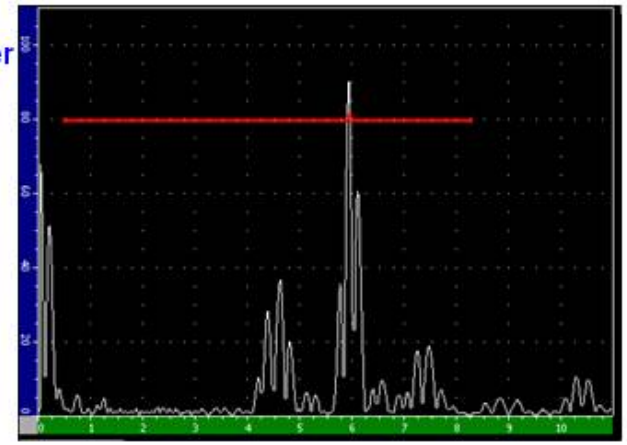

Cal In- 90% Amplitude/33.0dB (5.70mm)

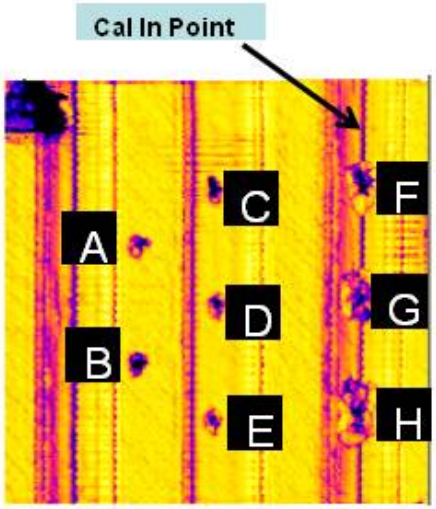

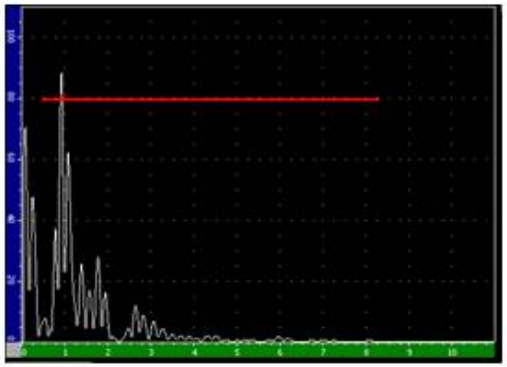

Point F-89% Amplitude

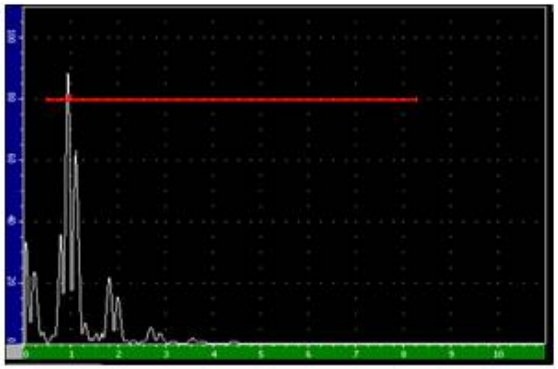

Point G-90% Amplitude

Point H-86.5% Amplitude

Note: Reduced Gain To 26.7dB for Point G and Point H

National Nuclear Security Administration

Sandia National Laboratories

FAA-I-1 Impact Panel
Flash Thermography (IR)

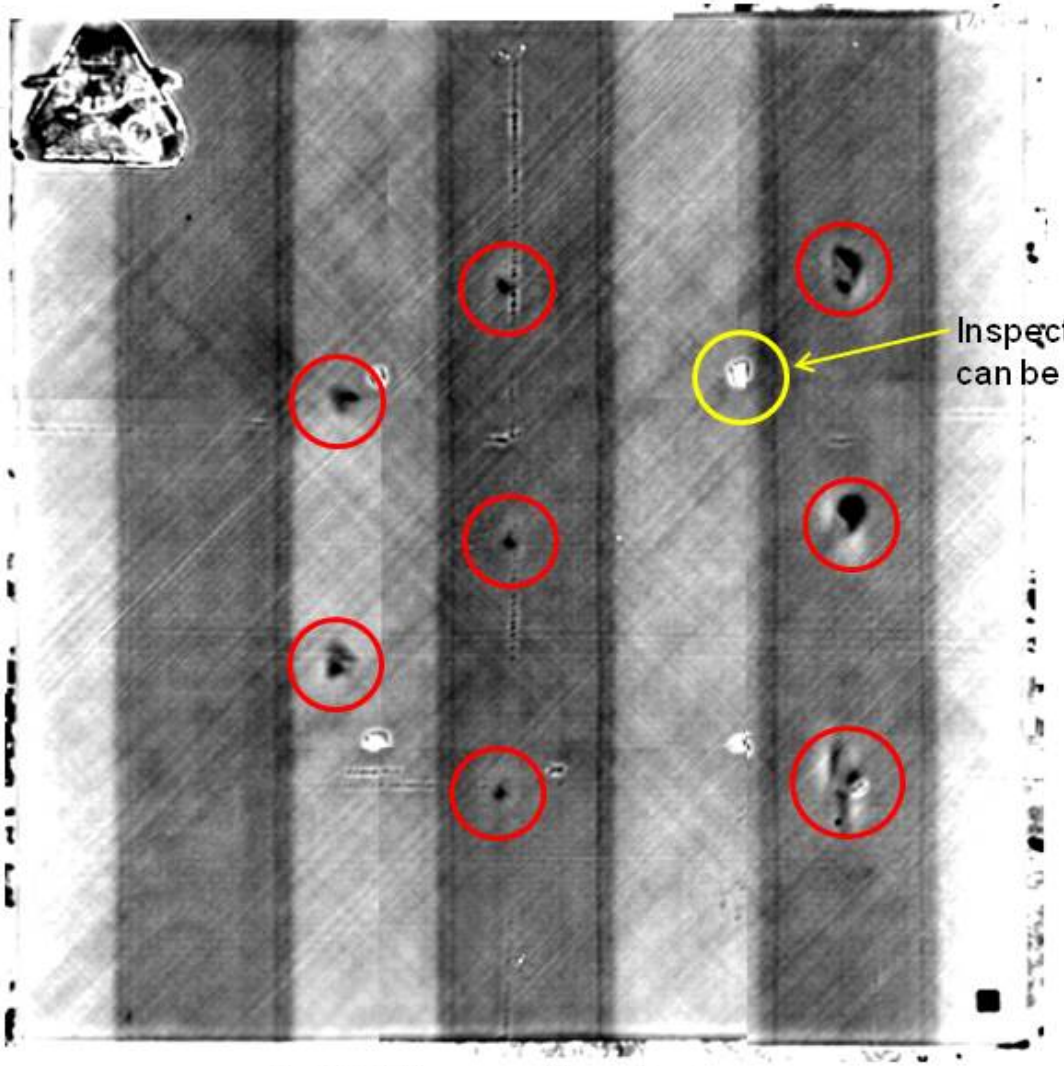

2d 1.201 sec after flash

National Nuclear Security Administration

Sandia National Laboratories

I Beam Stiffened Panel FAA-I-2 Bell-Innovative, Image Based NDE for Modern Rotorcraft Sustainment

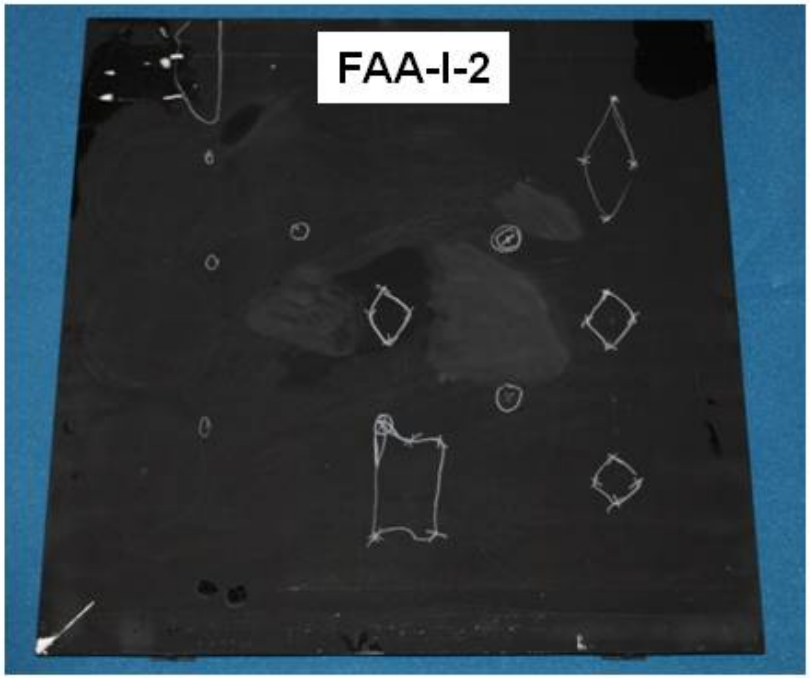

Top

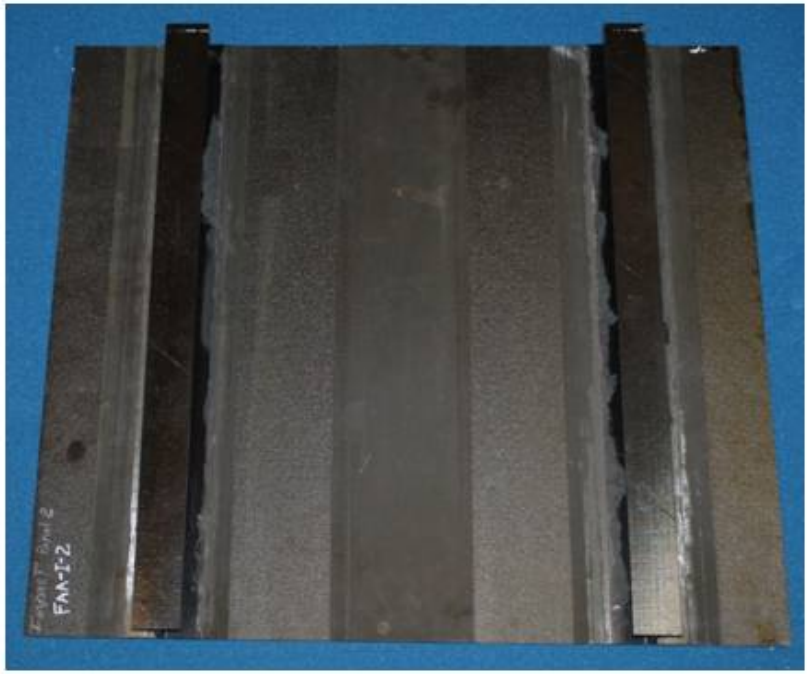

Bottom

National Nuclear Security Administration

Sandia National Laboratories

I Beam Stiffened Panel FAA-I-2 Bell-Innovative, Image Based NDE for Modern Rotorcraft Sustainment
Omniscan 5L64 (5 MHZ) Phased Array Aqalene Wedge

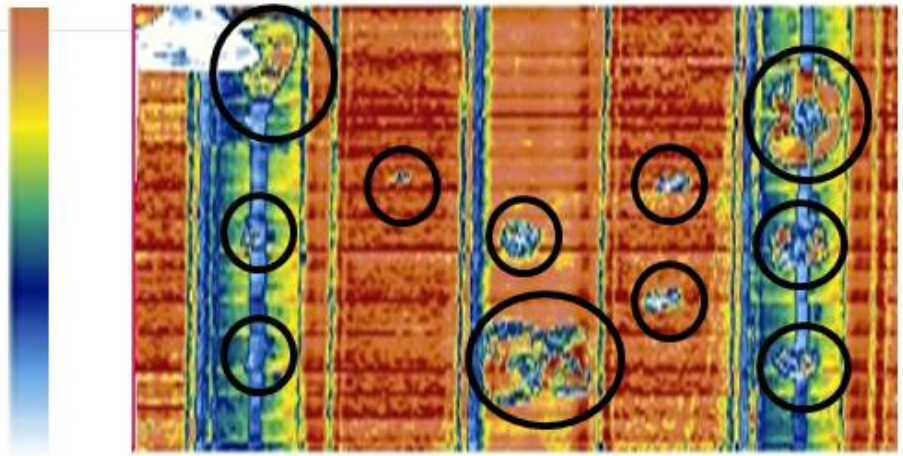

Amplitude

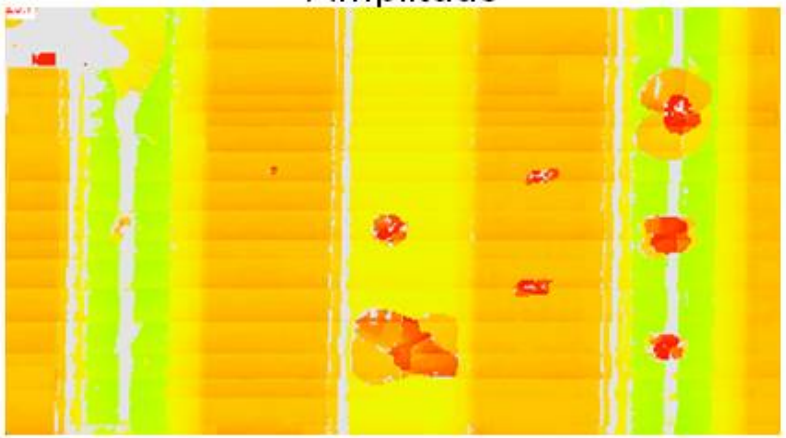

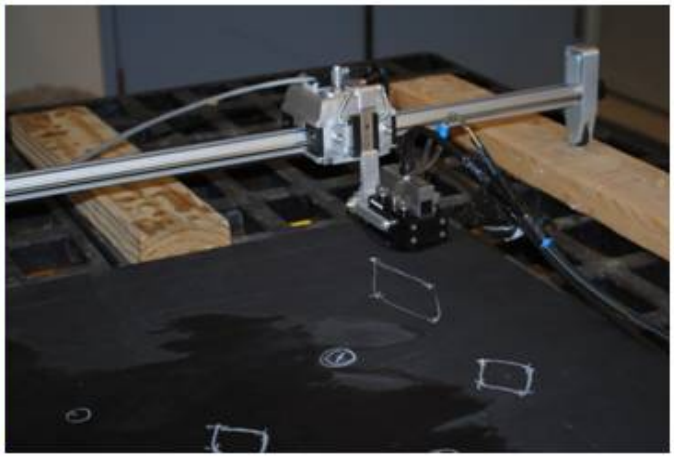

TOF

National Nuclear Security Administration

Sandia National Laboratories

I Beam Stiffened Panel FAA-I-2 Bell-Innovative, Image Based NDE for Modern Rotorcraft Sustainment Omniscan 5 MHZ/.25" Diameter Contact Testing

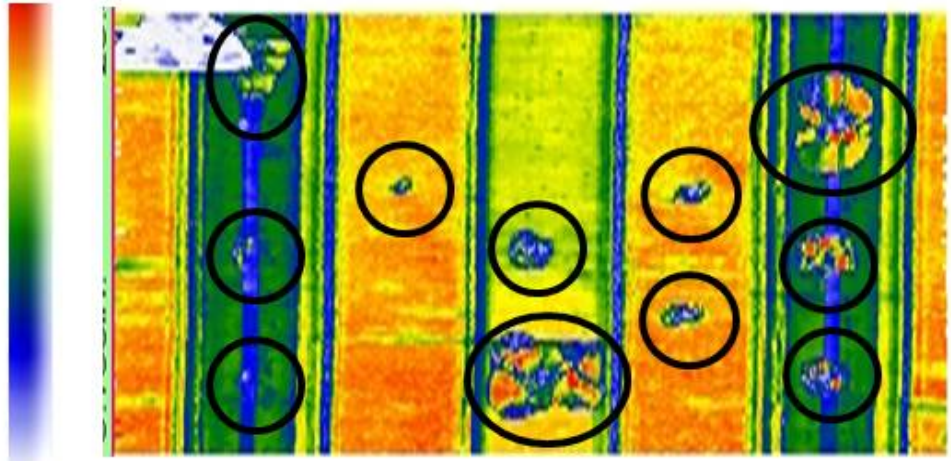

Amplitude

Note: I was able to improve image resolution by reducing the index increment and probe diameter.

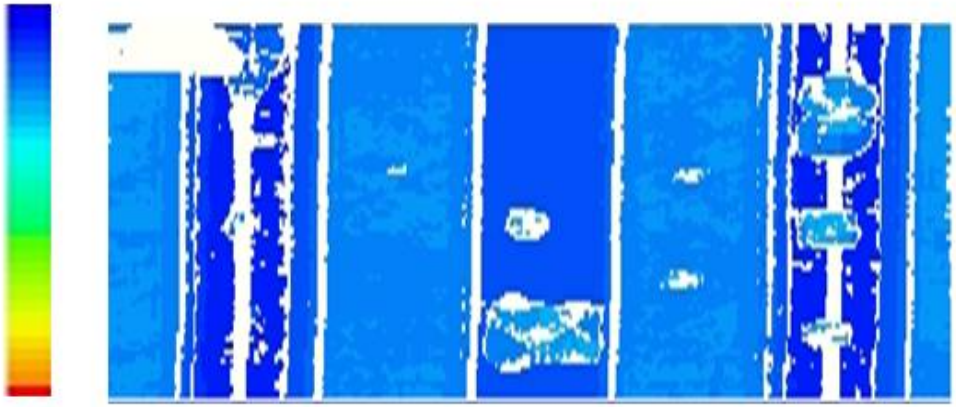

TOF

I Beam Stiffened Panel FAA-I-2 Bell-Innovative, Image Based NDE for Modern Rotorcraft Sustainment MAUS V Pulse Echo 5 MHZ Contact Testing

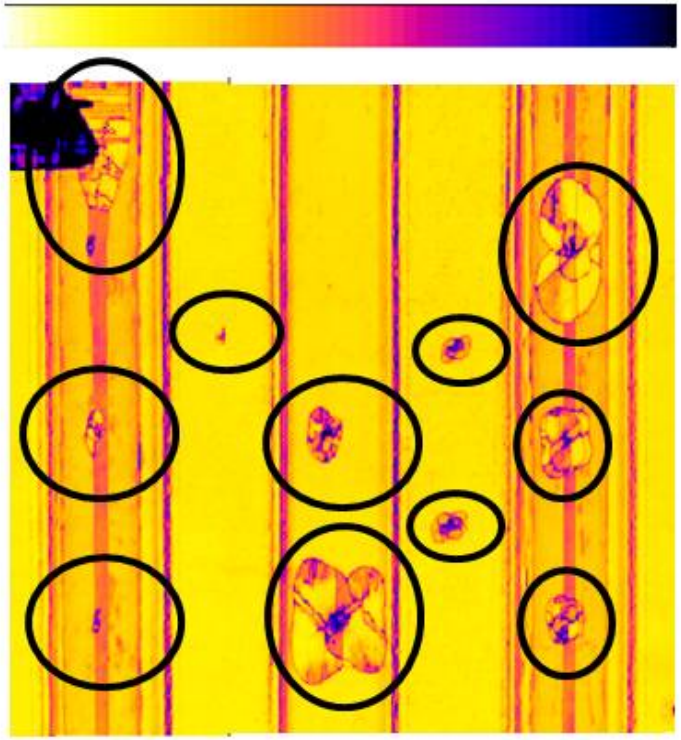

Amplitude

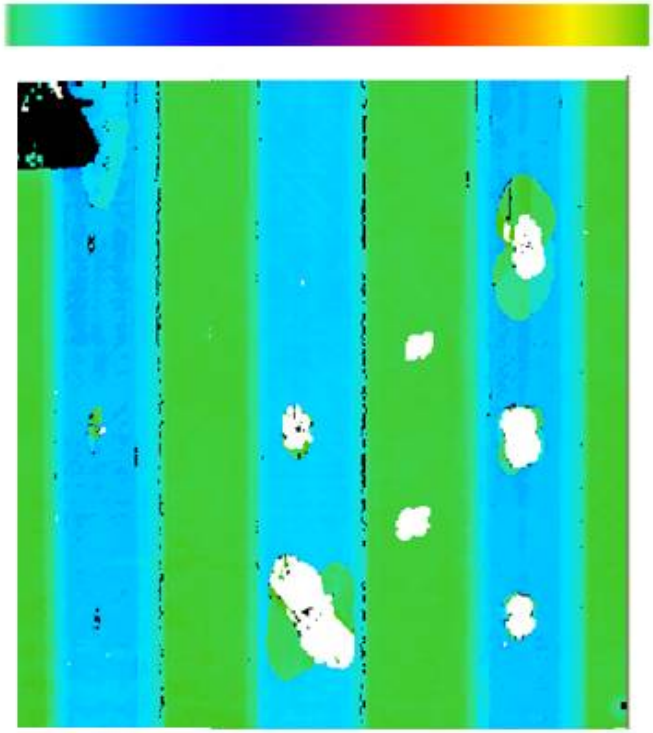

Depth- TOF

National Nuclear Security Administration

Sandia National Laboratories

I Beam Stiffened Panel FAA-I-2 Bell-Innovative, Image Based NDE for Modern Rotorcraft Sustainment MAUS V Resonance Testing 301 KHZ

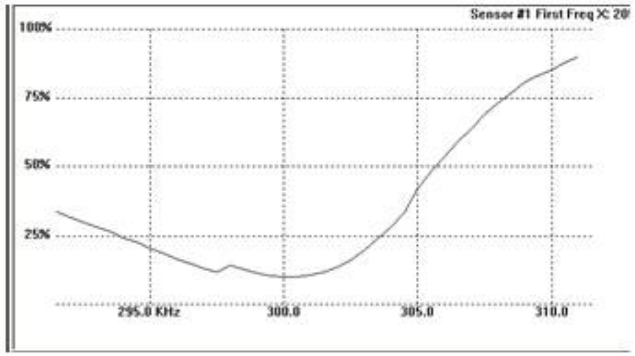

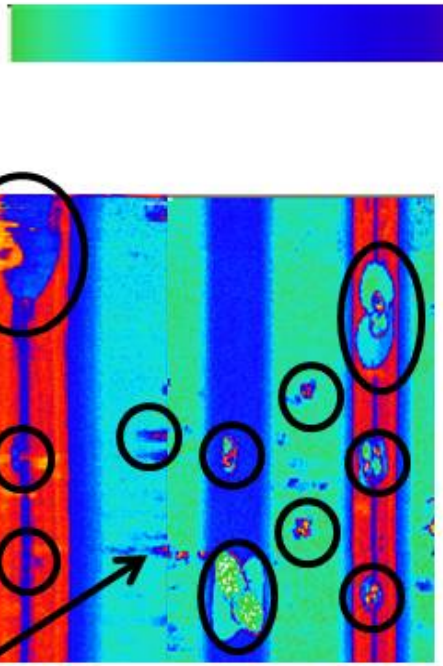

Unknown X-Plot

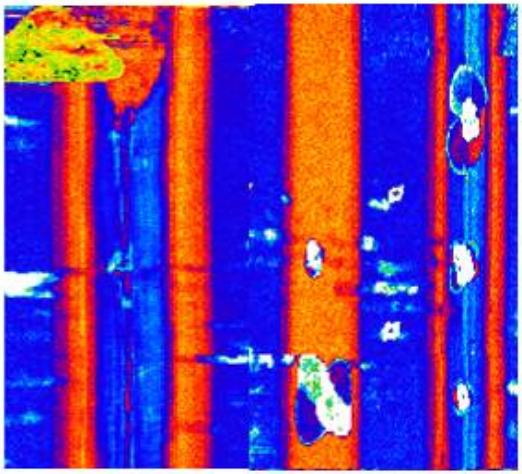

Y-Plot

Tried 301 KHZ To Try To Enhance Smallest Impacts

National Nuclear Security Administration

Sandia National Laboratories

I Beam Stiffened Panel FAA-I-2 Bell-Innovative, Image Based NDE for Modern Rotorcraft Sustainment

1000i Olympus Ultrasonic Tester 5 MHZ Contact A-Scans

Ramp Damage Checker/Bondmaster Results

Point A- Bad/Bad
Point B- Good/Bad
Point C-Good/Bad

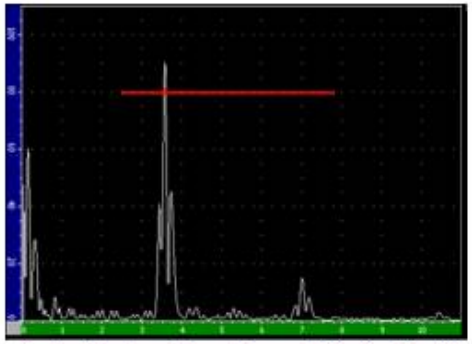

Point A Top By Tag- 34.4 db 90% Amplitude

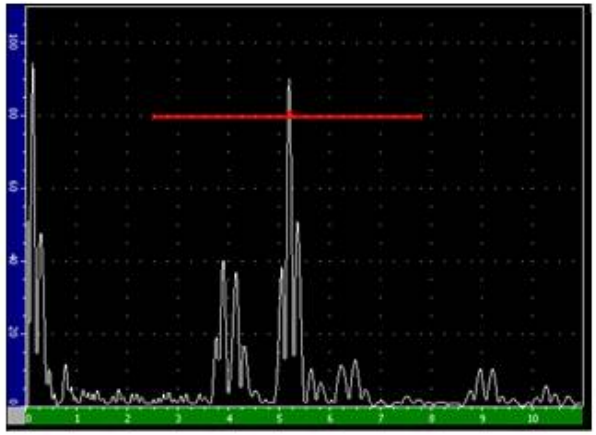

Cal In- 90% Amplitude/37.2db (5.37mm)

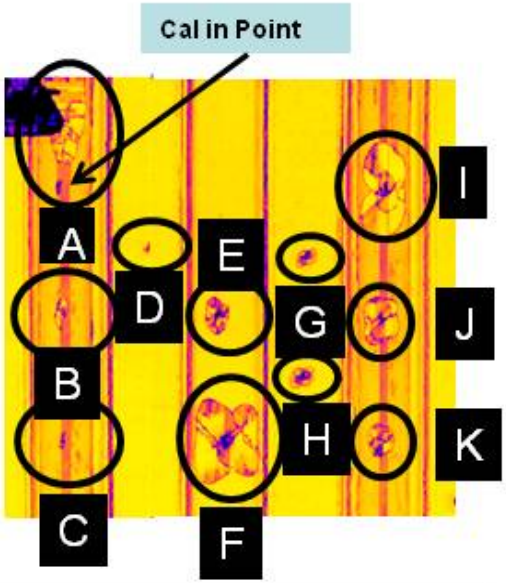

Point A Bottom Dark Area- 34.4 dB 15% Amplitude

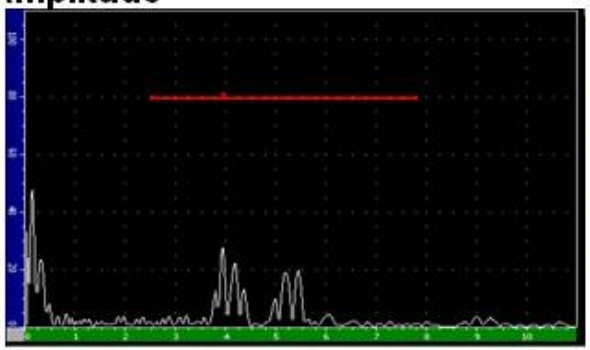

Point B- 34.4dB 27.7% Amplitude

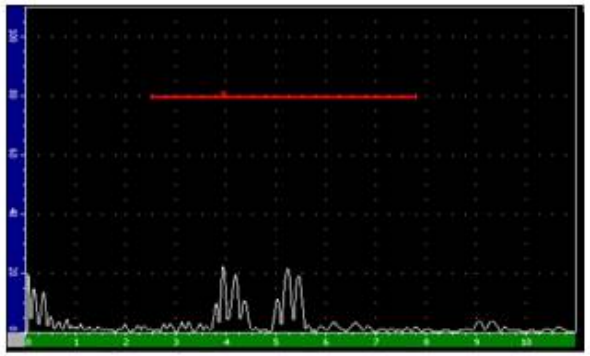

Point C- 34.4dB 22.75% Amplitude

NOTE: Noted dB and Amplitude Changes different from the Cal In

National Nuclear Security Administration

Sandia National Laboratories

I Beam Stiffened Panel FAA-I-2 Bell-Innovative, Image Based NDE for Modern Rotorcraft Sustainment
1000i Olympus Ultrasonic Tester 5 MHZ Contact A-Scans

Ramp Damage Checker/Bondmaster Results

Point D- Good/Bad

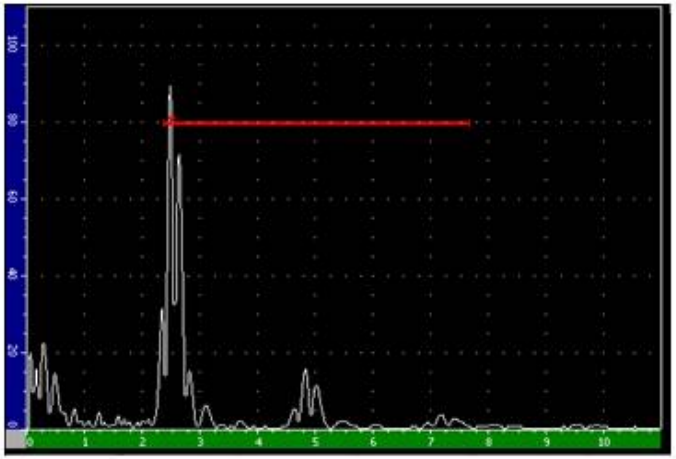

Cal In- 90% Amplitude/34.0db (2.71mm)

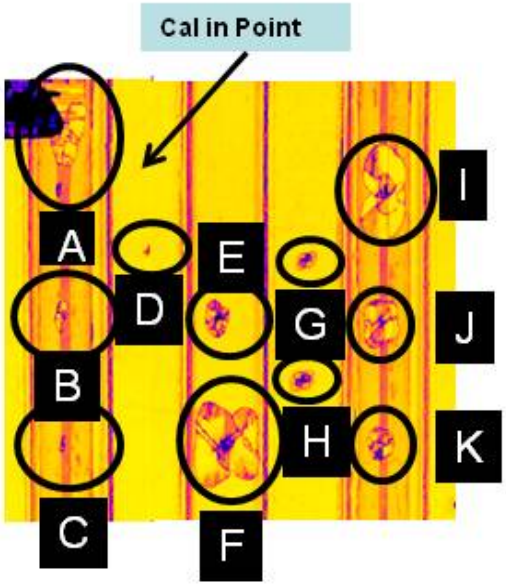

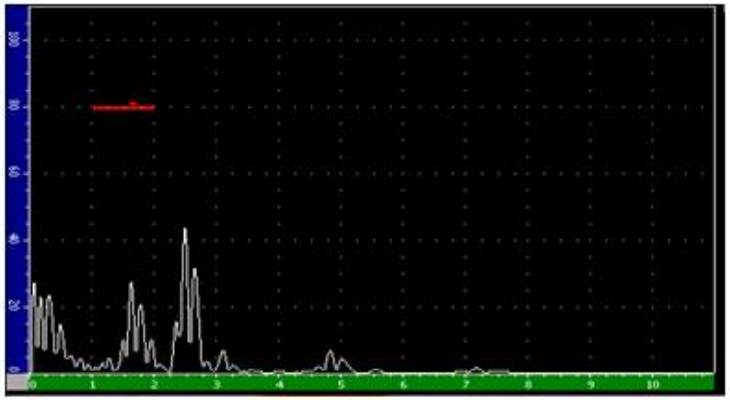

Point D- 27.5% Amplitude

NOTE: Noted dB and Amplitude Changes different from the Cal In

I Beam Stiffened Panel FAA-I-2 Bell-Innovative, Image Based NDE for Modern Rotorcraft Sustainment
1000i Olympus Ultrasonic Tester 5 MHZ Contact A-Scans

Ramp Damage Checker/Bondmaster Results

Point E- Bad/Bad
Point F- Bad/Bad

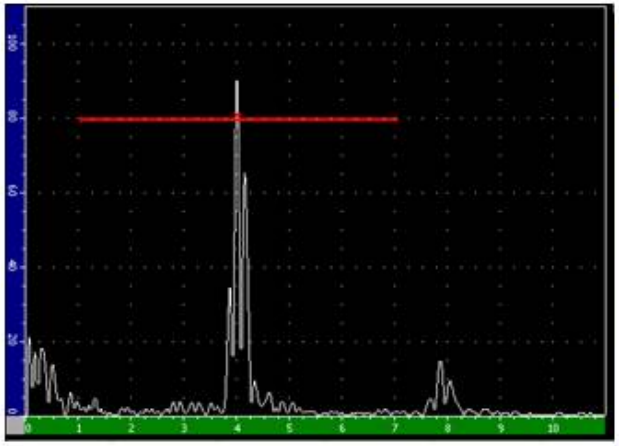

Cal In- 90% Amplitude/34.2db (4.15mm)

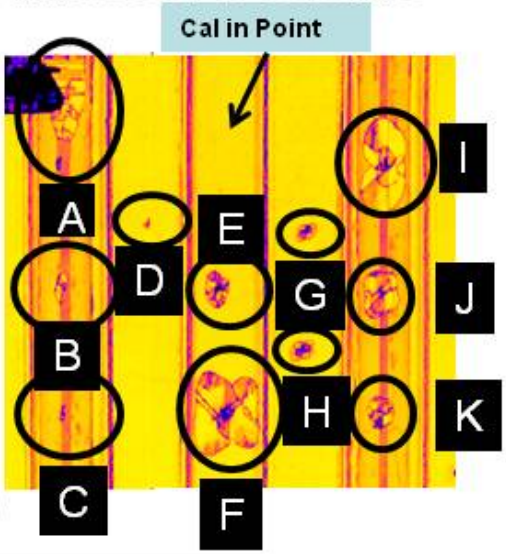

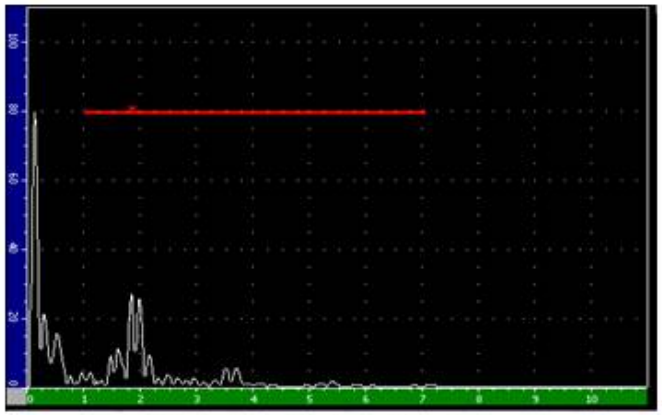

Point E- 27% Amplitude

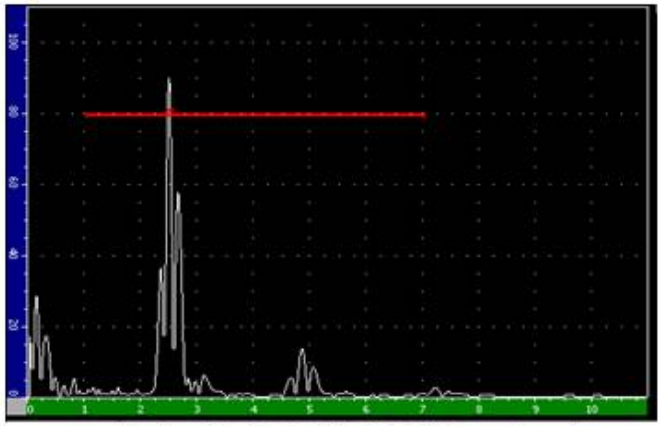

Point F- 30.9dB 90% Amplitude

NOTE: Noted dB and Amplitude Changes different from the Cal In

National Nuclear Security Administration

Sandia National Laboratories

I Beam Stiffened Panel FAA-I-2 Bell-Innovative, Image Based NDE for Modern Rotorcraft Sustainment
1000i Olympus Ultrasonic Tester 5 MHZ Contact A-Scans

Ramp Damage Checker/ Bondmaster Results

Point G- Bad/Bad
Point H- Bad/Bad

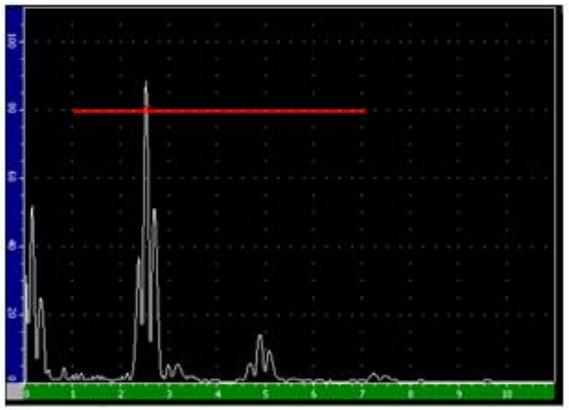

Cal In- 90% Amplitude/32.2db (2.98mm)

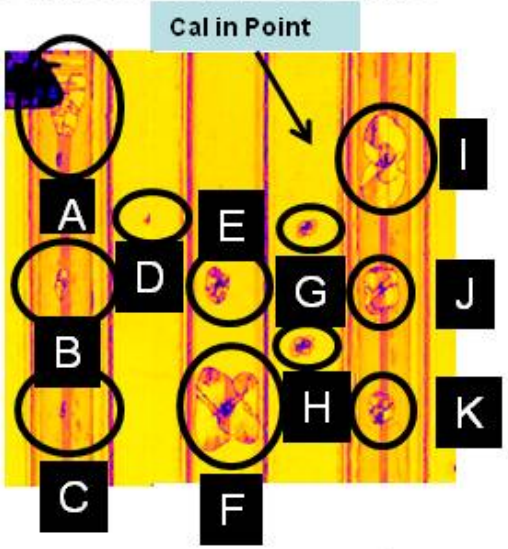

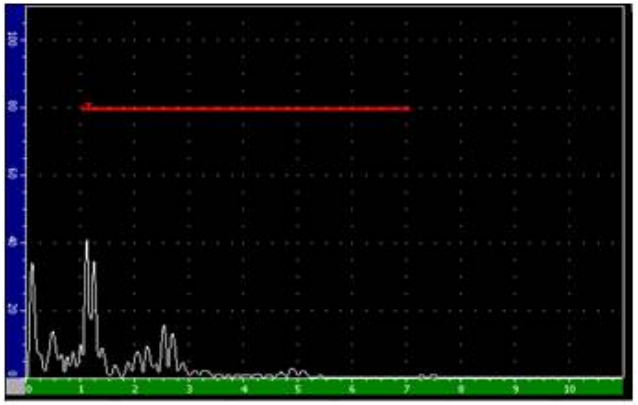

Point G- 41% Amplitude

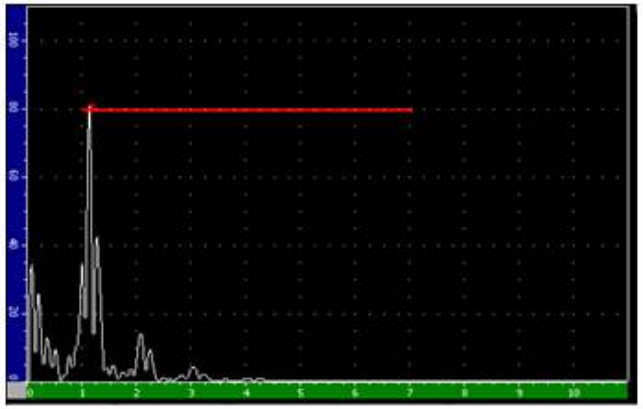

Point H- 81.75% Amplitude

NNSA National Nuclear Security Administration

NOTE: Noted dB and Amplitude Changes different from the Cal In

Sandia National Laboratories

I Beam Stiffened Panel FAA-I-2 Bell-Innovative, Image Based NDE for Modern Rotorcraft Sustainment
1000i Olympus Ultrasonic Tester 5 MHZ Contact A-Scans

Ramp Damage Checker/Bondmaster Results

Point I- Bad/Bad
Point J- Bad/Bad
Point K- Bad/Bad

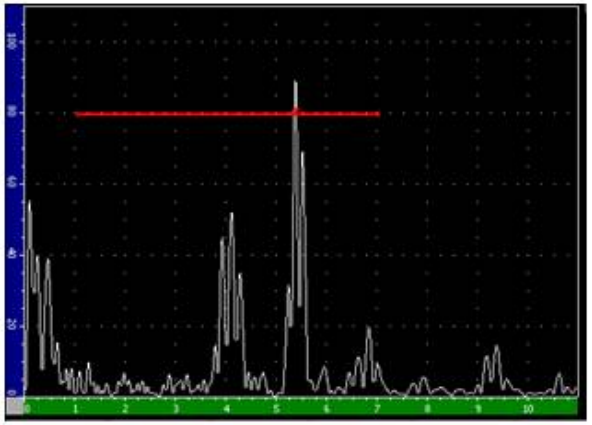

Cal In- 90% Amplitude/40.6db (5.71mm)

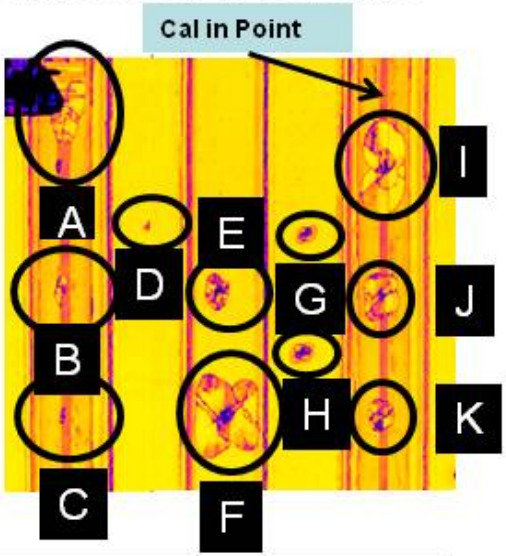

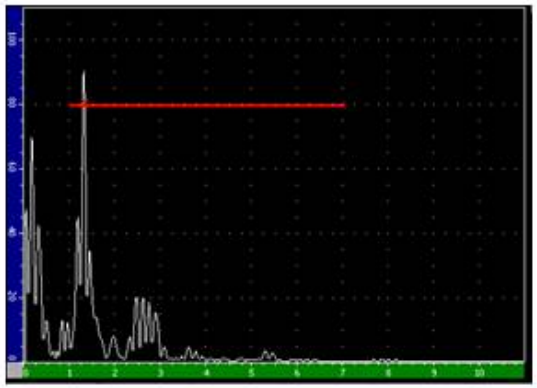

Point I- 35.3dB 90% Amplitude

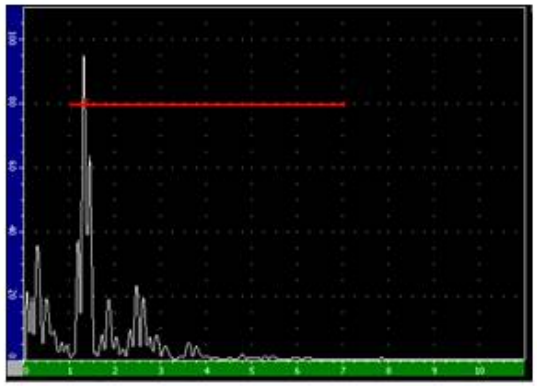

Point J- 35.35 dB 96.75%Amplitude

Point K- 32.8 dB 90% Amplitude

NOTE: Noted dB and Amplitude Changes different from the Cal In

FAA-I-2 Impact Panel
Flash Thermography (IR)

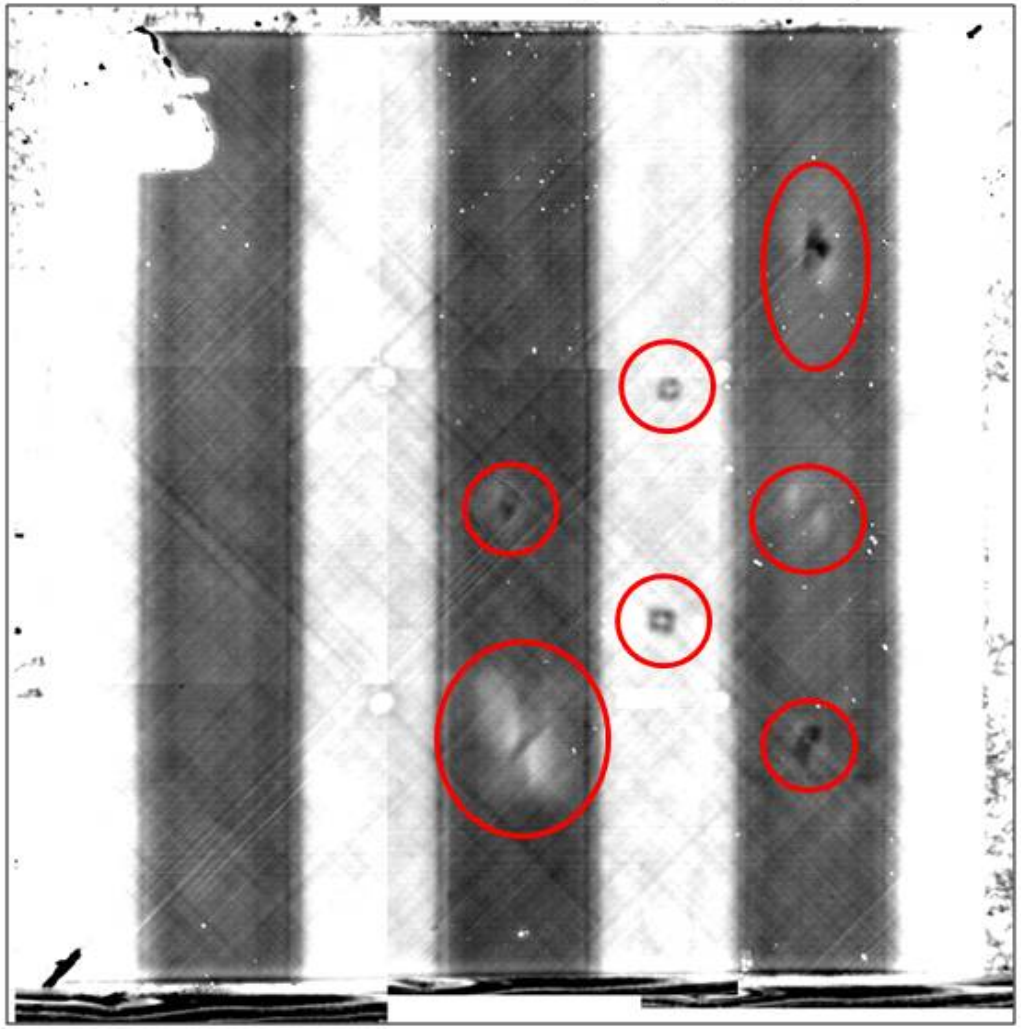

1d .0684 sec after flash

National Nuclear Security Administration

Sandia National Laboratories

I Beam Stiffened Panel FAA-I-003 Bell-Innovative, Image Based NDE for Modern Rotorcraft Sustainment

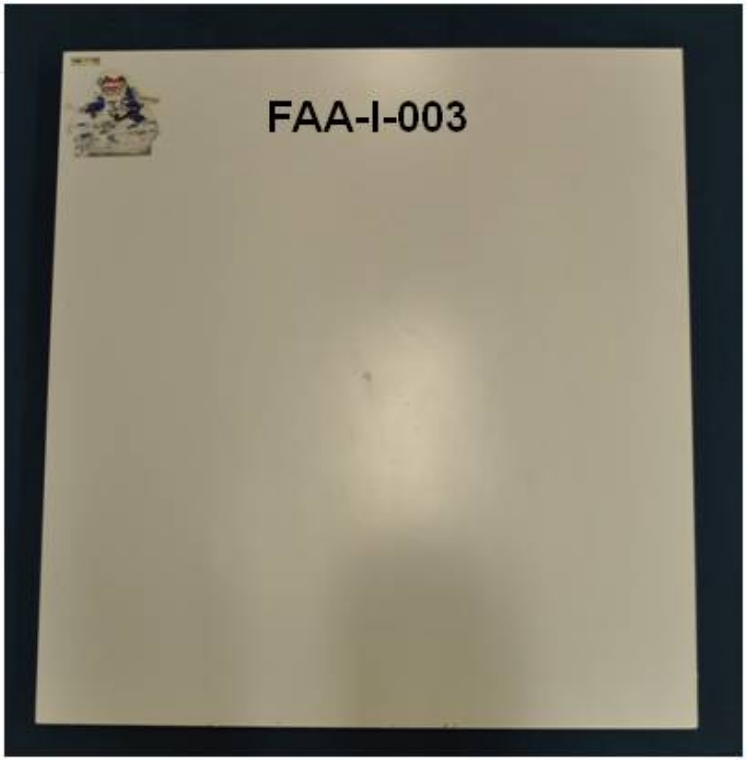

Top

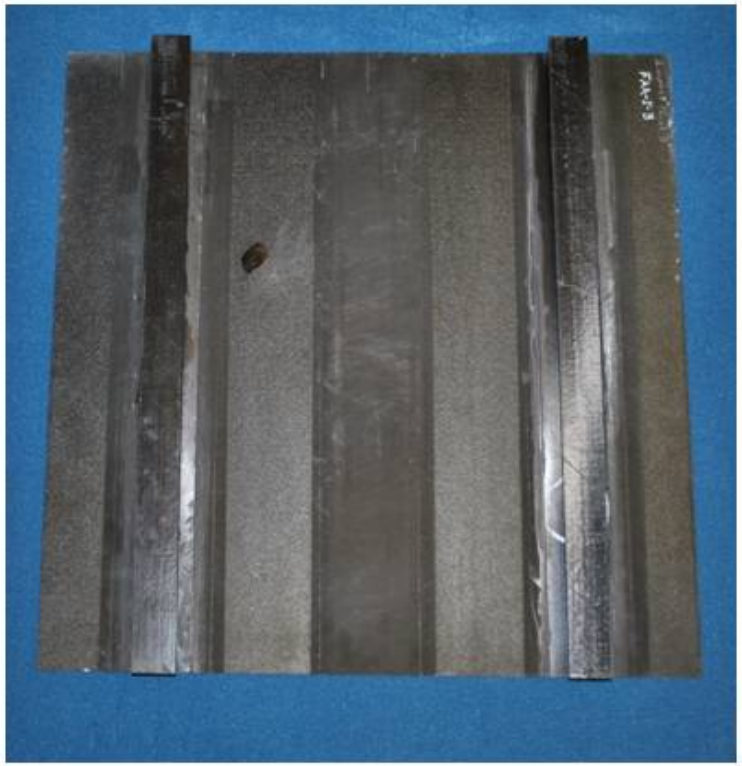

Bottom

National Nuclear Security Administration

Sandia National Laboratories

I Beam Stiffened Panel FAA-I-003 Bell-Innovative, Image Based NDE for Modern Rotorcraft Sustainment Omniscan 10L64 (10 MHZ) Phased Array Plastic Wedge

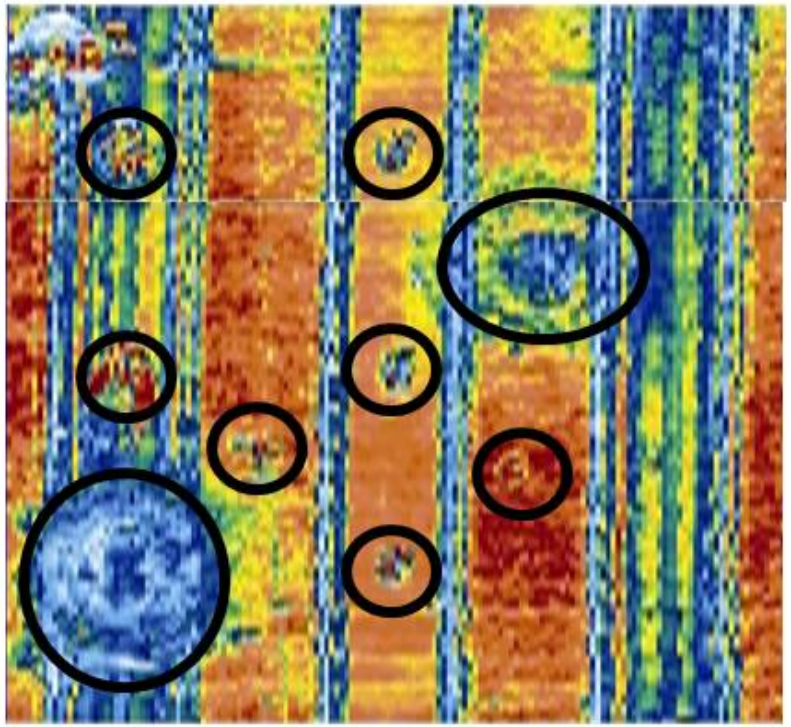

Amplitude

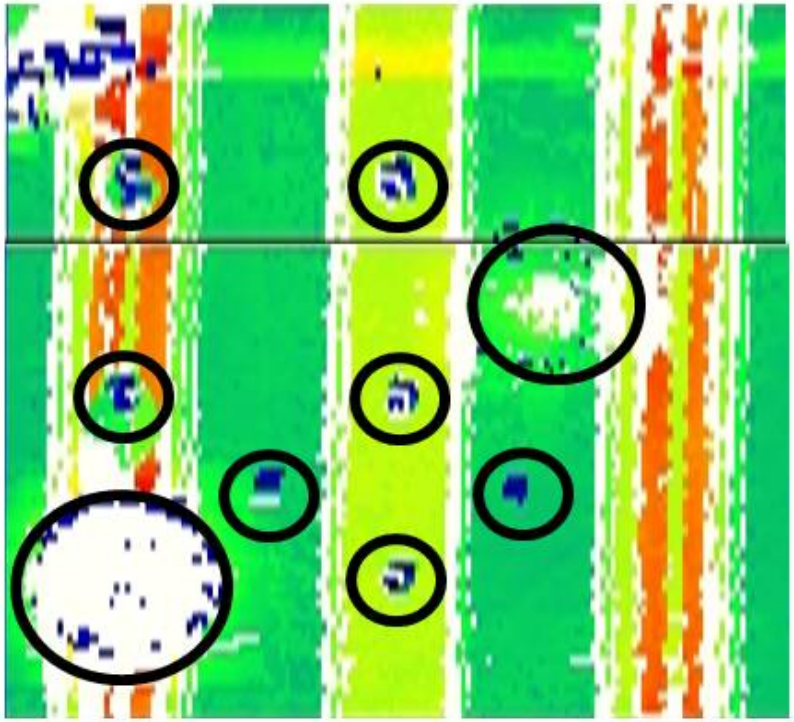

TOF

National Nuclear Security Administration

Sandia National Laboratories

I Beam Stiffened Panel FAA-I-003 Bell-Innovative, Image Based NDE for Modern Rotorcraft Sustainment Omniscan 5 MHZ/.5" Diameter Contact Testing

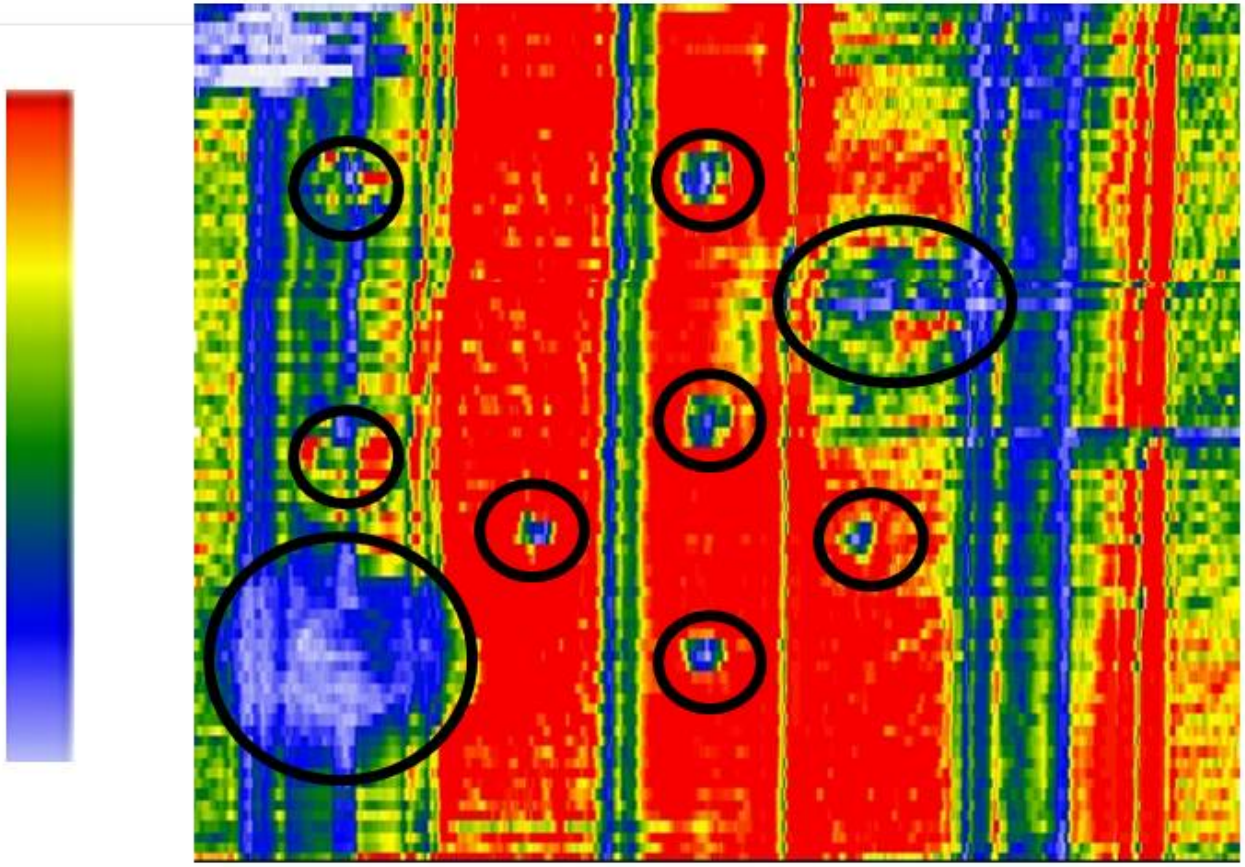

National Nuclear Security Administration

Sandia National Laboratories

I Beam Stiffened Panel FAA-I-003 Bell-Innovative, Image Based NDE for Modern Rotorcraft Sustainment MAUS V Pulse Echo 5 MHZ Contact Testing

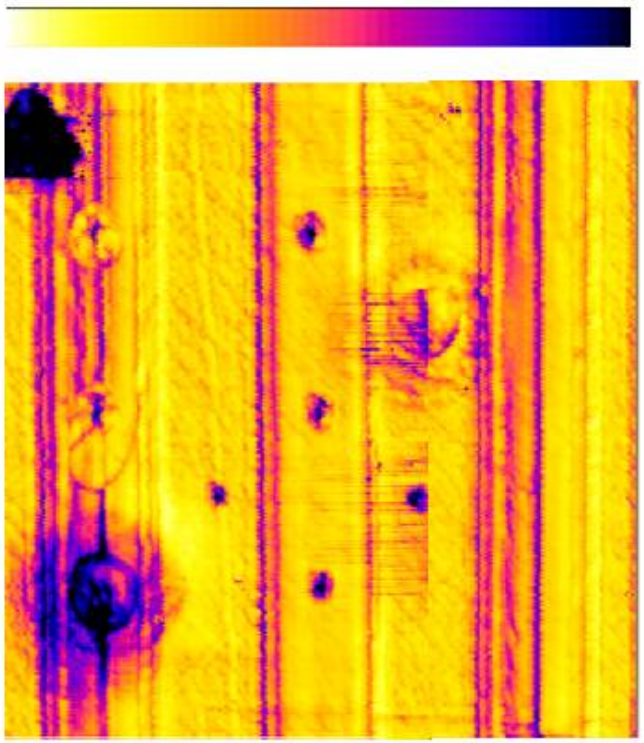

Amplitude

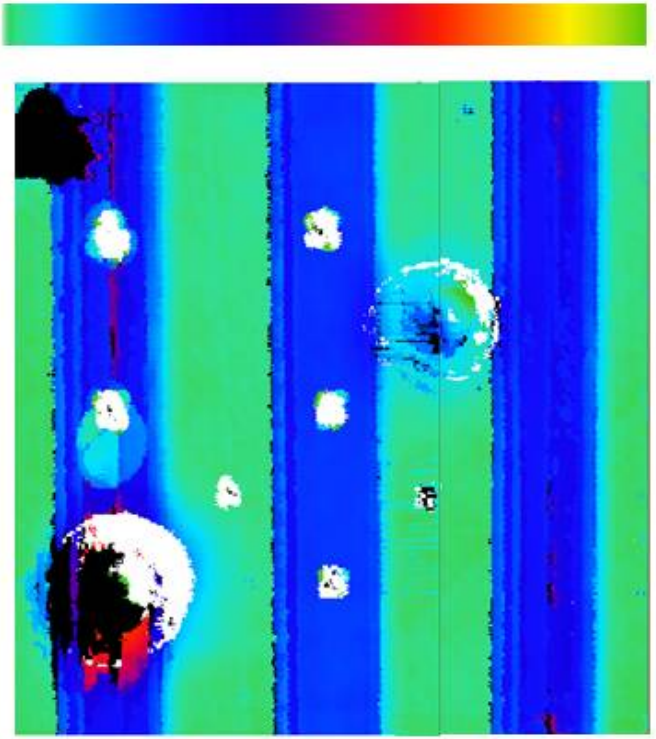

Depth- TOF

National Nuclear Security Administration

Sandia National Laboratories

I Beam Stiffened Panel FAA-I-003 Bell-Innovative, Image Based NDE for Modern Rotorcraft Sustainment MAUS V Resonance Testing 301 KHZ

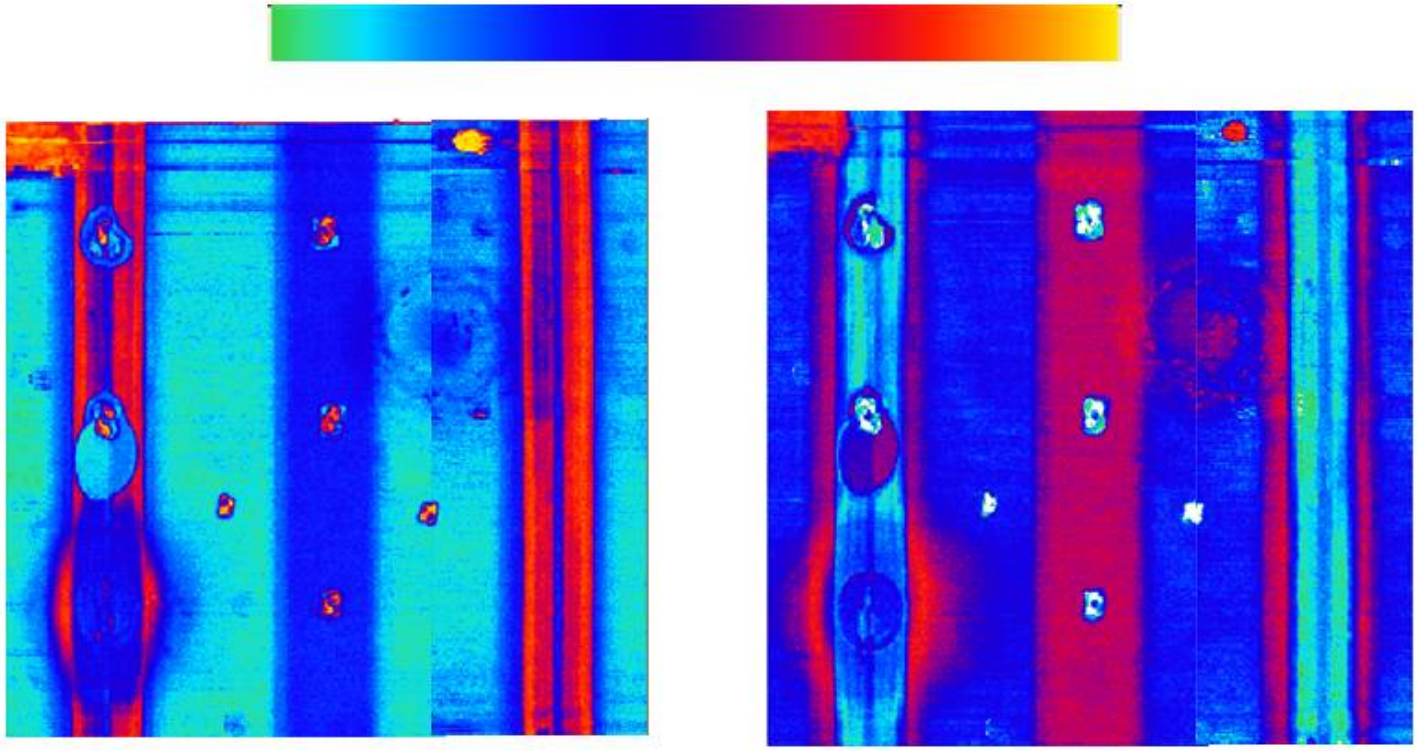

X-Plot

Y-Plot

National Nuclear Security Administration

Sandia National Laboratories

I Beam Stiffened Panel FAA-I-003 Bell-Innovative, Image Based NDE for Modern Rotorcraft Sustainment 1000i Olympus Ultrasonic Tester 5 MHZ Contact A-Scans

Ramp Damage Checker/Bondmaster Results

Point A- Bad/Bad
Point B- Bad/Bad
Point C- Bad/Bad

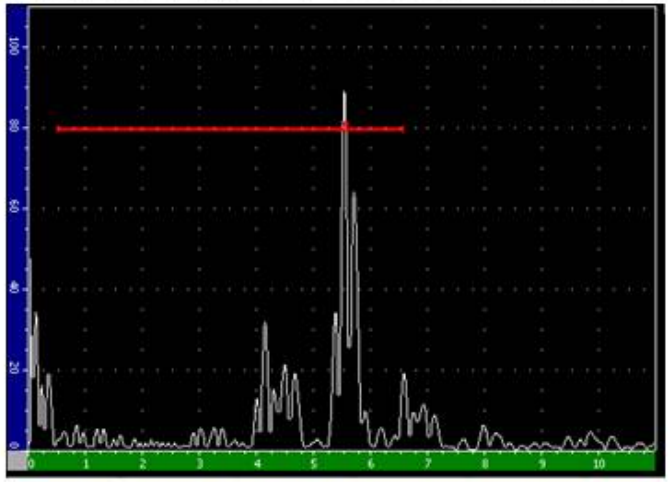

Cal In- 90% Amplitude/34.1db (5.5mm)

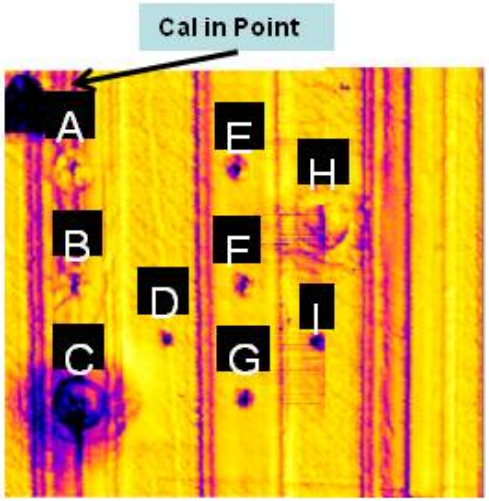

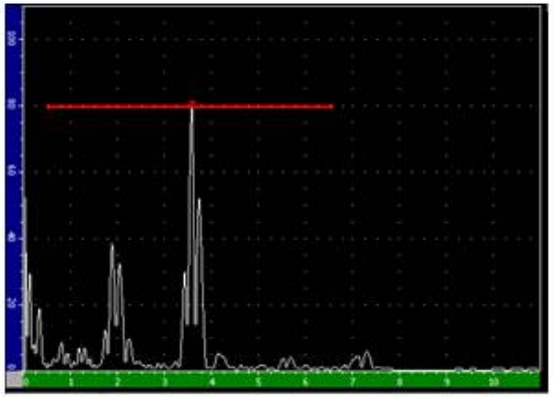

Point A- 81% Amplitude

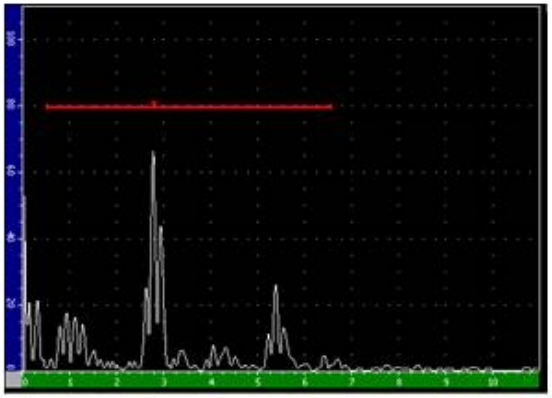

Point B- 66.25% Amplitude

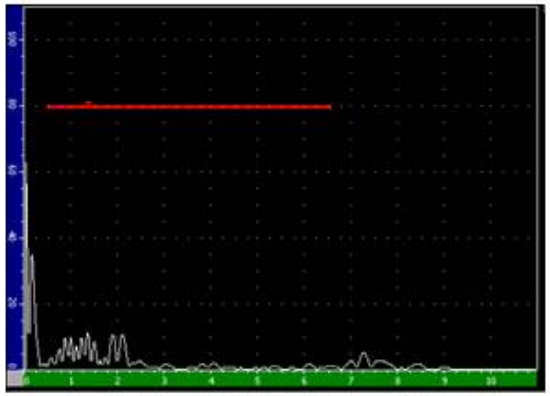

Point C- 5% Amplitude

NOTE: Noted dB and Amplitude Changes different from the Cal In

I Beam Stiffened Panel FAA-I-003 Bell-Innovative, Image Based NDE for Modern Rotorcraft Sustainment 1000i Olympus Ultrasonic Tester 5 MHZ Contact A-Scans

Ramp Damage Checker/Bondmaster Results

Point D- Bad/Bad

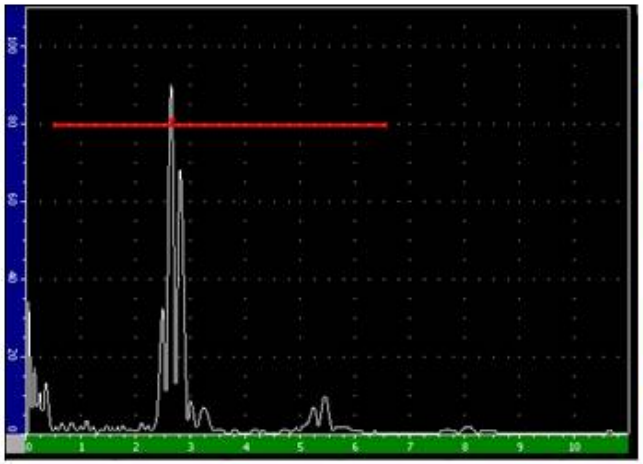

Cal In- 90% Amplitude/30.1db (2.78mm)

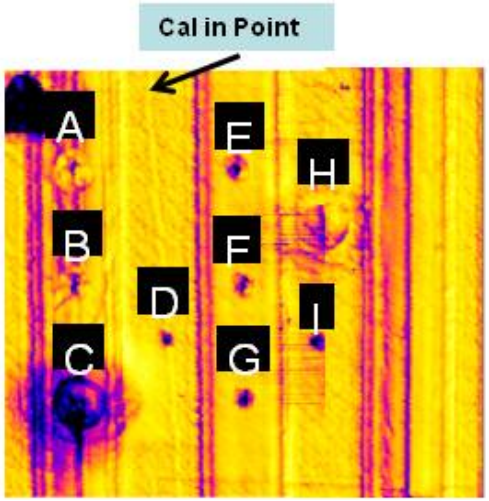

NOTE: Noted dB and Amplitude Changes different from the Cal In

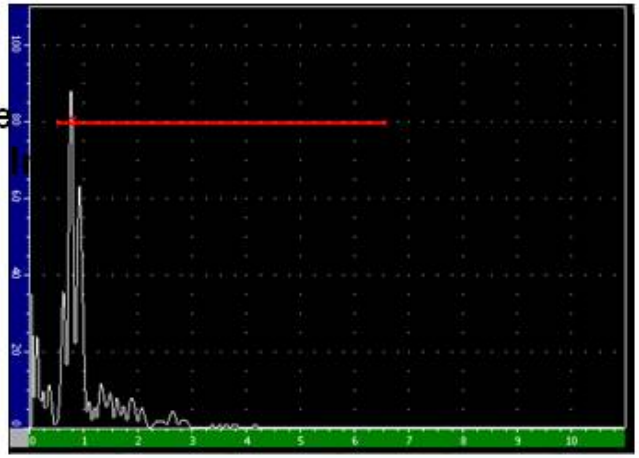

Point D- 89% Amplitude

National Nuclear Security Administration

Sandia National Laboratories

I Beam Stiffened Panel FAA-I-003 Bell-Innovative, Image Based NDE for Modern Rotorcraft Sustainment 1000i Olympus Ultrasonic Tester 5 MHZ Contact A-Scans

Ramp Damage Checker/ Bondmaster Results

Point E- Bad/Bad
Point F- Bad/Bad
Point G- Bad/Bad

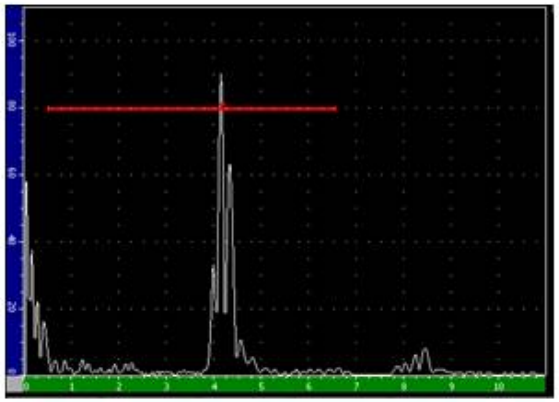

Cal In- 90% Amplitude/33.8db (4.07mm)

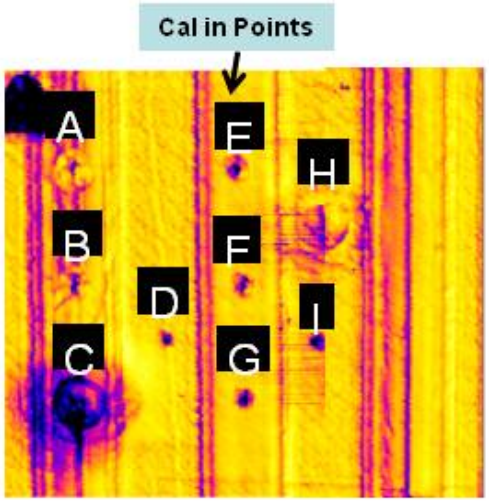

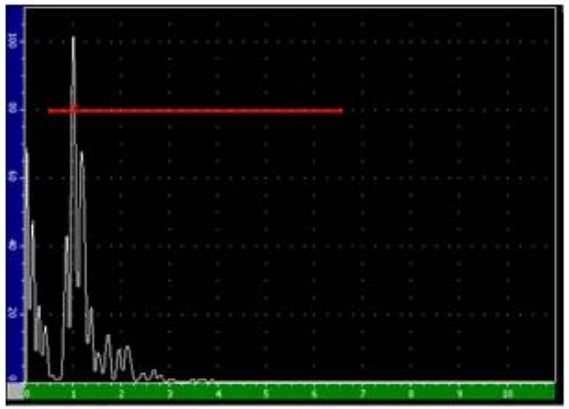

Point E- 102.25% Amplitude

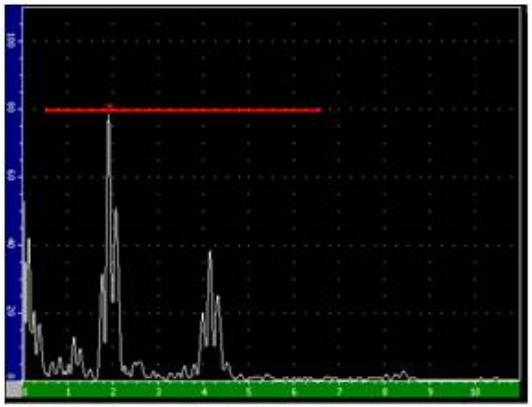

Point F- 79.0% Amplitude

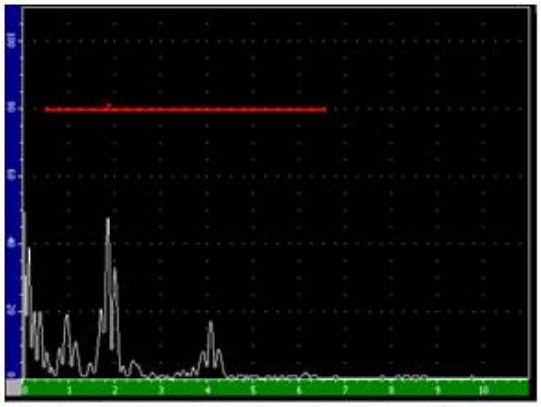

Point G- 47.75% Amplitude

NOTE: Noted dB and Amplitude Changes different from the Cal In

I Beam Stiffened Panel FAA-I-003 Bell-Innovative, Image Based NDE for Modern Rotorcraft Sustainment 1000i Olympus Ultrasonic Tester 5 MHZ Contact A-Scans

Ramp Damage Checker/Bondmaster Results

Point H- Bad/Bad
Point I- Bad/Bad

Note: Point H Kept Reading Cal Beyond Thickness

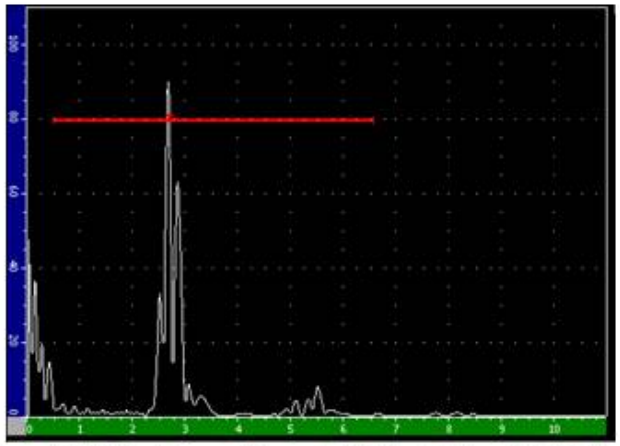

Cal In- 90% Amplitude/31.4db (2.73mm)

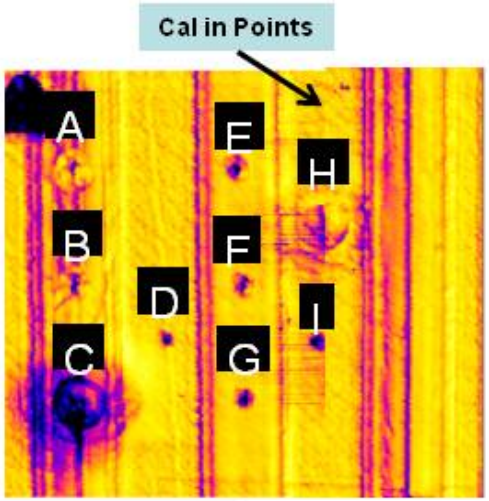

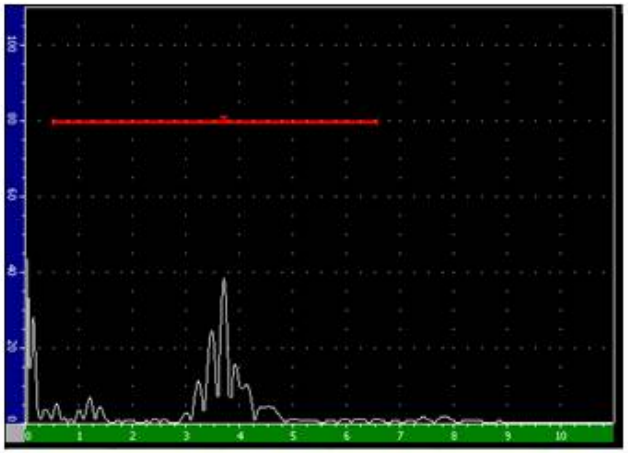

Point H- 38.5% Amplitude

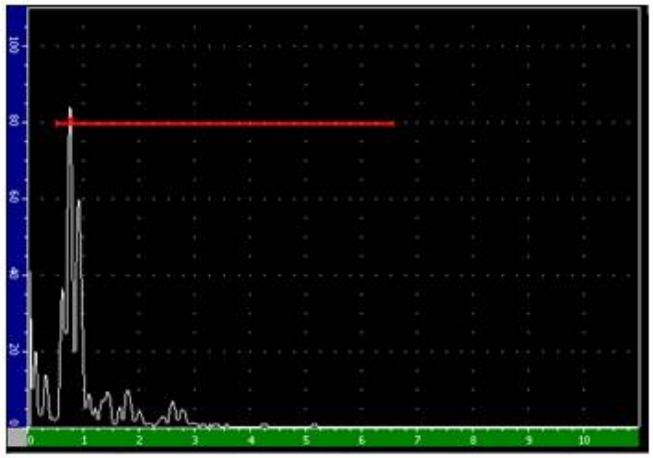

Point I- 84.5% Amplitude

NOTE: Noted dB and Amplitude Changes different from the Cal In

National Nuclear Security Administration

Sandia National Laboratories

FAA-I-003 Impact Panel
Flash Thermography (IR)

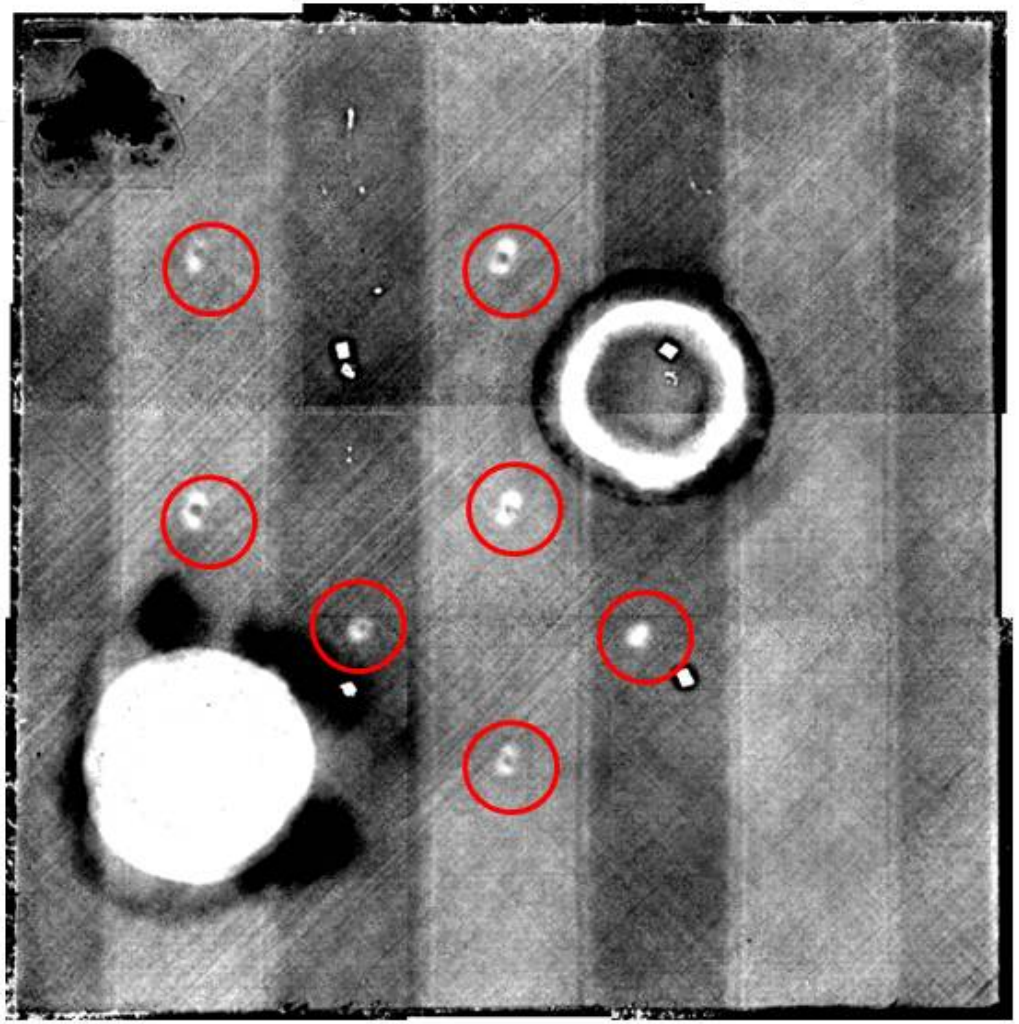

1d .0684 sec after flash

National Nuclear Security Administration

Sandia National Laboratories

Hat Stiffened Panel FAA-H-001 Bell-Innovative, Image Based NDE for Modern Rotorcraft Sustainment

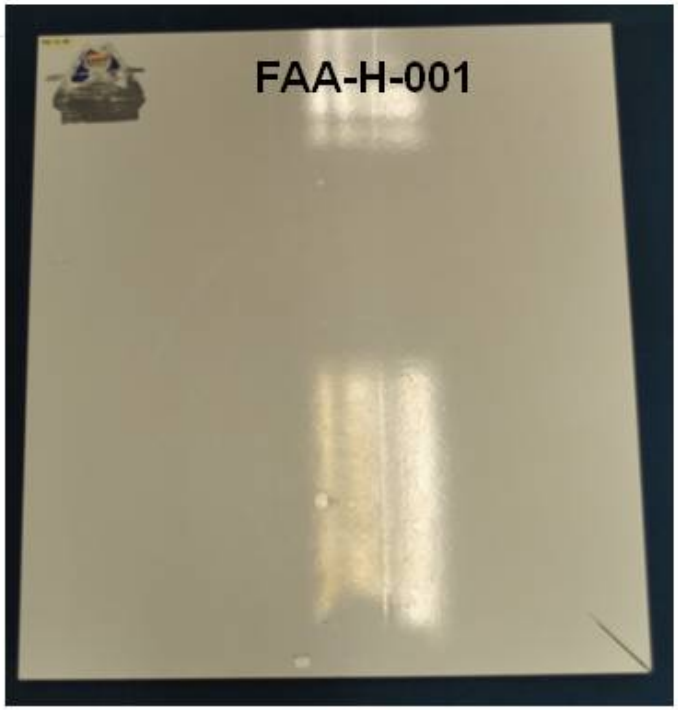

Top

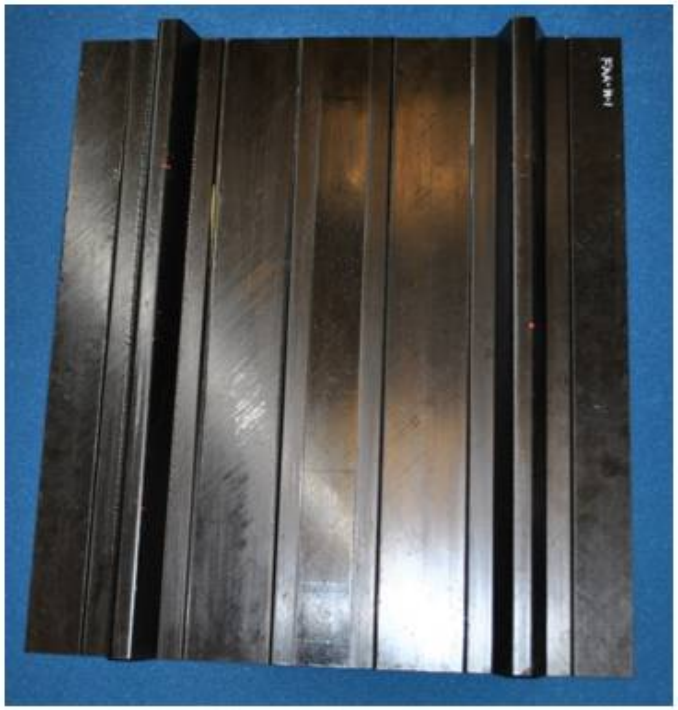

Bottom

National Nuclear Security Administration

Sandia National Laboratories

Hat Stiffened Panel FAA-H-001 Bell-Innovative, Image Based NDE for Modern Rotorcraft Sustainment
Omniscan 10L64 (10 MHZ) Phased Array With Aqualene Block

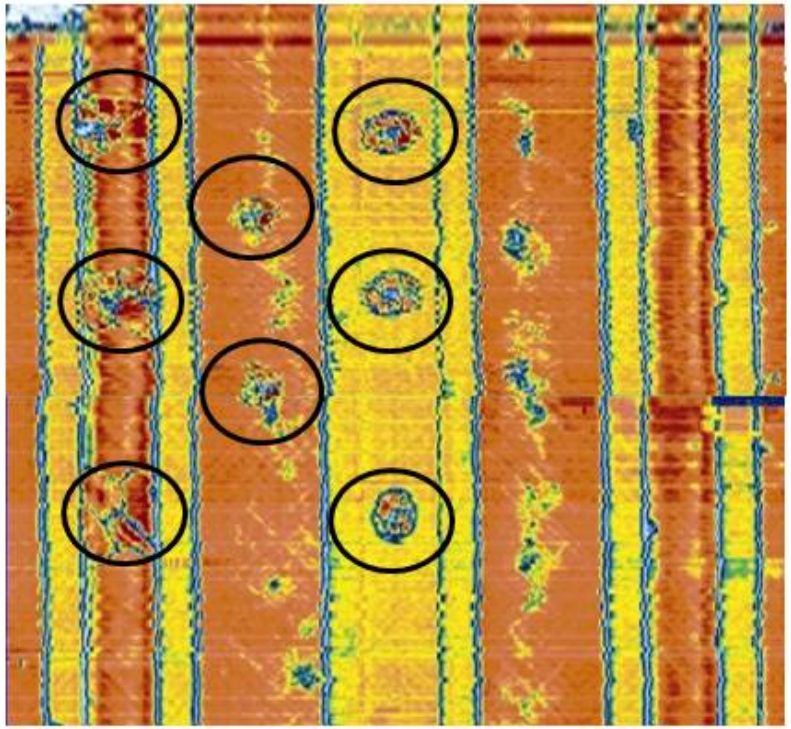

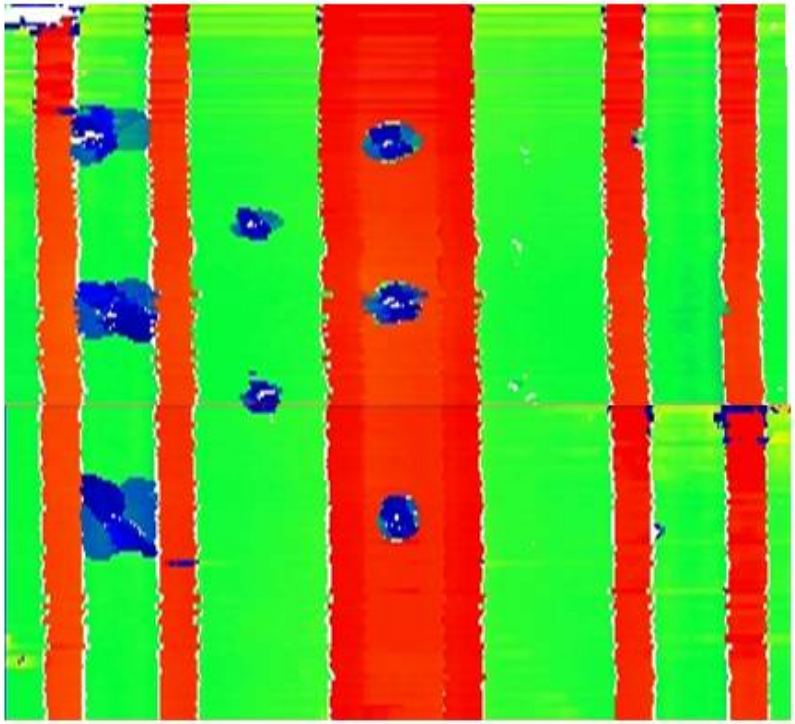

National Nuclear Security Administration

Sandia National Laboratories

Hat Stiffened Panel FAA-H-001 Bell-Innovative, Image Based NDE for Modern Rotorcraft Sustainment Omniscan 5L64 (5 MHZ) Phased Array With Aqualene Block

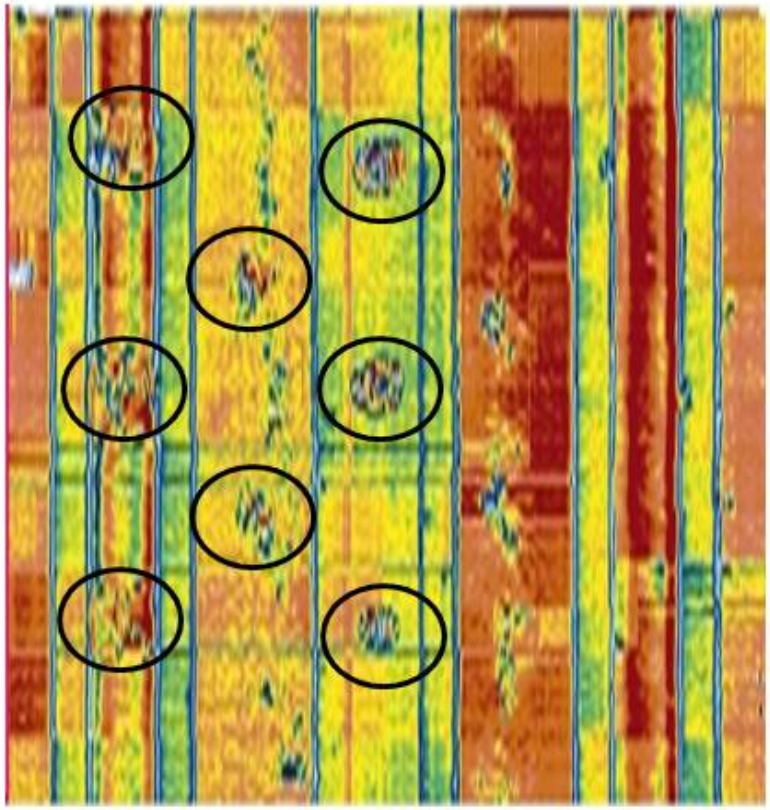

Amplitude

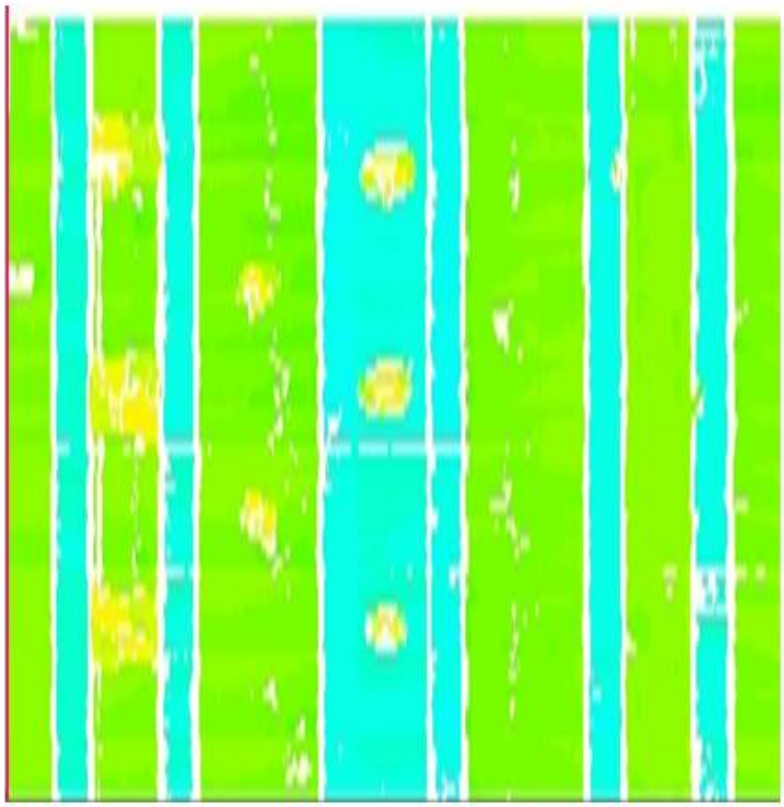

TOF

National Nuclear Security Administration

Sandia National Laboratories

Hat Stiffened Panel FAA-H-001 Bell-Innovative, Image Based NDE for Modern Rotorcraft Sustainment MAUS V Pulse Echo 5 MHZ

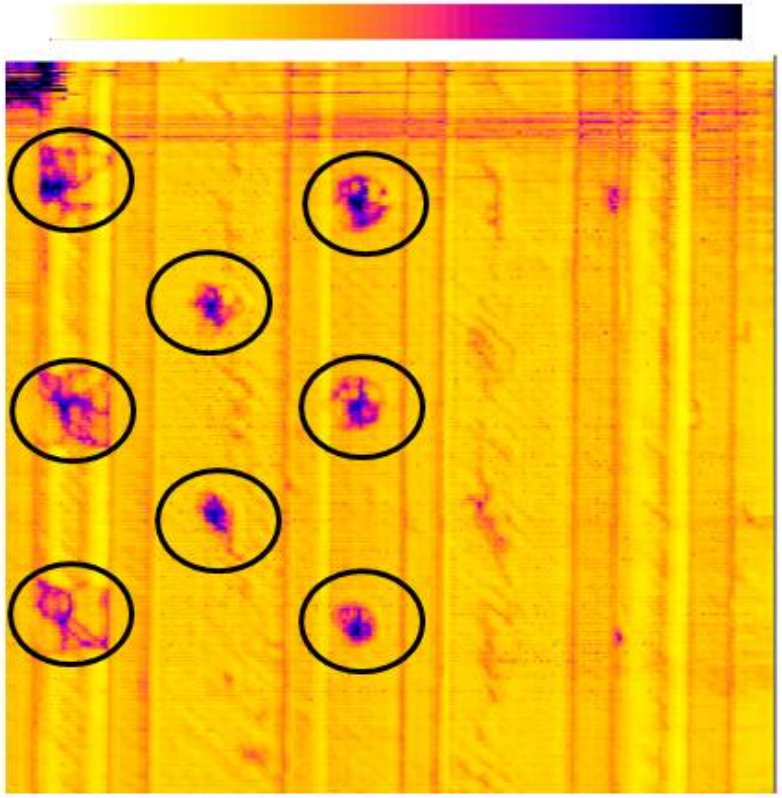

Amplitude

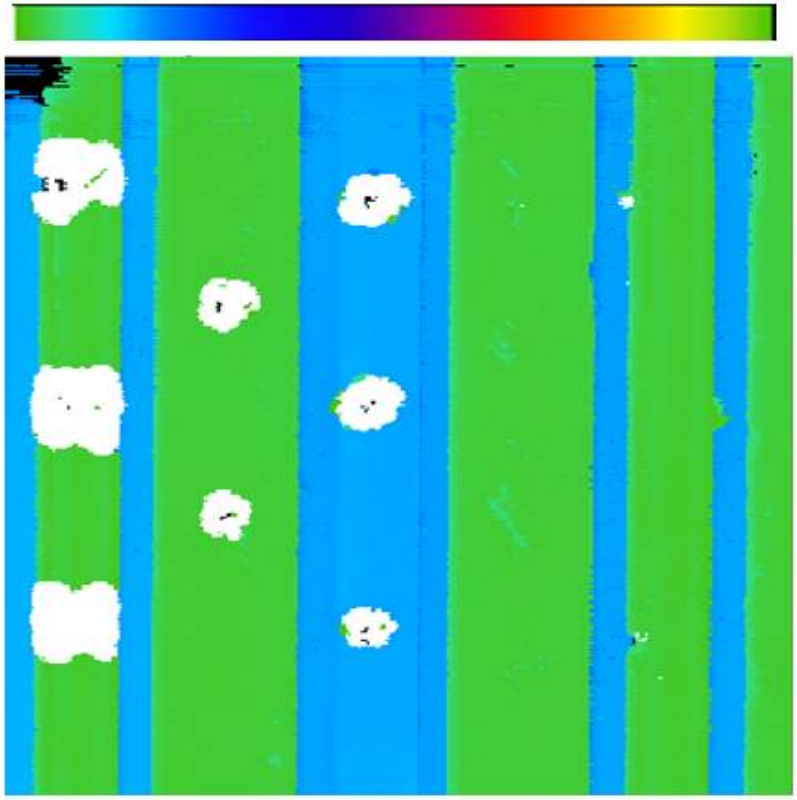

Depth- TOF

National Nuclear Security Administration

Sandia National Laboratories

Hat Stiffened Panel FAA-H-001 Bell-Innovative, Image Based NDE for Modern Rotorcraft Sustainment MAUS V Resonance Testing 277 KHZ

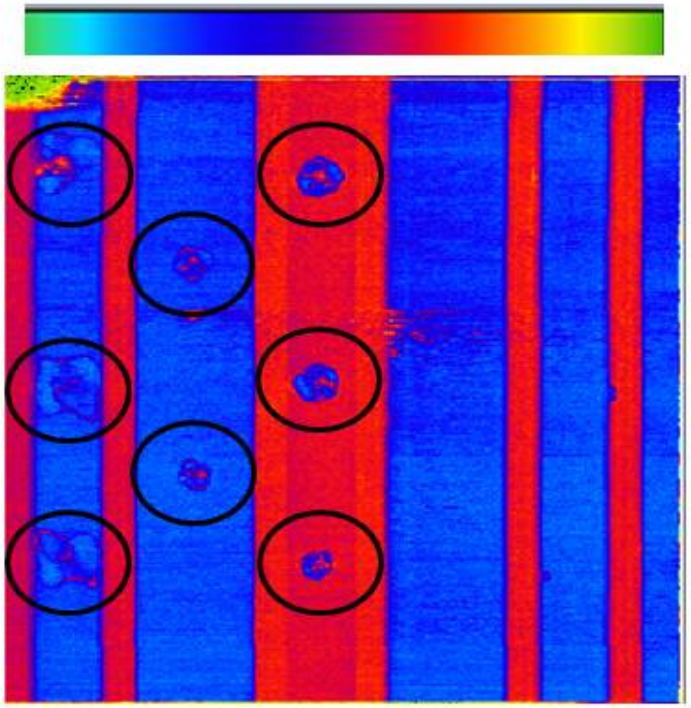

X-Plot

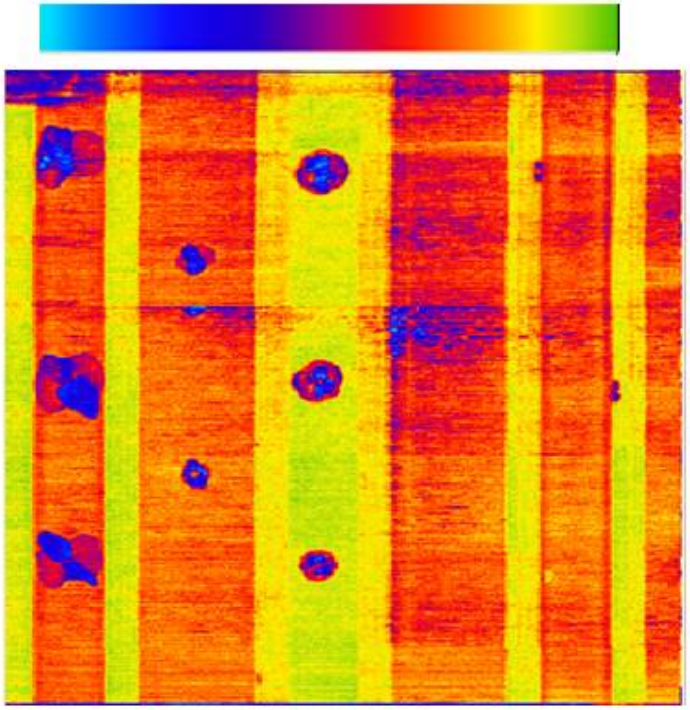

Y-Plot

National Nuclear Security Administration

Sandia National Laboratories

Hat Stiffened Panel FAA-H-001 Bell-Innovative, Image Based NDE for Modern Rotorcraft Sustainment
1000i Olympus Ultrasonic Tester 5 MHZ Contact A-Scans

Ramp Damage Checker/Bondmaster Results

Point A- Bad/Bad
Point B- Bad/Bad
Point C- Bad/Bad

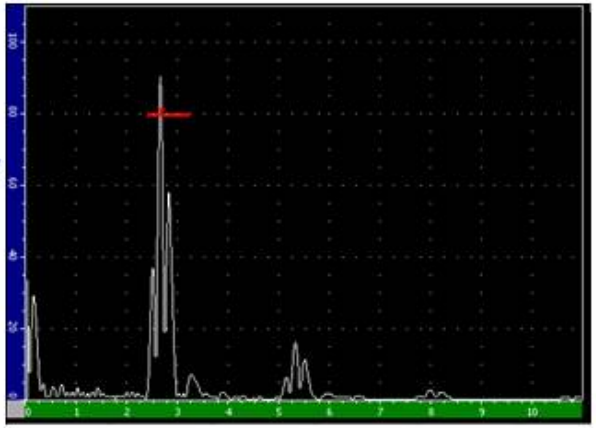

Cal In- 90% Amplitude/28.5db (2.64mm)

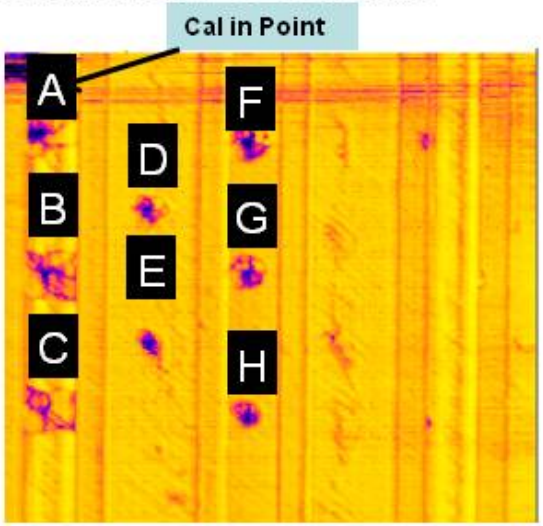

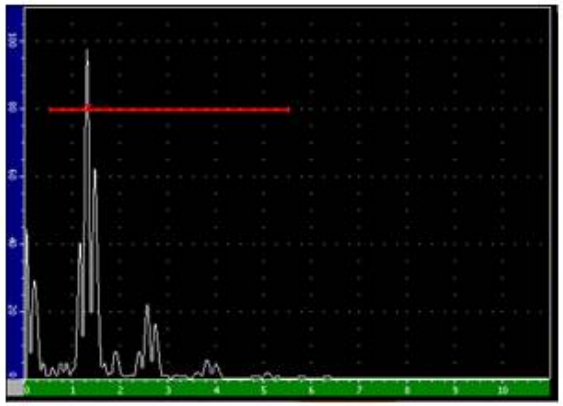

Point A- 98% Amplitude

Point B- 106.25% Amplitude

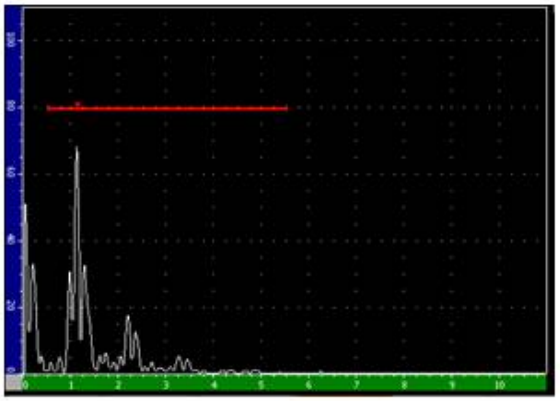

Point C- 68.5% Amplitude

NNSA National Nuclear Security Administration

NOTE: Noted dB and Amplitude Changes different from the Cal In

Sandia National Laboratories

Hat Stiffened Panel FAA-H-001 Bell-Innovative, Image Based NDE for Modern Rotorcraft Sustainment
1000i Olympus Ultrasonic Tester 5 MHZ Contact A-Scan

Ramp Damage Checker/Bondmaster Results

Point D- Bad/Bad
Point E- Bad/Bad

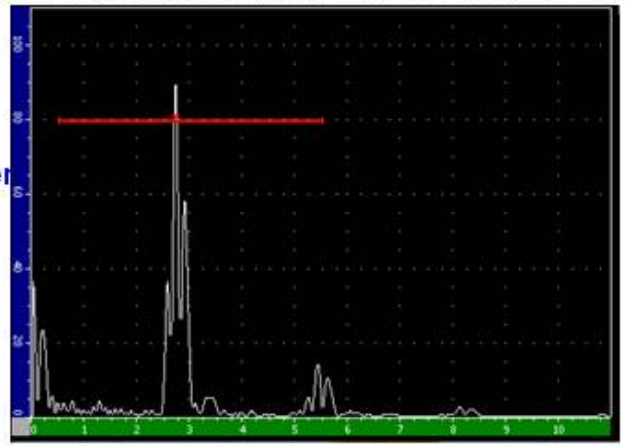

Cal In- 90% Amplitude/28.5db (2.64mm)

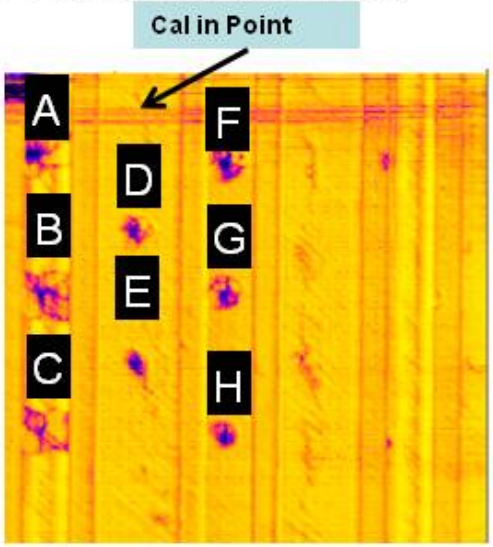

Point D- 47.25% Amplitude

Point E- 49% Amplitude

NOTE: Noted dB and Amplitude Changes different from the Cal In

National Nuclear Security Administration

Sandia National Laboratories

Hat Stiffened Panel FAA-H-001 Bell-Innovative, Image Based NDE for Modern Rotorcraft Sustainment
1000i Olympus Ultrasonic Tester 5 MHZ Contact A-Scan

Ramp Damage Checker/Bondmaster Results

Point F- Bad/Bad
Point G- Bad/Bad
Point H- Bad/Bad

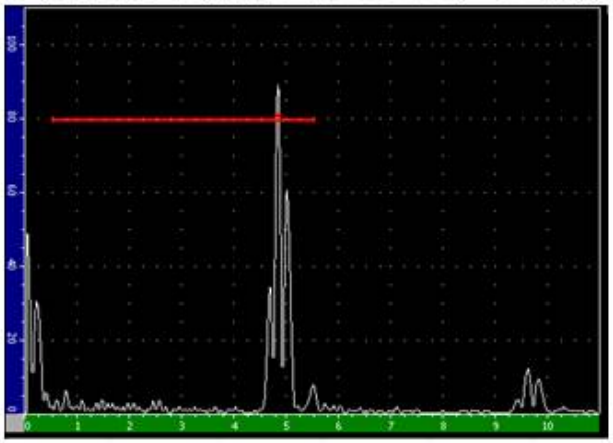

Cal In- 90% Amplitude/30.6db (4.58mm)

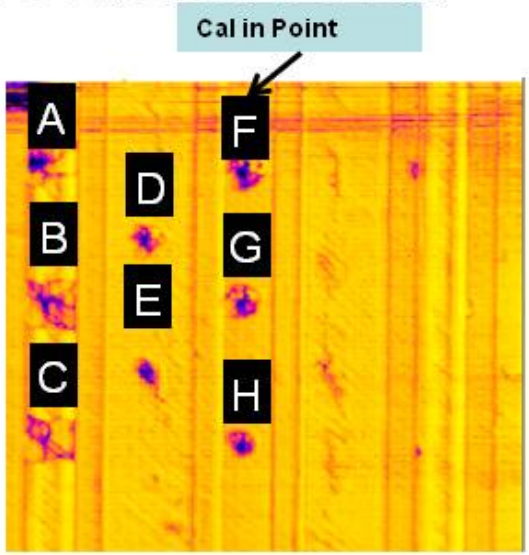

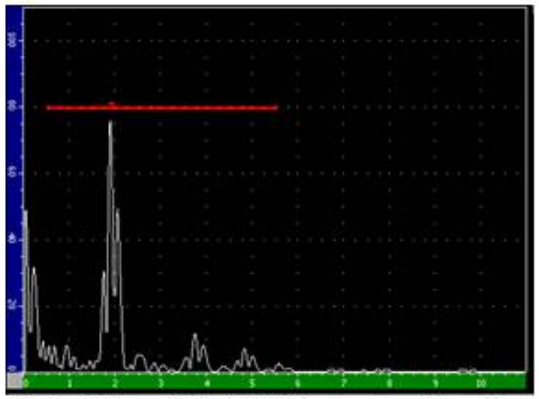

Point F- 60.75% Amplitude

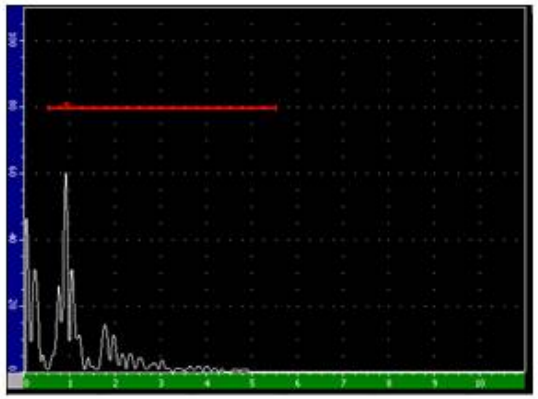

Point G- 76.5% Amplitude

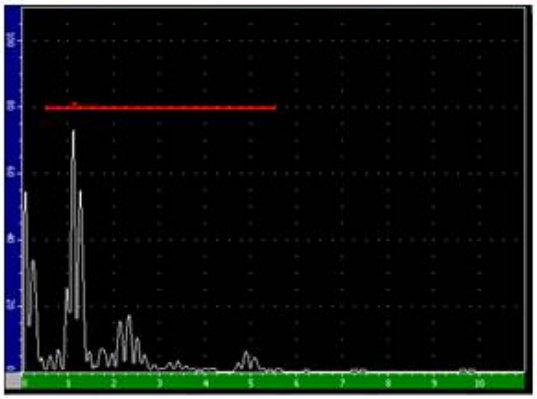

Point H- 73.5% Amplitude

NNSA National Nuclear Security Administration

NOTE: Noted dB and Amplitude Changes different from the Cal In

Sandia National Laboratories

FAA-H-001 Impact Panel
Flash Thermography (IR)

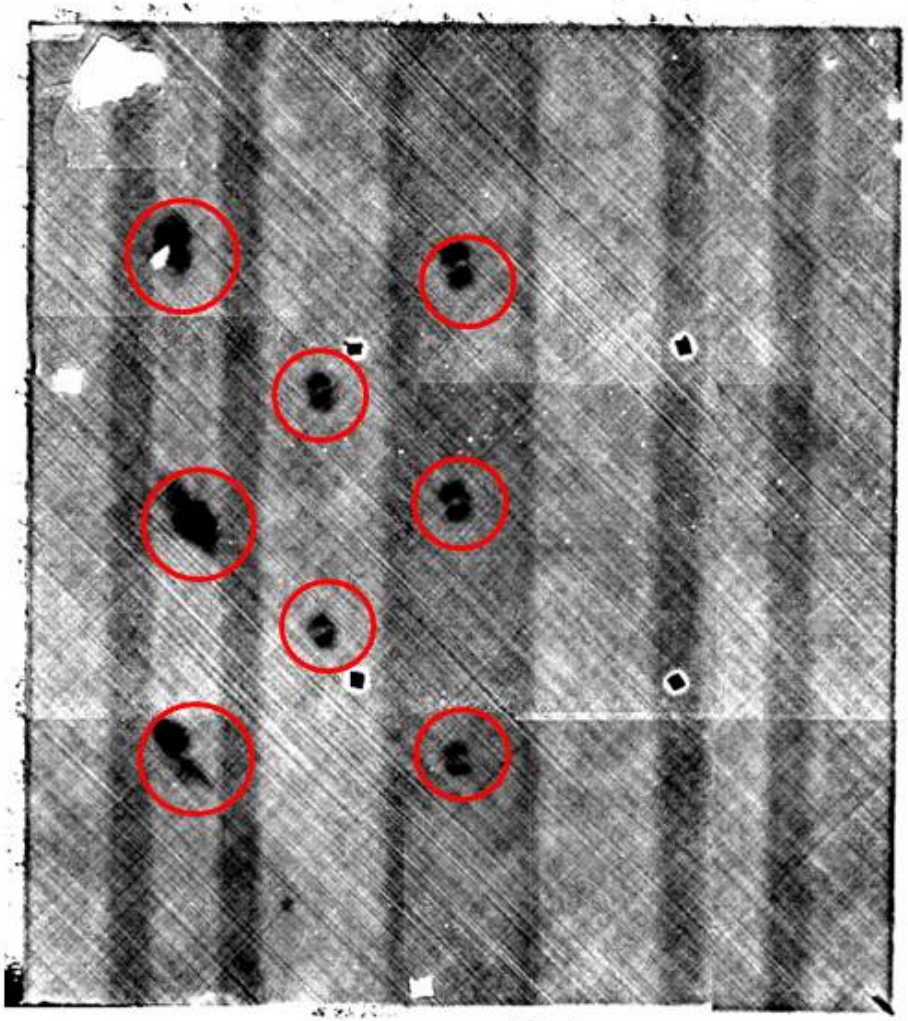

1d 0.601 sec after flash

National Nuclear Security Administration

Sandia National Laboratories

Hat Stiffened Panel FAA-H-002 Bell-Innovative, Image Based NDE for Modern Rotorcraft Sustainment

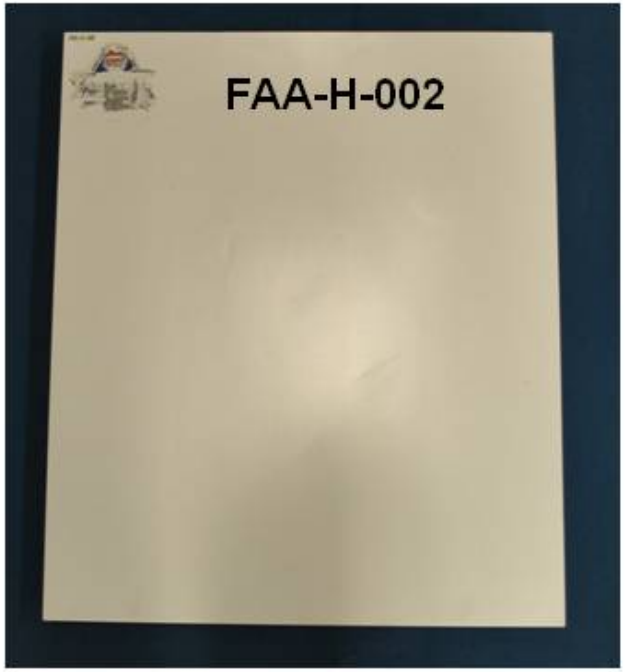

Top

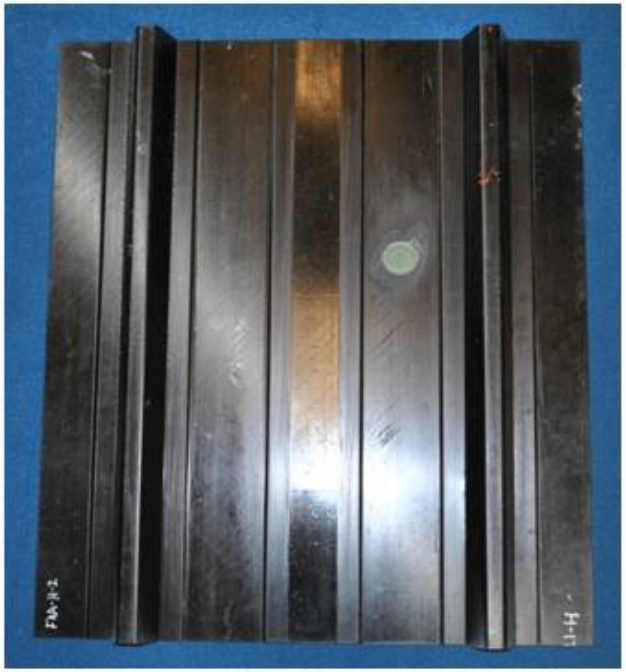

Bottom

National Nuclear Security Administration

Sandia National Laboratories

Hat Stiffened Panel FAA-H-002 Bell-Innovative, Image Based NDE for Modern Rotorcraft Sustainment Omniscan 10L64 (10 MHZ) Phased Array Plastic Wedge

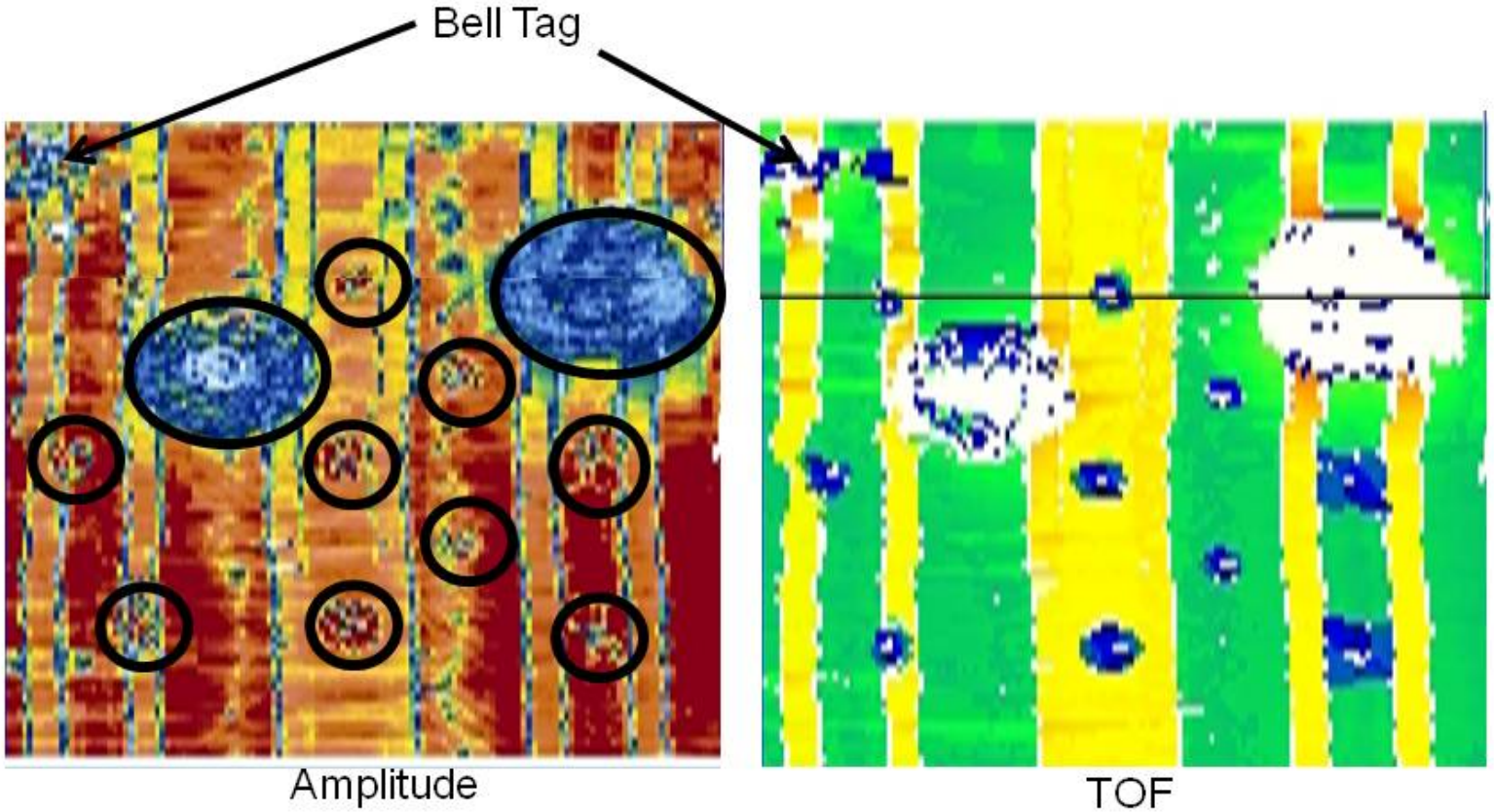

Hat Stiffened Panel FAA-H-002 Bell-Innovative, Image Based NDE for Modern Rotorcraft Sustainment Omniscan 5L64 (5 MHZ) Phased Array Aqualene

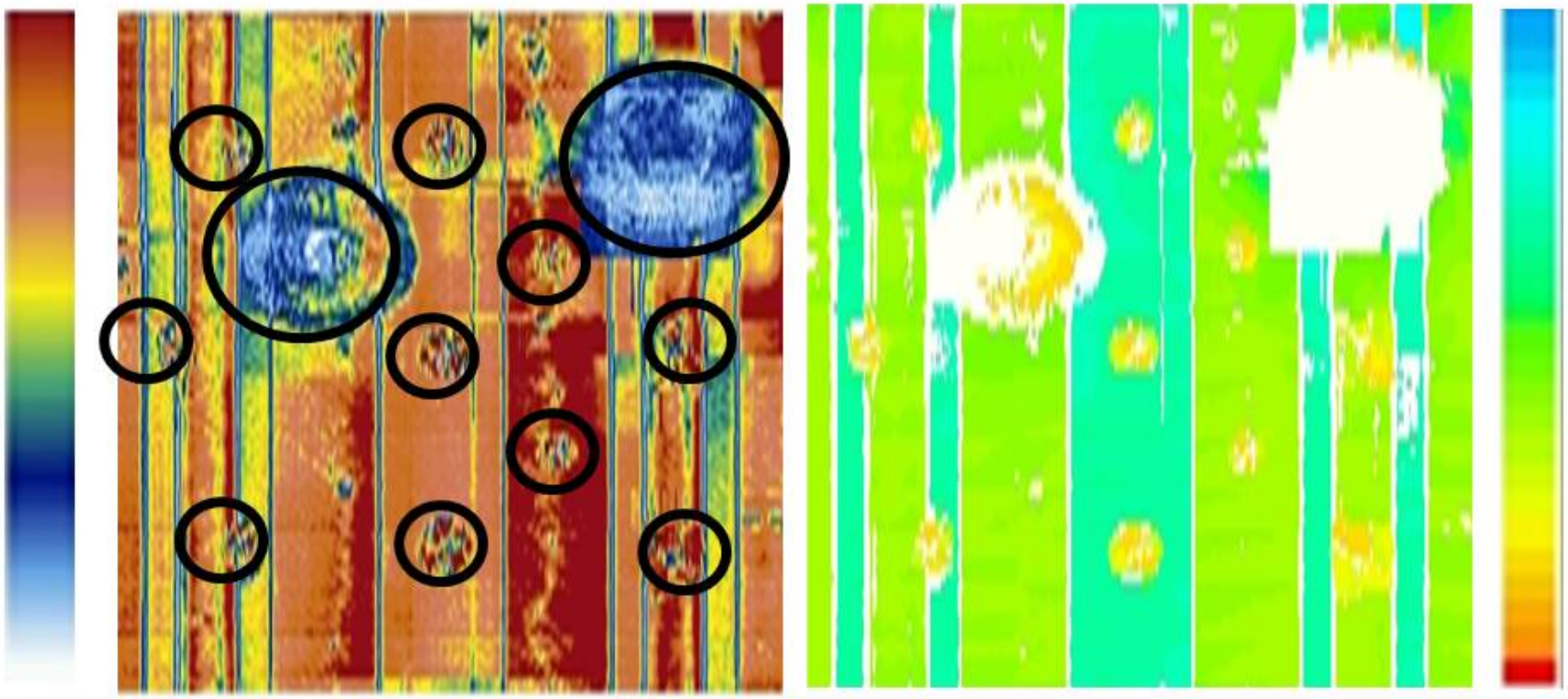

Amplitude

TOF

Hat Stiffened Panel FAA-H-002 Bell-Innovative, Image Based NDE for Modern Rotorcraft Sustainment Omniscan 5 MHZ Contact Testing

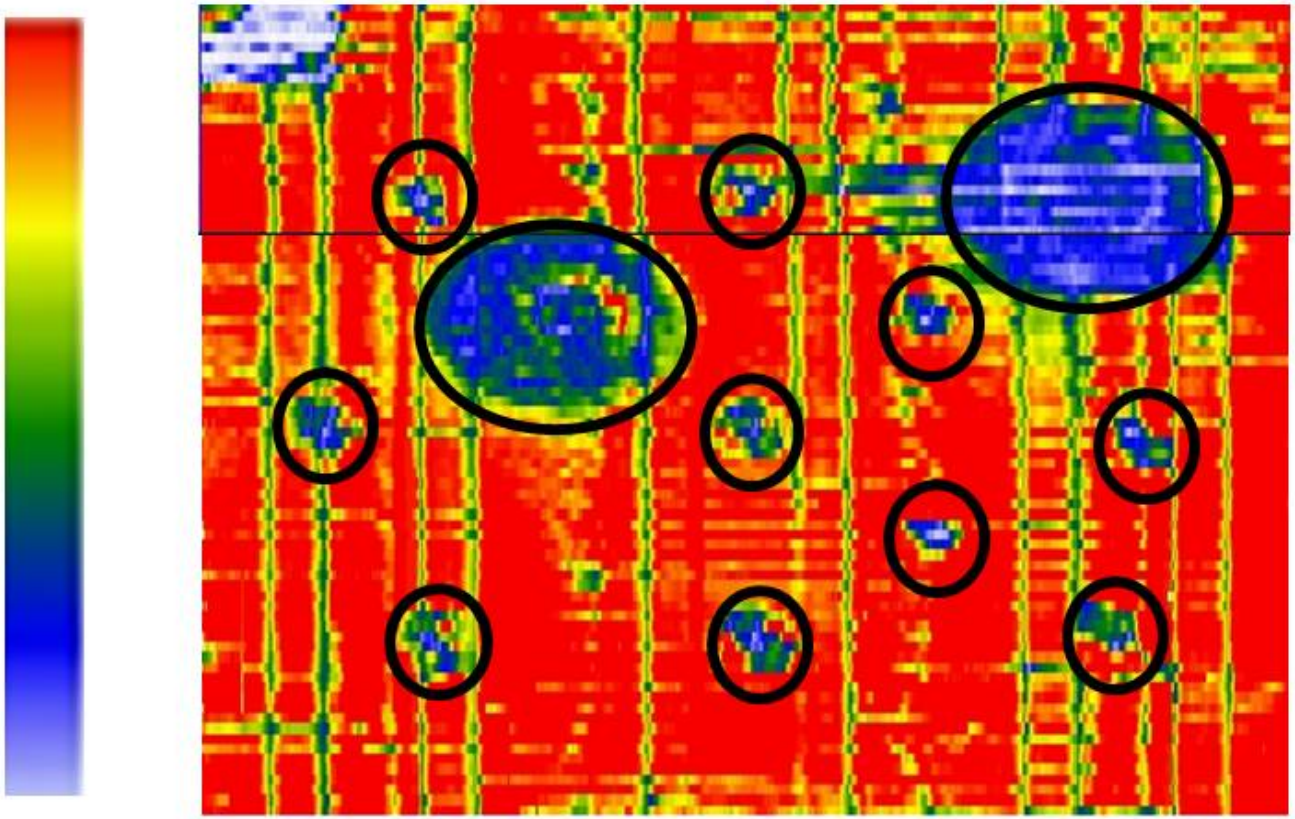

National Nuclear Security Administration

Sandia National Laboratories

Hat Stiffened Panel FAA-H-002 Bell-Innovative, Image Based NDE for Modern Rotorcraft Sustainment MAUS V Pulse Echo 5 MHZ Contact Testing

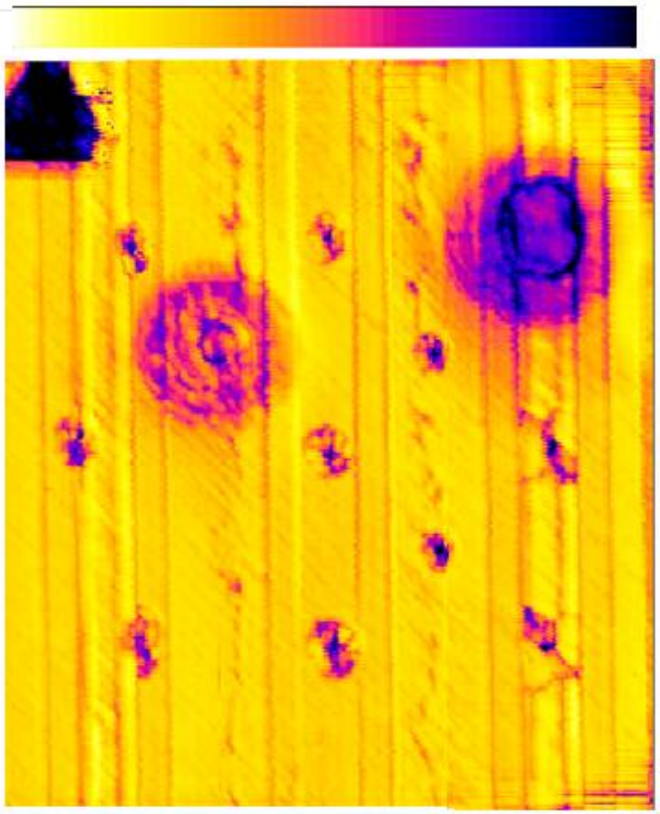

Amplitude

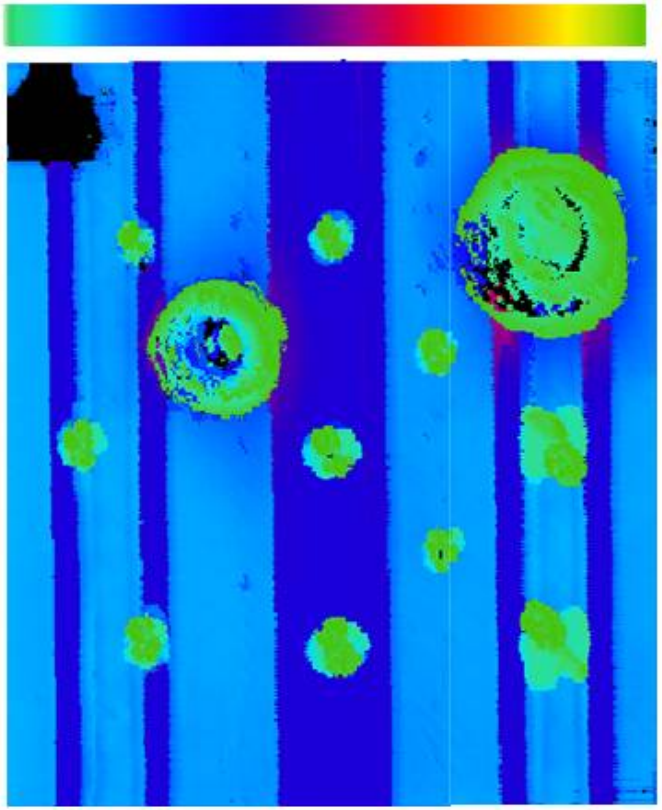

Depth- TOF

National Nuclear Security Administration

Sandia National Laboratories

Hat Stiffened Panel FAA-H-002 Bell-Innovative, Image Based NDE for Modern Rotorcraft Sustainment MAUS V Resonance 295 KHZ

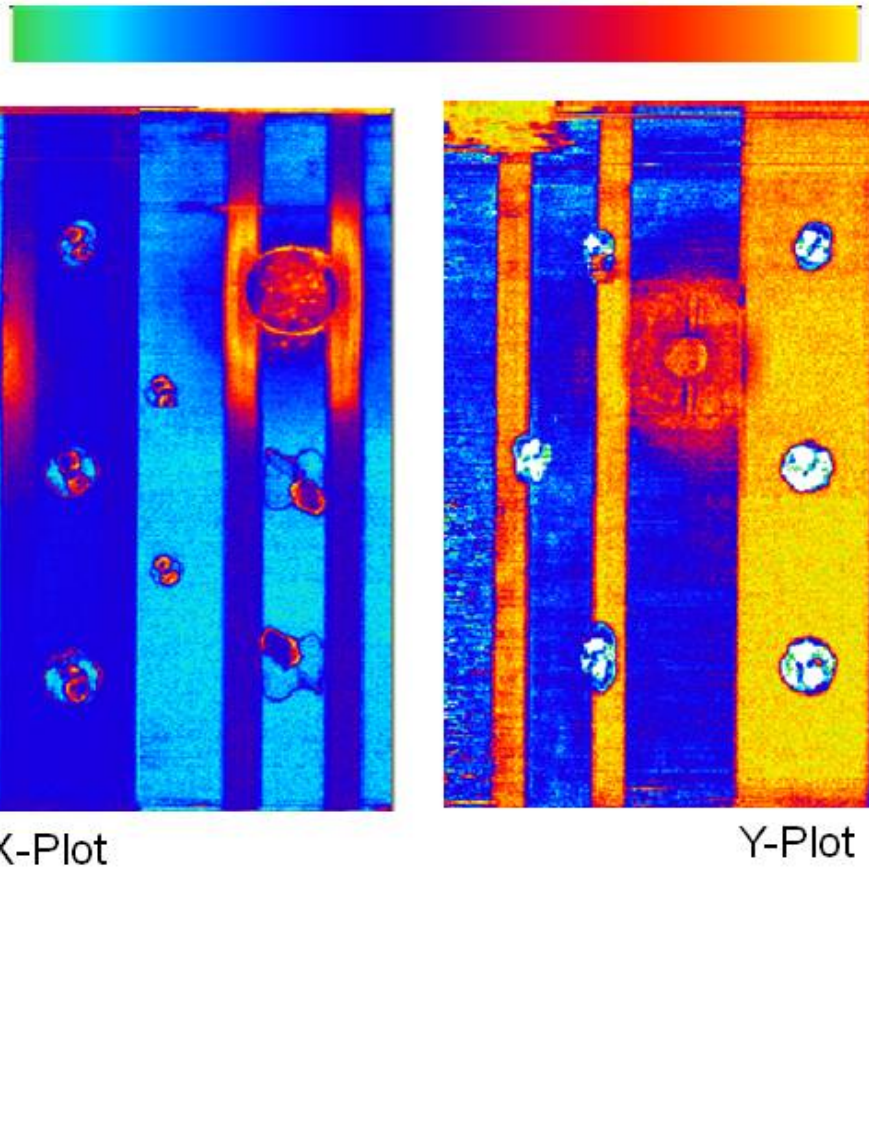

X-Plot

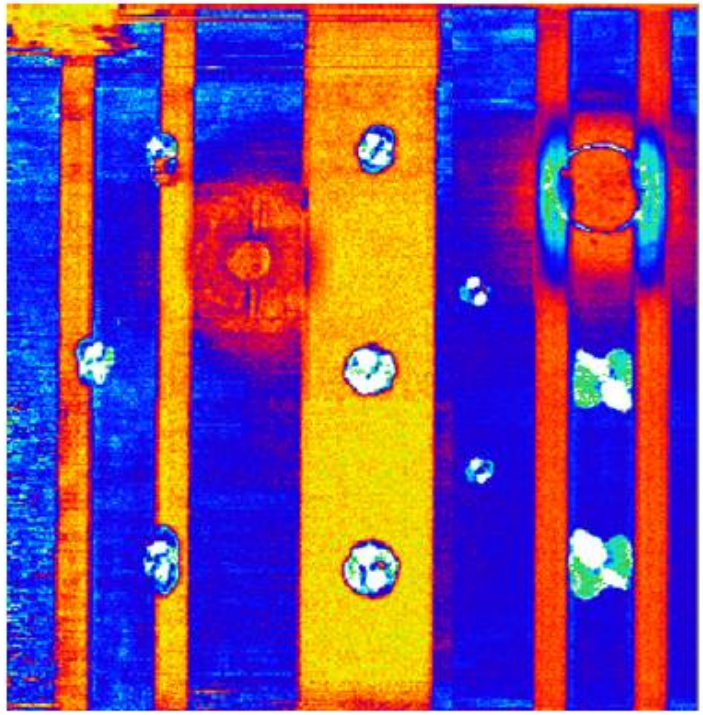

Y-Plot

National Nuclear Security Administration

Sandia National Laboratories

Hat Stiffened Panel FAA-H-002 Bell-Innovative, Image Based NDE for Modern Rotorcraft Sustainment
1000i Olympus Ultrasonic Tester 5 MHZ Contact A-Scan

Ramp Damage Checker/Bondmaster Results

Point A- Bad/Bad
Point B- Bad/Bad
Point C- Bad/Bad

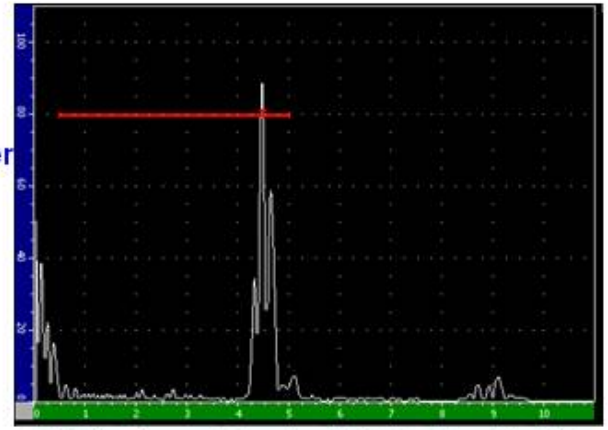

Cal In- 90% Amplitude/30.6db (4.52mm)

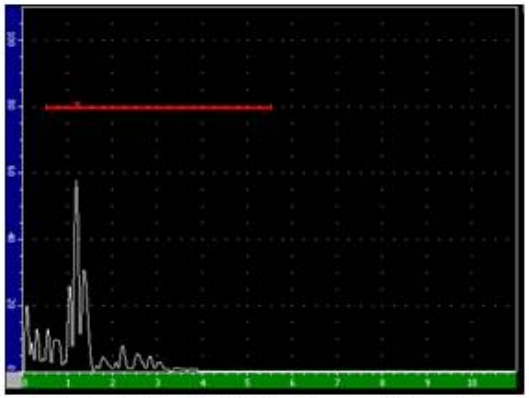

Point A- 58% Amplitude

Point B- 41.5% Amplitude

Point C- 49.0% Amplitude

NOTE: Noted dB and Amplitude Changes different from the Cal In

National Nuclear Security Administration

Sandia National Laboratories

Hat Stiffened Panel FAA-H-002 Bell-Innovative, Image Based NDE for Modern Rotorcraft Sustainment
1000i Olympus Ultrasonic Tester 5 MHZ Contact A-Scan

Ramp Damage Checker/Bondmaster Results

Point D- Bad/Bad

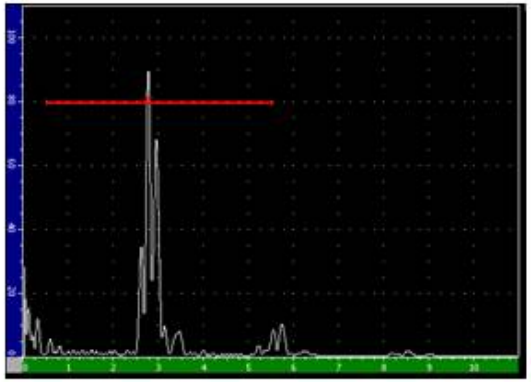

Cal In- 90% Amplitude/30.3db (2.56mm)

NOTE: Noted dB and Amplitude Changes different from the Cal In

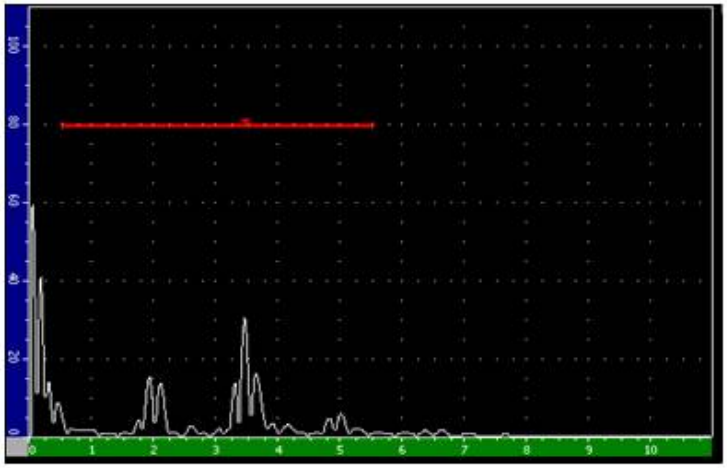

Point D- 26.5% Amplitude

Note: Repaired Area- Bondmaster Said Beyond Thickness

National Nuclear Security Administration

Sandia National Laboratories

Hat Stiffened Panel FAA-H-002 Bell-Innovative, Image Based NDE for Modern Rotorcraft Sustainment
1000i Olympus Ultrasonic Tester 5 MHZ Contact A-Scan

Ramp Damage Checker/Bondmaster Results

Point E- Bad/Bad
Point F- Bad/Bad
Point G- Bad/Bad

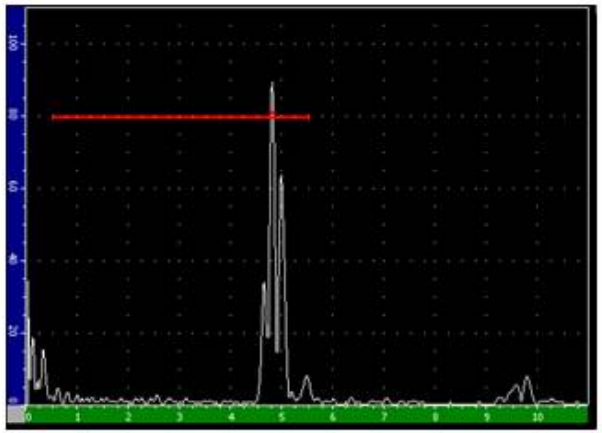

Cal In- 90% Amplitude/31.0db (4.51mm)

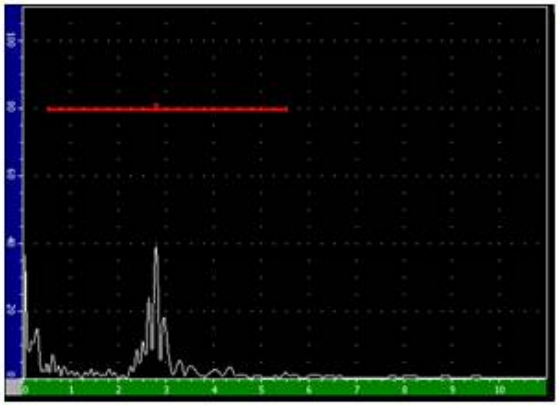

Point E- 39% Amplitude

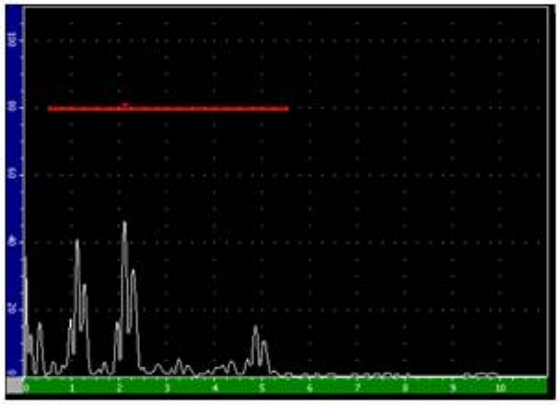

Point F- 46.5% Amplitude

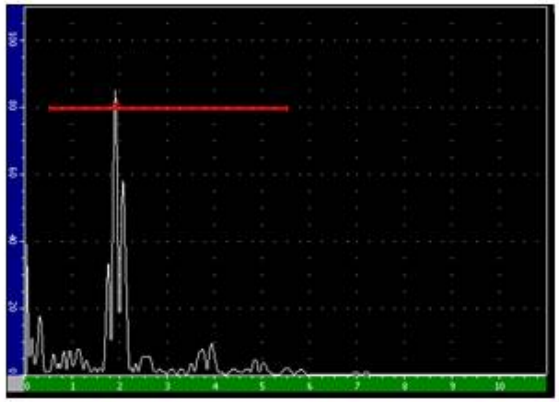

Point G- 85.2% Amplitude

NOTE: Noted dB and Amplitude Changes different from the Cal In

Hat Stiffened Panel FAA-H-002 Bell-Innovative, Image Based NDE for Modern Rotorcraft Sustainment
1000i Olympus Ultrasonic Tester 5 MHZ Contact A-Scan

Ramp Damage Checker/Bondmaster Results

Point H- Bad/Bad
Point I- Bad/Bad

Cal In- 90% Amplitude/30.6db (2.78mm)

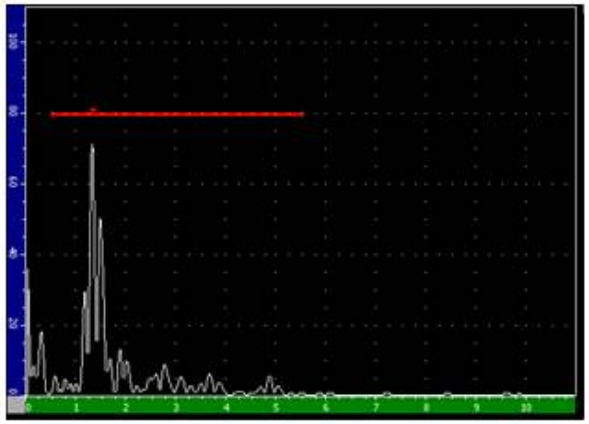

Point H- 71.75% Amplitude

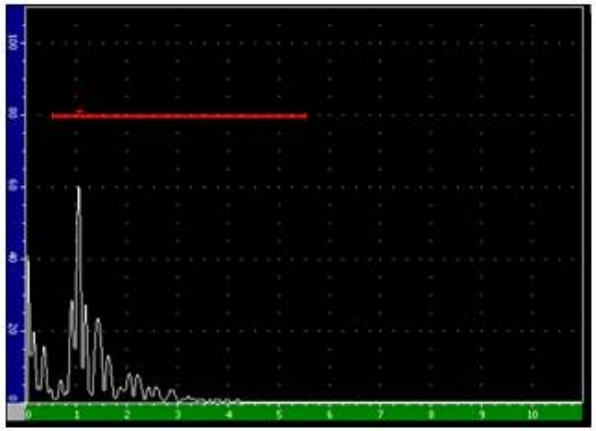

Point I- 60.75% Amplitude

NOTE: Noted dB and Amplitude Changes different from the Cal In

Hat Stiffened Panel FAA-H-002 Bell-Innovative, Image Based NDE for Modern Rotorcraft Sustainment
1000i Olympus Ultrasonic Tester 5 MHZ Contact A-Scan

Ramp Damage Checker/Bondmaster Results

Point J- Bad/Bad
Point K- Bad/Bad
Point L- Bad/Bad

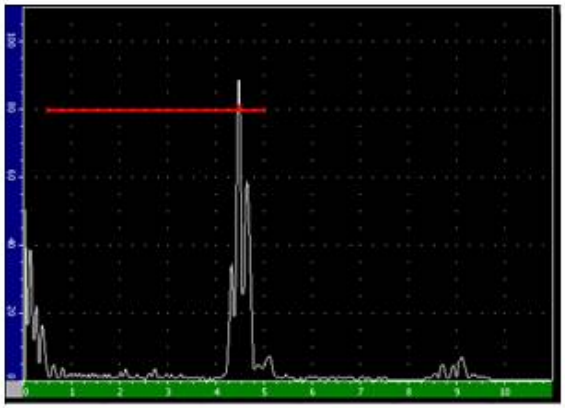

Cal In- 90% Amplitude/32.5db (4.44mm)

Point J- 76.25% Amplitude

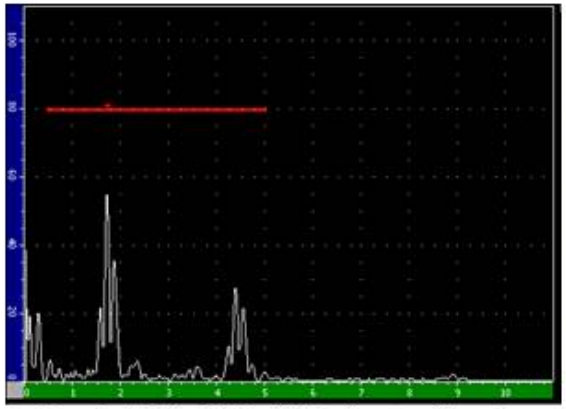

Point K- 55.1% Amplitude

Point L- 60.0% Amplitude

NOTE: Noted dB and Amplitude Changes different from the Cal In

FAA-H-002 Impact Panel
Flash Thermography (IR)

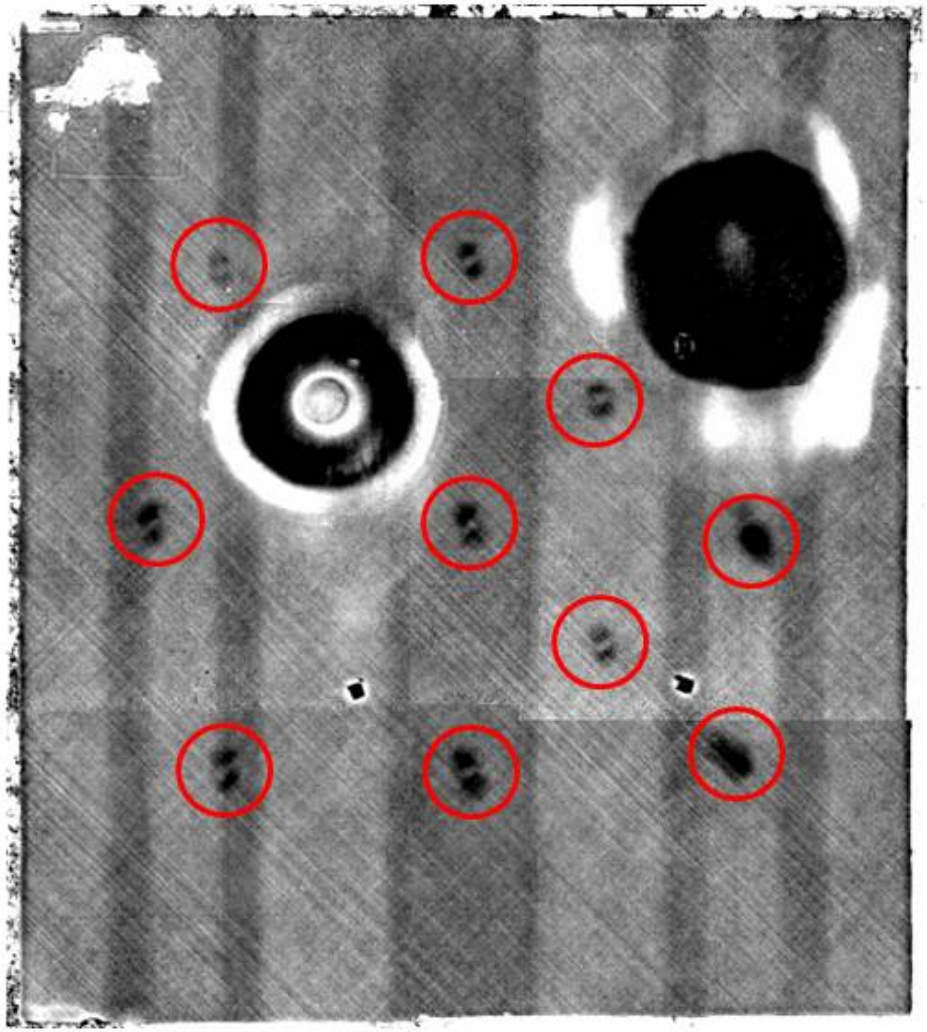

1d 0.851sec after flash

National Nuclear Security Administration

Sandia National Laboratories

Hat Stiffened Panel FAA-H-003 Bell-Innovative, Image Based NDE for Modern Rotorcraft Sustainment

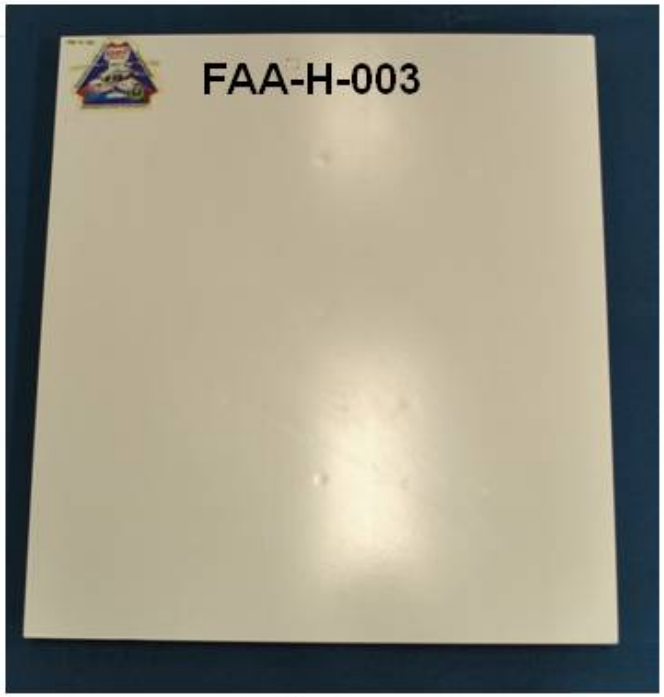

Top

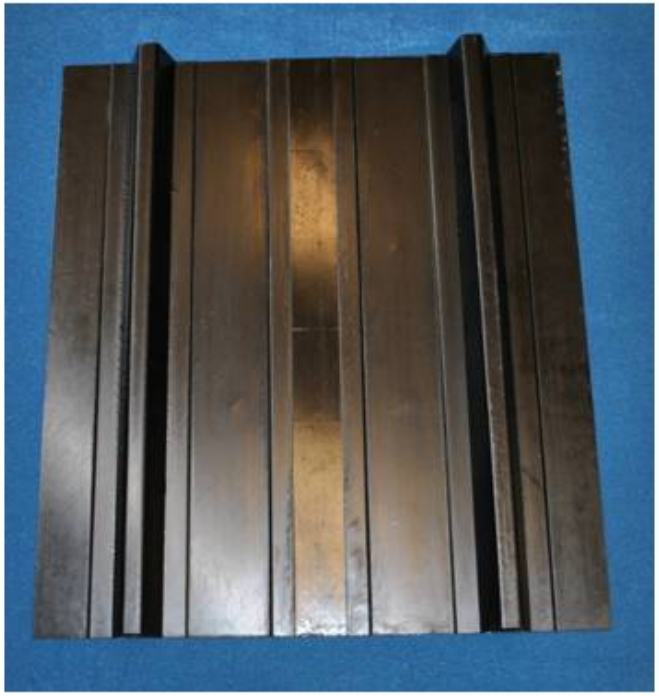

Bottom

National Nuclear Security Administration

Sandia National Laboratories

Hat Stiffened Panel FAA-H-003 Bell-Innovative, Image Based NDE for Modern Rotorcraft Sustainment Omniscan 10L64 (10 MHZ) Phased Array Plastic Wedge

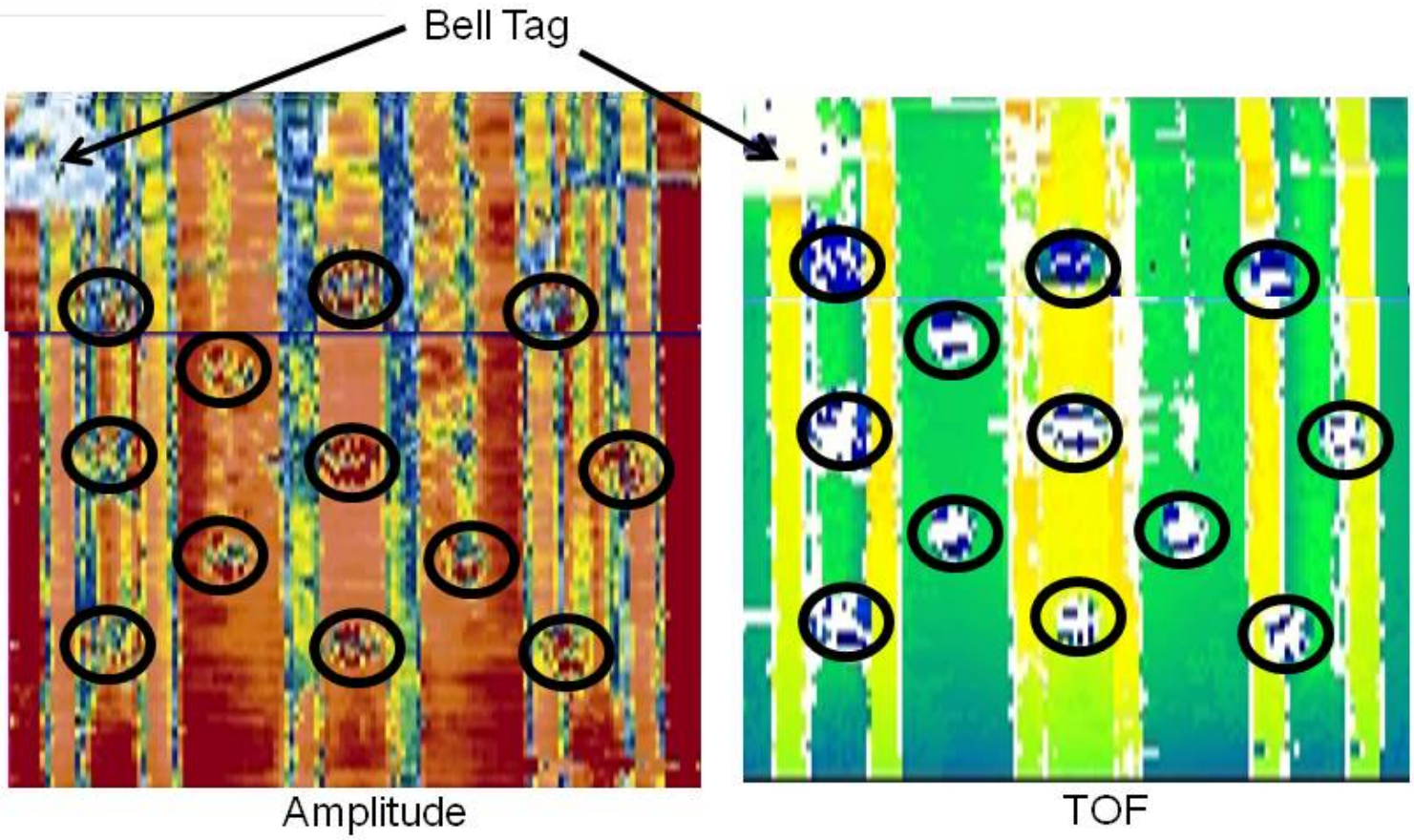

Hat Stiffened Panel FAA-H-003 Bell-Innovative, Image Based NDE for Modern Rotorcraft Sustainment Omniscan 5L64 (5 MHZ) Phased Array Aqualene

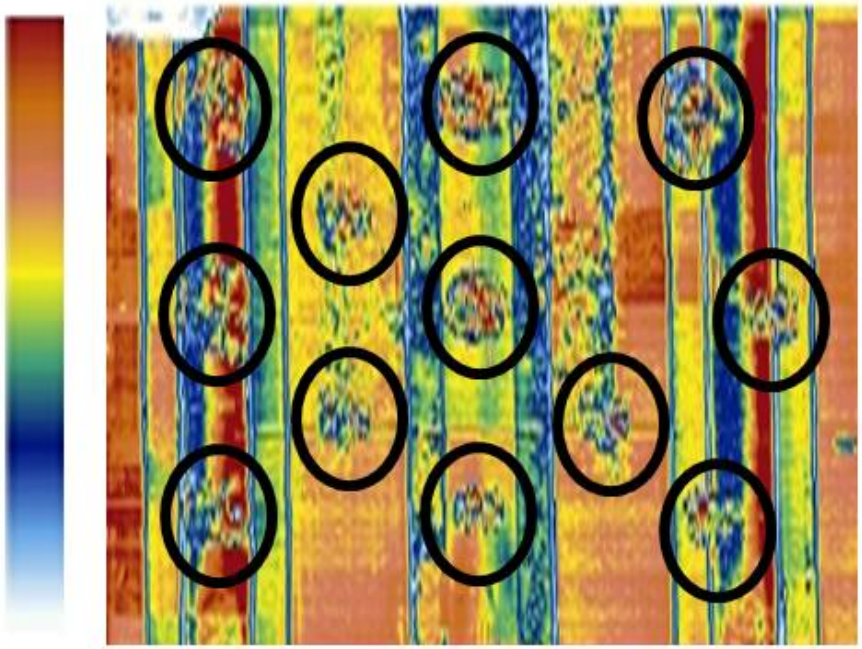

Amplitude

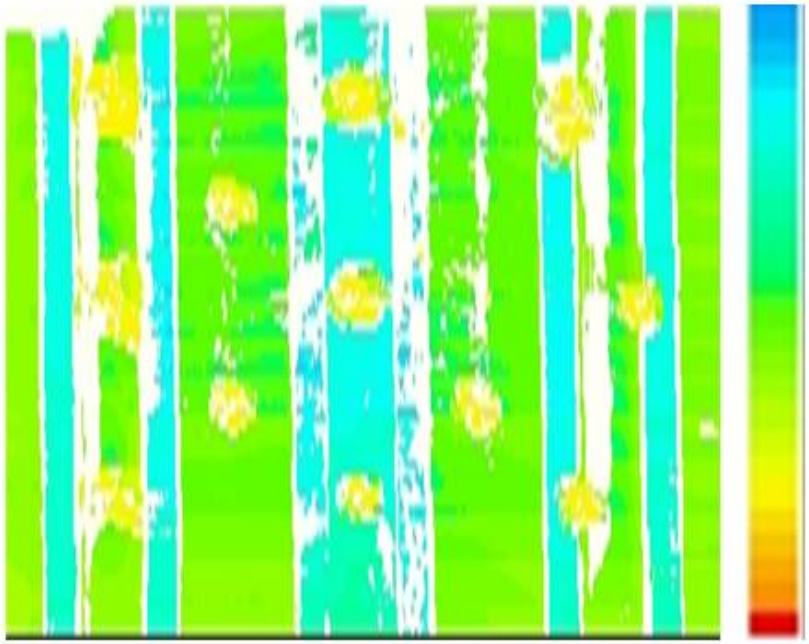

TOF

National Nuclear Security Administration

Sandia National Laboratories

Hat Stiffened Panel FAA-H-003 Bell-Innovative, Image Based NDE for Modern Rotorcraft Sustainment Omniscan 5 MHZ Contact Testing

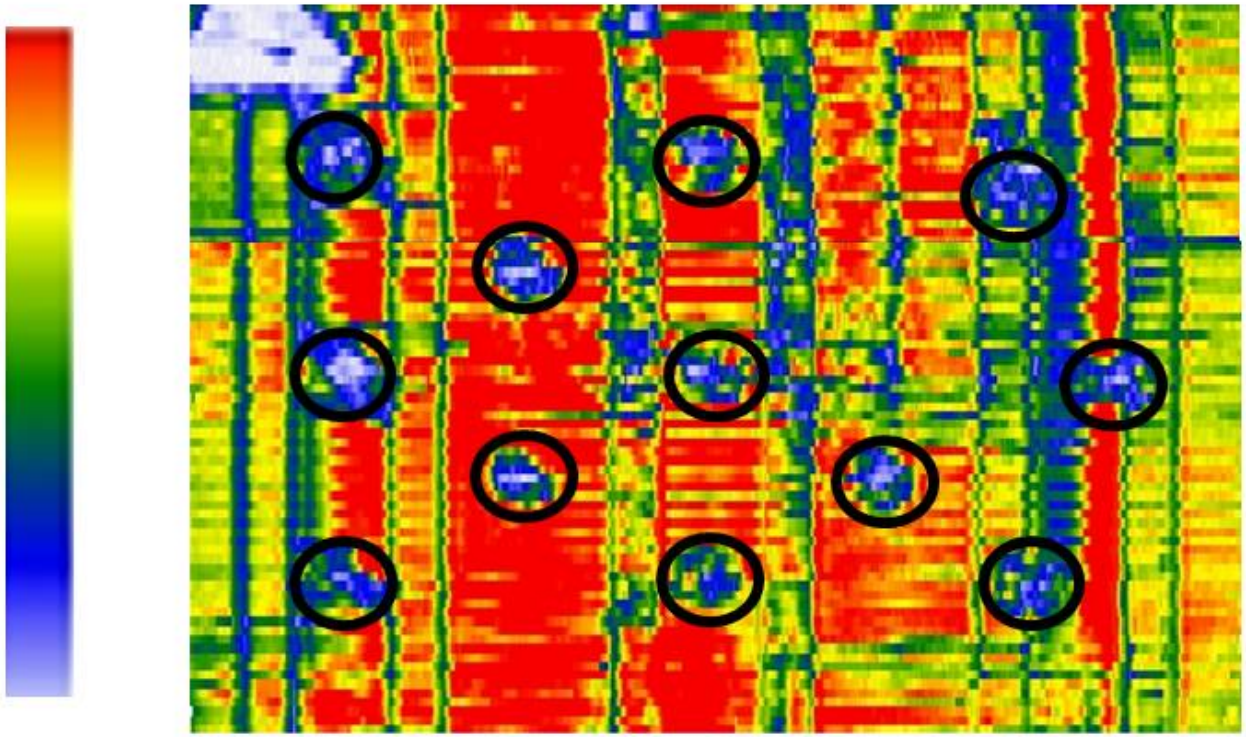

Amplitude

National Nuclear Security Administration

Sandia National Laboratories

Hat Stiffened Panel FAA-H-003 Bell-Innovative, Image Based NDE for Modern Rotorcraft Sustainment MAUS V Pulse Echo 5 MHZ Contact Testing

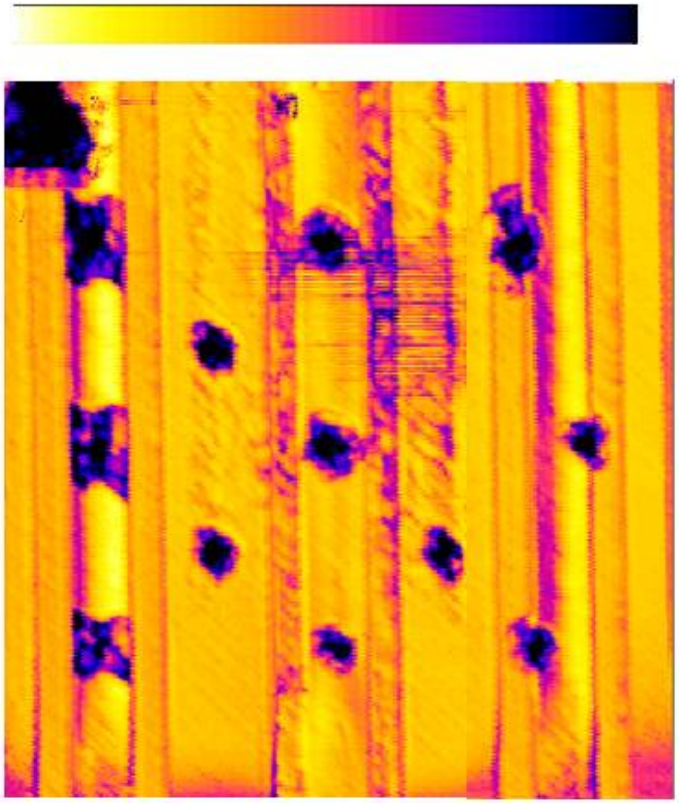

Amplitude

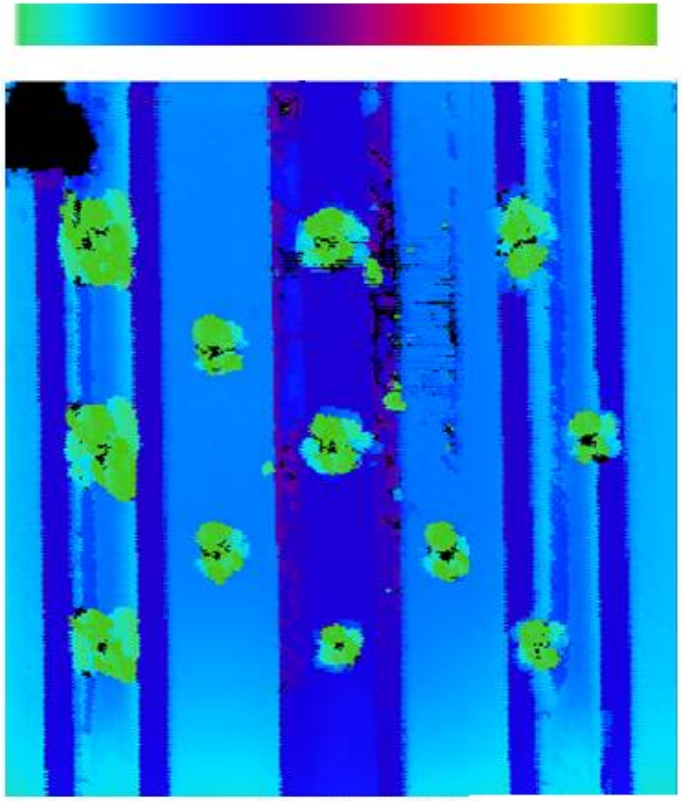

Depth- TOF

National Nuclear Security Administration

Sandia National Laboratories

Hat Stiffened Panel FAA-H-003 Bell-Innovative, Image Based NDE for Modern Rotorcraft Sustainment MAUS V Resonance Testing 295 KHZ

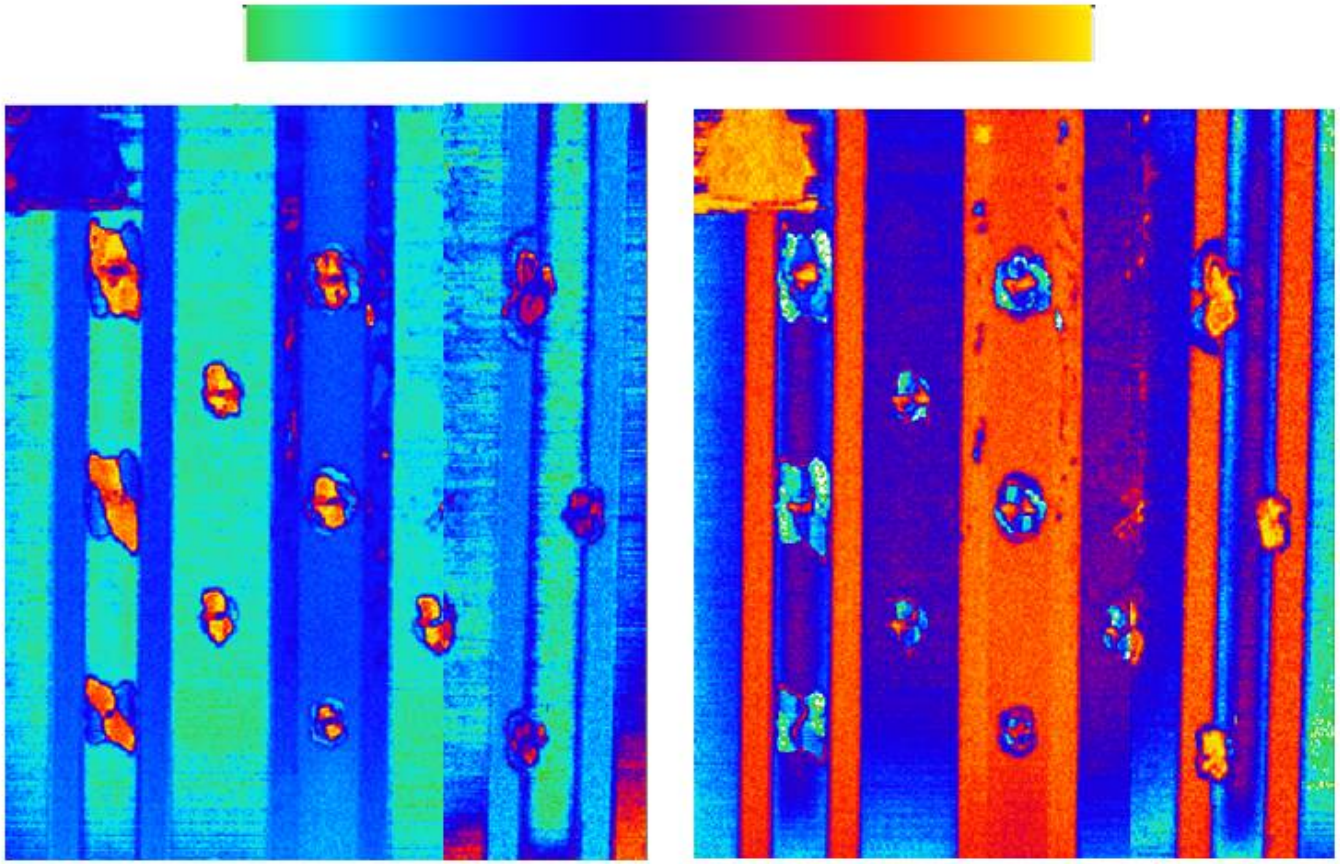

X-Plot Y-Plot

National Nuclear Security Administration

Sandia National Laboratories

Hat Stiffened Panel FAA-H-003 Bell-Innovative, Image Based NDE for Modern Rotorcraft Sustainment
1000i Olympus Ultrasonic Tester 5 MHZ Contact A-Scans

Ramp Damage Checker/Bondmaster Results

Point A- Bad/Bad
Point B- Bad/Bad
Point C- Bad/Bad

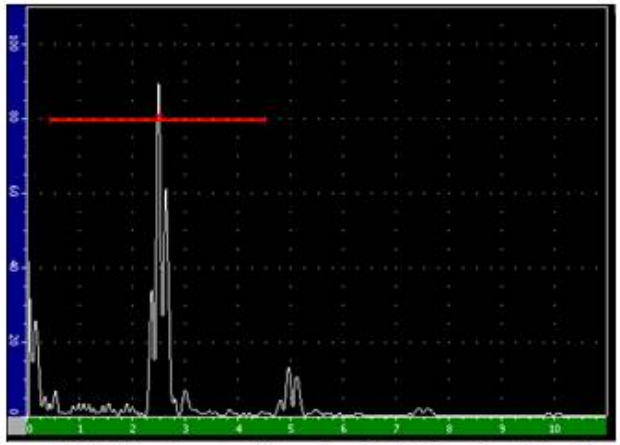

Cal In- 90% Amplitude/29.5db (2.07mm)

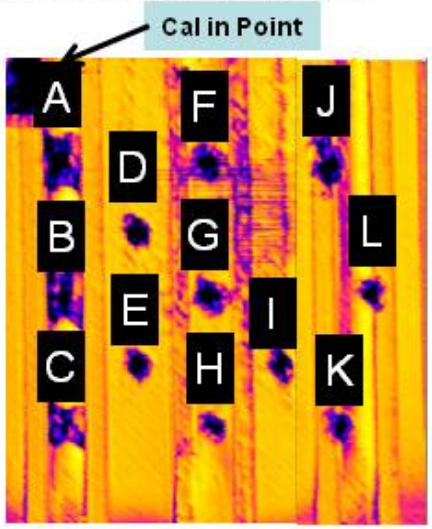

Point A- 94.25% Amplitude

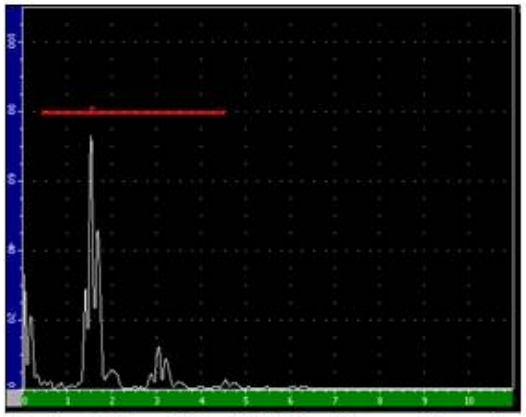

Point B- 73.75% Amplitude

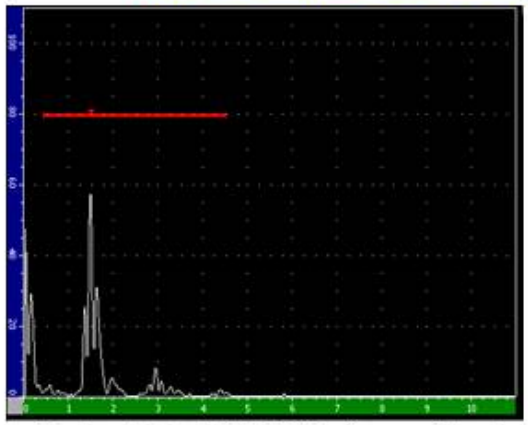

Point C- 57.5% Amplitude

NOTE: Noted dB and Amplitude Changes different from the Cal In

Hat Stiffened Panel FAA-H-003 Bell-Innovative, Image Based NDE for Modern Rotorcraft Sustainment
1000i Olympus Ultrasonic Tester 5 MHZ Contact A-Scan

Ramp Damage Checker/Bondmaster Results

Point D- Bad/Bad
Point E- Bad/Bad

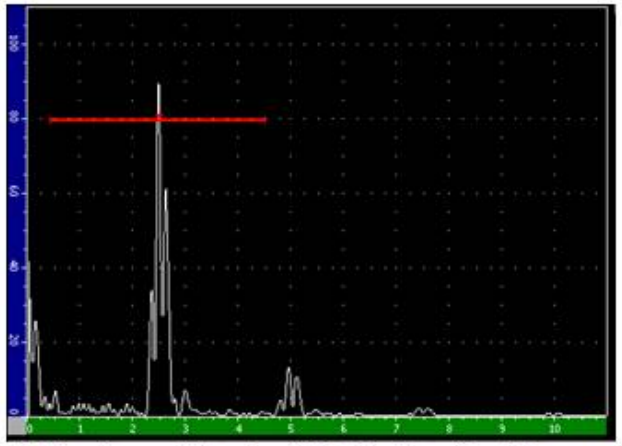

Cal In- 90% Amplitude/29.5db (2.10mm)

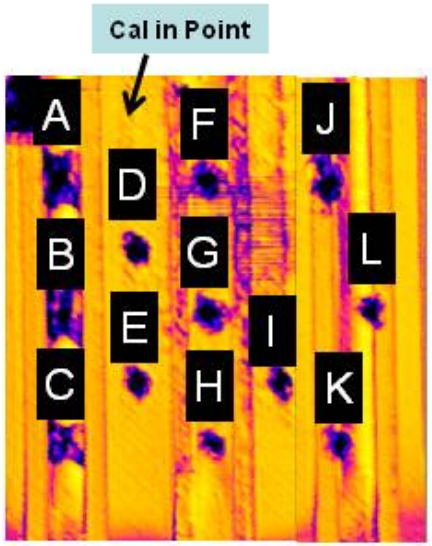

Point D- 94.75% Amplitude

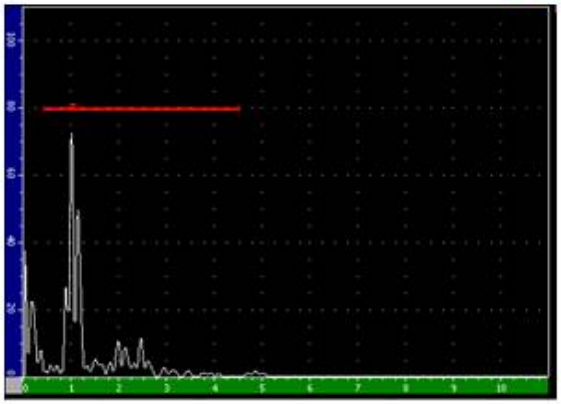

Point E- 73% Amplitude

NOTE: Noted dB and Amplitude Changes different from the Cal In

Hat Stiffened Panel FAA-H-003 Bell-Innovative, Image Based NDE for Modern Rotorcraft Sustainment
1000i Olympus Ultrasonic Tester 5 MHZ Contact A-Scan

Ramp Damage Checker/Bondmaster Results

Point F- Bad/Bad
Point G- Bad/Bad
Point H- Bad/Bad

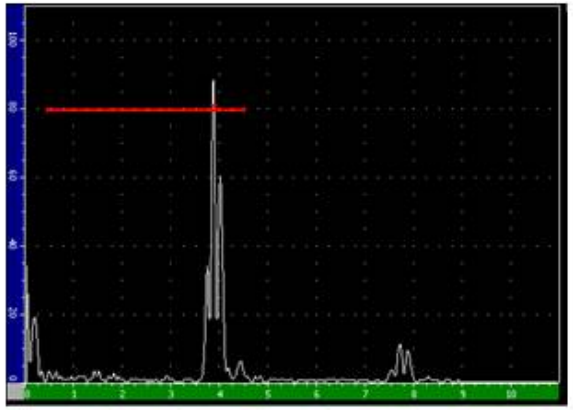

Cal In- 90% Amplitude/30.0db (3.68mm)

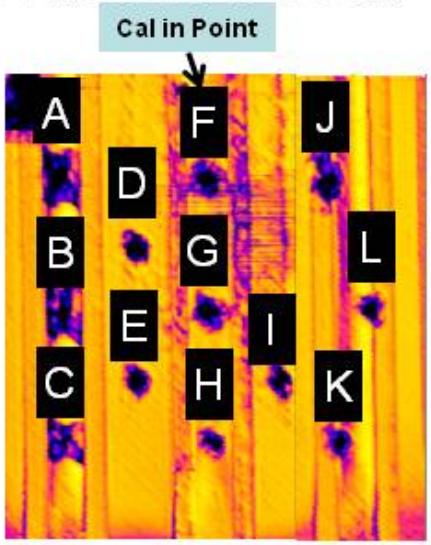

Point F- 91.5% Amplitude

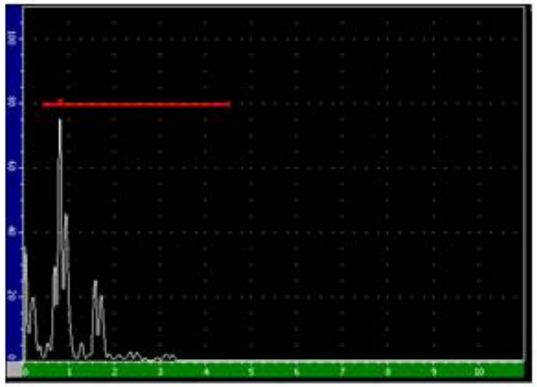

Point G- 75.5% Amplitude

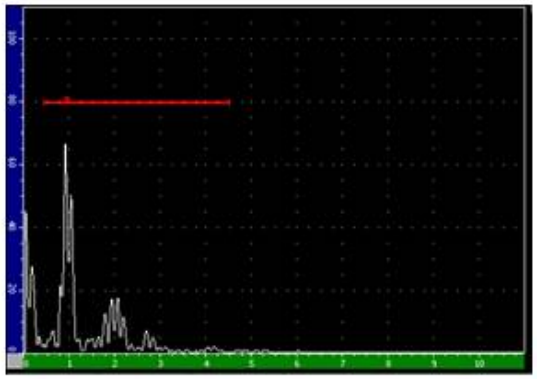

Point H- 67% Amplitude

NOTE: Noted dB and Amplitude Changes different from the Cal In

Hat Stiffened Panel FAA-H-003 Bell-Innovative, Image Based NDE for Modern Rotorcraft Sustainment
1000i Olympus Ultrasonic Tester 5 MHZ Contact A-Scan

Ramp Damage Checker/Bondmaster Results

Point I- Bad/Bad

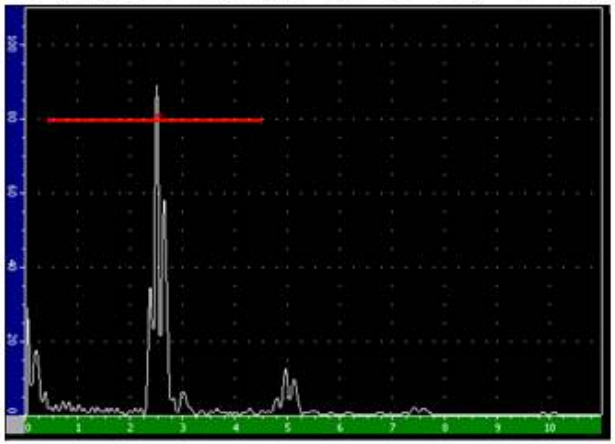

Cal In- 90% Amplitude/30.0db (2.18mm)

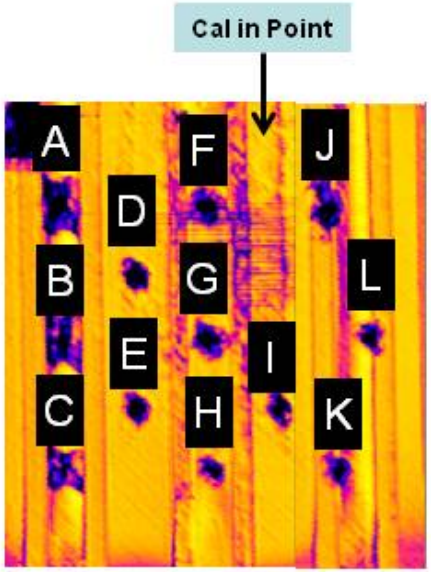

NOTE: Noted dB and Amplitude Changes different from the Cal In

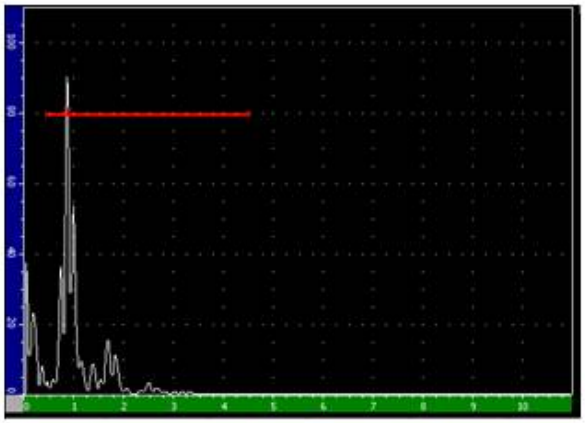

Point I- 91.25% Amplitude

National Nuclear Security Administration

Sandia National Laboratories

Hat Stiffened Panel FAA-H-003 Bell-Innovative, Image Based NDE for Modern Rotorcraft Sustainment
1000i Olympus Ultrasonic Tester 5 MHZ Contact A-Scan

Ramp Damage Checker/Bondmaster Results

Point J- Bad/Bad
Point K- Bad/Bad
Point L- Bad/Bad

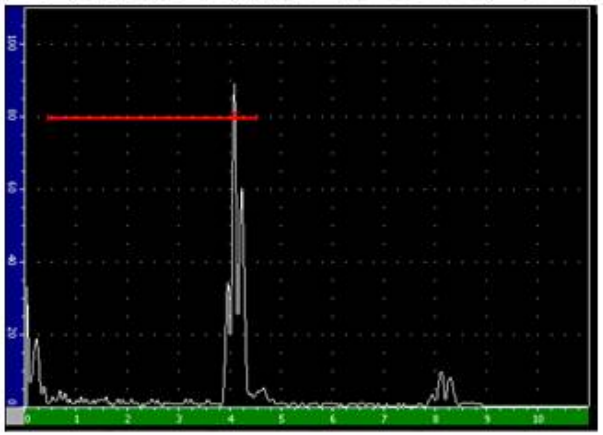

Cal In- 90% Amplitude/31.2db (3.93mm)

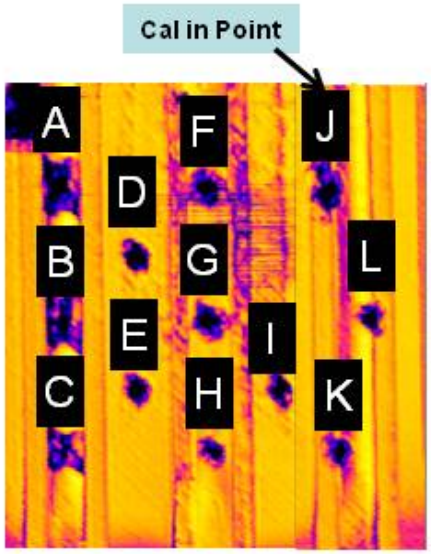

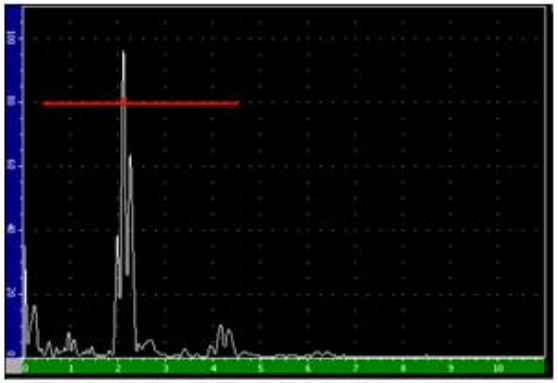

Point J- 97.25% Amplitude

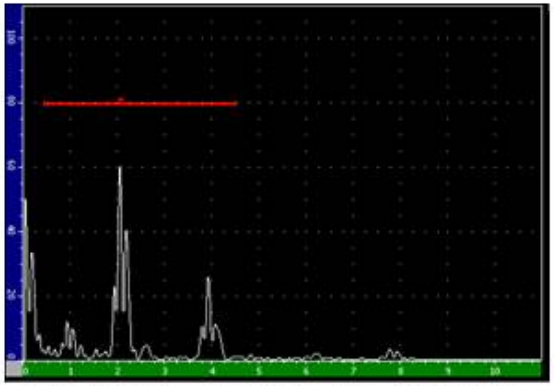

Point K- 60.5% Amplitude

Point L- 73.25% Amplitude

NOTE: Noted dB and Amplitude Changes different from the Cal In

FAA-H-003 Impact Panel
Flash Thermography (IR)

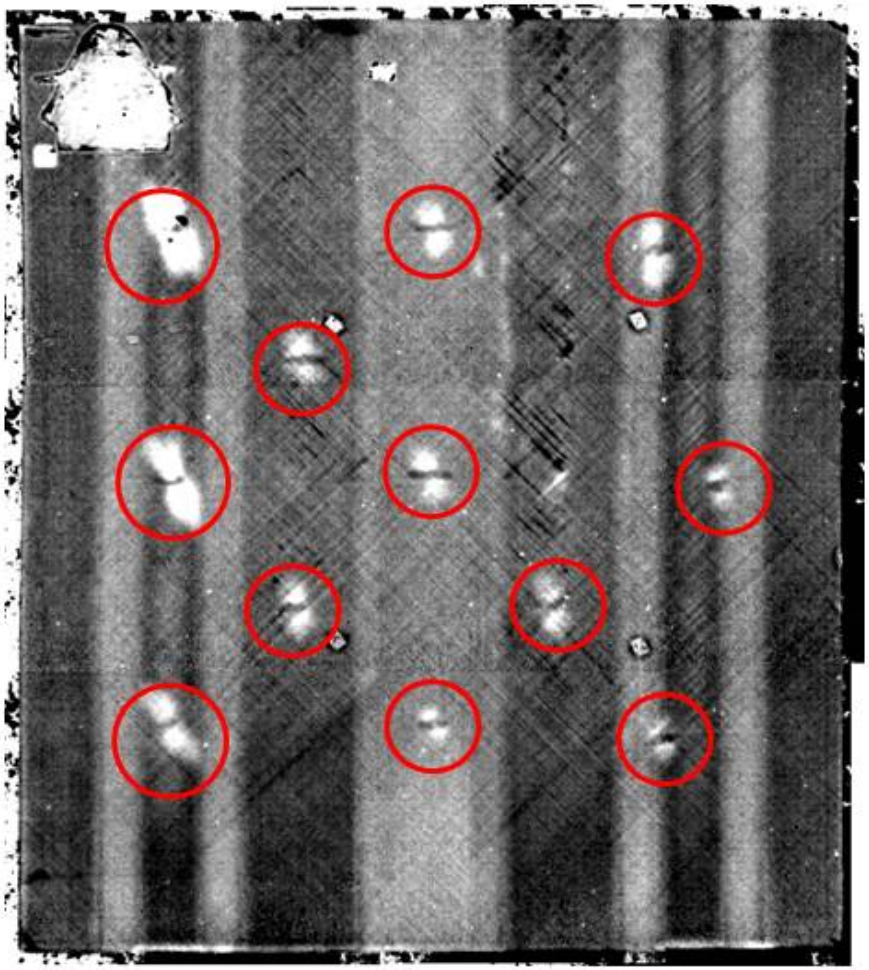

2d 0.300 sec after flash

National Nuclear Security Administration

Sandia National Laboratories

Bell-Innovative FOD Panels, Image Based NDE for Modern Rotorcraft Sustainment

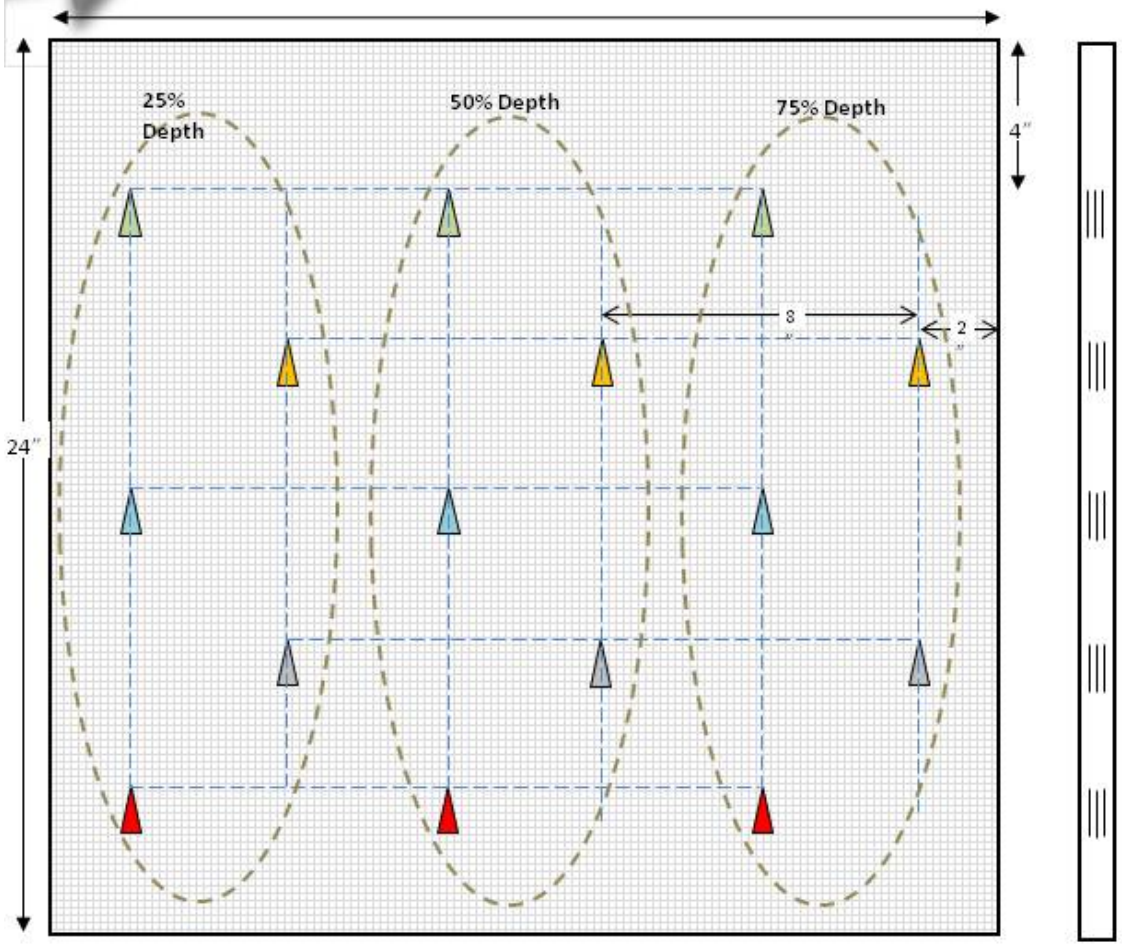

Green = Teflon / Tedlar, is orange Teflon Tape over Tedlar

Gold = Backing Film, 1 layer, Poly material, FM300 per 299-947-121

Blue = Paper, coated, from AF 163 per spec. 299-947-320

Silver = 1 Layer Aluminum Backing from material per 299-947-350

Red = AF 163 Adhesive film plastic Backing per 299-947-038

Note: Dart size is approximately 1.25" tall x 0.5" wide at base

21 Ply C/EP Tape per 297-947-330 TY35 CL2 Form 0 Grade 190 (as illustrated on ply table on Page 2)

Fod Layers between

Ply 5 and 6,

- Ply 10 and 11
- Ply15 and 16

FOD Inserts to be provided and applied by NDE Lab personnel.

RJ Barry Ext. 13253

National Nuclear Security Administration

FAA-FOD-01 Bell-Innovative, Image Based NDE for Modern Rotorcraft Sustainment

Top

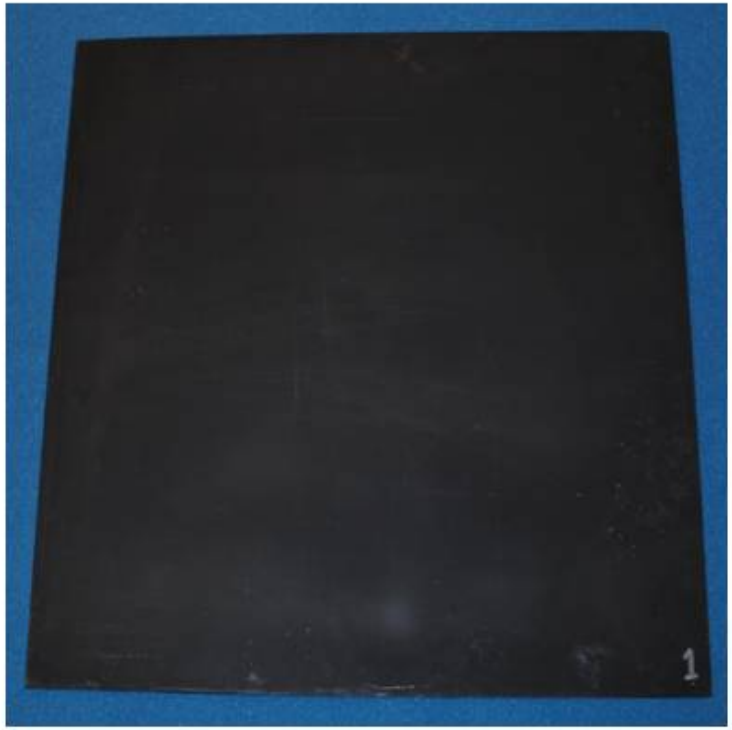

Bottom

National Nuclear Security Administration

Sandia National Laboratories

FAA-FOD-01 Bell-Innovative, Image Based NDE for Modern Rotorcraft Sustainment
Omniscan Unit 5L64 (5 MHZ) Aqualene Wedge Phased Array

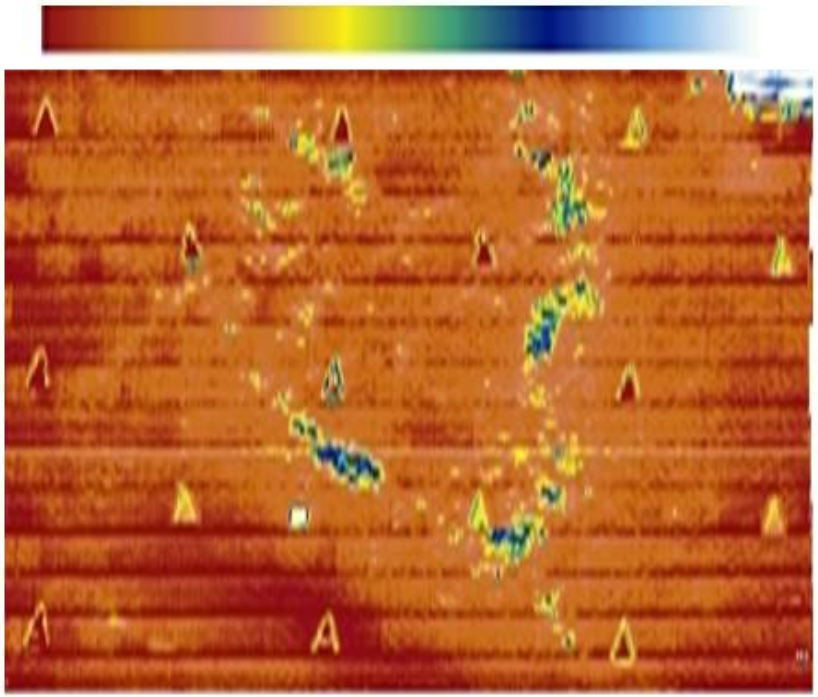

Amplitude

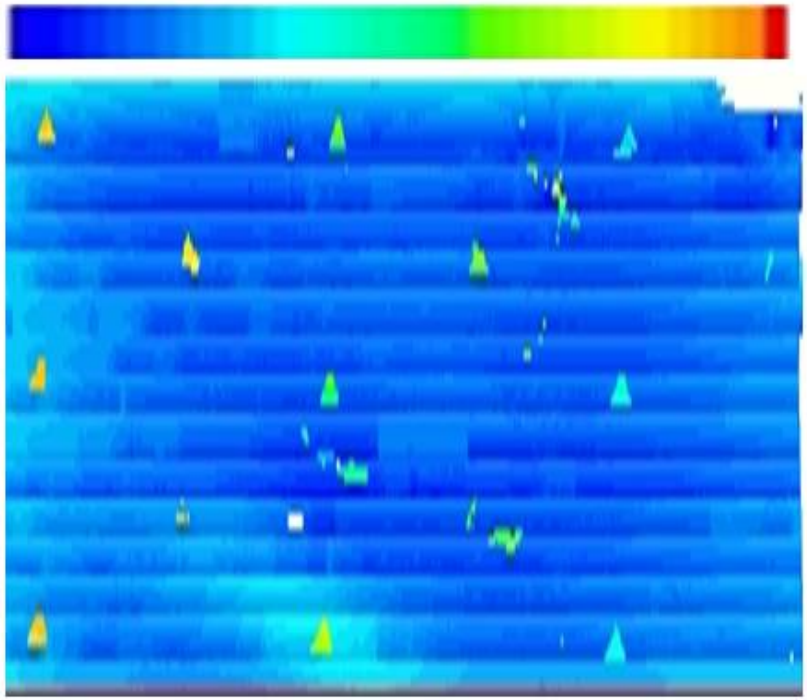

TOF

National Nuclear Security Administration

Sandia National Laboratories

FAA-FOD-01 Bell-Innovative, Image Based NDE for Modern Rotorcraft Sustainment
Omniscan Unit 5 MHZ Contact Testing

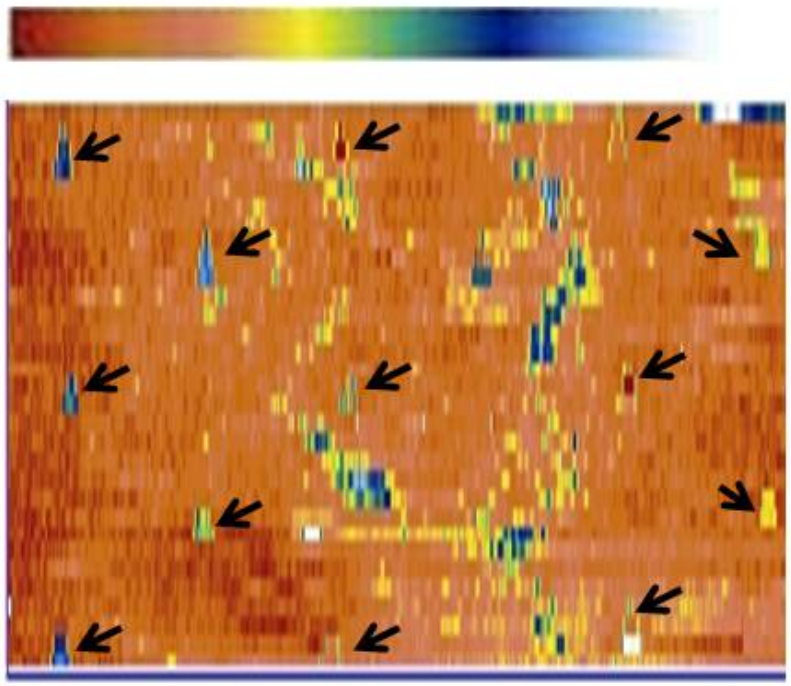

Amplitude

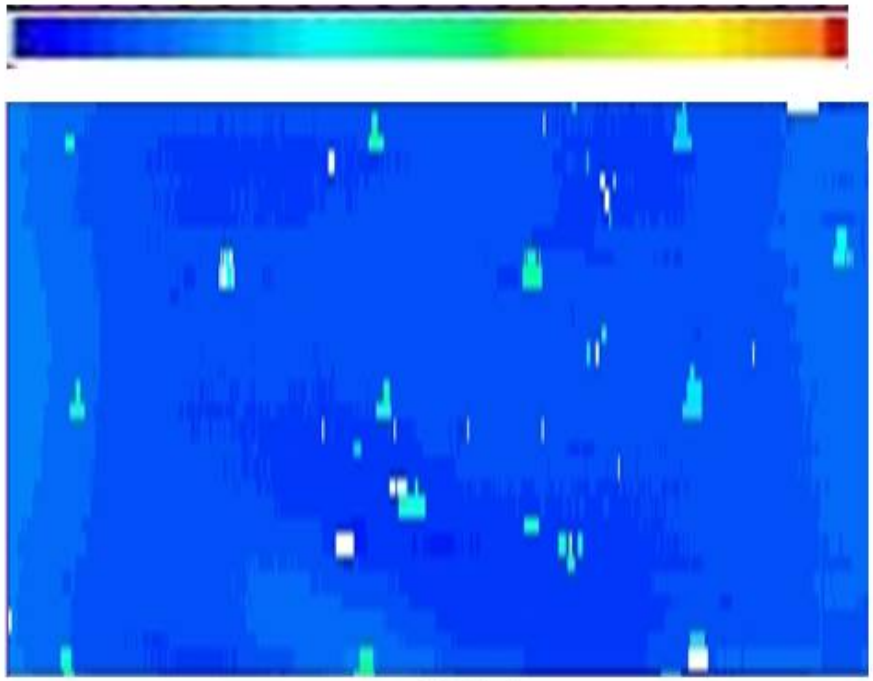

TOF

National Nuclear Security Administration

Sandia National Laboratories

FAA-FOD-01 Bell-Innovative, Image Based NDE for Modern Rotorcraft Sustainment
MAUS 5 Pulse Echo 5 MHZ Contact Testing

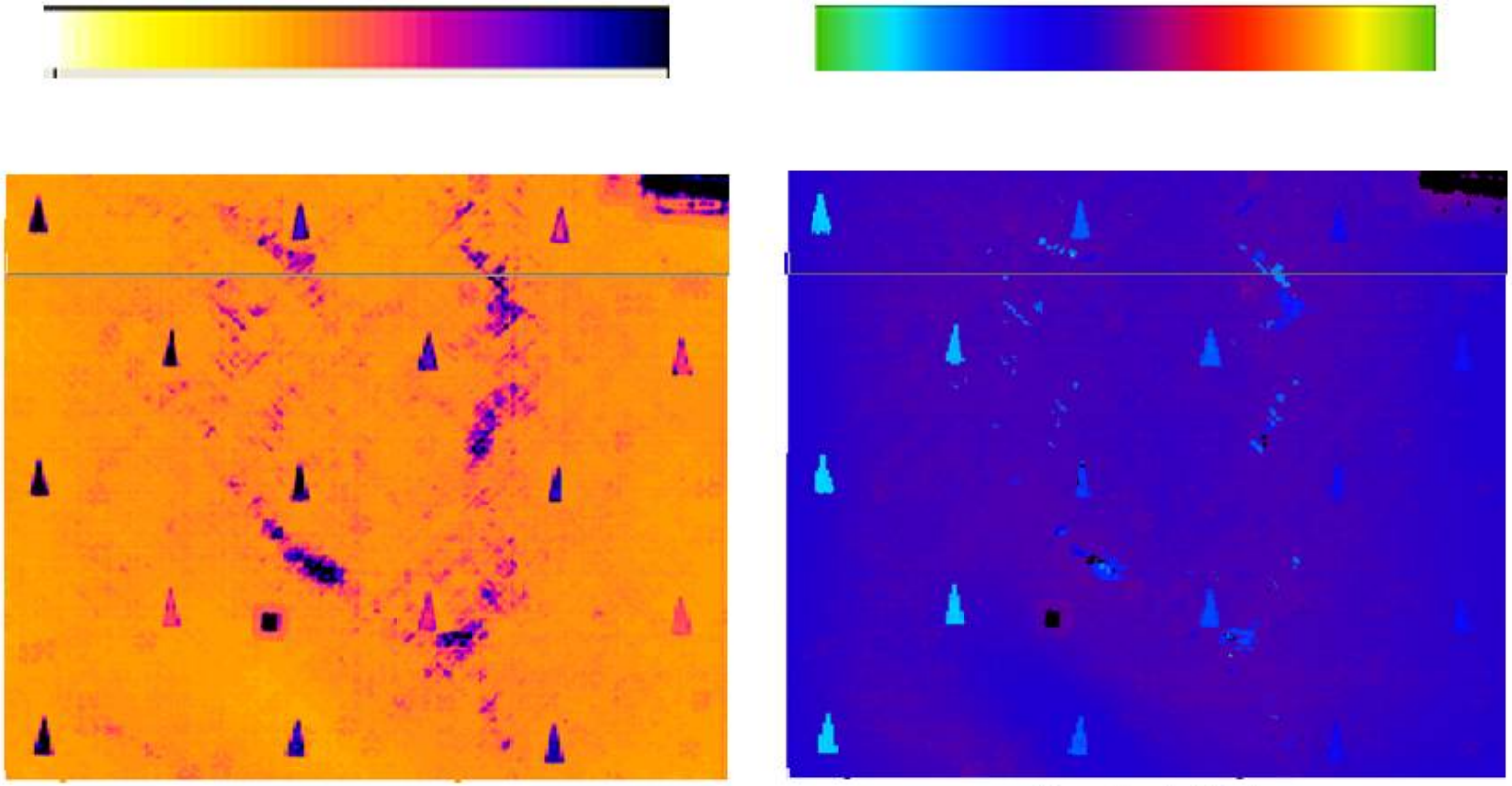

Amplitude

Depth- TOF

National Nuclear Security Administration

Sandia National Laboratories

FAA-FOD-01 Bell-Innovative, Image Based NDE for Modern Rotorcraft Sustainment
MAUS 5 Resonance Testing 313 KHZ

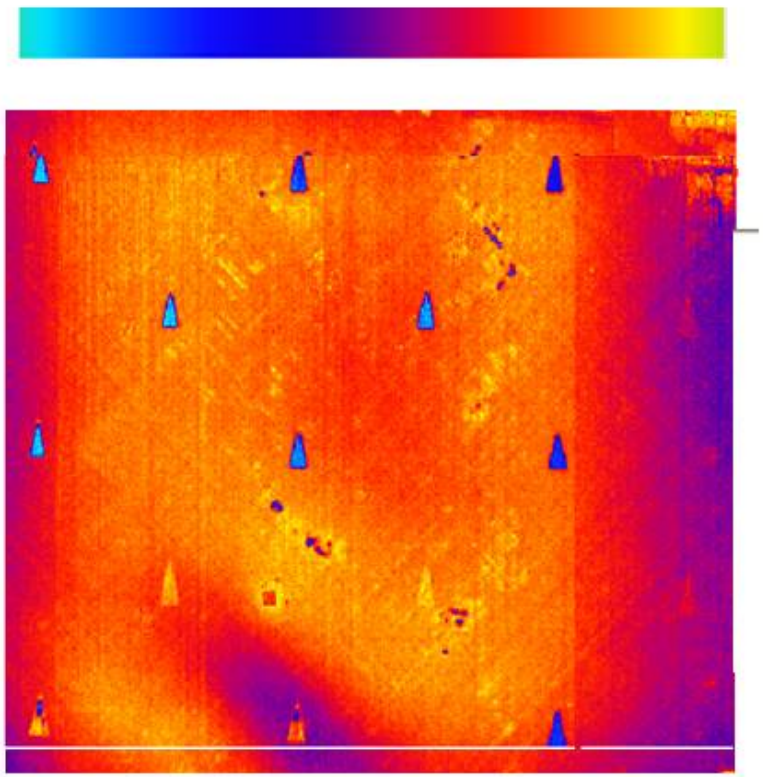

X-Plot

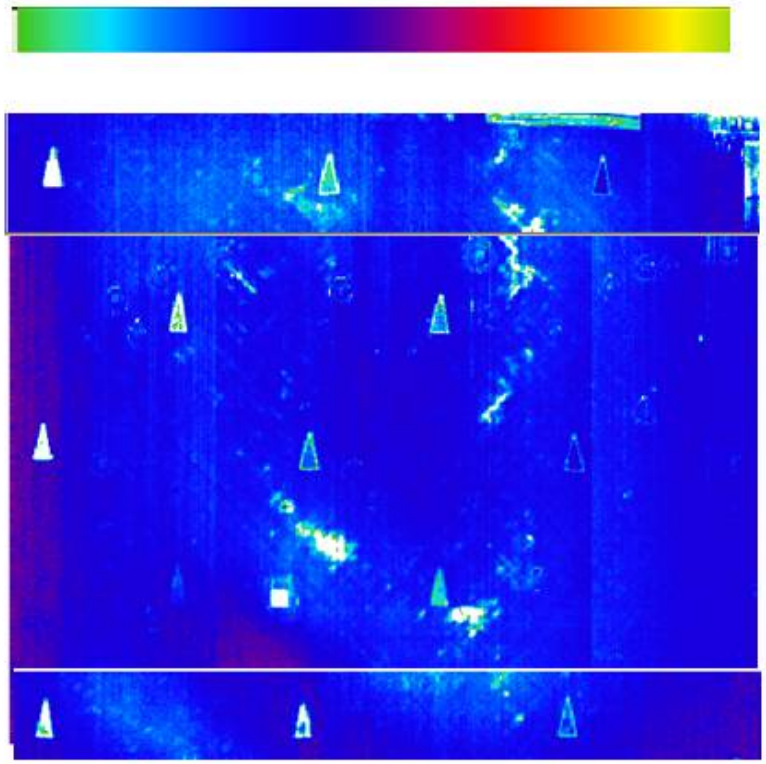

Y-Plot

NOTE: Part Had To Be Scanned In Sections

National Nuclear Security Administration

Sandia National Laboratories

FAA-FOD-01 Bell-Innovative, Image Based NDE for Modern Rotorcraft Sustainment

1000i Olympus Ultrasonic Tester 5 MHZ Contact A-Scan

Ramp Damage Checker/Bondmaster Results

Point A- Bad/Bad
Point B- Bad/Bad
Point C- Bad/Bad

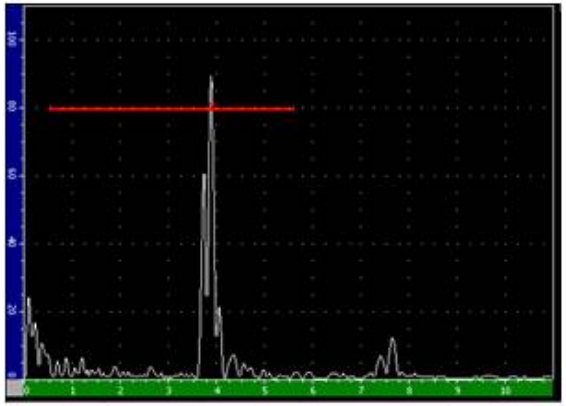

Cal In- 90% Amplitude/29.8db (4.0mm)

Note: FOD (1.0mm)(25%) Deep

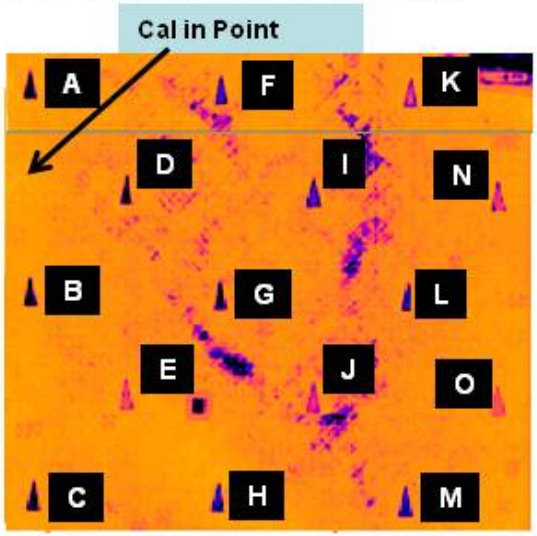

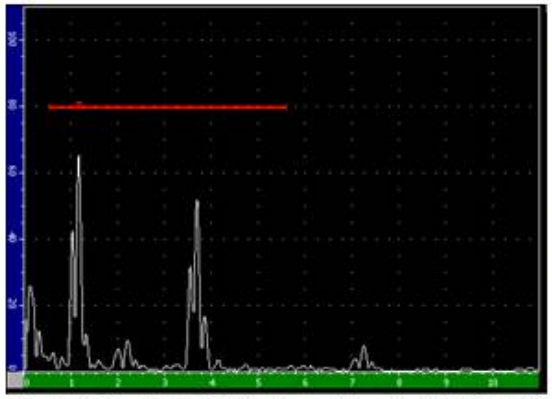

Point A- 65.75% Amplitude/29.8 dB

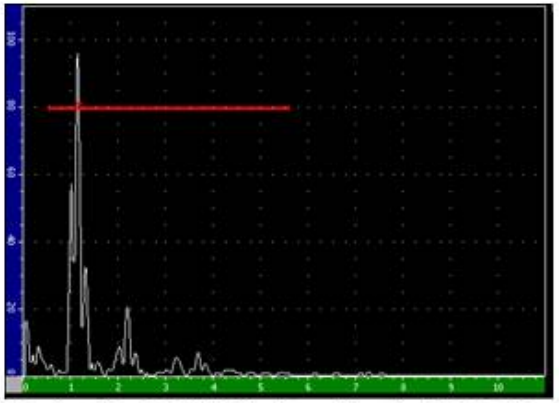

Point B- 96.75% Amplitude/29.8dB

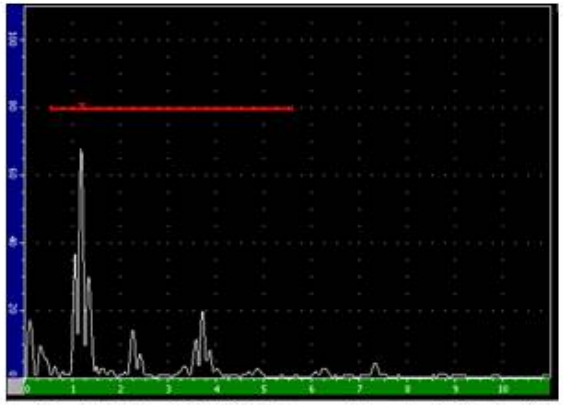

Point C- 68.0% Amplitude/29.8dB

NNSA National Nuclear Security Administration

NOTE: Noted dB and Amplitude Changes different from the Cal In

Sandia National Laboratories

FAA-FOD-01 Bell-Innovative, Image Based NDE for Modern Rotorcraft Sustainment
1000i Olympus Ultrasonic Tester 5 MHZ Contact A-Scan

Cal in Point

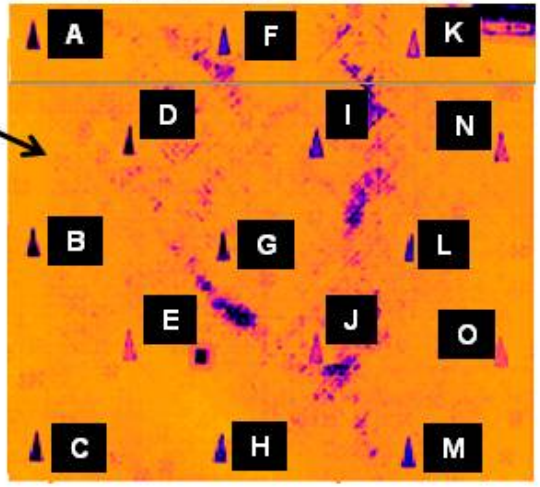

Ramp Damage Checker/Bondmaster Results

Point D- Bad/Bad
Point E- Good and Bad/Bad

Note: FOD (1.0mm)(25%) Deep

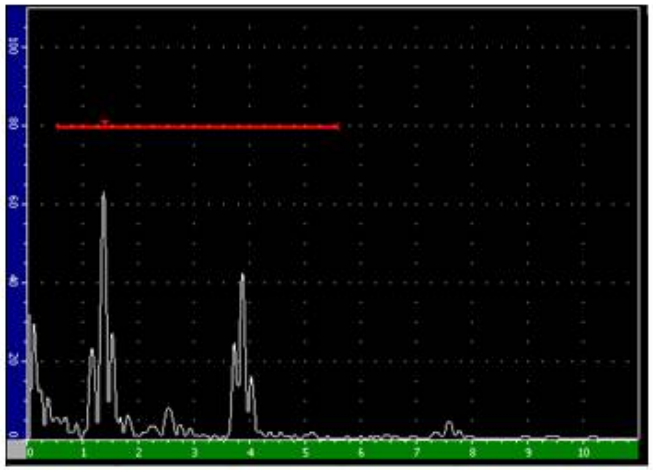

Point D- 63.5% Amplitude/29.8dB

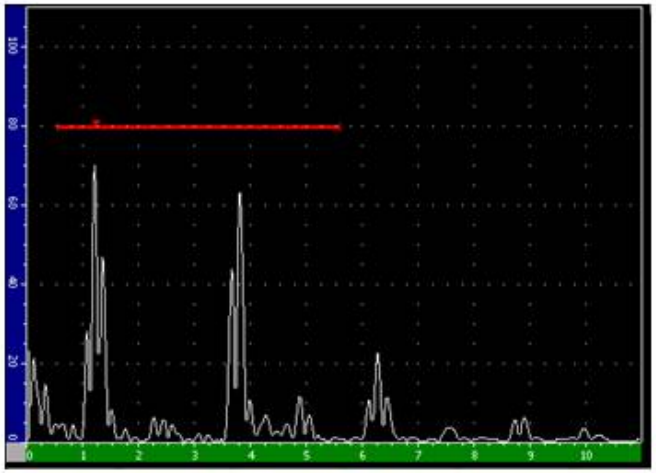

Point E- 70.5% Amplitude/29.8dB

National Nuclear Security Administration

Sandia National Laboratories

FAA-FOD-01 Bell-Innovative, Image Based NDE for Modern Rotorcraft Sustainment
1000i Olympus Ultrasonic Tester 5 MHZ Contact A-Scan

Cal in Point

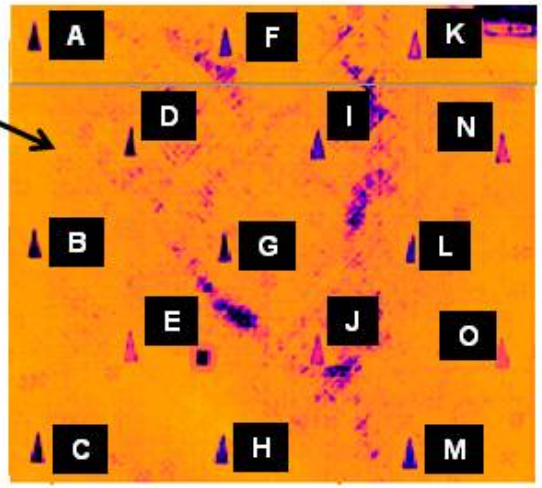

Ramp Damage Checker/Bondmaster Results

Point F- Bad/Bad
Point G- Bad/Bad
Point H- Bad/Bad

Note: FOD (2.0mm)(50%) Deep

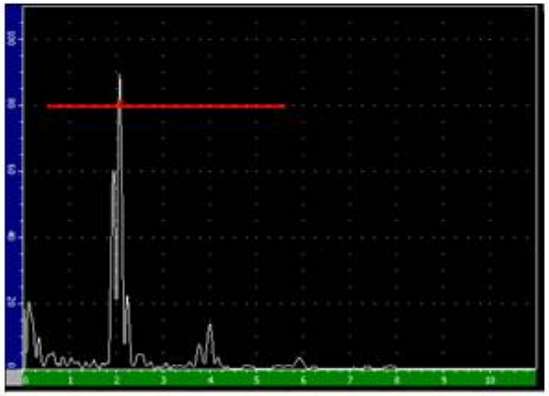

Point F- 90.0% Amplitude/26.6dB

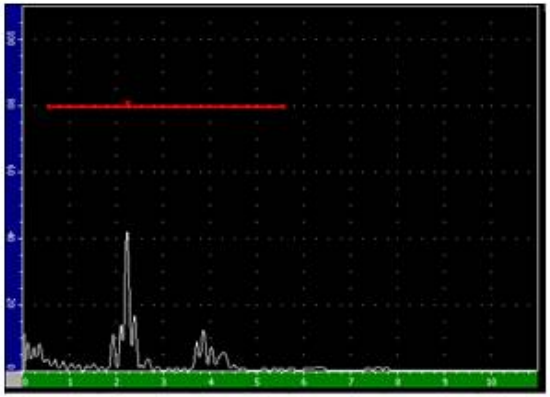

Point G- 42.25% Amplitude/26.6dB

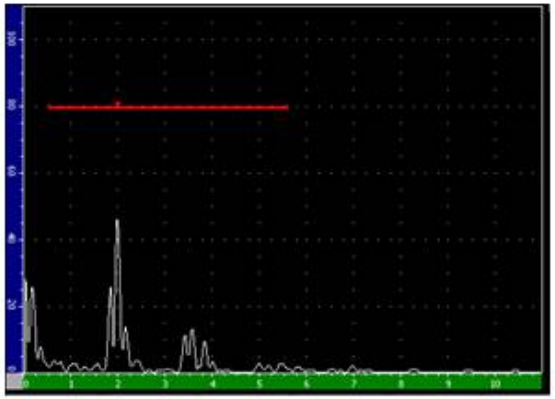

Point H- 46.25% Amplitude/26.6dB

National Nuclear Security Administration

Sandia National Laboratories

FAA-FOD-01 Bell-Innovative, Image Based NDE for Modern Rotorcraft Sustainment
1000i Olympus Ultrasonic Tester 5 MHZ Contact A-Scan

Cal in Point

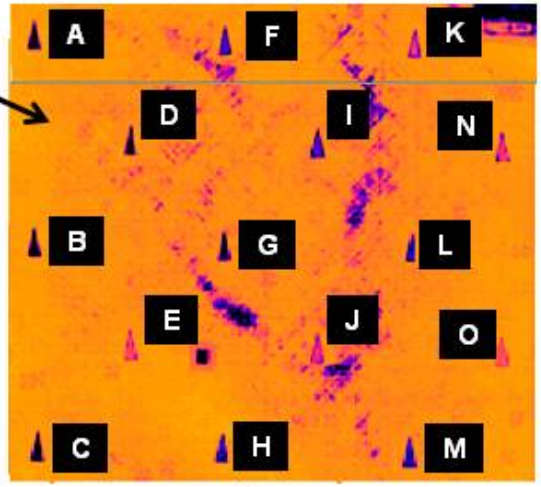

Ramp Damage Checker/Bondmaster Results

Point I- Bad/Bad
Point J- Good and Bad/Bad

Note: FOD (2.0mm)(50%) Deep

Point I- 60.0% Amplitude/26.6dB

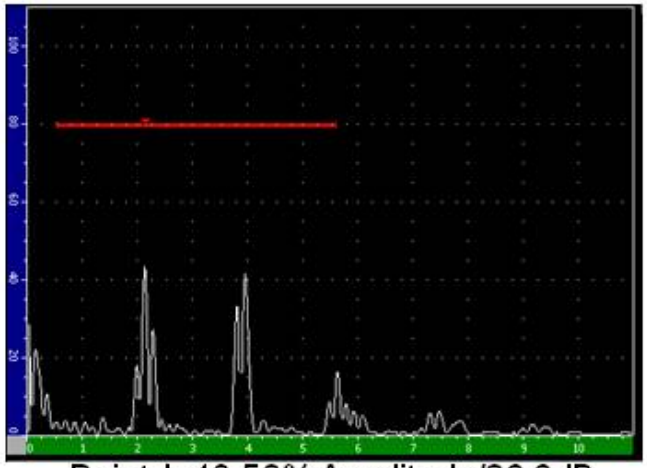

Point J- 43.50% Amplitude/26.6dB

National Nuclear Security Administration

Sandia National Laboratories

FAA-FOD-01 Bell-Innovative, Image Based NDE for Modern Rotorcraft Sustainment
1000i Olympus Ultrasonic Tester 5 MHZ Contact A-Scan

Cal in Point

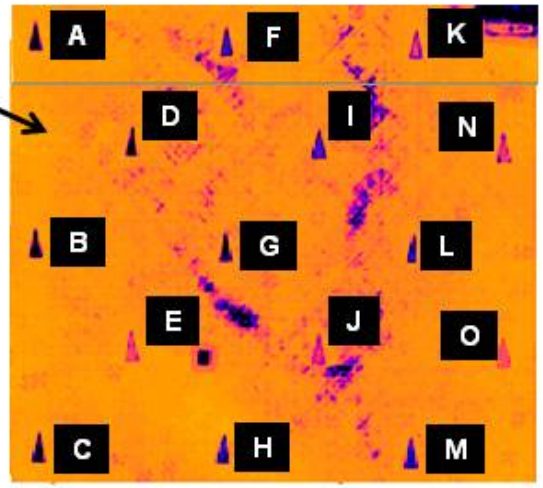

Ramp Damage Checker/Bondmaster Results

Point K- Bad/Bad
Point L- Bad/Bad
Point M- Bad/Bad

Note: FOD (3.0mm)(75%) Deep

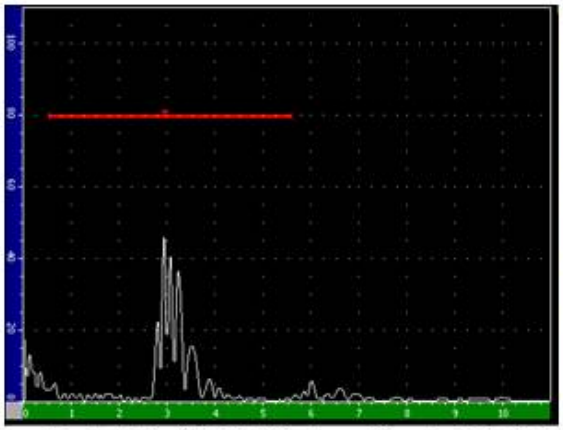

Point K- 46.25% Amplitude/26.6dB

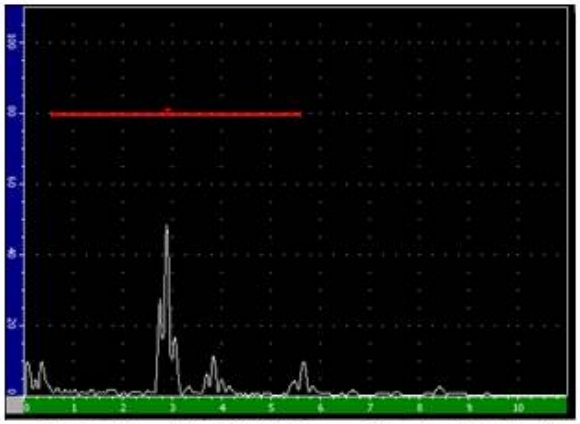

Point L- 48.50% Amplitude/26.6dB

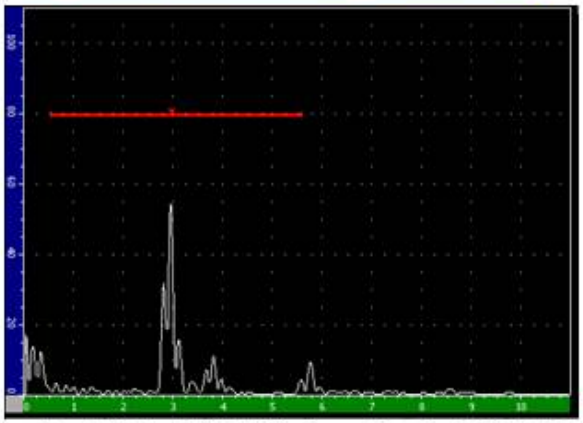

Point M- 54.75% Amplitude/26.6dB

National Nuclear Security Administration

Sandia National Laboratories

FAA-FOD-01 Bell-Innovative, Image Based NDE for Modern Rotorcraft Sustainment
1000i Olympus Ultrasonic Tester 5 MHZ Contact A-Scan

Cal in Point

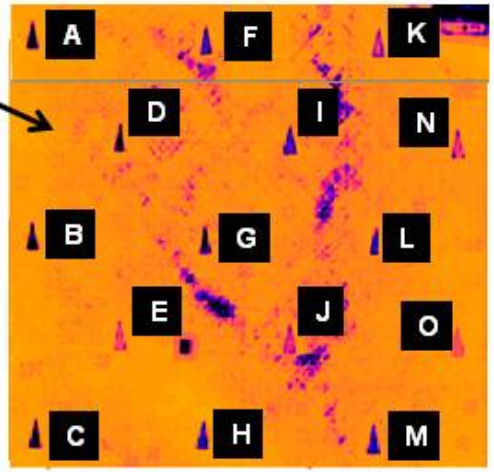

Ramp Damage Checker/Bondmaster Results

Point N- Bad/Bad
Point O- Good and Bad/Bad

Note: FOD (3.0mm)(75%)Deep

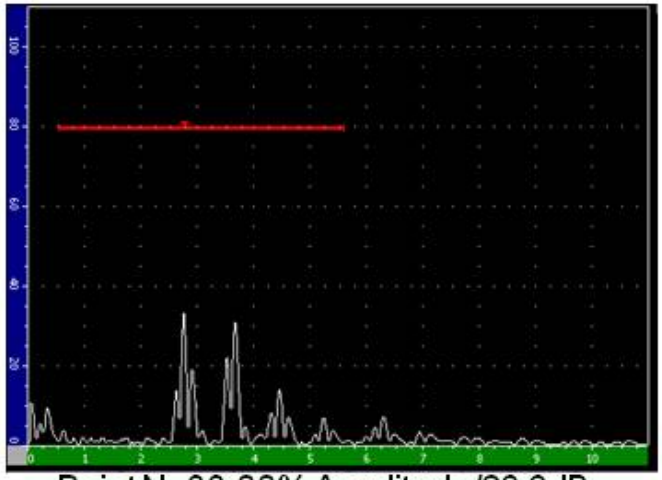

Point N- 33.00% Amplitude/26.6dB

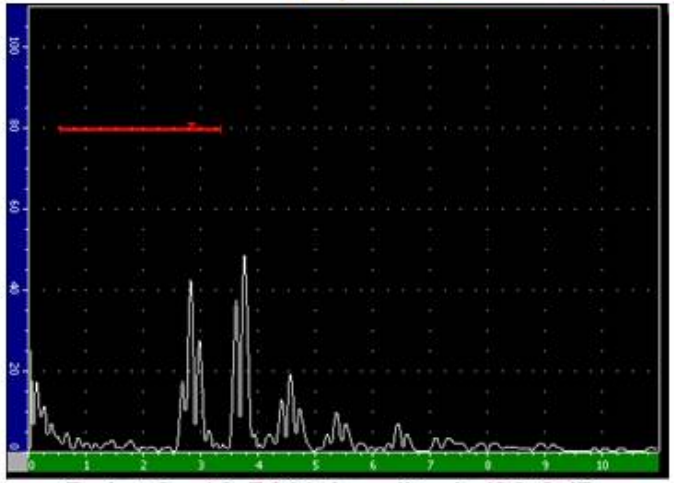

Point O- 42.50% Amplitude/26.6dB

National Nuclear Security Administration

Sandia National Laboratories

FAA-FOD-01 Bell-Innovative, Image Based NDE for Modern Rotorcraft Sustainment
Flash Thermography (IR)

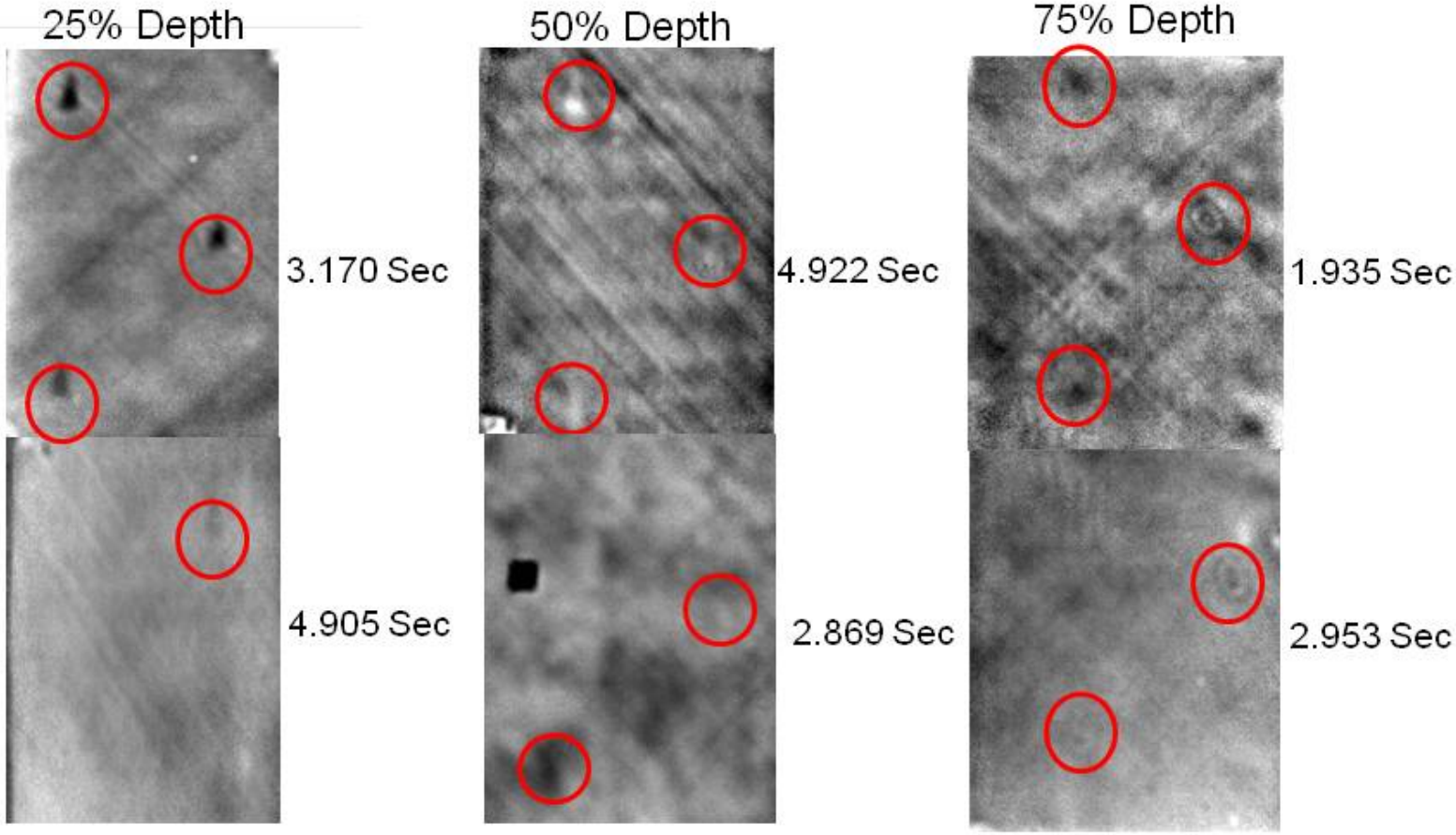

National Nuclear Security Administration

Sandia National Laboratories

Bell-Innovative FOD Panels, Image Based NDE for Modern Rotorcraft Sustainment

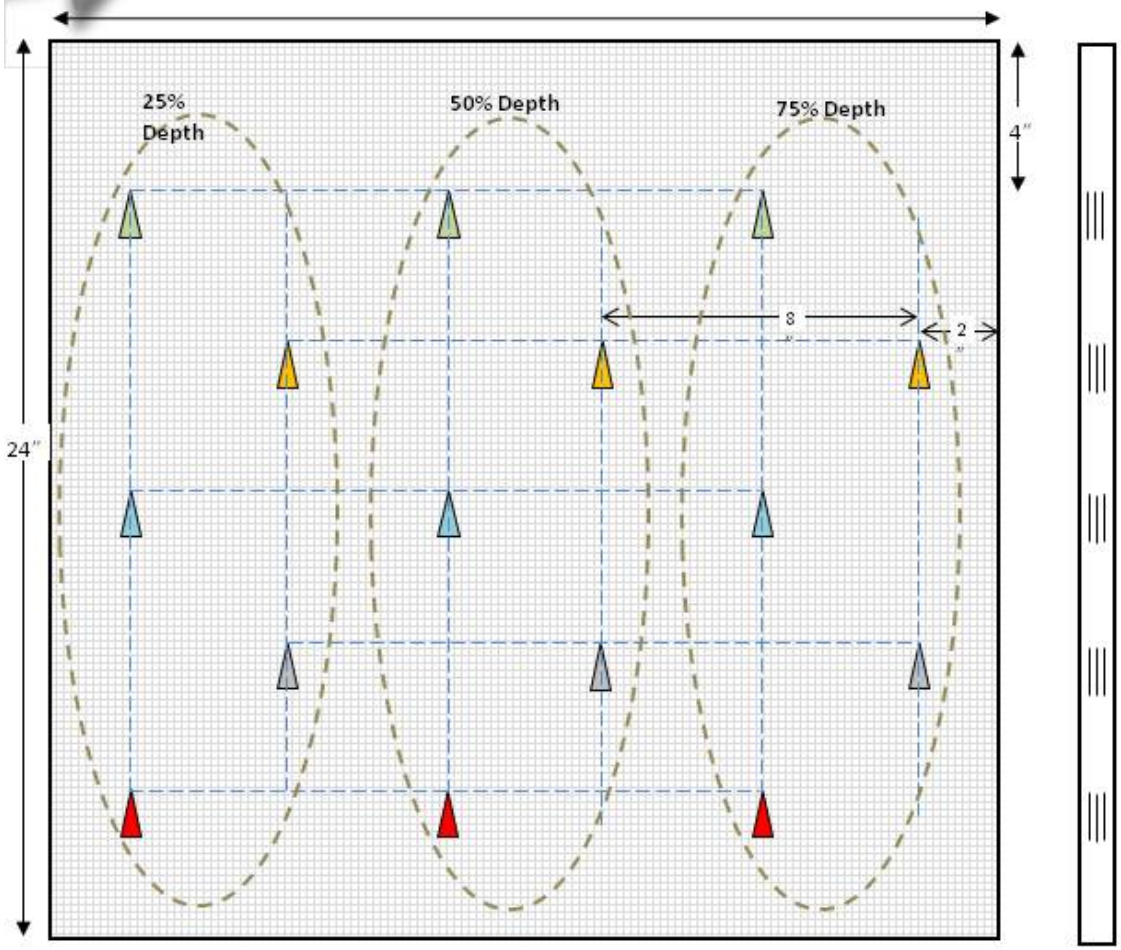

Green = Teflon / Tedlar, is orange Teflon Tape over Tedlar

Gold = Backing Film, 1 layer, Poly material, FM300 per 299-947-121

Blue = Paper, coated, from AF 163 per spec. 299-947-320

Silver = 1 Layer Aluminum Backing from material per 299-947-350

Red = AF 163 Adhesive film plastic Backing per 299-947-038

Note: Dart size is approximately 1.25" tall x 0.5" wide at base

21 Ply C/EP Tape per 297-947-330 TY35 CL2 Form 0 Grade 190 (as illustrated on ply table on Page 2)

Fod Layers between

Ply 5 and 6,

- Ply 10 and 11
- Ply15 and 16

FOD Inserts to be provided and applied by NDE Lab personnel.

RJ Barry Ext. 13253

National Nuclear Security Administration

FAA-FOD-02 Bell-Innovative, Image Based NDE for Modern Rotorcraft Sustainment

Top

Bottom

National Nuclear Security Administration

Sandia National Laboratories

FAA-FOD-02 Bell-Innovative, Image Based NDE for Modern Rotorcraft Sustainment
Omniscan Unit 5L64 (5 MHZ) Aqualene Wedge Phased Array

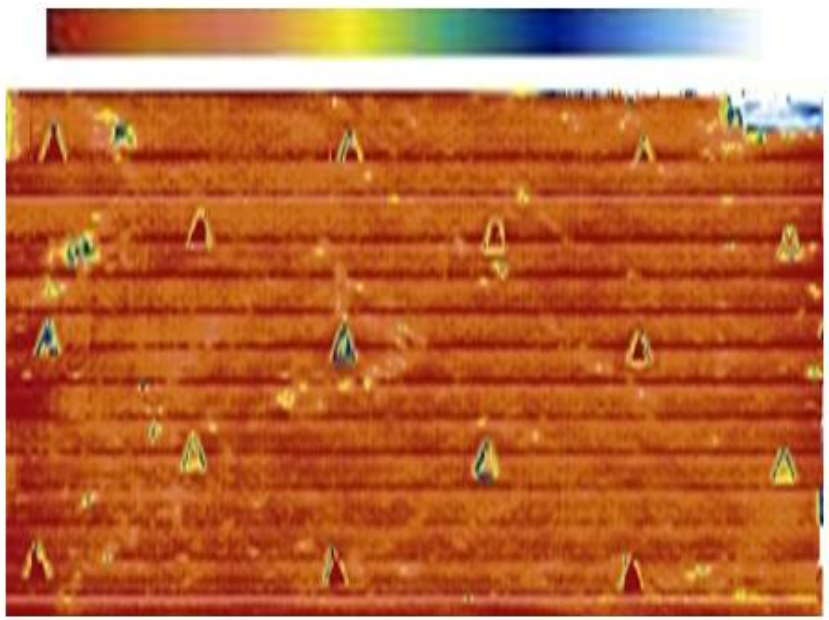

Amplitude

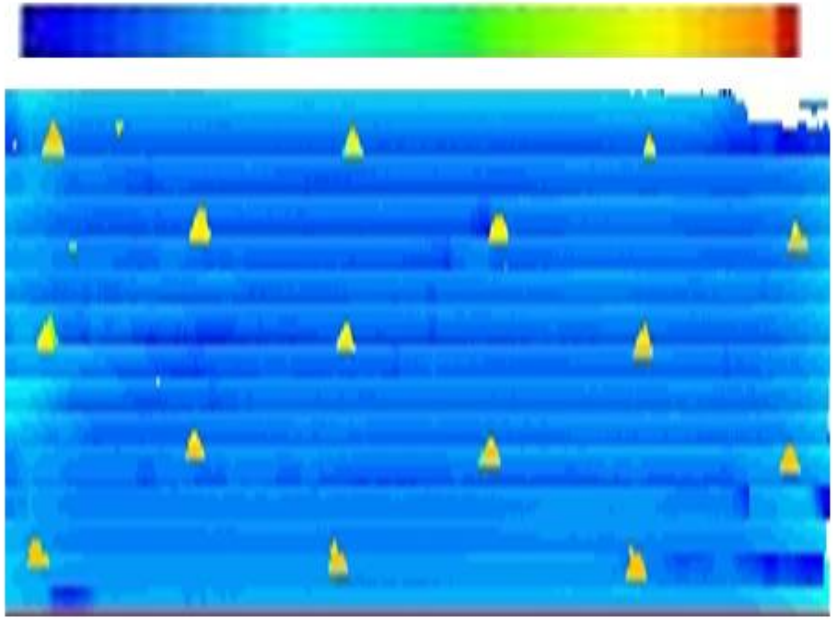

TOF

National Nuclear Security Administration

Sandia National Laboratories

FAA-FOD-02 Bell-Innovative, Image Based NDE for Modern Rotorcraft Sustainment
Omniscan Unit 5 MHZ Contact Testing

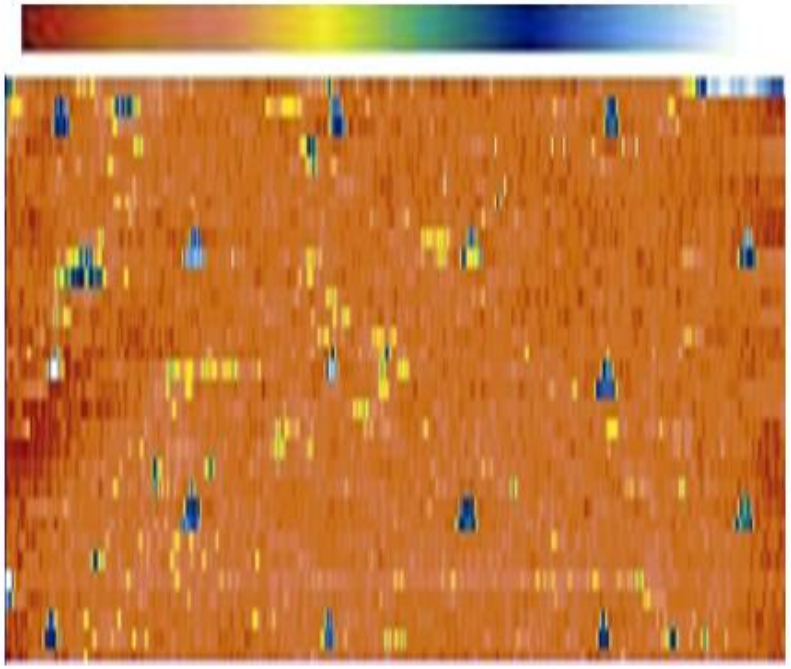

Amplitude

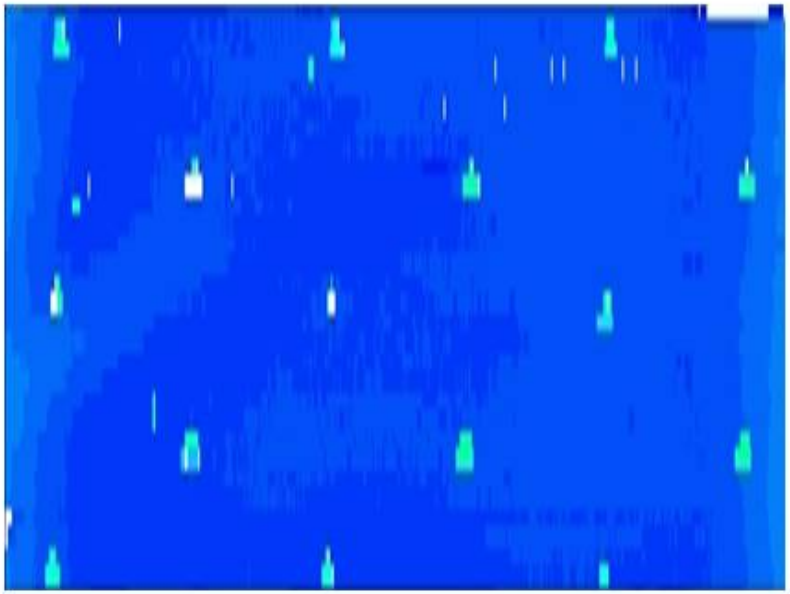

TOF

National Nuclear Security Administration

Sandia National Laboratories

FAA-FOD-02 Bell-Innovative, Image Based NDE for Modern Rotorcraft Sustainment
MAUS 5 Pulse Echo 5 MHZ Contact Testing

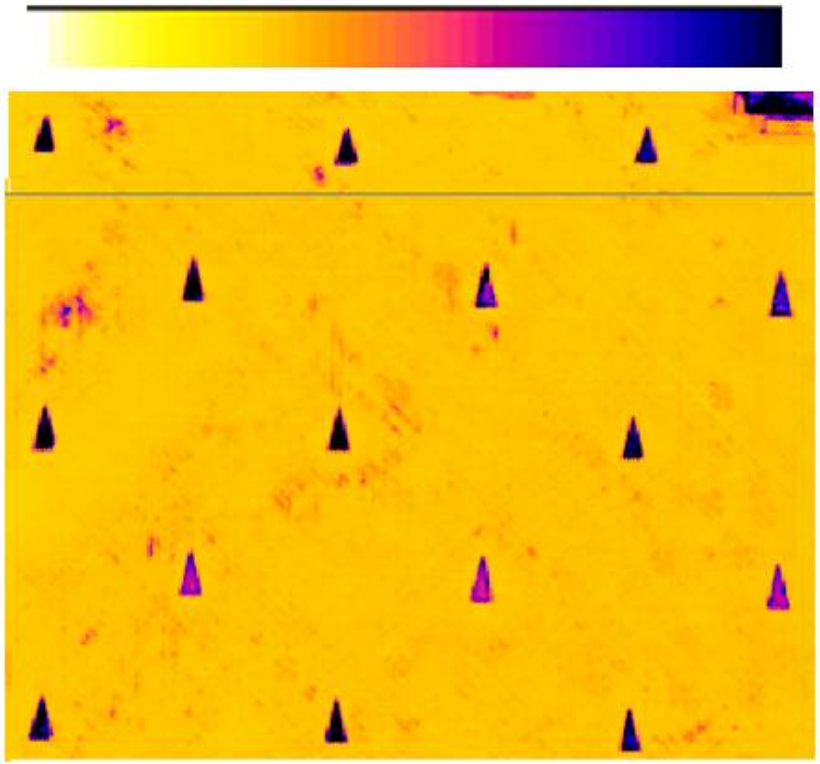

Amplitude

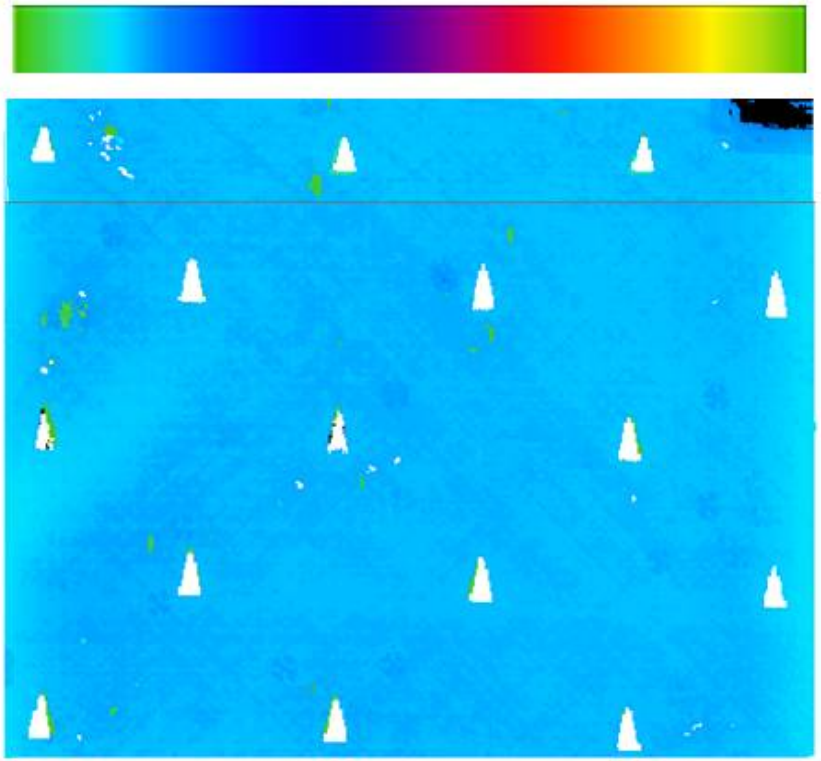

Depth- TOF

National Nuclear Security Administration

Sandia National Laboratories

FAA-FOD-02 Bell-Innovative, Image Based NDE for Modern Rotorcraft Sustainment
MAUS 5 Resonance Testing 313 KHZ

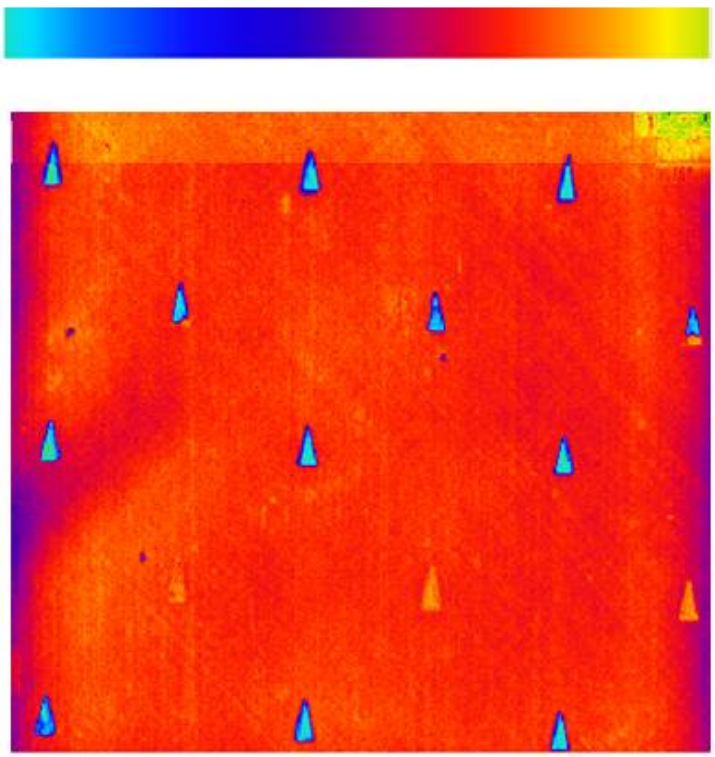

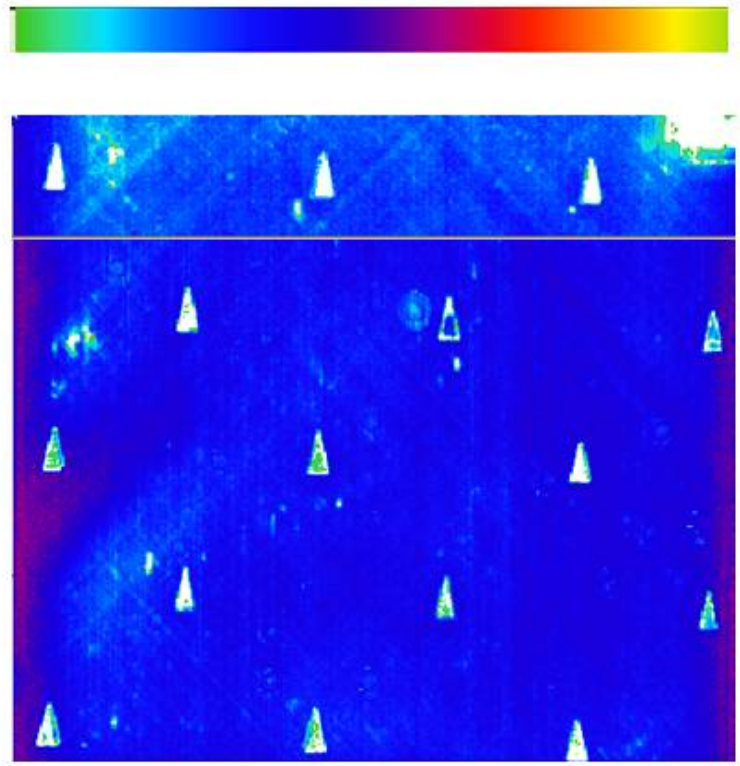

National Nuclear Security Administration

Sandia National Laboratories

FAA-FOD-02 Bell-Innovative, Image Based NDE for Modern Rotorcraft Sustainment

1000i Olympus Ultrasonic Tester 5 MHZ Contact A-Scan

Ramp Damage Checker/Bondmaster Results

Point A- Bad/Bad
Point B- Bad/Bad
Point C- Bad/Bad

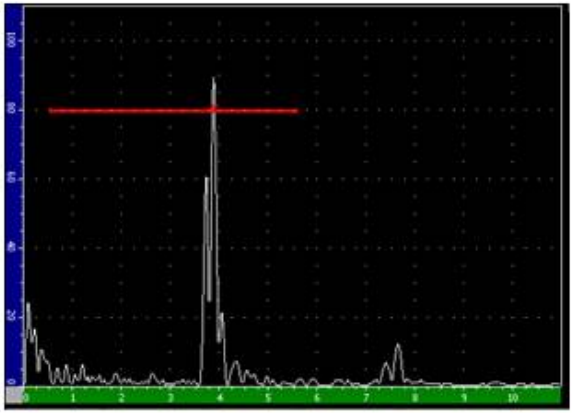

Cal In- 90% Amplitude/28.8db (4.0mm)

Note: FOD (1.0mm)(25%) Deep

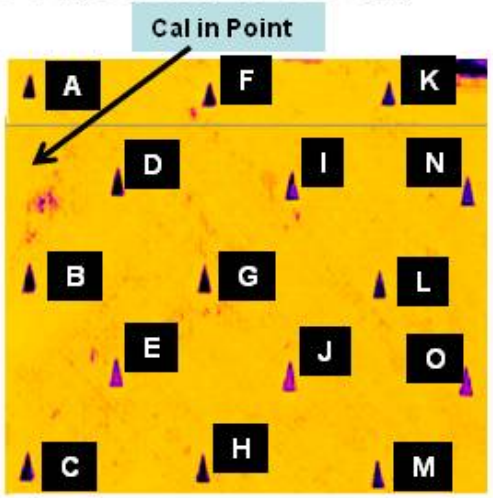

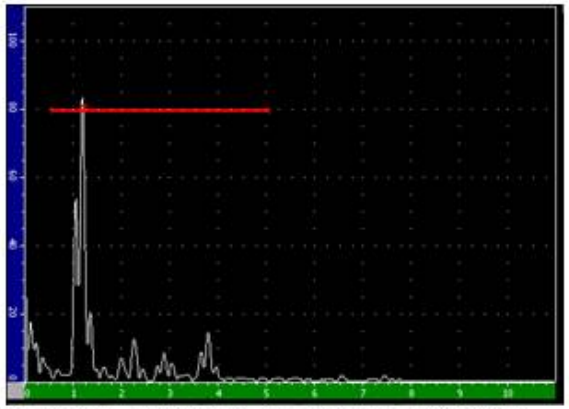

Point A- 84.25% Amplitude/28.8dB

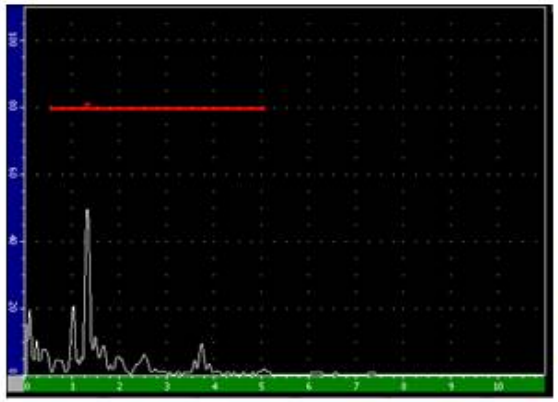

Point B- 50.25% Amplitude/28.8dB

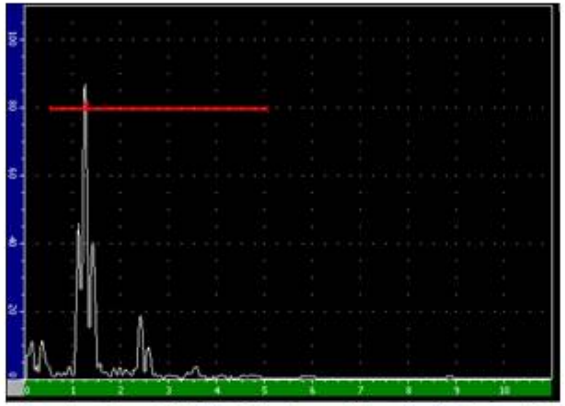

Point C- 87.50% Amplitude/28.8dB

National Nuclear Security Administration

Sandia National Laboratories

FAA-FOD-02 Bell-Innovative, Image Based NDE for Modern Rotorcraft Sustainment
1000i Olympus Ultrasonic Tester 5 MHZ Contact A-Scan

Cal in Point

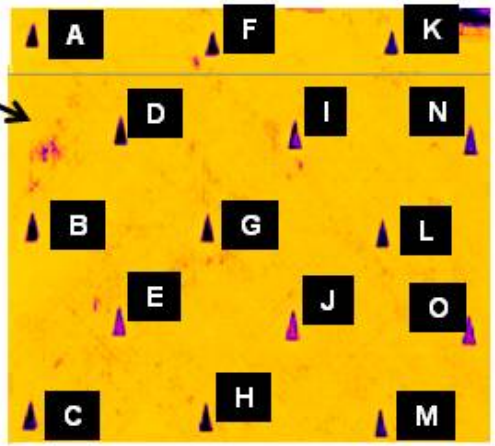

Ramp Damage Checker/Bondmaster Results

Point D- Bad/Bad
Point E- Good and Bad/Bad

Note: FOD (1.0mm)(25%) Deep

Point D- 109.00% Amplitude/28.8dB

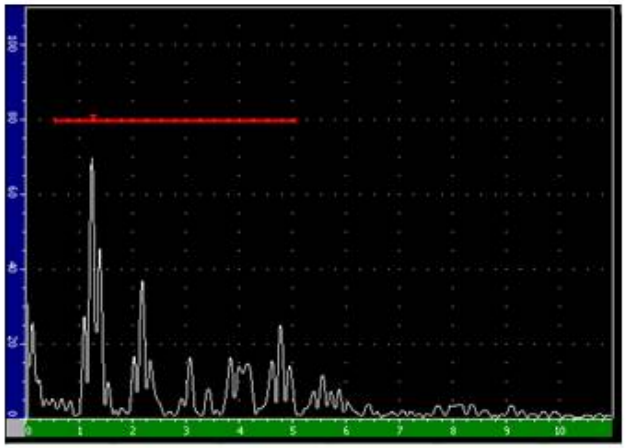

Point E- 70.25% Amplitude/28.8dB

National Nuclear Security Administration

Sandia National Laboratories

FAA-FOD-02 Bell-Innovative, Image Based NDE for Modern Rotorcraft Sustainment
1000i Olympus Ultrasonic Tester 5 MHZ Contact A-Scan

Cal in Point

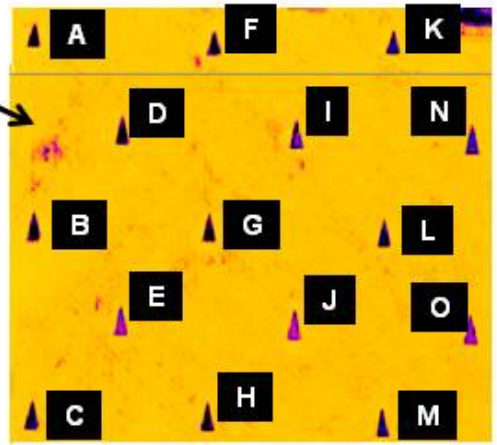

Ramp Damage Checker/Bondmaster Results

Point F- Bad/Bad
Point G- Bad/Bad
Point H- Bad/Bad

Note: FOD (2.0mm)(50%) Deep But Signal Showed at 1mm

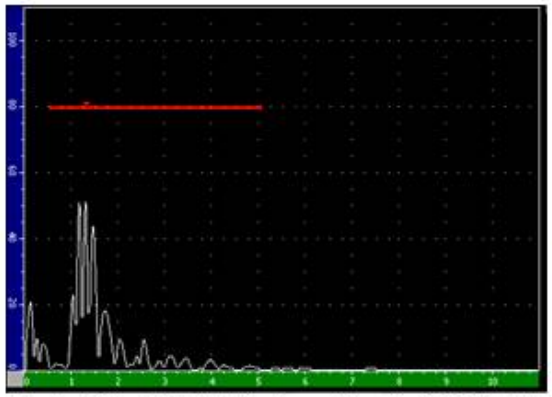

Point F- 51.50% Amplitude/28.8dB

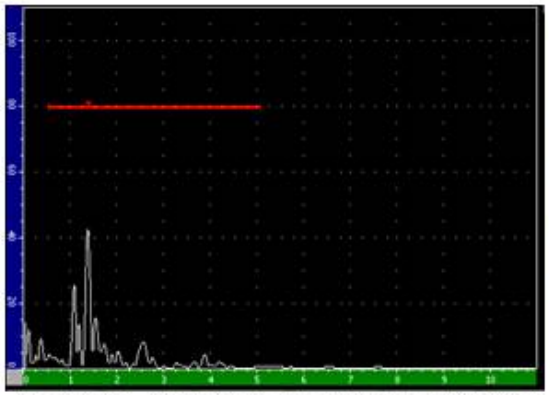

Point G- 42.75% Amplitude/28.8dB

Point H- 109.25% Amplitude/28.8dB

Note: FOD Should Have Shown at 2mm on Scale But Showed Up at 1mm

National Nuclear Security Administration

Sandia National Laboratories

FAA-FOD-02 Bell-Innovative, Image Based NDE for Modern Rotorcraft Sustainment
1000i Olympus Ultrasonic Tester 5 MHZ Contact A-Scan

Cal in Point

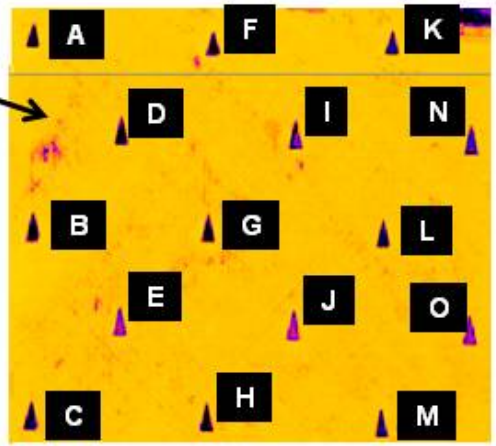

Ramp Damage Checker/Bondmaster Results

Point I- Bad/Bad
Point J- Good and Bad/Bad

Note: FOD (2.0mm)(50%) Deep But Signal Showed at 1mm

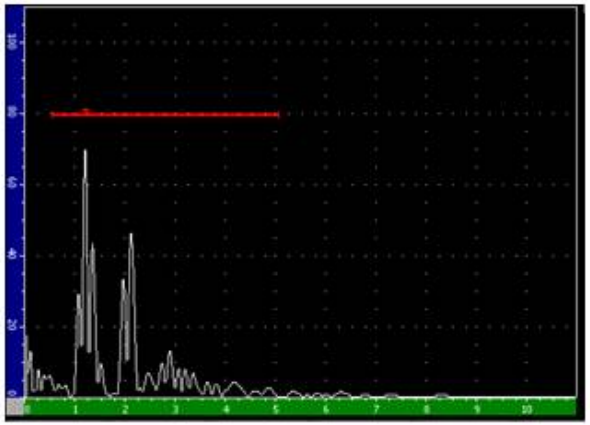

Point I- 70.25% Amplitude/28.8dB

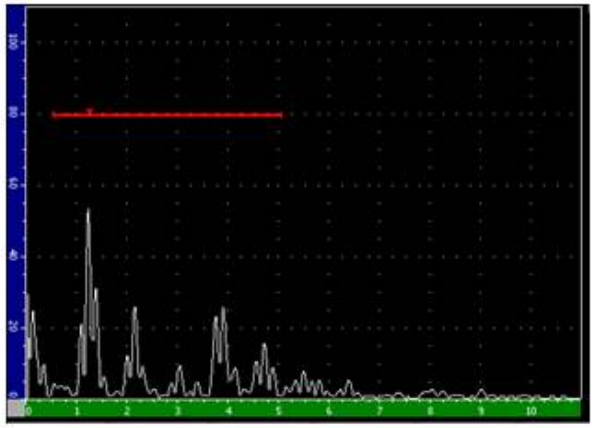

Point J- 53.50% Amplitude/28.8dB

Note: FOD Should Have Shown at 2mm on Scale But Showed Up at 1mm

National Nuclear Security Administration

Sandia National Laboratories

FAA-FOD-02 Bell-Innovative, Image Based NDE for Modern Rotorcraft Sustainment
1000i Olympus Ultrasonic Tester 5 MHZ Contact A-Scan

Cal in Point

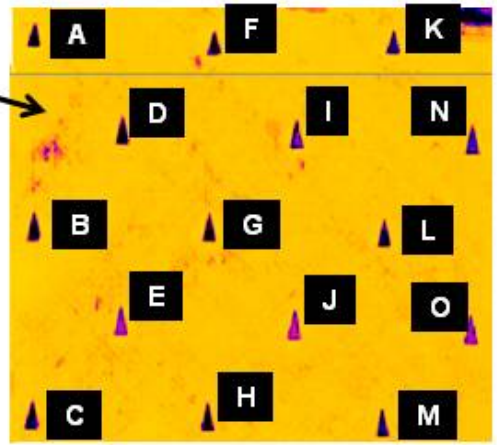

Ramp Damage Checker/Bondmaster Results

Point K- Bad/Bad
Point L- Bad/Bad
Point M- Bad/Bad

Note: FOD (3.0mm)(75%)Deep But Signal Showed Up at 1mm

Point K- 88.75% Amplitude/28.8dB

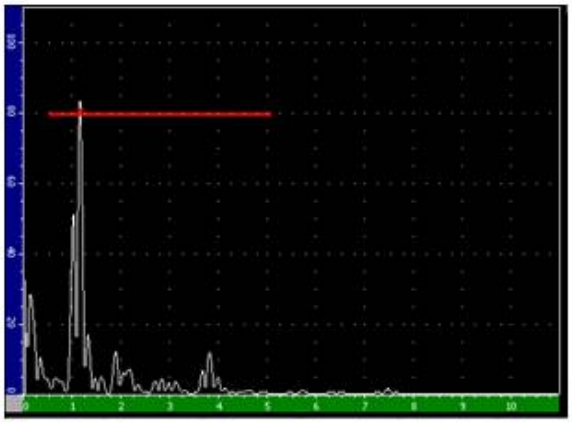

Point L- 84.00% Amplitude/28.8dB

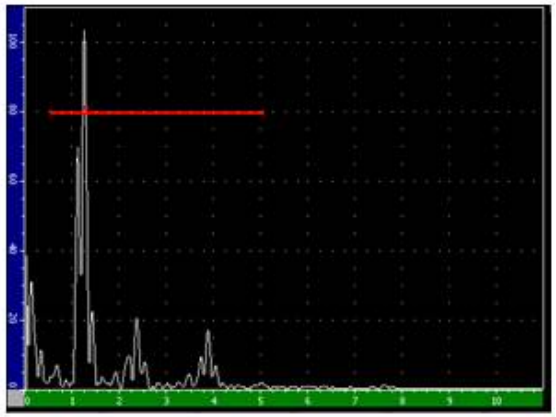

Point M- 104.00% Amplitude/28.8dB

Note: FOD Should Have Shown at 3mm on Scale But Showed Up at 1mm

National Nuclear Security Administration

Sandia National Laboratories

FAA-FOD-02 Bell-Innovative, Image Based NDE for Modern Rotorcraft Sustainment
1000i Olympus Ultrasonic Tester 5 MHZ Contact A-Scan

Cal in Point

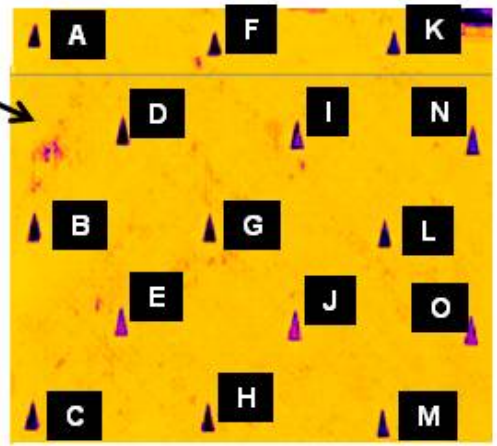

Ramp Damage Checker/Bondmaster Results

Point N- Bad/Bad
Point O- Good and Bad/Bad

Note: FOD (3.0mm)(75%)Deep But Signal Showed Up at 1mm

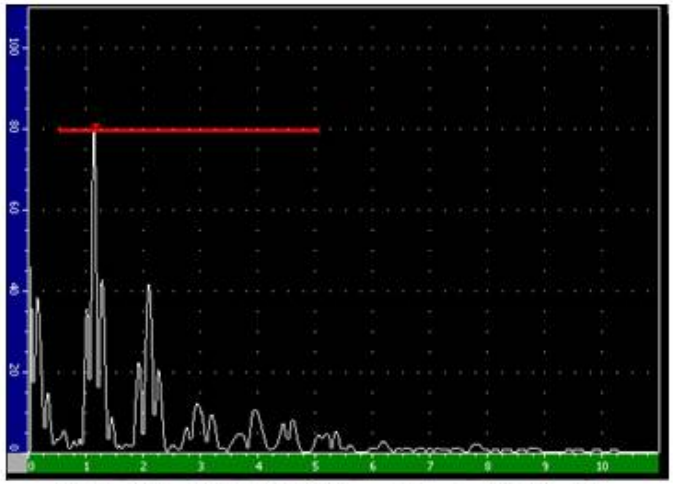

Point N- 80.25% Amplitude/28.8dB

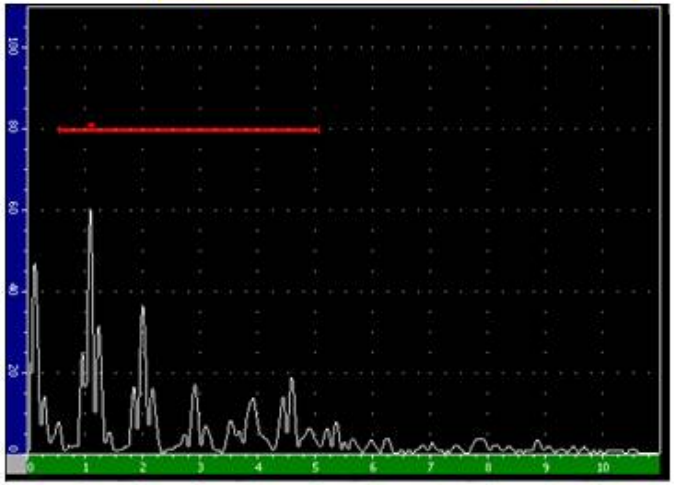

Point O- 60.75% Amplitude/28.8dB

Note: FOD Should Have Shown at 3mm on Scale But Showed Up at 1mm

National Nuclear Security Administration

Sandia National Laboratories
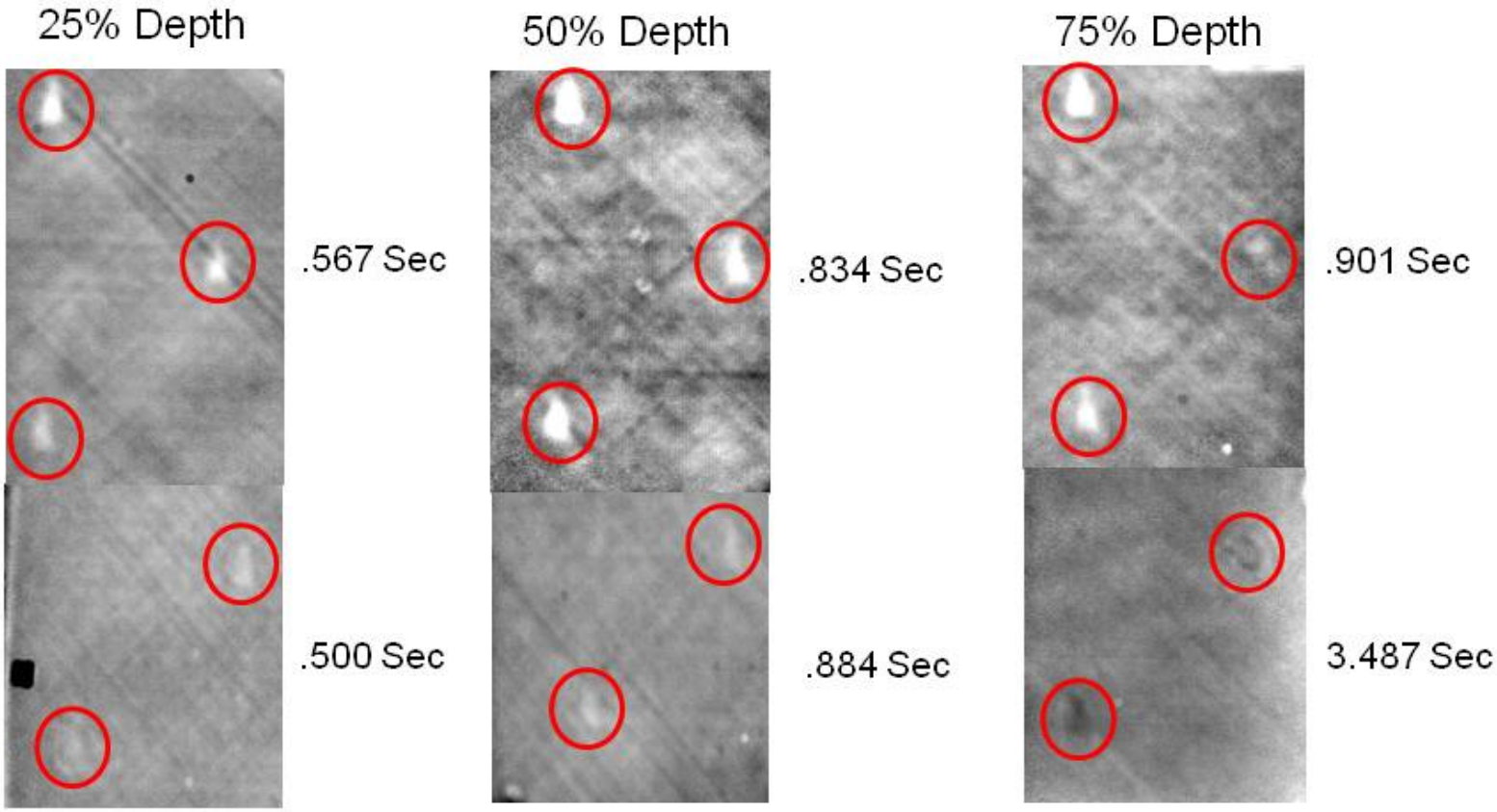
FAA-FOD-02 Bell-Innovative, Image Based NDE for Modern Rotorcraft Sustainment
Flash Thermography (IR)